Phenomenology Of The Minimal Supersymmetric Standard Model Without R–Parity

Benjamin Hugh O'Leary

Thesis submitted for the degree of Doctor of Philosophy

University of Edinburgh
2007

Abstract

This thesis is an investigation into the current bounds on the trilinear R–parity–violating couplings in the Minimal Supersymmetric Standard Model without R–parity conservation. The model is described, and its implications are discussed. Bounds on the couplings are obtained from leptonic and mesonic decay data, approximating mediating sfermions as much heavier than the decaying particles and assuming that only one set of couplings is non–zero for each decay. Those bounds from the purely leptonic decay data are compared to bounds from the LEP–II data, over a large range of sfermion masses. A potential signal of R–parity–violation at existing lepton colliders is calculated assuming that certain couplings are close to their bounds. The signal is found to be feasible and the backgrounds to the process are found to be negligible.

Declaration

This thesis has been wholly composed by me, and presents work carried out by me alone and work carried out by me in collaboration with Michael Krämer and Herbi Dreiner.

The first and second chapters are mainly background material.

The calculations in chapter 3 were performed by me and verified by Michael Krämer and Herbi Dreiner. The experimental data were taken from the results of the Particle Data Group as were available in December 2006.

The results of chapter 3 were published on the Internet as reference [1]:

- Bounds on R–Parity Violation from Leptonic and Semi–Leptonic Meson Decays, H. K. Dreiner, M. Krämer, Ben O'Leary, hep–ph/0612278

and have been submitted for publication to Physics Review D.

The calculations in chapter 4 were performed wholly by me, and have not been published outside this thesis.

The calculations in chapter 5 were performed wholly by me, in parts utilizing the programs FORM and FORMCalc.

The results of chapter 5 were published on the Internet as reference [2]:

- Single B production through R–parity violation, Ben O'Leary, hep–ph/0610413

which has been published in Physics Review D **75**:

- B. O'Leary, "Single B production through R-parity violation," Phys. Rev. D **75** (2007) 054027

Benjamin Hugh O'Leary June 21, 2007

Acknowledgements

I would like to thank Michael Krämer for accepting me as a student, for his patient explanations and for his valuable help with my work. I would like to thank Tilman Plehn for also accepting me as a student, for his dedication and for his motivating enthusiasm.

I am grateful to the Carnegie Trust for the Universities of Scotland for their support of my project.

I would like to thank Herbi Dreiner for fruitful collaboration, Thomas Binoth for helpful and interesting discussions, and Steve Playfer and Franz Muheim for practical and useful points of view.

Vorrei ringraziare i miei compagni dell'ufficio, Simone Marzani e Maria Ubiali, per il loro supporto, la loro amicizia e per avermi fatto scoprire l'italiano.

I would also like to thank my office–mates Tom Rippon and Dave Antonio for a friendly and intelligent working environment.

Ich möchte Eike Müller für den Entwurf meiner These mit Sorgfalt lesen und für das Beibringen mir einer kleinen Spitze des Deutschen danken.

Finally I would like to thank all my friends and my family for restoring my sanity during my free time.

Contents

Chapter 1

Introduction

Nature is well described at the smallest scales which we can probe in experiment by the Standard Model of Particle Physics. However, this model is generally not considered to be the most fundamental description of the universe. Its supersymmetric extension, the Minimal Supersymmetric Standard Model, is a very popular candidate for the next refinement of our understanding of short–distance physics, though there is as yet no direct evidence for its realization. The Minimal Supersymmetric Standard Model is defined with a discrete symmetry called R–parity, which is introduced for phenomenological reasons but which has no theoretical basis. This thesis investigates the experimental constraints on the R–parity–disallowed particle interaction couplings from heavy lepton and meson decay data, and considers whether collider searches could find signals of such interactions should the couplings be just under their bounds from the decay data.

The first chapter provides an introduction to the Standard Model as a quantum field theory and then attempts to motivate extending the Standard Model, especially by supersymmetry. The second chapter describes the model upon which this thesis is based, and illustrates some of its characteristics. The third chapter uses experimental data on the non–observation of particular rare decays to place bounds on the many of the parameters of the extended model. The fourth chapter investigates whether the non–observation of particular processes at the high energy LEP2 run enhance the associated bounds in any regions of the parameter space. The fifth chapter calculates the signal and background for single b quark production at current electron–positron colliders should the model's couplings be just below the bounds calculated in chapter 3. The sixth chapter reviews the thesis and discusses its results. The appendices provide descriptions of the conventions used, the input data used, the method of dealing with quantum chromodynamic bound states employed, and more details on topics touched upon in the main text.

1.1 Quantum Field Theory

The laws of physics of the fundamental particles as they are currently known are described almost completely within experimental limits by the Standard Model of Particle Physics (the SM). The SM is a quantum field theory: that is to say, the physical properties of every particle are described by *quantum fields*, which are objects which have values for properties for every single point in a continuous space–time. These quantum fields are not classical fields, in the sense that they are not necessarily sets of commuting (complex) numbers: they are represented by non–commuting operators acting on the vacuum state.

The quantum fields are analogous to the quantum mechanical *wavefunctions* of particles; however, they are more than that. The excitations of quantum fields are interpreted as particles,

in particular the plane–wave excitations are interpreted as particles with definite momenta. An exciting consequence of a quantum field theory is that it describes particle creation and annihilation.

1.2 The Standard Model of Particle Physics

The SM is a quantum field theory with Poincaré invariance (the laws of physics are the same under boosts, rotations and translations of frames of reference) and the preservation of unitarity (so that it preserves the inner product on its Hilbert space: this leads to the result that the inner products of quantum states can be interpreted as probabilities, since they are always between 0 and 1, and, if the states are normalized appropriately, unitarity ensures that the sum of the probabilities of all possible outcomes remains 1). The dynamics come from Heisenberg's Equation of Motion: for an operator $\mathcal{A}$, the time–evolution is given by $i\hbar\frac{\partial}{\partial t}\mathcal{A} = [\mathcal{A}, H]$, where H is the Hamiltonian operator. Equivalently, one can use the Path Integral approach developed by Feynman, also called the "Sum Over Histories" approach: the overlap of a final state with an initial state is given by $\langle\text{final state}\,|\text{initial state}\rangle = \int\mathcal{D}(\text{intermediate states})\exp(iS)$, where S is the action for a given intermediate state.

One might say that it is the *Lagrangian density* (where the action is the integral of the Lagrangian density over space and time), $\mathcal{L}$, of the SM which defines the model, as it contains all the fields of the model, along with all their interactions. The *Feynman rules* can be read off this Lagrangian density, and hence any interaction process can, in principle, be calculated, as long as the interaction *coupling constants* are small enough for a perturbative approach, yielding a power series in the coupling constants, to be valid. In this approach, the free–particle plane–wave eigenstates are the solutions of the basic Hamiltonian which is perturbed by interactions. This basic Hamiltonian is quadratic in all the fields, and therefore is solvable. Any term which involves three or more fields is an interaction term.

The SM is defined with the minimal amount of fields and symmetries for which there is evidence: the three flavors (or sometimes called generations) of charged leptons and neutrinos; the three flavors of up–type and down–type quarks, in each of their three $SU(3)_C$ charges; the gauge groups $U(1)_Y$ and $SU(2)_L$, which mix to become the electromagnetic and weak nuclear forces, and $SU(3)_C$, the strong nuclear force, and their associated vector bosons; plus the Higgs boson, which is required by the very successful Glashow–Weinberg–Salam model [3, 4, 5] of electroweak interactions but is as yet undetected. $U(1)_Y$ is a $U(1)$ Lie group associated with charges Y called hypercharges, $SU(2)_L$ is an $SU(2)$ Lie group which only affects "left–handed" chiralities of fermions, and $SU(3)_C$ is an $SU(3)$ Lie group of which the charges are known as "colors" since the antisymmetric combination of the three charges is neutral under this group's transformations, reminiscent of how the human eye interprets the activation of all three types of color–distinguishing photoreceptors as "colorless" white.

1.2.1 The SM Lagrangian Density

The Lagrangian density of the SM can be separated into four pieces: the *kinetic* part, $\mathcal{L}^{\text{SM}}_{\text{kin}}$, the *scalar potential* part, $\mathcal{L}^{\text{SM}}_{\text{pot}}$, the *Yukawa* part, $\mathcal{L}^{\text{SM}}_{\text{Yuk}}$, and the *Yang–Mills* part, $\mathcal{L}^{\text{SM}}_{\text{Y–M}}$.

The Kinetic Part The classical equation of motion for the field is that which has the action at an extremum. If one takes the kinetic part of the SM Lagrangian density only and ignores the couplings of the particles to the gauge fields, the equations of motion obtained are those of massless free particles in flat Minkowski space: *i.e.* the massless Dirac equation (equation (A.3) in appendix A) for fermionic fields (such as the electron) and the massless Klein–Gordon equation (equation (A.2) in appendix A) for scalar bosonic fields (which, in the SM, is only the Higgs boson). If now the gauge fields are included, the equations become those of massless

particles in external fields.

$$\mathcal{L}^{\rm SM}_{\rm kin} = i\bar{\psi}_j \not{D}\psi_j + (D^\mu\phi_j)^\dagger(D_\mu\phi_j) \tag{1.1}$$

where the ψ_j are the fermions: three flavors of charged leptons: electron (e), muon (μ) and tau lepton (τ); three flavors of neutrinos: electron–neutrino (ν_e), muon–neutrino (ν_μ) and tau–neutrino (ν_τ); three flavors of up–type quarks: up (u), charm (c) and top (t); and three flavors of down–type quark: down (d), strange (s) and bottom (b); also, there are three versions of each of these six flavors of quark forming an $SU(3)_C$ triplet; and the ϕ_j are the scalar bosons: in the SM, just the Higgs boson doublet (ϕ^0, ϕ^+). The D_μ are covariant derivatives, which are different for each fermionic field depending on their gauge–transformation properties.

The fermionic aspect of the $SU(2)_L$ gauge symmetry is most naturally expressed in terms of two–component chiral spinors or *Weyl* spinors, which are related to Dirac spinors through projection operators P_L (left–handed) and P_R (right–handed); the left–handed component of a Dirac spinor ψ is denoted by $\psi_L = P_L\psi$ and the right–handed component is denoted by $\psi_R = P_R\psi$. The sum of these components is exactly the Dirac spinor; that is to say $P_L + P_R = 1$.

The Scalar Potential Part The potential part of the Lagrangian density is, in the SM, just the potential energy density due to the Higgs boson field.

$$\mathcal{L}^{\rm SM}_{\rm pot} = \mu^2\phi^\dagger\cdot\phi - \lambda(\phi^\dagger\cdot\phi)^2 \tag{1.2}$$

where ϕ is the $SU(2)_L$ Higgs doublet. The relative difference in sign between the quadratic (mass) and the quartic (self–interaction) terms leads to the celebrated Higgs mechanism of spontaneously broken electroweak symmetry [6] (this mechanism was also discovered independently by Englert and Brout [7] and by Kibble, Guralnik and Hagen [8]). The relative sign difference means that the minimum of the potential is not at $|\phi| = 0$, but at $\mu/\sqrt{2\lambda}$, so re–writing the Higgs field as this constant plus fluctuations about it leads to the couplings of the $SU(2)_L$ gauge fields to the Higgs becoming couplings to the fluctuations plus quadratic gauge boson terms, *i.e.* mass terms for the gauge bosons. It also leads to mass terms for the fermions without breaking $SU(2)_L$ gauge–invariance.

The Yukawa Part The Yukawa [9] part is, in the SM, the interaction of the Higgs field with the fermions. The vacuum expectation value of the Higgs field leads to mass terms for the fermionic fields without breaking $SU(2)_L$ gauge–invariance: a naïve Dirac mass term $\bar{\psi}_j m\psi_j$ for the fermions mixes left– and right–handed chiralities, which have different transformations under the $SU(2)_L$ gauge, hence such a term is forbidden. The mismatch between the mass eigenstates and the $SU(2)_L$ flavor eigenstates, since the Yukawa coupling matrix is not diagonal in the $SU(2)_L$ flavor basis, leads to the Cabibbo–Kobayashi–Maskawa (CKM) matrix [10, 11] and weak–mediated mixing between flavors of quarks.

$$\mathcal{L}^{\rm SM}_{\rm Yuk} = -Y^l_{jk}\bar{L}_{jL}\cdot\phi\, e_{kR} - Y^d_{jk}\bar{Q}_{jL}\cdot\phi\, d_{kR} - Y^u_{jk}\bar{Q}_{jL\alpha}\epsilon_{\alpha\beta}\phi^*_\beta u_{kR} + \text{ Hermitian conjugate} \tag{1.3}$$

where L_{jL} is the left–handed lepton $SU(2)_L$ doublet (in Weyl spinor notation) of flavor j, e_{kR} is the right–handed charged lepton $SU(2)_L$ singlet of flavor k, Q_{jL} is the left–handed quark $SU(2)_L$ doublet of flavor j, ϕ is the Higgs doublet, d_{kR} is the right–handed down–type quark $SU(2)_L$ singlet of flavor k and u_{kR} is the right–handed up–type quark $SU(2)_L$ singlet of flavor k. The color indices have been suppressed: there are three copies of each of the bi–quark terms, in which both quark fields have the same color. The components of the $SU(2)_L$ doublets are indicated by the indices α and b, and $\epsilon_{\alpha\beta}$ is the rank two antisymmetric tensor; $\bar{Q}_{jL\alpha}\epsilon_{\alpha\beta}\phi^*_\beta$ is allowed as it is invariant under $SU(2)_L$.

The Yang–Mills Part The Yang–Mills part leads to Maxwell's equations (or the non–Abelian generalization) for vector bosonic fields (such as the photon) in the absence of charges. When combined with the fermion–vector boson interaction term from the kinetic part, it leads to the equations including charges and currents.

$$\mathcal{L}^{\mathrm{SM}}_{\mathrm{Y-M}} = \frac{-1}{4} \sum_{\text{gauge fields}} \mathrm{tr}(F_{\mu\nu}F^{\mu\nu}) \tag{1.4}$$

where $F_{\mu\nu} = g^{-1}[D_\mu, D_\nu]$ is the field strength tensor associated with each gauge symmetry, and $D_\mu = (\partial_\mu - igA^a_\mu t^a)$. The A^a_μ are the gauge fields of the symmetry, the t^a are the generators of the Lie group of the symmetry, and g is the coupling associated with the gauge. The quanta of these fields are the vector bosons: depending on whether the symmetry is $U(1)_Y$, $SU(2)_L$ or $SU(3)_C$, they are the photon, the charged W bosons and the Z boson (ignoring the mixing between the $U(1)_Y$ vector boson and the neutral $SU(2)_L$ vector boson arising from the Higgs mechanism), or the eight gluons.

1.3 Beyond The Standard Model

There are many reasons why one might not believe that the Standard Model is the last word in particle physics. Foremost is that it does not even attempt to model gravity. Other than that, most objections have an "aesthetic" feel to them. It can be claimed that the SM is not satisfactory in the respects that there are three seemingly unrelated gauge symmetries, three flavors of each fermion, differentiated only by their Higgs couplings, and perhaps most seriously that all the masses and gauge couplings in the SM Lagrangian density receive infinite corrections at the level of one–loop diagrams, at least perturbatively. These infinite renormalizations do not cause the theory to become unphysical, in the sense that perfectly accurate physical results are still predicted after some redefinitions, but they certainly cause at least some theorists discomfort. More seriously, if one regards the SM as an effective theory, as one must if one is to account for gravity, these infinite quantities are replaced by quantities depending on some scale, up to which the SM is a good theory, but above which the SM cannot be considered a good description of physics. Then the renormalization of quantities depends on this scale, and the exact fine–tuning of some parameters (specifically the Higgs boson mass) to be within physically acceptable values requires extremely precise cancellations. This is known as the hierarchy problem.

Many models have been proposed, which reduce to the Standard Model in certain limits, that address some or all of these concerns. Unfortunately, experimental agreement with the SM severely restricts such models.

1.3.1 Supersymmetry

The model of physics beyond the Standard Model which is considered in this thesis is the Minimal Supersymmetric Standard Model (MSSM) without R–parity. This model does not directly address any of the issues outlined above. There are, however, indirect motivations. First of all, supersymmetry (SUSY) must be described.

Supersymmetry is an extension of the normal space–time symmetries (rotations, translations and boosts) by a fermionic generator and its conjugate (or several of these) which pairs every fermion with a bosonic partner and every boson with a fermionic partner. No SM boson can be paired with any SM fermion without violating gauge symmetries (except perhaps pairing the Higgs boson with a neutrino, but this leads to other problems: most obviously the chiral anomaly), so introducing supersymmetry necessitates the introduction of at least one new particle for every known SM particle, to create the Minimal Supersymmetric Standard Model.

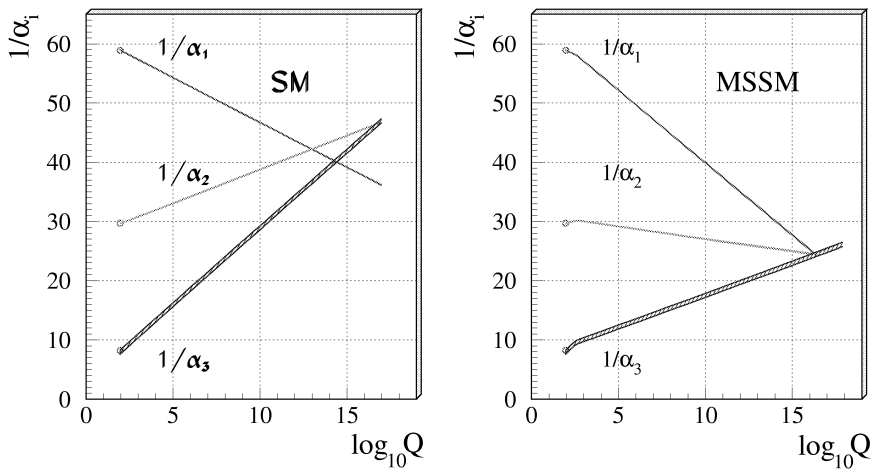

Figure 1.1: The running of the gauge couplings in the Standard Model (left) and Minimal Supersymmetric Standard Model (right) [17].

Many physicists [12, 13] have noted that the scale–dependence of the gauge couplings (induced by loop–corrections to gauge boson propagators) leads to an apparent meeting of the values at about 10^{16} GeV, the GUT scale (after Grand Unification Theory), at which energy the gauge couplings associated with $U(1)_Y$, $SU(2)_L$ and $SU(3)_C$ become equal. (Actually the $U(1)_Y$ coupling at the GUT scale is not *equal* to the other two: there is a group factor of $\sqrt{5/3}$. However, the strength of all three gauge couplings is directly dependent on only one free parameter, the GUT coupling.) This unification is not exact: the energy at which $U(1)_Y$ and $SU(2)_L$ unify is about two orders of magnitude below that at which $SU(2)_L$ and $SU(3)_C$ unify. However, with the extra particle content of the MSSM [14, 15] creates kinks in the runnings in just the right way (if the extra particles have masses of about 1 TeV) that they all unify at the same energy, within errors [14, 15, 16], as can be seen in figure 1.1.

Another motivation is that the MSSM reduces the hierarchy problem. If the SM is regarded as an effective theory which is valid up to some energy scale, in the sense that only processes that happen at a lower energy should be described well and that the integrals in loops should be evaluated only up to this scale, as above this scale new physics starts to play a significant part, then one finds that the gauge couplings, vector boson masses and fermion masses are all dependent on the logarithm of this scale. The Higgs boson mass–squared depends quadratically. Unfortunately the only natural energy scale without introducing new physics is the scale of gravity, the Planck mass, of the order of 10^{19} GeV. This would destroy the predictions of the current model of electroweak symmetry breaking. In the MSSM though, the extra fermionic Higgs loop reduces the divergence to logarithmic.

Another motivation is that superstring theory [18], the only known candidate for a Theory of Everything (ToE), a theory which combines quantum mechanics with gravity, requires some form of supersymmetry in its ten–dimensional form, which, in most models, persists as the MSSM once compactification has reduced the theory to a four–dimensional form.

Chapter 2

The R–Parity Violating Minimal Supersymmetric Standard Model

This thesis is concerned with the R–Parity Violating Minimal Supersymmetric Standard Model (the RPVMSSM) with baryon–number conservation. This model is most easily described by first describing the R–parity conserving Minimal Supersymmetric Standard Model (which is referred to as just the MSSM), before describing R–parity and R–parity violation. The baryon–number conservation aspect is described in section 3.1. Some details on supersymmetry can be found in appendices A and D, but for a detailed introduction to supersymmetry and the MSSM, see for example reference [19].

2.1 The Minimal Supersymmetric Standard Model

The Coleman–Mandula theorem [20] restricts the possible symmetries of the S–matrix (which is the limit of asymptotically free states in the far distant past and future of the evolution operator in the interaction representation [21], essentially the scattering amplitude for a quantum process), to the direct product of the Poincaré group with internal symmetries. If the assumptions of this theorem are relaxed to allow for *graded* Lie algebrae (where the generators obey anti–commutation relations as well as commutation relations), then one finds that instead of fermionic and bosonic fields being separate entities, there is a transformation which takes a fermionic field to a bosonic field, and vice versa. Hence fermions and bosons become components of *superfields*, which are invariant under *supersymmetry*. The Minimal Supersymmetric Standard Model is obtained by replacing all fields of the Standard Model, fermionic and bosonic, with the appropriate superfield.

The notation used in the literature to denote superfields and their components is not entirely consistent. Hence, for reasons outlined in appendix A, in this thesis an accent is used to denote the superfields, *e.g.* $\check{\nu}_e$ denotes the superfield containing the electron–neutrino fermion while ν_e is reserved exclusively to represent the electron–neutrino fermion.

The Lagrangian density is extended to be a function of the anticommuting coordinates associated with the fermionic generators. The kinetic part of the SM Lagrangian density is contained within the D–term part of the MSSM Lagrangian density, while the remainder is contained within the *superpotential* (these terms are explained in appendix D).

No SM boson can be identified with a SM fermion, so the MSSM doubles the particle content of the SM: for every quark, there is a scalar quark, or *squark*, which has the same gauge transformations as a quark, but is a boson; for every lepton, there is a *slepton*; there are fermionic partners of the vector bosons, the *winos*, *zinos*, *photinos* and *gluinos*, and fermionic partners of the Higgs bosons, *Higgsinos*. Collectively these extra particles are known as

superpartners or *sparticles*. The winos, zinos, photinos and gluinos are sometimes known as *gauginos*. The quarks and the leptons are the only fermions in the SM, hence the term *sfermions* refers to squarks and sleptons. In addition, there are actually two sfermions for every SM fermion, since the left– and right–handed chiralities in the SM are different fields transforming differently under $SU(2)_L$, hence there is a sfermion associated with the left–handed SM fermion and a sfermion associated with the right–handed SM fermion. The MSSM actually has more than double the fields of the SM — only *one* Higgs doublet is required in the SM to give masses to all the massive SM particles, through a Yukawa term involving the complex conjugate of the doublet, but the MSSM requires *two* as the superpotential must be an analytic function of the superfields. This can be seen by considering the third term in equation (1.3), or rather its Hermitian conjugate: the antisymmetric tensor allows two **2**s of $SU(2)$ to combine in an $SU(2)$–invariant way. Hence the ϕ^a can be replaced by $(H_u)_a$, the electrically neutral component of which may acquire a vacuum expectation value without breaking $U(1)_Y$. The problem in the MSSM is actually dealing with the other two terms, where ϕ_a must be replaced by $\epsilon_{ab}(H_d)^*_b$. This other Higgs doublet must have opposite hypercharge to the H_u to preserve invariance of these terms under $U(1)_Y$, which also allows a vacuum expectation value for its electrically neutral component to generate a mass term for the down–type quarks and charged leptons. The presence of a second Higgs superfield with opposite $U(1)_Y$ hypercharge is also required so that the pair of oppositely–charged Higgsinos cancel out their contributions to the chiral anomaly [22, 23]. Having two Higgs doublets leads to the MSSM having five Higgs bosons after electroweak symmetry–breaking: one with the same electric charge as the electron, denoted by H^-, one with the opposite charge, denoted by H^+, and three neutral ones, of which two are CP–even, the heavier denoted by H and the lighter by h, and the other is CP–odd, denoted by A. The other three degrees of freedom are "eaten" by the $SU(2)_L$ gauge bosons to allow them to have the correct number of degrees of freedom for massive vector bosons. The sparticles are identified by the same notation as the SM particles, but with a tilde over the letters. For instance, the scalar superpartner associated with the left–handed electron field denoted e_L is denoted by $\tilde{e}_L$. Being a scalar boson, $\tilde{e}_L$ does *not* have a chirality. However, as there is a separate scalar boson associated with each chirality of electron, they are usually labelled with the chiral subscripts to indicate with which fermion they are grouped with in their superfield, which also identifies whether the selectron is an $SU(2)_L$ singlet or part of a doublet, which fixes its coupling to the Z boson, for example.

The MSSM contains all the particles of the SM, with the same interactions, as well as the superpartners and interactions between the SM particles and the superpartners and between the superpartners themselves. With exact supersymmetry, the MSSM introduces no new parameters beyond the mass and couplings of the extra Higgs doublet. The interactions of the superpartners are fixed by the interactions of the SM particles: the superpartners couple to the gauge fields with the same couplings as their partnered SM particles, though the vertices have a different Lorentz structure. The masses of the superpartners are identical to those of their partnered SM particles. However, this is at odds with experimental evidence; scalar electrons with the same mass as the electron have not been observed, for example. Therefore supersymmetry cannot be an exact symmetry of Nature. If it is assumed that supersymmetry is broken at some energy scale, and ignorance of the workings of this breaking can be parametrized by adding terms to the Lagrangian density that break supersymmetry softly. A soft supersymmetry–breaking term is one which becomes irrelevant at high energy scales. The scale of the soft supersymmetry–breaking terms is often referred to as the SUSY scale. Typically the supersymmetry–breaking terms are chosen to be masses for the sfermions, the gauginos and the Higgsinos, along with trilinear terms coupling three bosonic fields in all combinations that respect gauge symmetries. This leads to mixing between the charged winos and charged Higgsinos, collectively *charginos*, and between the zinos, photinos and neutral Higgsinos, collectively *neutralinos*. The neutralinos and charginos are often denoted by $\tilde{\chi}^0$ and $\tilde{\chi}^\pm$ respectively.

The SUSY scale is currently expected to be of the order of 1 TeV — much greater than this, and the corrections to the Higgs boson mass are deemed to require too much fine–tuning and the unification of the gauge couplings ceases to be at one point within errors [24, 25].

2.2 R–Parity

If, instead of starting with the SM Lagrangian density and then promoting all fields to superfields in the appropriate manner, one starts with superfields for all the SM particles and then attempts to write down the most general renormalizable Lagrangian density with these superfields that respects the SM gauge symmetries, then one obtains all the terms that one would in the first scenario, but one also obtains an additional set of terms. These terms violate either lepton–number conservation or baryon–number conservation. Both lepton and baryon–number conservations appear in the SM as *accidental* symmetries: it is not possible to write down renormalizable terms using the SM fields that violate these symmetries without violating gauge symmetries. The existence of these terms is problematic: if they were all of the order of 1 and if the sfermion masses were about 1 TeV, then protons would decay with a lifetime of under a picosecond [26].

To forbid these unwanted terms, the MSSM introduces a new symmetry, *R–parity* (R_p). This could be the discrete remnant of a continuous (global) $U(1)$ *R–symmetry*, which is carried by the supersymmetry generators as well as the superfields.

2.2.1 R–symmetry

The transformations of superfields under this $U(1)$ R–symmetry are defined as follows:

$$\begin{aligned} V(x^\mu, \theta, \bar{\theta}) &\rightarrow V(x^\mu, \theta \exp(-i\alpha), \bar{\theta}\exp(i\alpha)) \\ C(x^\mu, \theta) &\rightarrow \exp(iq_R\alpha) C(x^\mu, \theta\exp(-i\alpha)) \end{aligned} \tag{2.1}$$

where V is a vector superfield and C is a chiral superfield, and q_R is defined as 0 for the Higgs superfields and +1 for the left–handed quark and lepton superfields and the left–handed superfields for the charge conjugates of the right–handed quarks and leptons. This then leads to the "F–term" of the trilinear Yukawa terms of the MSSM superpotential (see equation (D.20)) being invariant under R–symmetry, while all the terms in equation (2.4) in the next section are forbidden. However, the required H_u coupling to the H_d in the MSSM is also forbidden under this symmetry, and this symmetry must also be broken to allow gauginos and gravitinos (the fermionic partners of gravitons, the conjectured carriers of gravity) to have mass terms [27].

2.2.2 Discrete R–Parity

Regardless of its origin, R_p is defined by

$$R_p = (-1)^{(3B+L+2s)} \tag{2.2}$$

where B is baryon–number, L is lepton–number and s is spin. Since lepton–number seems only to be integer–valued, R_p can be equivalently defined by

$$R_p = (-1)^{(3(B-L)+2s)} \tag{2.3}$$

This latter definition, equation (2.3), is favored by those who advocate models where $(B-L)$ is the charge of a particle under a $U(1)$ gauge symmetry, such as left–right–symmetric models [28]. R_p is a multiplicatively conserved quantum number, and only terms which have an overall positive R_p are permitted in the MSSM superpotential. The forbidden terms are known as *R–parity violating terms.*

R_p is of paramount importance when considering experimental signatures of the superpartners. Not only does it forbid terms which could lead to proton decay, it also forbids the creation and annihilation of single sparticles. Sparticles must be produced and annihilated in pairs. Consequently, any sparticle decay must have an odd number of sparticles in the final state, as well as any number of SM particles. Hence, the lightest supersymmetric particle, the *LSP*, is stable, and thus provides a candidate particle for Dark Matter [29]. From cosmological considerations [30], the LSP should be electrically neutral. The lack of superheavy stable hadrons implies that the LSP is a color singlet [31]. The most popular candidates for the LSP are the lightest neutralino and the lightest sneutrino. The relative mixture of photino, zino and Higgsino of which the lightest neutralino consists, or the relative mixture of left– and right–handed–associated electron–, muon– and τ–sneutrino of which the lightest sneutrino consists depend on the specific model of SUSY breaking considered. Both candidates provide the experimental signature of a large amount of missing energy, taken away as the LSP escapes the detector, since it only interacts through the weak force.

2.3 R–Parity Violation

The unwanted terms that R_p forbids follow from the observation that without R_p, the Higgs doublet with the vacuum expectation value which generates mass for the down–type quarks (denoted $\breve{H}_d$) has the same quantum numbers as the lepton doublets, hence replacing this Higgs doublet with each of the three lepton doublets does not break any symmetries. One can also write down a trilinear quark term which also preserves supersymmetry and the SM gauge symmetries, since now there is a color–carrying scalar in the model.

The R–parity–violating (RPV) terms in the superpotential are (using the same conventions as reference [26])

$$\begin{aligned} W_{\not R_p} &= \mu'_i(\breve{L}_{iL})_\alpha \epsilon_{\alpha\beta}(\breve{H}_u)_\beta \\ &\quad + \frac{1}{2}\lambda_{ijk}(\breve{L}_{iL})_\alpha \epsilon_{\alpha\beta}(\breve{L}_{jL})_\beta \breve{e}^c_{kR} + \lambda'_{ijk}(\breve{L}_{iL})_\alpha \epsilon_{\alpha\beta}(\breve{Q}_{jL})^p_\beta (\breve{d}^c_{kR})^p \\ &\quad + \frac{1}{2}\lambda''_{ijk}\epsilon_{pqr}(\breve{u}^c_{iR})^p (\breve{d}^c_{jR})^q (\breve{d}^c_{kR})^r \end{aligned} \tag{2.4}$$

where i, j and k are flavor indices, α and β are $SU(2)_L$ indices and p, q and r are $SU(3)_C$ indices. The superscript c denotes charge conjugation, and this notation is explained in section A.3.2. The final term in equation (2.4) is $SU(3)_C$–invariant because of the antisymmetric tensor, analogously to how the other terms are $SU(2)_L$–invariant because of their antisymmetric tensors. The indices have been explicitly shown in this expression to show how the terms are invariant under the gauge groups. For the rest of this thesis, $SU(3)_C$ indices are suppressed unless explicitly stated — it is implicit that every color–carrying field which does not have its color index shown represents three copies, one for each color. $\breve{L}_{iL} = \begin{pmatrix} \breve{\nu}_{iL} \\ \breve{e}_{iL} \end{pmatrix}$ is the left–handed lepton $SU(2)_L$ doublet of flavor i, $\breve{e}^c_{kR}$ is the left–handed charged anti–lepton $SU(2)_L$ singlet of flavor k, $\breve{Q}_{jL} = \begin{pmatrix} \breve{u}_{jL} \\ \breve{d}_{jL} \end{pmatrix}$ is the left–handed quark $SU(2)_L$ doublet of flavor j, $\breve{d}^c_{jR}$ is the left–handed down–type anti–quark $SU(2)_L$ singlet of flavor j, $\breve{u}^c_{iR}$ is the left–handed up–type anti–quark $SU(2)_L$ singlet doublet of flavor i and $\breve{H}_u = \begin{pmatrix} \breve{H}^+_u \\ \breve{H}^0_u \end{pmatrix}$ is the Higgs doublet which gives mass to the up–type quarks. The subscript R here denotes that the charge conjugate of the superfield contains the right–handed SM fermion, *e.g.* $(\breve{e}^c_{1R})^\dagger$ is a right–handed chiral superfield which has the right–handed electron $SU(2)_L$ singlet as its fermionic component. The first term in equation (2.4) is analogous to the MSSM Higgs mixing term $\mu(\breve{H}_d)_\alpha \epsilon_{\alpha\beta}(\breve{H}_u)_\beta$. The second two terms in equation (2.4) are analogous to the lepton– and down–type quark–mass generating terms, and both violate lepton number. The third term in equation (2.4) has no MSSM–analogous term, and violates baryon number.

The factor of $^1/_2$ before the λ term is conventional: one sees that $\lambda_{ijk} = -\lambda_{jik}$ by relabelling a to b and vice-versa in the first term of equation (2.4), hence the extra factor of $^1/_2$ sets the coupling of the $\breve{\nu}_i \breve{e}_{jL} \breve{e}^c_{kR}$ term to be λ_{ijk} rather than $2\lambda_{ijk}$. Likewise λ''_{ijk} is antisymmetric in j and k, hence its factor of $^1/_2$.

For example, consider the second term with $i = 1$, $j = 2$ and $k = 3$, plus its Hermitian conjugate. Then the Lagrangian density obtained from these terms once the fermionic coordinates have been integrated over is given by two parts (restoring $SU(3)_C$ indices, labelled p and q):
a Yukawa part:

$$\begin{aligned}
\mathcal{L}^{e.g.}_{\rm Yuk} &= \lambda'_{123}(-\tilde{\nu}_{eL}(b^c_R)^p(s_L)^p - (\tilde{s}_L)^p(b^c_R)^p\nu_{eL} - (\tilde{b}^c_R)^p\nu^T_{eL}(s_L)^p \\
&\quad +\tilde{e}_L(b^c_R)^p(c_L)^p + (\tilde{c}_L)^p(b^c_R)^p e_L + (\tilde{b}^c_R)^p e^T_L(c_L)^p) + \text{ Hermitian conjugate} \\
&= -\lambda'_{123}(\tilde{\nu}_{eL}(\bar{b})^p P_L(s)^p + (\tilde{s}_L)^p(\bar{b})^p P_L\nu_e - i(\tilde{b}^c_R)^p\nu^T_e\gamma^0\gamma^2 P_L(s)^p \\
&\quad -\tilde{e}_L(\bar{b})^p P_L(c)^p - (\tilde{c}_L)^p(\bar{b})^p P_L e + i(\tilde{b}^c_R)^p e^T\gamma^0\gamma^2 P_L(c)^p) + \text{ Hermitian conjugate}
\end{aligned} \tag{2.5}$$

and a four–scalar potential part:

$$\begin{aligned}
\mathcal{L}^{e.g.}_{\rm pot} &= -|\lambda'_{123}|^2[(\tilde{\nu}^*_{eL}(\tilde{s}^*_L)^p - \tilde{e}^*_L(\tilde{c}^*_L)^p)(\tilde{\nu}_{eL}(\tilde{s}_L)^p - \tilde{e}_L(\tilde{c}_L)^p) && \text{[A]} \\
&\quad +((\tilde{s}^*_L)^p(\tilde{b}^{c*}_R)^p(\tilde{s}_L)^q(\tilde{b}^c_R)^q) && \text{[B]} \\
&\quad +(\tilde{\nu}^*_{eL}(\tilde{b}^{c*}_R)^p\tilde{\nu}_{eL}(\tilde{b}^c_R)^p) && \text{[C]} \\
&\quad +((\tilde{c}^*_L)^p(\tilde{b}^{c*}_R)^p(\tilde{c}_L)^q(\tilde{b}^c_R)^q) && \text{[D]} \\
&\quad +(\tilde{e}^*_L(\tilde{b}^{c*}_R)^p\tilde{e}_L(\tilde{b}^c_R)^p)] && \text{[E]}
\end{aligned} \tag{2.6}$$

Here b is the bottom quark field, s the strange quark field and ν_e the electron–neutrino field. The terms in equation (2.6) denoted by [A] are from the F–term for $\breve{b}^c_R$, [B] from the F–term for $\breve{\nu}_{eL}$, [C] from that for $\breve{s}_L$, [D] from that for $\breve{e}_L$ and [E] from that for $\breve{c}_L$.

Note that the terms in equation (2.6) are *not* independently allowable as soft SUSY–breaking terms, as in general soft SUSY–breaking terms must have couplings with dimensions of at least one power of mass.

The Feynman rules resulting from equation (2.5) are shown in figure 2.1 and those from equation (2.6) are shown in figure 2.2.

In this example one can see a particular aspect of supersymmetry that distinguishes it from merely the addition of extra bosonic and fermionic fields: a single term in the superpotential fixes the couplings for all the interactions derived from it. All the Yukawa terms from the superpotential term have the same coupling, and the four–scalar terms have this coupling squared as their coefficients (along with factors associated with the three $SU(3)_C$ colors of squark).

In the Yukawa part, the first term on the right–hand side allows an electron–sneutrino to decay to a strange anti–quark and a bottom quark, and in combination with the unconjugated term allows bottom quarks to scatter off strange anti–quarks by the exchange of an electron sneutrino, and since the sneutrino is a zero–spin particle, this would have a different angular dependence than the same scattering by the exchange of a vector boson, such as a gluon. The Yukawa part also allows strange squarks to decay to electron–neutrinos and bottom quarks, and bottom squarks to decay to electron anti–neutrinos and strange quarks. The Feynman diagram corresponding to this last process (which corresponds to the Hermitian conjugate of the rightmost Feynman diagram in the top line of diagrams in figure 2.1, remembering that $\tilde{b}^{c*}_R$ is usually called a squark rather than an anti–squark since it is the scalar partner of a right–handed quark) has the arrows on both fermion lines pointing away from the vertex, which is impossible in the SM, but not forbidden because of any fundamental theoretical reason. Care must be taken with momentum flows in this case.

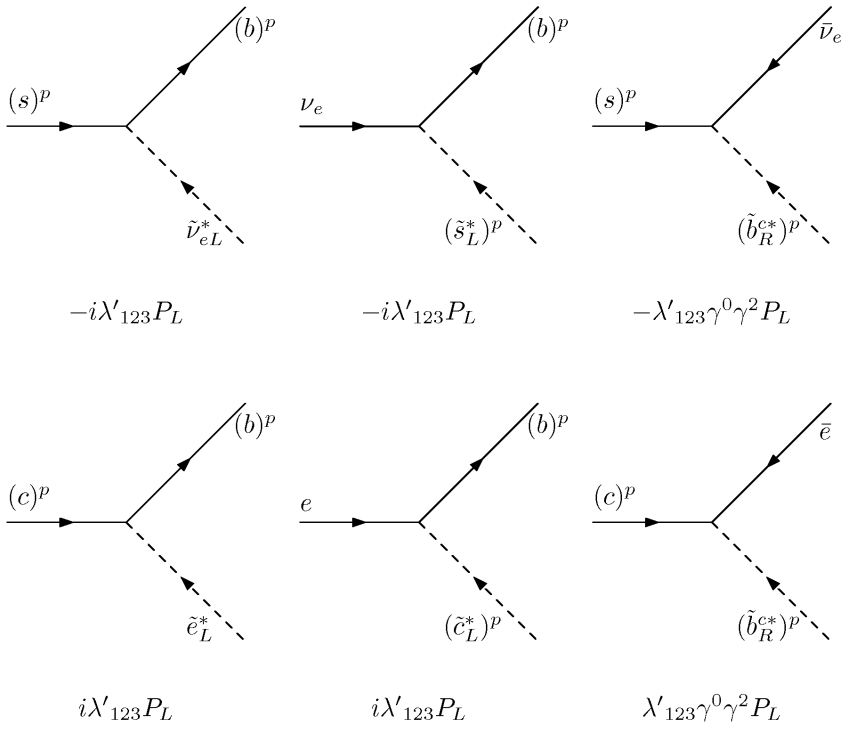

Figure 2.1: Yukawa vertex rules from non–zero λ'_{123}.

The four–scalar potential part allows the appropriate scalar bosons to scatter, or to annihilate and pair–produce, and so on.

The presence of the bilinear term $\mu'_1(\breve{L}_{1L})_a\epsilon_{ab}(\breve{H}_u)_b$ as well would generate additional three–scalar vertices, proportional to μ'_1.

2.3.1 Spontaneously Broken R–Parity

Even if one believes that the Lagrangian density must be R_p–conserving, there are ways in which R_p may be broken spontaneously. The sneutrino fields may acquire vacuum expectation values through soft SUSY–breaking terms in the same way that the Higgs fields do [32], though this is very constrained by experiment [33]. If one adds a right–handed $SU(2)_L$ singlet neutrino to the MSSM in a way that gives the left–handed neutrinos small masses through the see–saw mechanism [34, 35] (as described in section 2.4.4, though of course the right–handed neutrino replaces the Higgsino), the right–handed sneutrino could acquire a vacuum expectation value and this is not particularly constrained [36].

If a left–handed sneutrino gains a vacuum expectation value, then the charged leptons mix with the charged Higgsinos in the same way that the Higgs boson vacuum expectation value leads to mixing between the left– and right–handed chiralities of the charged leptons. The charged lepton mass–generating term in the superpotential is shown in equation (2.7). The Yukawa terms that result from integrating over the fermionic coordinates are shown in equations (2.8) and (2.9). A vacuum expectation value for H^0_d results in the first term on the right hand side of equation (2.8) (along with its Hermitian conjugate) generating a mass term for the charged leptons, once the coupling matrix Y^l_{ik} is diagonalized. Likewise, if $\tilde{\nu}_{iL}$ were to have a vacuum expectation value, the second term on the right hand side of equation (2.9)

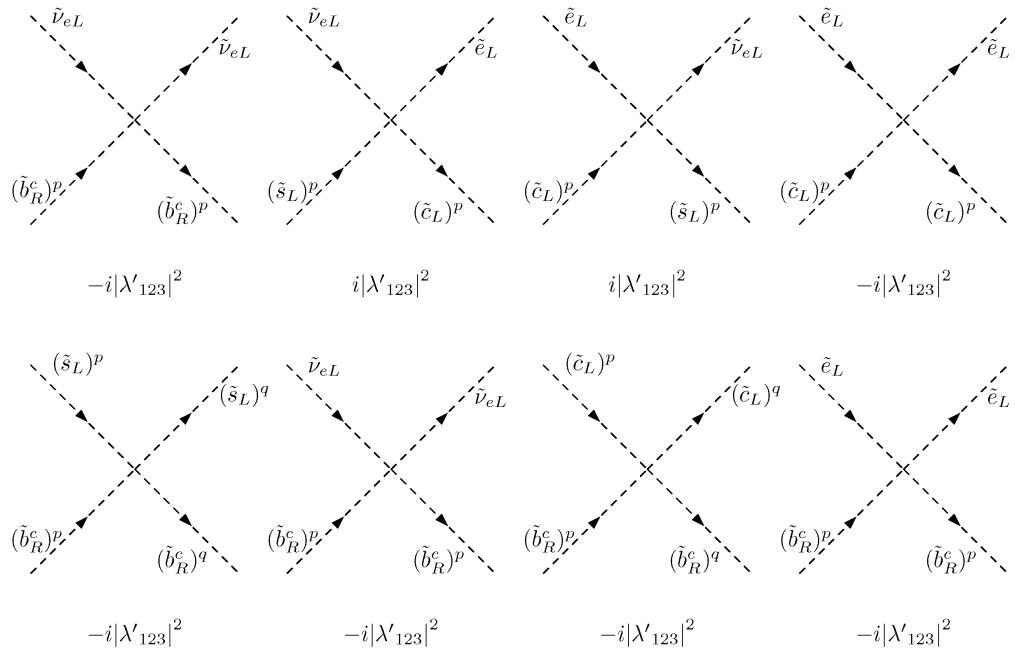

Figure 2.2: Four–scalar vertex rules from non–zero λ'_{123}.

would generate a term that would mix the charged leptons and the charged Higgsinos. This mixing explicitly breaks R_p.

$$Y^l_{ik}(\breve{L}_i)_a\epsilon_{ab}(\breve{H}_d)_b\breve{e}^c_{kR} = Y^l_{ik}(\breve{\nu}_i\breve{H}^-_d\breve{e}^c_{kR} - \breve{e}_{iL}\breve{H}^0_d\breve{e}^c_{kR}) \quad (2.7)$$

$$\left[Y^l_{ik}\breve{e}_{iL}\breve{H}^0_d\breve{e}^c_{kR}\right]_{\theta\theta} = Y^l_{ik}H^0_d\bar{e}_kP_Le_i + Y^l_{ik}\tilde{e}_{iL}\bar{e}_kP_L\tilde{H}^0_d + Y^l_{ik}\tilde{e}^c_{kR}\tilde{H}^{0T}_dP_Le_i + (\text{purely bosonic terms}) \quad (2.8)$$

$$\left[Y^l_{ik}\breve{\nu}_i\breve{H}^-_d\breve{e}^c_{kR}\right]_{\theta\theta} = Y^l_{ik}H^-_d\bar{e}_kP_L\nu_i + Y^l_{ik}\tilde{\nu}_{iL}\bar{e}_kP_L\tilde{H}^-_d + Y^l_{ik}\tilde{e}^c_{kR}\tilde{H}^{-T}_dP_L\nu_i + (\text{purely bosonic terms}) \quad (2.9)$$

When adding right–handed neutrinos N^c_k to the MSSM, one usually adds the analogue of the up–type quark–Higgs coupling, replacing Q_{iL} with L_{iL} and u^c_k with N^c_k, and an independent matrix of Yukawa couplings, to obtain $Y'^l_{ik}(\breve{L}_i)_a\epsilon_{ab}(\breve{H}_u)_b\breve{\nu}^c_{kR}$. If a right–handed sneutrino gains a vacuum expectation value, then this would lead to both neutral Higgsinos mixing with left–handed neutrinos *and* charged leptons mixing with charged Higgsinos, in this very same way. It leads to a term of the form of the bilinear term $\mu'_i(\breve{L}_i)_a\epsilon_{ab}(\breve{H}_u)_b$, the first term on the right–hand side of equation (2.4), though in this case μ'_i is the vacuum expectation value of the sneutrino multiplied by the coupling to the Higgs doublet with the lepton doublet.

In both these cases, the mixing has a see–saw–mechanism–type suppression of the mixing parameter squared divided by the Higgsino mass squared, and this is where one can constrain the vacuum expectation values.

The superpotential described above is very general. In the scenarios of R_p–breaking just described there are relationships between the couplings μ', λ and λ' and the Yukawa couplings of the H_d Higgs field to the lepton and quark fields, and the only new variable added is the

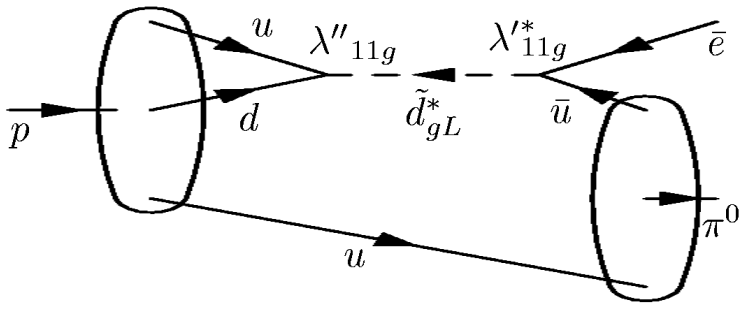

Figure 2.3: The Feynman diagram for a proton decaying into a positron plus a neutral pion through non–zero λ''_{11g} and λ'_{11g}.

vacuum expectation value of the sneutrino. However, in this thesis no assumptions as to how the RPV couplings could arise are made and the most general form of the RPV part of the superpotential is used.

2.4 The Consequences Of R–Parity Violation

There are two immediate consequences of the RPV interactions: lepton and baryon number violation, and flavor violation in both the quark and lepton sectors.

2.4.1 Lepton Number Violation

Both the λ and λ' terms give rise to vertices that violate lepton number by one unit. As a consequence of this, single sneutrinos or charged sleptons could be produced through a non–zero λ or λ'. For instance, a non–zero λ_{211} would allow electron–positron annihilation into a muon sneutrino. Conversely, single sleptons would be allowed to decay. A non–zero λ_{211} would allow a muon sneutrino to decay into an electron–positron pair.

The λ' terms allow single slepton creation through quark fusion, and also allow squark decay to a quark plus lepton. The second term in equation (2.1) due to λ'_{123}, for example, allows a strange squark to decay to a bottom quark plus an electron anti–neutrino. Note, though, that both λ and λ' terms conserve baryon number.

2.4.2 Baryon Number Violation

Analogously the λ'' terms give rise to vertices that violate baryon number by one unit. Consequently, single squarks could decay through a non–zero λ'', though in this case it would be to a pair of anti–quarks.

Proton Decay

If only one of either lepton number or baryon number were violated, then protons would be (at least perturbatively) stable. However, should both be violated, then protons could decay. An example Feynman diagram is shown in figure 2.3, where a pair of valence quarks from the proton annihilate to form an anti–squark, which then decays into an anti–electron and an anti–quark, which goes on to bind with the remaining valence quark from the proton to form a meson.

There are very stringent constraints on proton decay. The current lower bound on the nucleon mean lifetime is 2.1×10^{29} years from neutron disappearance searches [37]; the bound

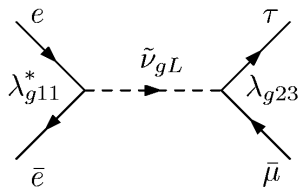

Figure 2.4: Example lepton flavor violation through $e\bar{e}$ annihilating via a sneutrino to become a $\tau\bar{\mu}$ pair.

extends to $1.6{\times}10^{33}$ years for proton decay into a positron plus pion [38]. This leads to a bound on the combination of the couplings involved of the order of 10^{-27}, for sfermion masses of 100 GeV [26].

2.4.3 Flavor Violation

As mentioned in section 1.2, the perturbative approach views the solutions of the part of the Hamiltonian which is quadratic in the fields as the basic eigenstates. At the level of the Lagrangian density, the only quadratic terms for fermions in the SM Hamiltonian are the kinetic parts, without the gauge–coupled interactions. At this point one is free to choose a basis which consists of independent flavors of fermions, with appropriate gauge–covariant derivatives. However, the couplings to the Higgs fields are not diagonal in this basis. Hence once the Higgs field acquires a vacuum expectation value, the mass terms generated are not diagonal. Diagonalizing the mass matrix mixes the flavors through the $SU(2)_L$ gauge couplings — it is impossible to simultaneously diagonalize the isospin $+1$ and -1 components of the doublets with their singlet partners in both the $SU(2)_L$ flavor basis and the mass eigenstate basis. In the same way that the Higgs couplings to the leptons and quarks are not diagonal in the $SU(2)_L$ flavor basis, the RPV couplings are not obliged to be diagonal in this basis either. This could lead to enhanced rates of flavor violation both for leptons and for quarks.

Lepton Flavor Violation

Before the discovery of neutrino flavor oscillations, there was no evidence that neutrinos were not massless, and the SM was constructed with only the left–handed chirality. In this case, it is possible to simultaneously diagonalize the charged lepton states in both the $SU(2)_L$ flavor basis and the mass eigenstate basis along with the neutrino flavors. However, experiments [39, 40, 41] have measured a reduction in the flux of neutrinos from sources that is dependent on the distance between the source and the detector, and this can be explained by postulating that neutrinos have mass and that the mass eigenstates are not aligned with the $SU(2)_L$ flavor eigenstates [42]. This gives rise to lepton flavor violation in the SM.

Unfortunately even the detection of neutrinos is extremely hard, and outside of specialized neutrino oscillation experiments it is practically impossible to detect flavor violation in the neutrino sector, so there is no opportunity to look for R_p–violation.

However, the mixing of the charged lepton states occurs in the SM at the one–loop level, and is proportional to $\alpha\delta m_\nu^2/m_W^2$, which is roughly 10^{-24} (δm_ν^2 is the difference of the square of the masses of the neutrinos and is of the order of 1 eV^2). This is small enough to be entirely discounted as a source of any observed flavor violation in the charged lepton sector, hence lepton flavor violation is generally considered to be a clean signal of new physics beyond the SM. In the case of the RPVMSSM, such lepton flavor violation can occur at tree–level, through interactions mediated by squarks or sneutrinos. An example of this is shown in figure 2.4.

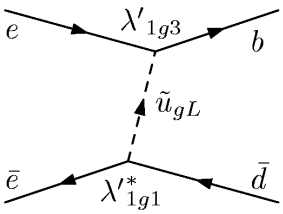

Figure 2.5: Example quark flavor violation through $e\bar{e}$ exchanging an up–type squark to become a $b\bar{d}$ pair.

The RPVMSSM is not the only model with lepton flavor violation: for example, MSSM models with soft SUSY–breaking terms that mix sneutrinos and sleptons (*e.g.* through renormalization effects from the right–handed neutrino sector [43] or from Grand Unification concerns [44]), Little Higgs models with T–parity [45], general two–Higgs–doublet models [46], Left–Right Symmetric models [47] and topcolor models [48] all have the potential for detectable lepton flavor violation. Distinguishing these models would be very important should lepton flavor violation be experimentally measured.

Quark Flavor Violation

The quark flavor violation inherent in the SM manifests in the CKM matrix, which relates the quark $SU(2)_L$ flavor eigenstates to the quark mass eigenstates. While the quarks do not escape detectors like neutrinos do (and therefore do not evade identification), searching for R_p–violation through quark flavor violation is complicated by the fact that flavor violation in the SM is not negligible as it is in the charged lepton sector. The suppression on lepton–flavor–violating loops due to the smallness of the neutrino masses is not present for quarks ($m_t \approx 2m_W$), however there is a suppression due to the smallness of the off–diagonal CKM matrix elements. Still, this is not a particularly strong suppression, and even the rate of the doubly–Cabibbo–suppressed quark–flavor–violating decay $b \to s\gamma$ within the SM is large enough to be measured, and indeed has been measured, in agreement with the SM prediction [49].

Fortunately, the rate of flavor violation is small enough that the enhancements through R_p–violation could be significant, and therefore measurable. Again, in the RPVMSSM, quark flavor violation can occur at tree–level through interactions mediated by squarks or sneutrinos, with an example shown in figure 2.5.

2.4.4 Neutrino Mass

R_p–violation leads to two mechanisms for neutrino mass [50]. One is a see–saw effect from the neutrino–Higgsino mixing bilinear term with the soft SUSY–breaking Higgsino mass, and the other is through quantum loop effects from the trilinear terms with heavy sfermions in the loop.

Bilinear See–Saw Mechanism

The bilinear $\mu'_i(\breve{L}_i)_a\epsilon_{ab}(\breve{H}_u)_b$ in the first line of equation (2.4) leads to mixing between the neutrinos and the up–mass–generating Higgsinos. This then leads to a see–saw mechanism where the neutrinos gain mass proportional to $\mu'^2_i/m_{\tilde{h}^0_u}$. This can be seen by considering the

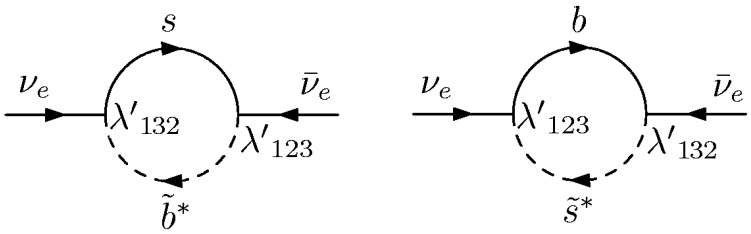

Figure 2.6: The Feynman diagrams for the loop contributions to the neutrino (Majorana) mass term.

(Majorana) mass matrix for these particles with the vector $(\nu_e, \nu_\mu, \nu_\tau, \tilde{h}_u^0)^T$:

$$M_{\nu,\tilde{h}} = \begin{pmatrix} 0 & 0 & 0 & \mu'_1 \\ 0 & 0 & 0 & \mu'_2 \\ 0 & 0 & 0 & \mu'_3 \\ \mu'_1 & \mu'_2 & \mu'_3 & m_{\tilde{h}_u^0} \end{pmatrix} \tag{2.10}$$

This matrix has two zero eigenvalues, one eigenvalue of $-\sum_i \mu'^2_i / m_{\tilde{h}_u^0} + \mathcal{O}\left(\mu'^4_i / m^3_{\tilde{h}_u^0}\right)$ and one eigenvalue of $m_{\tilde{h}_u^0} + \sum_i \mu'^2_i / m_{\tilde{h}_u^0} + \mathcal{O}\left(\mu'^4_i / m^3_{\tilde{h}_u^0}\right)$. So this leads to one massive neutrino and two massless neutrinos. However, the bilinear also mixes the charged leptons with the charged Higgsinos, and in general the mass eigenstates after this mixing are not the $SU(2)_L$ eigenstates, and this leads to further corrections which lift the degeneracy of the masses for the remaining neutrinos.

Trilinear Loop Effects

The trilinear terms $\lambda_{ijk}(\breve{L}_i)_a \epsilon_{ab} (\breve{L}_j)_b \breve{e}^c_{kR}$ and $\lambda'_{ijk}(\breve{L}_i)_a \epsilon_{ab} (\breve{Q}_j)_b \breve{D}^c_k$ of the second line of equation (2.4) allow neutrinos to gain quantum corrections to their masses through self–energy diagrams. The mass terms generated are Majorana; the diagrams that would give Dirac masses actually give corrections to the kinetic term and can be absorbed into the normalization of the kinetic term. To see this, consider the contribution from the λ'_{123} term in equation (2.5), along with the contribution of λ'_{132} (which is the same as that of λ'_{123} with the b and s swapped) as the λ'_{123} term alone cannot generate a neutrino mass term. The relevant Feynman diagrams are shown in figure 2.6.

To first order in each of λ'_{123} and λ'_{132} the two–point function corresponding to a Majorana

neutrino mass term due to the example trilinear terms is given by

$$\begin{aligned}
\langle\bar{\nu}_{eL}|m_{\nu_e}|\nu_{eL}\rangle &= \int_{-\infty}^{\infty}\frac{\mathrm{d}^4k}{(2\pi)^4}\langle 0|T\left((\lambda'_{123}\tilde{b}_R^c\nu_e^T i\gamma^0\gamma^2 P_L s)(-\lambda'_{132}\tilde{b}_L\bar{s}P_L\nu_e)\right.\\
&\quad\left.+\,(\lambda'_{132}\tilde{s}_R^c\nu_e^T i\gamma^0\gamma^2 P_L b)(-\lambda'_{123}\tilde{s}_L\bar{b}P_L\nu_e)\right)|0\rangle\\
&= \int_{-\infty}^{\infty}\frac{\mathrm{d}^4k}{(2\pi)^4}\langle 0|T\left(i(\lambda'_{123}(\sin(\theta_b)\tilde{b}_1-\cos(\theta_b)\tilde{b}_2)^*\nu_e^T\gamma^0\gamma^2P_Ls)\right.\\
&\quad\times(-\lambda'_{132}(\cos(\theta_b)\tilde{b}_1+\sin(\theta_b)\tilde{b}_2)\bar{s}P_L\nu_e)\\
&\quad+i(\lambda'_{132}(\sin(\theta_s)\tilde{s}_1-\cos(\theta_s)\tilde{s}_2)^*\nu_e^T\gamma^0\gamma^2P_Lb)\\
&\quad\left.\times\,(-\lambda'_{123}(\cos(\theta_s)\tilde{s}_1+\sin(\theta_s)\tilde{s}_2)\bar{b}P_L\nu_e)\right)|0\rangle\\
&= \int_{-\infty}^{\infty}\frac{\mathrm{d}^4k}{(2\pi)^4}\langle 0|T\left(-\nu_e^T i\gamma^0\gamma^2P_L\lambda'_{123}\lambda'_{132}\left[\left(\frac{\sin(2\theta_b)}{2}\right)(\tilde{b}_1^*\tilde{b}_1-\tilde{b}_2^*\tilde{b}_2)s\bar{s}\right.\right.\\
&\quad\left.\left.+\left(\frac{\sin(2\theta_s)}{2}\right)(\tilde{s}_1^*\tilde{s}_1-\tilde{s}_2^*\tilde{s}_2)b\bar{b}\right]P_L\nu_e+\text{ non–contractible terms}\right)|0\rangle
\end{aligned}\tag{2.11}$$

where $\tilde{b}_R^c$ and $\tilde{b}_L$ have been written out as orthogonal combinations of the two mass eigenstates $\tilde{b}_1$ and $\tilde{b}_2$ with mixing angle θ_b, and likewise for the strange squarks. Also, equation (A.40) was used to rewrite the Yukawa terms with Dirac spinors rather than Weyl spinors.

Performing the contractions on the quarks and squarks and integrating over all possible loop momenta leads to

$$\begin{aligned}
m_{\nu_e}\nu_e^T(-i)\gamma^0\gamma^2P_L\nu_e &= 3\int_{-\infty}^{\infty}\frac{\mathrm{d}^4k}{(2\pi)^4}\nu_e^T(-i)\gamma^0\gamma^2\lambda'_{123}\lambda'_{132}P_L\times\\
&\quad\left[\left(\frac{\sin(2\theta_b)}{2}\right)\left(\frac{i}{(k^2-m^2_{\tilde{b}_1})}-\frac{i}{(k^2-m^2_{\tilde{b}_2})}\right)\left(\frac{i(\not{k}+m_s)}{(k^2-m_s^2)}\right)\right.\\
&\quad\left.+\left(\frac{\sin(2\theta_s)}{2}\right)\left(\frac{i}{(k^2-m^2_{\tilde{s}_1})}-\frac{i}{(k^2-m^2_{\tilde{s}_2})}\right)\left(\frac{i(\not{k}+m_b)}{(k^2-m_b^2)}\right)\right]P_L\nu_e
\end{aligned}\tag{2.12}$$

which leads to

$$\begin{aligned}
m_{\nu_e} &= \left[\frac{3\lambda'_{123}\lambda'_{132}}{(4\pi)^2}\left(\frac{\sin(2\theta_b)}{2}m_s\left(\frac{m^2_{\tilde{b}_2}}{m^2_{\tilde{b}_1}}-1-\left(\frac{m^2_{\tilde{b}_2}}{m^2_{\tilde{b}_1}}\right)\ln\left(\frac{m^2_{\tilde{b}_2}}{m^2_{\tilde{b}_1}}\right)\right)\right.\right.\\
&\quad\left.\left.+\,\frac{\sin(2\theta_s)}{2}m_b\left(\frac{m^2_{\tilde{s}_2}}{m^2_{\tilde{s}_1}}-1-\left(\frac{m^2_{\tilde{s}_2}}{m^2_{\tilde{s}_1}}\right)\ln\left(\frac{m^2_{\tilde{s}_2}}{m^2_{\tilde{s}_1}}\right)\right)\right)\right]
\end{aligned}\tag{2.13}$$

where the factor of 3 comes from the three copies of the color–carrying fields.

Assuming a common mass of $\tilde{m}$ for $\tilde{b}_R^c$, $\tilde{b}_L$, $\tilde{s}_R^c$ and $\tilde{s}_L$, maximal mixing (*i.e.* that both θ_b and θ_s are $\pi/4$), and setting trilinear soft SUSY–breaking terms coupling $\tilde{b}$, $\tilde{s}$ and H_d to zero, this becomes

$$\nu_e^T(-i)\gamma^0\gamma^2m_{\nu_e}\nu_e=\left[\frac{-3\lambda'_{123}\lambda'_{132}}{(4\pi)^2}\mu\tan(\beta)\frac{m_sm_b}{\tilde{m}^2}\right]\nu_e^T(-i)\gamma^0\gamma^2P_L\nu_e \tag{2.14}$$

where μ is the H_u–H_d coupling and tanβ is the ratio of the two Higgs vacuum expectation values.

Chapter 3

Bounds On R–Parity Violating Terms From Particle Decays

The non–observation of certain flavor–violating decays of τ leptons, muons and mesons constrains many combinations of RPV couplings with sfermion masses more tightly than other means.

The results presented in this chapter have been published in reference [1]. This chapter is a comprehensive review of the tree–level bounds on trilinear baryon–number–conserving RPV couplings (in combination with sfermion masses) from the bounds on the purely leptonic decays of muons, τ leptons and neutral mesons, and the decays of a τ lepton into a neutral meson plus either a muon or an electron, using all the available published data available from the Particle Data Group (P.D.G.) [51] in December 2006.

The chapter is organized as follows: first the assumptions used in the calculations are presented; then the Feynman diagrams, matrix elements and decay widths are presented for each class of decay; then the numerical results from comparison with experimental data are tabulated.

3.1 Assumptions

Extracting bounds on the trilinear RPV couplings is not straightforward. There are so many unknowns associated with each process that no meaningful bounds can be set without making sweeping assumptions. Initially general formulae will be presented, but expressions will be simplified and numerical results will be based on the following assumptions:

No Baryon Number Violation The main incentive to applying R_p to the MSSM is the prevention of proton decay. No serious model can allow simultaneous lepton and baryon number violation without extremely strong suppression mechanisms. In this thesis baryon number conservation is assumed, hence λ''_{ijk} is set to be 0 for all i, j and k. No further assumptions about the nature of the conservation are made. This assumption is, admittedly, as *ad hoc* as R_p itself, but allowing the other RPV terms does provide neutrino mass mechanisms, as mentioned in section 2.4.4. A further point is that R_p does not forbid proton decay through (non–renormalizable) dimension–5 terms and must be strengthened to a discrete $\mathbf{Z}_6$ symmetry, baryon hexagonality [52], when considering the MSSM as an effective theory; imposing baryon triality [53, 54] forbids proton decay while still allowing the λ_{ijk} and λ'_{ijk} terms.

Heavy Mediating Sfermions The sfermion masses are assumed to be so heavy that their propagators $i/(p^2_{\tilde{f}} - m^2_{\tilde{f}})$ can be approximated as $-i/m^2_{\tilde{f}}$. This assumption is very reasonable,

since experimental constraints on sparticle masses put them $\gtrsim$100 GeV [55], though such bounds on sfermion masses are quite model–dependent, while the momentum–squared carried by the sfermion is at most equal to the mass–squared of the decaying particle (the heaviest particle considered is the B_s meson, of mass 5.37 GeV $\ll m_{\tilde{f}}$).

Double Coupling Dominance The main assumption made is that one sfermion dominates the signal process, either because it is much lighter than the others or because it has a much larger coupling product. This is called the quadratic coupling dominance convention in the literature, as in reference [26], presumably because the matrix element is dependent on the product of two couplings. This assumption has little justification, other than it allows bounds to be extracted at all, and the precedent that, in the SM, the Higgs Yukawa couplings to fermions other than the top quark are all smaller by orders of magnitude than the top–Higgs coupling. Therefore there is no sum over g, the index used to denote the flavor of the mediating sfermion. Subsequent expressions with an index g are implicitly for only one value of g, though one may always reverse the process and replace expressions like $\left|\lambda'_{gjk}\lambda'_{glm}/m^2_{\tilde{u}_{gL}}\right|^2$ with $\left|\sum_g \lambda'_{gjk}\lambda'_{glm}/m^2_{\tilde{u}_{gL}}\right|^2$ and so on. The Einstein summation convention is held to unless otherwise stated, and in particular is not held for the cases where there are three of the same index, as happens when there is two index–dependent couplings combined with an index–dependent propagator. In this thesis, this only occurs in the case of two RPV couplings combined with the sfermion mass–squared, and will always be labelled with the index g.

Negligible Sfermion Mixing The final assumption is that the sneutrinos of each flavor and the H_d Higgs boson mix negligibly with each other, *i.e.* setting μ'_i to 0 for all i along with the relevant soft SUSY–breaking terms, and also the mixing of the squarks is ignored. Such mixings just add to the notational burden. If one insists on accounting for mixing, one can make the replacement $\left|\lambda'_{gjk}\lambda'_{glm}/m^2_{\tilde{u}_{gL}}\right|^2 \rightarrow \left|\sum_{g,x,y}\lambda'_{xjk}U_{xg}U^\dagger_{gy}\lambda'_{ylm}/m^2_{\tilde{u}_{gL}}\right|^2$ for squark mixing matrices U, with a similar expression for mixing between the sneutrinos and Higgs bosons.

No Mass–Splitting Between CP–Even And CP–Odd Sneutrinos There is the possibility of allowing soft SUSY–breaking terms that assign differing masses to the real (CP–even) and imaginary (CP–odd) parts of the sneutrino field [56]. Accounting for this in the processes considered can be done in the same way as accounting for sneutrino–Higgs mixing, *i.e.* reading the couplings to include mixing matrices as well, though in this case the associated vectors have ten components: the real and imaginary parts of three flavors of sneutrino plus four neutral Higgs boson components. This is not the same as CP–violation, which is when a process is not the same under the simultaneous charge conjugation of all particles (C, for charge) and spatial inversion of all vectors (P, for parity). CP–violation enters the SM through a single phase of the CKM matrix. CP–violation leads to interesting other effects, but those are beyond the scope of this thesis (for an examination of the general CP–violating phases that can appear in the MSSM, see reference [57]).

3.2 Analytic Expressions

The bounds are calculated by comparing the decay widths in terms of the unknowns (the RPV couplings and the sfermion masses) to the measured upper bounds on the decay widths. The matrix elements for the cross–sections are calculated using the Feynman rules given in appendix D, combined, in the cases involving mesons, with the QCD bound state approximations in appendix F.

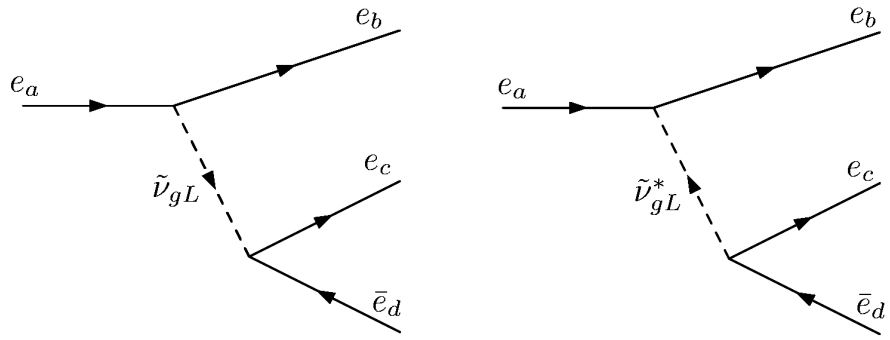

Figure 3.1: The Feynman diagrams for a heavy charged lepton of flavor a decaying to charged leptons of flavors b and c and a charged anti–lepton of flavor d.

3.2.1 Effective Lagrangian Density

The replacement of the full sfermion propagator with $-i/m^2_{\tilde{f}}$ is equivalent to integrating out the sfermionic degrees of freedom to obtain an effective interaction Lagrangian density[1], and taking only the leading term in an expansion in inverse sfermion mass, given by

$$\begin{aligned}
\mathcal{L}_{\text{eff}} \quad = \quad & \tfrac{1}{m^2_{\tilde{\nu}_{gL}}}\lambda_{gab}\lambda^*_{gcd}(\bar{e}_c P_R e_d)(\bar{e}_b P_L e_a) && \text{(A)} \\
+ \quad & \left(\tfrac{1}{m^2_{\tilde{\nu}_{gL}}}\lambda_{gik}\lambda'^*_{gnm}(\bar{d}_n P_R d_m)(\bar{e}_k P_L e_i) + \text{ Hermitian conjugate}\right) && \text{(B)} \\
- \quad & \left(\tfrac{1}{2m^2_{\tilde{u}_{gL}}}\lambda'_{ign}\lambda'^*_{kgm}(\bar{d}_n \gamma^\mu P_R d_m)(\bar{e}_k \gamma_\mu P_L e_i) + \text{ Hermitian conjugate}\right) && \text{(C)} \\
+ \quad & \left(\tfrac{1}{2m^2_{\tilde{d}_{gR}}}\lambda'_{img}\lambda'^*_{kng}(\bar{u}_n \gamma^\mu P_L u_m)(\bar{e}_k \gamma_\mu P_L e_i) + \text{ Hermitian conjugate}\right) && \text{(D)}
\end{aligned} \tag{3.1}$$

where (A) and (B) come from integrating out the sneutrino fields, and (C) and (D) come from integrating out the up–type and down–type squark fields respectively, using some Fierz identities (see section B.5). Adherence to the Einstein summation convention on the indices a, b, c and d means that (A) already contains Hermitian–conjugate pairs.

3.2.2 Purely Leptonic Decays

Non–zero RPV couplings of the λ_{ijk}–type allow lepton–flavor–violating decays of τ leptons and muons through couplings to a sneutrino. The Feynman diagrams for such a process are shown in figure 3.1.

[1] This effective Lagrangian density can be compared with those in references [58], [59], [60], [61] and [62], noting that both references [58] and [62] use the convention where there is *no* factor of $^1/_2$ before the λ_{ijk} term in the superpotential. It disagrees with the form of the effective Lagrangians in references [59] and [60], agreeing with those in references [58], [61] and [62], though noting that through projection onto vector or pseudoscalar quark bilinears the difference with reference [60] reduces to a simple overall sign error of the matrix element, which is then eliminated by squaring. This has no ill effects in the quadratic coupling dominance convention. Also, in the case of reference [59] it is merely that the wrong coupling in the second term of their equation (7) has the "$*$" denoting complex conjugation.

Matrix Element

The tree–level matrix element for this decay is given by

$$i\mathcal{M}_{e_a\to e_b e_c \bar{e}_d} = \langle e_b(p_{e_b}), e_c(p_{e_c}), \bar{e}_d(p_{\bar{e}_d})|T([\bar{e}_k(-i)\lambda_{jik}P_L e_i \tilde{\nu}_{jL}][\bar{e}_l(-i)\lambda^*_{mln}P_R e_n \tilde{\nu}^*_{mL}])|e_a(p_{e_a})\rangle \tag{3.2}$$

Performing the contractions over the fields gives

$$\begin{aligned} i\mathcal{M}_{e_a\to e_b e_c \bar{e}_d} = \frac{i}{m^2_{\tilde{\nu}_{gL}}}\big(& [\bar{u}(p_{e_c})\lambda_{gdc}P_L v(p_{\bar{e}_d})][\bar{u}(p_{e_b})\lambda^*_{gba}P_R u(p_{e_a})] \\ & +[\bar{u}(p_{e_b})\lambda_{gab}P_L u(p_{e_a})][\bar{u}(p_{e_c})\lambda^*_{gcd}P_R v(p_{\bar{e}_d})] \\ & -[\bar{u}(p_{e_b})\lambda_{gdb}P_L v(p_{\bar{e}_d})][\bar{u}(p_{e_c})\lambda^*_{gca}P_R u(p_{e_a})] \\ & -[\bar{u}(p_{e_c})\lambda_{gac}P_L u(p_{e_a})][\bar{u}(p_{e_b})\lambda^*_{gbd}P_R v(p_{\bar{e}_d})]\big) \end{aligned} \tag{3.3}$$

Decay Width

Squaring the matrix element, summing over final spins and averaging over initial spins, then integrating over the phase–space of the final–state particles gives the following decay width:

$$\Gamma_{e_a\to e_b e_c \bar{e}_d} = \frac{m^5_{e_a}}{6144\pi^3 m^4_{\tilde{\nu}_{gL}}}(|\lambda_{gdc}|^2|\lambda_{gba}|^2 + |\lambda_{gcd}|^2|\lambda_{gab}|^2 + |\lambda_{gdb}|^2|\lambda_{gca}|^2 + |\lambda_{gbd}|^2|\lambda_{gac}|^2) \tag{3.4}$$

approximating the final state (anti–)leptons as massless compared to the mass of the decaying lepton. Considering τ lepton decay, m_μ/m_τ is roughly 0.06 and m_e/m_τ is roughly 0.0003, and considering the decay $\mu\to ee\bar{e}$, m_e/m_μ is roughly 0.005.

Care must be taken for the case $b = c$, since there are now identical particles in the final state. The matrix element remains the same (with $c\to b$), but the phase space picks up a factor of $^1/_2$ to avoid overcounting final states.

$$\begin{aligned} \Gamma_{e_a\to e_b e_b \bar{e}_d} &= \frac{m^5_{e_a}}{12288\pi^3 m^4_{\tilde{\nu}_{gL}}}(|\lambda_{gdb}|^2|\lambda_{gba}|^2 + |\lambda_{gbd}|^2|\lambda_{gab}|^2 + |\lambda_{gdb}|^2|\lambda_{gba}|^2 + |\lambda_{gbd}|^2|\lambda_{gab}|^2) \\ &= \frac{m^5_{e_a}}{6144\pi^3 m^4_{\tilde{\nu}_{gL}}}(|\lambda_{gdb}|^2|\lambda_{gba}|^2 + |\lambda_{gbd}|^2|\lambda_{gab}|^2) \end{aligned} \tag{3.5}$$

3.2.3 Decays Involving A Vector Meson

Non–zero RPV couplings of the λ'_{ijk}–type allow lepton– and quark–flavor–violating decays of τ leptons to a muon or an electron plus a vector meson through couplings to a squark. Muons are not heavy enough to decay into even the lightest vector mesons, the ρ mesons. The Feynman diagrams for such a process are shown in figure 3.2. Through replacing some incoming particles with outgoing anti–particles *etc.*, the diagrams and matrix elements for the related process, shown in figure 3.3, of a vector meson decaying to a charged lepton and a charged anti–lepton (of the same flavor or of different flavors) can be obtained.

Matrix Element

The tree–level matrix element for the process of a charged lepton of flavor i decaying to a charged lepton of flavor k and a neutral vector meson V is given by

$$\begin{aligned} i\mathcal{M}_{e_i\to e_k V} = & \langle e_k V|T\left([i\lambda'_{ijn}\bar{d}_{Rn}e_{iL}\tilde{u}_{jL}][i\lambda'^*_{ktm}\bar{e}_{kL}d_{mR}\tilde{u}^*_{tL}]\right. \\ & \left.+[i\lambda'_{imj}e_{iL}u_{mL}\tilde{d}_{jR}][i\lambda'^*_{knt}\bar{u}_{nL}\bar{e}_{kL}\tilde{d}^*_{tR}]\right)|e_i\rangle \end{aligned} \tag{3.6}$$

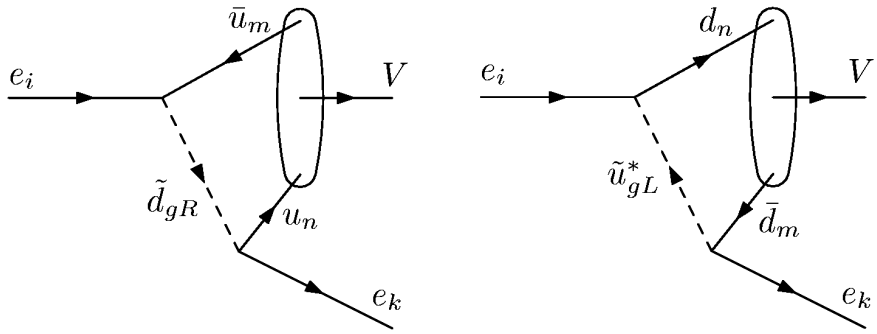

Figure 3.2: The Feynman diagrams for a heavy charged lepton of flavor i decaying to a charged lepton of flavor k and a vector meson V.

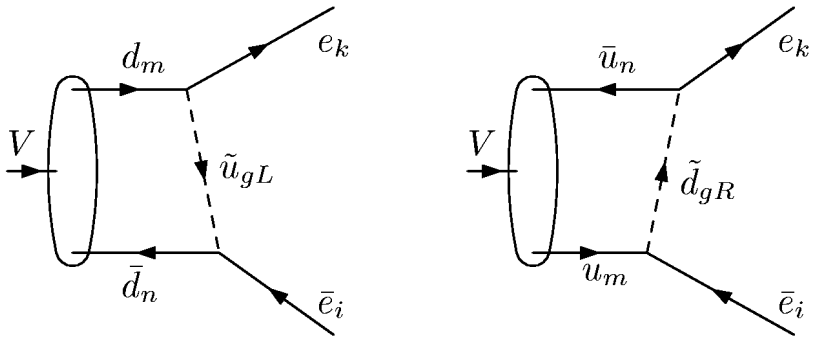

Figure 3.3: The Feynman diagrams for a vector meson V decaying to a charged lepton of flavor k and a charged anti–lepton of flavor i.

After some use of Fierz identities (see section B.5),

$$\begin{aligned} i\mathcal{M}_{e_i\to e_kV} &= \langle e_kV|\frac{1}{4}T\left([\lambda'_{ijn}\lambda'^{*}_{ktm}\tilde{u}_{jL}\tilde{u}^{*}_{tL}\bar{d}_n(\gamma^\mu+\gamma^\mu\gamma^5)d_m\right. \\ &\quad \left.-\lambda'_{imj}\lambda'^{*}_{knt}\tilde{d}_{jR}\tilde{d}^{*}_{tR}\bar{u}_n(\gamma^\mu-\gamma^\mu\gamma^5)u_m][\bar{e}_k\gamma_\mu P_L e_i]\right)|e_i\rangle \end{aligned} \tag{3.7}$$

Contracting the charged lepton fields with the external charged lepton states and the meson state with the quark bilinear (see appendix F),

$$\begin{aligned} i\mathcal{M}_{e_i\to e_kV} &= \frac{1}{4}\left[\sum_{\text{d–type}}\lambda'_{ign}\lambda'^{*}_{kgm}H_V^{mn*}\left(\frac{-i}{m^2_{\tilde{u}_{gL}}}\right)-\sum_{\text{u–type}}\lambda'_{img}\lambda'^{*}_{kng}H_V^{mn*}\left(\frac{-i}{m^2_{\tilde{d}_{gR}}}\right)\right] \\ &\quad\times[\bar{u}(p_{e_k})\gamma_\mu P_L u(p_{e_i})](-i)F_V^* m_V\epsilon_V^{\mu*} \end{aligned} \tag{3.8}$$

as agrees with equation (25) in reference [61], with the introduction of the notation $\sum_{\text{d–type}}$ to mean only summing over the down–type quarks in the meson and $\sum_{\text{u–type}}$ to mean summing over the up–type quarks, so now the m and n in H_V^{mn} (and, later in the equations involving pseudoscalar mesons and sneutrinos, in μ_P^{mn} — this notation is defined in appendix F) correspond to the flavor indices of the appropriate quarks, and both these indices are summed over. For example, the matrix element for the decay $\tau\to e\rho^0$ is given by

$$\begin{aligned} i\mathcal{M}_{\tau\to e\rho^0} &= \frac{1}{4}\left[\sum_{\text{d–type}}\lambda'_{3gn}\lambda'^{*}_{1gm}H_{\rho^0}^{mn*}\left(\frac{-i}{m^2_{\tilde{u}_{gL}}}\right)\right. \\ &\quad\left.-\sum_{\text{u–type}}\lambda'_{3mg}\lambda'^{*}_{1ng}H_{\rho^0}^{mn*}\left(\frac{-i}{m^2_{\tilde{d}_{gR}}}\right)\right][\bar{u}(p_e)\gamma^\mu P_L u(p_\tau)](-i)F^*_{\rho^0}m_{\rho^0}\epsilon^*_{\rho^0\mu} \\ &= \frac{-1}{4}[\bar{u}(p_e)\gamma^\mu P_L u(p_\tau)]\left[\frac{i}{m^2_{\tilde{u}_{gL}}}(\lambda'_{3g1}\lambda'^{*}_{1g1}H_{\rho^0}^{dd*}+\lambda'_{3g1}\lambda'^{*}_{1g2}H_{\rho^0}^{ds*}\right. \\ &\quad+\lambda'_{3g1}\lambda'^{*}_{1g3}H_{\rho^0}^{db*}+\lambda'_{3g2}\lambda'^{*}_{1g1}H_{\rho^0}^{sd*}+\ldots) \\ &\quad\left.-\frac{i}{m^2_{\tilde{d}_{gR}}}(\lambda'_{31g}\lambda'^{*}_{11g}H_{\rho^0}^{uu*}+\lambda'_{31g}\lambda'^{*}_{12g}H_{\rho^0}^{uc*}+\ldots)\right](-i)F^*_{\rho^0}m_{\rho^0}\epsilon^*_{\rho^0\mu} \\ &= \frac{-1}{4}[\bar{u}(p_e)\gamma^\mu P_L u(p_\tau)]\left[\frac{i}{m^2_{\tilde{u}_{gL}}}(\lambda'_{3g1}\lambda'^{*}_{1g1}\times(\frac{-1}{\sqrt{2}})+\lambda'_{3g1}\lambda'^{*}_{1g2}\times 0\right. \\ &\quad+\lambda'_{3g1}\lambda'^{*}_{1g3}\times 0+\lambda'_{3g2}\lambda'^{*}_{1g1}\times 0+\ldots) \\ &\quad\left.-\frac{i}{m^2_{\tilde{d}_{gR}}}(\lambda'_{31g}\lambda'^{*}_{11g}\times(\frac{1}{\sqrt{2}})+\lambda'_{31g}\lambda'^{*}_{12g}\times 0+\ldots)\right](-i)F^*_{\rho^0}m_{\rho^0}\epsilon^*_{\rho^0\mu} \end{aligned} \tag{3.9}$$

For the case of a vector meson V decaying to a charged lepton of flavor k and a charged anti–lepton of flavor i, the matrix elements are identical through crossing symmetry up to making the appropriate index substitutions in the couplings (*i.e.* swapping n and m, as the meson now consists of quarks labelled by m and anti–quarks labelled by n).

Decay Width

Again, squaring the matrix element, summing over final spins and averaging over initial spins leads to the following two cases for a heavy lepton of flavor i decaying into a lepton of flavor k

and a vector meson V:
up–type squark–mediated:

$$\Gamma_{e_i\to e_k V} = \left|\sum_{\text{d–type}} (\lambda'_{ign}\lambda'_{kgm}) H_V^{mn}\right|^2 \frac{(m_{e_i}^2 - m_V^2)^2}{512\pi m_{\tilde{u}_{gL}}^4} \frac{|F_V|^2 (m_{e_i}^2 + 2m_V^2)}{m_{e_i}^3} \left(1 + \mathcal{O}\left(\frac{m_{e_k}}{m_{e_i}}\right)\right) \tag{3.10}$$

as agrees with equation (31) in reference [61] and equation (11) in reference [60], or down–type squark–mediated:

$$\Gamma_{e_i\to e_k V} = \left|\sum_{\text{u–type}} (\lambda'_{img}\lambda'_{kng}) H_V^{mn}\right|^2 \frac{(m_{e_i}^2 - m_V^2)^2}{512\pi m_{\tilde{d}_{gR}}^4} \frac{|F_V|^2 (m_{e_i}^2 + 2m_V^2)}{m_{e_i}^3} \left(1 + \mathcal{O}\left(\frac{m_{e_k}}{m_{e_i}}\right)\right) \tag{3.11}$$

as also agrees with equation (31) in reference [61] and equation (11) in reference [60].

For a vector meson V decaying into a lepton of generation i and an anti–lepton of generation k, there are again two cases:
up–type squark–mediated:

$$\Gamma_{V\to e_k \bar{e}_i} = \left|\sum_{\text{d–type}} (\lambda'_{ign}\lambda'_{kgm}) H_V^{nm}\right|^2 \frac{(m_V^2 - m_{e_k}^2)^2}{768\pi m_{\tilde{u}_{gL}}^4} \frac{|F_V|^2 (2m_V^2 + m_{e_k}^2)}{m_V^3} \left(1 + \mathcal{O}\left(\frac{m_{e_i}}{m_V}\right)\right) \tag{3.12}$$

or down–type squark–mediated:

$$\Gamma_{V\to e_k \bar{e}_i} = \left|\sum_{\text{u–type}} (\lambda'_{img}\lambda'_{kng}) H_V^{nm}\right|^2 \frac{(m_V^2 - m_{e_k}^2)^2}{768\pi m_{\tilde{d}_{gR}}^4} \frac{|F_V|^2 (2m_V^2 + m_{e_k}^2)}{m_V^3} \left(1 + \mathcal{O}\left(\frac{m_{e_i}}{m_{e_k}}\right)\right) \tag{3.13}$$

3.2.4 Decays Involving A Pseudoscalar Meson

Non–zero RPV couplings of the λ'_{ijk}–type also allow lepton– and quark–flavor–violating decays of τ leptons to a muon or an electron plus a pseudoscalar meson through couplings to a squark. Muons are not heavy enough to decay into even the lightest pseudoscalar mesons, pions, either. The diagrams are shown in figure 3.4, along with the additional diagram that is possible if both couplings of the λ'_{ijk}– and the λ_{ijk}–type are non–zero. As before, the Feynman diagrams (shown in figure 3.5) and the matrix elements for the related process of a pseudoscalar meson decaying to a charged lepton and a charged anti–lepton (of the same flavor or of different flavors) are obtained by replacing some incoming particles with outgoing anti–particles and so on.

Matrix Element

The contribution from the squark–mediated diagrams is obtained from equation (3.7) with different out states, and is given by

$$\begin{aligned} i\mathcal{M}^{\tilde{q}}_{e_i\to e_k P} &= \langle e_k P|\frac{1}{4}T\Big([\lambda'_{ijn}\lambda'^*_{ktm}\tilde{u}_{jL}\tilde{u}^*_{tL}\bar{d}_n(\gamma^\mu+\gamma^\mu\gamma^5)d_m \\ &\quad -\lambda'_{imj}\lambda'^*_{knt}\tilde{d}_{jR}\tilde{d}^*_{Rt}\bar{u}_n(\gamma^\mu-\gamma^\mu\gamma^5)u_m][\bar{e}_k\gamma_\mu P_L e_i]\Big)|e_i\rangle \end{aligned} \tag{3.14}$$

Contracting the charged lepton fields with the external charged lepton states and the meson

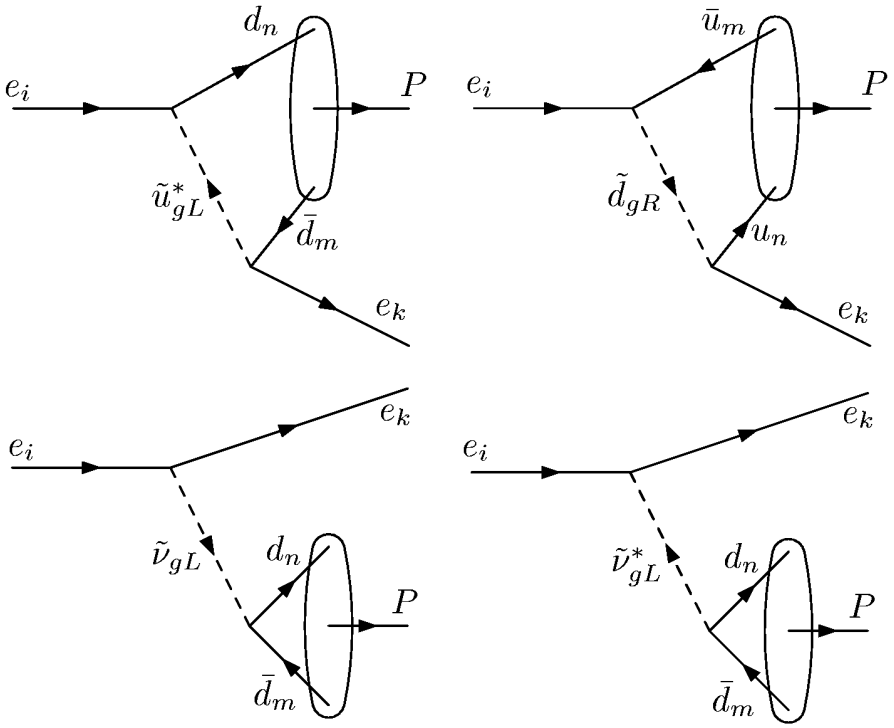

Figure 3.4: The Feynman diagrams for a heavy charged lepton of flavor i decaying to a charged lepton of flavor k and a pseudoscalar meson P.

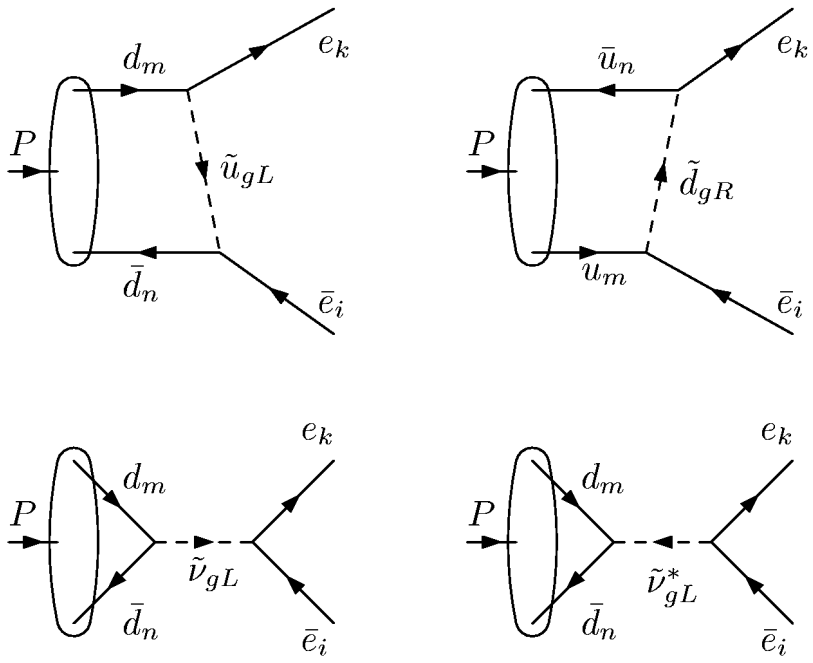

Figure 3.5: The Feynman diagrams for a pseudoscalar meson P decaying to a charged lepton of flavor k and a charged anti–lepton of flavor i.

state with the quark bilinear (see appendix F),

$$\begin{aligned} i\mathcal{M}^{\tilde{q}}_{e_i\to e_k P} &= \frac{1}{4}\left[\sum_{\text{d–type}} \lambda'_{ign}\lambda'^*_{kgm} H_P^{mn*}\left(\frac{-i}{m^2_{\tilde{u}_{gL}}}\right) - \sum_{\text{u–type}} \lambda'_{img}\lambda'^*_{kng} H_P^{mn*}\left(\frac{-i}{m^2_{\tilde{d}_{gR}}}\right)\right] \\ &\quad \times[\bar{u}(p_{e_k})\gamma_\mu P_L u(p_{e_i})](-i)F_P^* p_P^\mu \end{aligned} \tag{3.15}$$

as agrees with equation (33) in reference [61].

The contribution from the sneutrino–mediated diagrams is given by

$$\begin{aligned} i\mathcal{M}^{\tilde{\nu}}_{e_i\to e_k P} &= \langle e_k P|T\left([\bar{e}_k(-i)(\lambda_{jik}P_L\tilde{\nu}_{jL} + \lambda^*_{jki}\tilde{\nu}^*_{jL}P_R)e_i]\right. \\ &\quad \left.\times\,[\bar{d}_n(-i)(\lambda'_{tmn}P_L\tilde{\nu}_{tL} + \lambda'^*_{tnm}P_R\tilde{\nu}^*_{tL})d_m]\right)|e_i\rangle \\ &= \frac{-i}{2m^2_{\tilde{\nu}_{gL}}}\sum_{\text{d–type}}[\bar{u}(p_{e_k})\lambda_{gik}P_L u(p_{e_i})\lambda'^*_{gnm} - \bar{u}(p_{e_k})\lambda^*_{gki}P_R u(p_{e_i})\lambda'_{gmn}] \\ &\quad \times\left[\frac{iH_P^{mn}F_P m_P^2}{\mu_P^{mn}}\right]^* \end{aligned} \tag{3.16}$$

as also agrees with equation (33) in reference [61], noting that the sneutrino does not couple to up–type quarks.

For the case of a pseudoscalar meson P decaying to a charged lepton of flavor k and a charged anti–lepton of flavor i, the matrix elements are identical through crossing symmetry up to making the appropriate index substitutions in the couplings (*i.e.* swapping n and m, as the meson now consists of quarks labelled by m and anti–quarks labelled by n).

Decay Width

Once more, squaring the matrix element, summing over final spins and averaging over initial spins leads to the following three cases for a heavy lepton of flavor i decaying into a lepton of flavor k and a pseudoscalar meson P:
up–type squark–mediated:

$$\Gamma_{e_i\to e_k P} = \left|\sum_{\text{d–type}} (\lambda'_{ign}\lambda'_{kgm}) H_P^{mn}\right|^2 \frac{(m_{e_i}^2 - m_P^2)^2}{512\pi m_{\tilde{u}_{gL}}^4} \frac{|F_P|^2}{m_{e_i}} \left(1 + \mathcal{O}\left(\frac{m_{e_k}}{m_{e_i}}\right)\right) \tag{3.17}$$

as agrees with equation (34) in reference [61] and equation (11) in reference [60], down–type squark–mediated:

$$\Gamma_{e_i\to e_k P} = \left|\sum_{\text{u–type}} (\lambda'_{img}\lambda'_{kng}) H_P^{mn}\right|^2 \frac{(m_{e_i}^2 - m_P^2)^2}{512\pi m_{\tilde{d}_{gR}}^4} \frac{|F_P|^2}{m_{e_i}} \left(1 + \mathcal{O}\left(\frac{m_{e_k}}{m_{e_i}}\right)\right) \tag{3.18}$$

as also agrees with equation (34) in reference [61] and equation (11) in reference [60], or sneutrino–mediated:

$$\begin{aligned}\Gamma_{e_i\to e_k P} &= \frac{(m_{e_i}^2 - m_P^2)^2}{128\pi m_{\tilde{\nu}_{gL}}^4} \frac{|F_P|^2 m_P^4}{m_{e_i}^3} \left(\left|\sum_{\text{d–type}} \lambda^*_{gki}\lambda'_{gmn} \frac{H_P^{mn*}}{\mu_P^{mn*}}\right|^2 \right. \\ &\left. + \left|\sum_{\text{d–type}} \lambda_{gik}\lambda'^*_{gnm} \frac{H_P^{mn*}}{\mu_P^{mn*}}\right|^2\right) \left(1 + \mathcal{O}\left(\frac{m_{e_k}}{m_{e_i}}\right)\right)\end{aligned} \tag{3.19}$$

as also agrees with equation (34) in reference [61] and equation (11) in reference [60].

For a pseudoscalar meson P decaying into a lepton of generation i and an anti–lepton of generation k, there are again three cases:
up–type squark–mediated:

$$\Gamma_{P\to e_k \bar{e}_i} = \left|\sum_{\text{d–type}} (\lambda'_{ign}\lambda'_{kgm}) H_P^{nm}\right|^2 \frac{(m_P^2 - m_{e_k}^2)^2}{256\pi m_{\tilde{u}_{gL}}^4} \frac{|F_P|^2 m_{e_k}^2}{m_P^3} \left(1 + \mathcal{O}\left(\frac{m_{e_i}}{m_P}\right)\right) \tag{3.20}$$

as agrees with equation (14) in reference [60], down–type squark–mediated:

$$\Gamma_{P\to e_k \bar{e}_i} = \left|\sum_{\text{u–type}} (\lambda'_{img}\lambda'_{kng}) H_P^{nm}\right|^2 \frac{(m_P^2 - m_{e_k}^2)^2}{256\pi m_{\tilde{d}_{gR}}^4} \frac{|F_P|^2 m_{e_k}^2}{m_P^3} \left(1 + \mathcal{O}\left(\frac{m_{e_i}}{m_P}\right)\right) \tag{3.21}$$

as also agrees with equation (14) in reference [60], or sneutrino–mediated:

$$\begin{aligned}\Gamma_{P\to e_k \bar{e}_i} &= \frac{(m_P^2 - m_{e_k}^2)^2}{64\pi m_{\tilde{\nu}_{gL}}^4} |F_P|^2 m_P \left(\left|\sum_{\text{d–type}} \lambda^*_{gki}\lambda'_{gmn} \frac{H_P^{nm}}{\mu_P^{nm}}\right|^2 \right. \\ &\left. + \left|\sum_{\text{d–type}} \lambda_{gik}\lambda'^*_{gnm} \frac{H_P^{nm}}{\mu_P^{nm}}\right|^2\right) \left(1 + \mathcal{O}\left(\frac{m_{e_i}}{m_P}\right)\right)\end{aligned} \tag{3.22}$$

which does not agree with equation (13) in reference [60]. This is addressed in section 3.4.2.

3.3 Numerical Results

In tables 3.1 to 3.13, $[\tilde{f}]$ denotes $m_{\tilde{f}}/100$ GeV, *i.e.* the sfermion mass in units of 100 GeV (following the convention in reference [26]). This also indicates the mediating sfermion for the decay.

In the rightmost columns of tables 3.2 and 3.3, and tables 3.5 to 3.13,

- "New" indicates a result unpublished before reference [1],
- "Upd." indicates that the bound has been updated and tightened in reference [1],
- "Agr." indicates that the bound has not changed and reference [1] agrees with the previously published result,
- "Unimp." indicates that reference [1]'s bound from decay data is less strong than the previously published result, which in these cases is from a different experimental source (*e.g.* the non–observation of $\mu \to e$ in ^{48}Ti gives a better bound on $\lambda_{121}\lambda'_{111}[\tilde{\nu}_{L1}]^2$ than that of $\pi^0 \to e\bar{\mu}$),
- "Corr." indicates disagreement with the previously published result,
  - "Corr.(<)" indicating a result stronger than the incorrect previous bound
  - "Corr.(>)" indicating a result less strong.
- $^{\dagger(-)}$ indicates that this bound comes from a decay which involves a difference of couplings with the same mediating sfermion, so there could be a cancellation which would lead to the double coupling dominance hypothesis giving an excessively tight bound, since the couplings might be of the same order while there would be no suppression of one or the other from a heavier mediating sfermion mass.

In all the Agr. cases, it turns out that reference [1] is agreeing with reference [63], though reference [63] only gives the bounds to the first significant figure, and it is assumed that the differences (6.7×10^{-9} compared to 6×10^{-9} and 2.7×10^{-7} compared to 3×10^{-7}) arise from rounding errors.

The reference in this rightmost column, labelled "Key", gives the previous published bound. Where two references are given, the comparison is between the calculated bound on a product of two couplings and the product of the bounds on individual couplings.

The indices have been arranged so that the number made from reading off the indices to make a six–digit number ascends, with the exception that the first two indices on λ_{ijk} have not been rearranged to give the lowest number (through the antisymmetry of the coupling on its first two indices), rather they are such that the first index is that of the flavor of the sneutrino involved in the bound through its mass.

3.3.1 Highlights

To save the reader's eyesight and sanity, additional tables precede the main tables, containing what may be considered the most interesting results. The coupling combinations which had no bounds previous to reference [1] are presented in table 3.1. Those combinations which have improved by a factor of 30 or more are presented in table 3.2, and the cases where the previous tightest bound was given by a product of individual bounds but the combined bound is now better are presented in table 3.3.

Coupling combination	Bound	Decay
$\lambda_{g21}\lambda'_{g22}$	2.1 $[\tilde{\nu}_{gL}]^2$	$\eta \to \mu\bar{e} + e\bar{\mu}$
$\lambda_{g12}\lambda'_{g22}$		
$\lambda_{g13}\lambda'_{g12}$	9.7×10^{-4} $[\tilde{\nu}_{gL}]^2$	$\tau \to eK_S$
$\lambda_{g31}\lambda'_{g21}$		
$\lambda_{g23}\lambda'_{g12}$	1.0×10^{-3} $[\tilde{\nu}_{gL}]^2$	$\tau \to \mu K_S$
$\lambda_{g32}\lambda'_{g21}$		
$\lambda'_{1g1}\lambda'_{3g2}$	2.3×10^{-3} $[\tilde{u}_{gL}]^2$	$\tau \to eK_S$
$\lambda'_{1g2}\lambda'_{2g2}$	$1.5\times10^{+2}$ $[\tilde{u}_{gL}]^2$	$\eta \to \mu\bar{e} + e\bar{\mu}$
$\lambda'_{1g2}\lambda'_{3g2}$ $^{\dagger(-)}$	1.2×10^{-3} $[\tilde{u}_{gL}]^2$	$\tau \to e\eta$
$\lambda'_{1g2}\lambda'_{3g2}$	3.4×10^{-3} $[\tilde{u}_{gL}]^2$	$\tau \to e\phi$
$\lambda'_{2g1}\lambda'_{3g2}$	2.4×10^{-3} $[\tilde{u}_{gL}]^2$	$\tau \to \mu K_S$
$\lambda'_{2g2}\lambda'_{3g2}$ $^{\dagger(-)}$	1.6×10^{-3} $[\tilde{u}_{gL}]^2$	$\tau \to \mu\eta$
$\lambda'_{2g2}\lambda'_{3g2}$	3.4×10^{-3} $[\tilde{u}_{gL}]^2$	$\tau \to \mu\phi$

Table 3.1: Coupling combinations which had no bounds previous to reference [1].

Coupling combination	From reference [1]		Previously published		
	Bound	Decay	Bound	Decay	Key
$\lambda_{g13}\ \lambda'_{g22}$	4.6×10^{-4} $[\tilde{\nu}_{gL}]^2$	$\tau \to e\eta$	1.6×10^{-2} $[\tilde{\nu}_{gL}]^2$	$\tau \to e\eta$	Upd. [64]
$\lambda_{g31}\ \lambda'_{g22}$					
$\lambda_{g13}\ \lambda'_{g21}$	9.7×10^{-4} $[\tilde{\nu}_{gL}]^2$	$\tau \to eK_S$	8.5×10^{-2} $[\tilde{\nu}_{gL}]^2$	$\tau \to eK^0$	Upd. [64]
$\lambda_{g31}\ \lambda'_{g12}$					
$\lambda_{g23}\ \lambda'_{g21}$	1.0×10^{-3} $[\tilde{\nu}_{gL}]^2$	$\tau \to \mu K_S$	7.6×10^{-2} $[\tilde{\nu}_{gL}]^2$	$\tau \to \mu K^0$	Upd. [64]
$\lambda_{g32}\ \lambda'_{g12}$					
$\lambda_{g32}\ \lambda'_{g11}$	6.7×10^{-5} $[\tilde{\nu}_{gL}]^2$	$\tau \to \mu\eta$	1.7×10^{-3} $[\tilde{\nu}_{gL}]^2$	$\tau \to \mu\eta$	Upd. [64]
$\lambda_{g23}\ \lambda'_{g22}$	3.7×10^{-4} $[\tilde{\nu}_{gL}]^2$	$\tau \to \mu\eta$	1.7×10^{-2} $[\tilde{\nu}_{gL}]^2$	$\tau \to \mu\eta$	Upd. [64]
$\lambda_{g32}\ \lambda'_{g22}$					

Table 3.2: Coupling combinations which have improved by a factor of 30 or more compared to those published before reference [1].

Coupling combination	From reference [1]		Previously published		
	Bound	Decay	Bound	Decay	Key
$\lambda'_{11g}\ \lambda'_{31g}$	$1.2\times10^{-3}\ [\tilde{d}_{gR}]^2$	$\tau\to e\pi^0$	$0.02\ [\tilde{d}_{gR}]$ $\times0.12\ [\tilde{d}_{gR}]$	APV in Cs $\frac{\tau\to\pi^-\nu}{\pi^-\to\mu\bar{\nu}}$	Upd. [26], [26]
$\lambda'_{12g}\ \lambda'_{21g}$	$9.0\times10^{-3}\ [\tilde{d}_{gR}]^2$	$D^0\to\mu\bar{e}$	$0.21\ [\tilde{d}_{gR}]$ $\times5.9\ \times10^{-2}\ [\tilde{d}_{gR}]$	A^c_{FB} $\frac{\pi^-\to e\bar{\nu}}{\pi^-\to\mu\bar{\nu}}$	Upd. [26], [65]

Table 3.3: Cases where the combined bound is now better than the product of the individual bounds.

3.4 Discussion

3.4.1 $\lambda_{\mathbf{ijk}}\lambda_{\mathbf{lmn}}$

The bounds on $(\lambda_{ijk}\lambda_{lmn})$ from τ decay in table 3.4 tighten by a factor of about 3 those in reference [66], as the relevant bounds have increased by roughly an order of magnitude each. The muon decay bounds have not tightened.

3.4.2 $\lambda_{\mathbf{ijk}}\lambda'_{\mathbf{lmn}}$

The bounds in tables 3.5, 3.6 and 3.7 generally update those already published, most recently in reference [26] (excepting reference [1]).

Those associated with B meson rare decays do not agree with the bounds presented in reference [26], which are just those taken from reference [60]. This disagreement can be traced back to equation (13) in reference [60],

$$\Gamma(B_{q_i}\to l_l^- l_m^+) = \frac{f^2_{B_{q_i}}}{16\pi\tilde{m}^4 M^3_{B_{q_i}}} C(M_{B_{q_i}}, m_{l_l}, m_{l_m}) P_1(M_{B_{q_i}}, m_{l_l}, m_{l_m}) \left|\lambda_{nlm}\lambda'_{ni3}\right|^2 \tag{3.23}$$

For comparison with this work's equation (3.22), note that

$$f_{B_{q_i}} = F_{B_{d/s}} \qquad \text{(taken to be 200 MeV in both cases)} \tag{3.24}$$

$$\tilde{m} = m_{\tilde{\nu}_{gL}} \tag{3.25}$$

$$M_{B_{q_i}} = m_{B_{d/s}},\ m_{l_l} = m_{e_l} \qquad \text{and so on.}$$

$$C(M_{B_{q_i}}, m_{l_l}, m_{l_m}) = (m^2_{B_{d/s}} - m^2_{e_l})\left(1 + \mathcal{O}\left(\frac{m_{e_l}}{m_{B_{d/s}}}\right)\right) \tag{3.26}$$

$$P_1(M_{B_{q_i}}, m_{l_l}, m_{l_m}) = m^2_{B_{d/s}}(m^2_{B_{d/s}} - m^2_{e_l})\left(1 + \mathcal{O}\left(\frac{m_{e_l}}{m_{B_{d/s}}}\right)\right) \tag{3.27}$$

In this case $\mu^{bs}_{B_{d/s}} = m_b + m_{q_i}$.

It can then be seen that the ratio of reference [60]'s decay width over the decay width in equation (3.22) is $4(m_b + m_{q_i})^2/M^2_{B_{q_i}} = 2.67$ for the B_d case or 2.70 for the B_s case, which implies that reference [60]'s bound on $\left|\lambda_{nlm}\lambda'_{ni3}\right|^2$ is about 2.7 times too tight, so reference [60]'s bound on $|\lambda_{nlm}\lambda'_{ni3}|$ is about 1.6 times too tight. The bounds for the many of the rare B decay branching ratios have tightened, which is why many of the bounds in tables 3.5 to 3.8 for the couplings associated with these decays are tighter than in reference [60]. However, equation (3.22) agrees with equation (14) in reference [60], and note that the coefficients of

$(\lambda_{ijk}\ \lambda_{lmn})$	From reference [1]		Previously published	
$ijk\ lmn$	Bound	Decay	Bound	Key
121 123	$7.0\times10^{-4}\ [\tilde{\nu}_{1L}]^2$	$\tau\to\mu e\bar{\mu}$	$2.1\times10^{-3}\ [\tilde{\nu}_{1L}]^2$	Upd. [66]
121 131	$6.8\times10^{-4}\ [\tilde{\nu}_{1L}]^2$	$\tau\to\mu e\bar{e}$	$2.0\times10^{-3}\ [\tilde{\nu}_{1L}]^2$	Upd. [66]
121 132	$5.6\times10^{-4}\ [\tilde{\nu}_{1L}]^2$	$\tau\to\mu\mu\bar{e}$	$1.9\times10^{-3}\ [\tilde{\nu}_{1L}]^2$	Upd. [66]
122 123	$6.8\times10^{-4}\ [\tilde{\nu}_{1L}]^2$	$\tau\to\mu\mu\bar{\mu}$	$2.2\times10^{-3}\ [\tilde{\nu}_{1L}]^2$	Upd. [66]
122 131	$7.0\times10^{-4}\ [\tilde{\nu}_{1L}]^2$	$\tau\to\mu e\bar{\mu}$	$2.1\times10^{-3}\ [\tilde{\nu}_{1L}]^2$	Upd. [66]
122 132	$6.8\times10^{-4}\ [\tilde{\nu}_{1L}]^2$	$\tau\to\mu\mu\bar{\mu}$	$2.2\times10^{-3}\ [\tilde{\nu}_{1L}]^2$	Upd. [66]
211 212	$6.6\times10^{-7}\ [\tilde{\nu}_{2L}]^2$	$\mu\to ee\bar{e}$	$6.6\times10^{-7}\ [\tilde{\nu}_{2L}]^2$	Agr. [59]
211 213	$7.0\times10^{-4}\ [\tilde{\nu}_{2L}]^2$	$\tau\to ee\bar{e}$	$2.7\times10^{-3}\ [\tilde{\nu}_{2L}]^2$	Upd. [66]
211 231	$7.0\times10^{-4}\ [\tilde{\nu}_{2L}]^2$	$\tau\to ee\bar{e}$	$2.7\times10^{-3}\ [\tilde{\nu}_{2L}]^2$	Upd. [66]
211 232	$6.8\times10^{-4}\ [\tilde{\nu}_{2L}]^2$	$\tau\to\mu e\bar{e}$	$2.0\times10^{-3}\ [\tilde{\nu}_{2L}]^2$	Upd. [66]
212 213	$6.8\times10^{-4}\ [\tilde{\nu}_{2L}]^2$	$\tau\to\mu e\bar{e}$	$2.0\times10^{-3}\ [\tilde{\nu}_{2L}]^2$	Upd. [66]
212 231	$5.2\times10^{-4}\ [\tilde{\nu}_{2L}]^2$	$\tau\to ee\bar{\mu}$	$1.9\times10^{-3}\ [\tilde{\nu}_{2L}]^2$	Upd. [66]
212 232	$7.0\times10^{-4}\ [\tilde{\nu}_{2L}]^2$	$\tau\to\mu e\bar{\mu}$	$2.1\times10^{-3}\ [\tilde{\nu}_{2L}]^2$	Upd. [66]
311 312	$6.6\times10^{-7}\ [\tilde{\nu}_{3L}]^2$	$\mu\to ee\bar{e}$	$6.6\times10^{-7}\ [\tilde{\nu}_{3L}]^2$	Agr. [59]
311 313	$7.0\times10^{-4}\ [\tilde{\nu}_{3L}]^2$	$\tau\to ee\bar{e}$	$2.7\times10^{-3}\ [\tilde{\nu}_{3L}]^2$	Upd. [66]
311 321	$6.6\times10^{-7}\ [\tilde{\nu}_{3L}]^2$	$\mu\to ee\bar{e}$	$6.6\times10^{-7}\ [\tilde{\nu}_{3L}]^2$	Agr. [59]
311 323	$6.8\times10^{-4}\ [\tilde{\nu}_{3L}]^2$	$\tau\to\mu e\bar{e}$	$2.0\times10^{-3}\ [\tilde{\nu}_{3L}]^2$	Upd. [66]
312 313	$6.8\times10^{-4}\ [\tilde{\nu}_{3L}]^2$	$\tau\to\mu e\bar{e}$	$2.0\times10^{-3}\ [\tilde{\nu}_{3L}]^2$	Upd. [66]
312 323	$5.6\times10^{-4}\ [\tilde{\nu}_{3L}]^2$	$\tau\to\mu\mu\bar{e}$	$1.9\times10^{-3}\ [\tilde{\nu}_{3L}]^2$	Upd. [66]
313 321	$5.2\times10^{-4}\ [\tilde{\nu}_{3L}]^2$	$\tau\to ee\bar{\mu}$	$1.9\times10^{-3}\ [\tilde{\nu}_{3L}]^2$	Upd. [66]
313 322	$7.0\times10^{-4}\ [\tilde{\nu}_{3L}]^2$	$\tau\to\mu e\bar{\mu}$	$2.1\times10^{-3}\ [\tilde{\nu}_{3L}]^2$	Upd. [66]
321 323	$7.0\times10^{-4}\ [\tilde{\nu}_{3L}]^2$	$\tau\to\mu e\bar{\mu}$	$2.1\times10^{-3}\ [\tilde{\nu}_{3L}]^2$	Upd. [66]
322 323	$6.8\times10^{-4}\ [\tilde{\nu}_{3L}]^2$	$\tau\to\mu\mu\bar{\mu}$	$2.2\times10^{-3}\ [\tilde{\nu}_{3L}]^2$	Upd. [66]

Table 3.4: Bounds on $(\lambda_{\mathbf{ijk}}\lambda_{\mathbf{lmn}})$: all but those from $\mu\to ee\bar{e}$ are updated from reference [66]. The presented $\mu\to ee\bar{e}$ bounds agree with those in reference [59].

the four–fermion terms in equation (2) in reference [60] differ by a factor of 2 between the sneutrino–mediating and the squark–mediating terms in the effective Hamiltonian, so it is puzzling as to how the sneutrino–mediated and the squark–mediated decay widths differ by a factor of 16 rather than 4. Further to this, equation (13) in reference [60] appears to be the same as equation (8) in reference [62]; however reference [62] defines the couplings λ such that the superpotential does *not* have the factor of $^1/_2$ before the trilinear lepton term. Taking this into account, equation (3.22) agrees with the equations in reference [62].

In general, the updates on the other bounds in tables 3.5 to 3.8 arise from tighter experimental bounds, though some are tightened through considering $\tau \to K_S l^-$ instead of $\tau \to K^0 l^-$.

There are also new bounds on couplings that had not been published before reference [1], associated with the decays $\tau \to e K_S$ and $\tau \to \mu K_S$, which are of the same order as the other bounds, and with the decay $\eta \to \mu\bar{e} + e\bar{\mu}$, which is not a particularly tight bound at all.

The tightest bounds in tables 3.5 to 3.8 are associated with K_L decays. Since K_L is an antisymmetric combination of K^0 and $\bar{K}^0$, there is easily the possibility that contributions from λ'_{g12} and λ'_{g21} interfere destructively — if $\lambda'_{g12} = \lambda'_{g21}$, then no bounds can be extracted from K_L decays at all.

3.4.3 $\lambda'_{\mathbf{ijk}}\lambda'_{\mathbf{lmn}}$

Again, most of the bounds in tables 3.9 to 3.14 update those already published, most recently in reference [26] (excepting reference [1]), generally through tighter experimental bounds. Again, there are also new bounds on couplings that had not been published before reference [1], associated with the decays $\tau \to e K_S$ and $\tau \to \mu K_S$, which are of the same order as the other bounds, and with the decay $\eta \to \mu\bar{e} + e\bar{\mu}$, which is not a particularly tight bound at all. In addition, there are new bounds from $\tau \to e\eta$. (The bounds from $\tau \to l^-\eta$ are tighter than $\tau \to l^-\phi$, but $\tau \to l^-\phi$ has not the potential for the mediating squark coupling to both down and strange quarks creating interference as the η case has.)

In general, the pseudoscalar meson decay widths associated with $\lambda'_{ijk}\lambda'_{lmn}$–combinations suffer from suppression by $m^2_{e_i}/m^2_P$ compared to the decay width from $\lambda_{ijk}\lambda'_{lmn}$–combinations, leading to poor bounds from decays of heavy pseudoscalar mesons to light leptons, *e.g.* $B \to \mu\bar{e}$. This leads to many more unimproved bounds than in tables 3.9 to 3.14.

Also, the tightest bounds are again associated with K_L decays, which are not robust upon relaxation of the assumption that only one pair of couplings dominate the signal.

3.4.4 Comparison To SM Yukawa Couplings

If the sfermion mass is set to 100 GeV and it is assumed that the square root of the bound on the quadratic combination $\lambda^{(\prime)}_{ijk}\lambda^{(\prime)}_{lmn}$ gives a rough bound on the magnitude of each coupling, the bounds obtained are generally of the order of 10^{-2}. On one hand, this number is small. The coupling of a W boson to a quark is $\sqrt{2\pi\alpha}/\sin(\theta_W) \approx 0.45$. On the other hand, this is quite consistent with the Yukawa couplings present in the SM. As mentioned in section 2.4.3, there is enough freedom in the SM to rotate the fields such that the up–type quark Yukawa couplings are diagonal while remaining as $SU(2)_L$ flavor eigenstates, yet not enough to do this for the down–type quarks. This mismatch is generally moved from the Yukawa couplings to the CKM matrix. However, for comparison, the Yukawa couplings of the down–type–mass–generating Higgs boson to the down–type quarks in the MSSM in the $SU(2)_L$ flavor basis, once

the up–type quark Yukawa couplings have been diagonalized, are given by:

$$Y_d = \left(\frac{0.02}{\cos(\beta)}\right) \begin{pmatrix} 1.4\times10^{-4}\exp(2.9i) & 6.5\times10^{-3}\exp(0.0011i) & 3.9\times10^{-3}\exp(-1.0i) \\ 6.6\times10^{-3}\exp(3.1i) & 2.9\times10^{-2}\exp(0.000086i) & 4.1\times10^{-3}\exp(-0.0052i) \\ 7.9\times10^{-3}\exp(2.7i) & 2.6\times10^{-3}\exp(-2.8i) & 1 \end{pmatrix} \tag{3.28}$$

where $\tan\beta$ is, as in equation (2.14), the ratio of the Higgs vacuum expectation values: specifically, $\tan\beta = v_u/v_d$, where v_u is the vacuum expectation value of the up–type–mass–generating Higgs boson and v_d is the vacuum expectation value of the down–type–mass–generating Higgs boson. In the SM, the formula is the same, but with a prefactor of m_b/m_t instead of $0.02/\cos\beta$. This is equivalent to using the value of $\tan\beta = 1$. For large $\tan\beta$, $1/\cos\beta \approx \tan\beta$, and for the value $\tan\beta \approx 50$, the coupling to the bottom quark to the H_d Higgs field is the same as the top quark to the H_u Higgs field, the difference in the masses of the top and bottom quarks being solely due to the difference in vacuum expectation values of the Higgs fields.

In comparison to the bottom quark coupling to the Higgs boson, the magnitudes of all the other couplings are of the order of 10^{-2} or less. This implies the possibility that high–precision rare–decay searches are very close to detecting the RPV couplings, should they be of a similar magnitude to the other Yukawa couplings in the model.

$(\lambda_{ijk}\ \lambda'_{lmn})$	From reference [1]		Previously published		
$ijk\ lmn$	Bound	Decay	Bound	Decay	Key
121 111	$1.2\ \times 10^{-2}\ [\tilde{\nu}_{1L}]^2$	$\pi^0 \to e\bar{\mu}$	$2.1\times 10^{-8}\ [\tilde{\nu}_{1L}]^2$	$\mu \to e$ in ^{48}Ti	Unimp. [67]
	$0.39\ [\tilde{\nu}_{1L}]^2$	$\eta \to \mu\bar{e} + e\bar{\mu}$			
	$0.41\ [\tilde{\nu}_{1L}]^2$	$\pi^0 \to \mu\bar{e}$			
	$16\ [\tilde{\nu}_{1L}]^2$	$\eta' \to \mu\bar{e}/e\bar{\mu}$			
121 112	$6.7\ \times 10^{-9}\ [\tilde{\nu}_{1L}]^2$	$K_L^0 \to \mu\bar{e}/e\bar{\mu}$	$6\ \times 10^{-9}\ [\tilde{\nu}_{1L}]^2$	$K_L^0 \to \mu\bar{e}/e\bar{\mu}$	$^{\dagger(-)}$ Agr. [63]
121 113	$1.3\ \times 10^{-5}\ [\tilde{\nu}_{1L}]^2$	$B_d^0 \to \mu\bar{e}$	$2.3\times 10^{-5}\ [\tilde{\nu}_{1L}]^2$	$B_d^0 \to \mu\bar{e}$	Corr.(<) [60]
121 121	$6.7\ \times 10^{-9}\ [\tilde{\nu}_{1L}]^2$	$K_L^0 \to \mu\bar{e}/e\bar{\mu}$	$6\ \times 10^{-9}\ [\tilde{\nu}_{1L}]^2$	$K_L^0 \to \mu\bar{e}/e\bar{\mu}$	$^{\dagger(-)}$ Agr. [63]
121 122	$2.1\ [\tilde{\nu}_{1L}]^2$	$\eta \to \mu\bar{e} + e\bar{\mu}$	none	n/a	New
	$3.6\ \times 10^{+4}\ [\tilde{\nu}_{1L}]^2$	$\eta' \to \mu\bar{e}/e\bar{\mu}$			
121 123	$7.6\ \times 10^{-5}\ [\tilde{\nu}_{1L}]^2$	$B_s^0 \to \mu\bar{e}$	$4.7\times 10^{-5}\ [\tilde{\nu}_{1L}]^2$	$B_s^0 \to \mu\bar{e}$	Corr.(>) [60]
121 131	$1.3\ \times 10^{-5}\ [\tilde{\nu}_{1L}]^2$	$B_d^0 \to e\bar{\mu}$	$2.3\times 10^{-5}\ [\tilde{\nu}_{1L}]^2$	$B_d^0 \to e\bar{\mu}$	Corr.(<) [60]
121 132	$7.6\ \times 10^{-5}\ [\tilde{\nu}_{1L}]^2$	$B_s^0 \to e\bar{\mu}$	$4.7\times 10^{-5}\ [\tilde{\nu}_{1L}]^2$	$B_s^0 \to e\bar{\mu}$	Corr.(>) [60]
122 113	$6.2\ \times 10^{-6}\ [\tilde{\nu}_{1L}]^2$	$B_d^0 \to \mu\bar{\mu}$	$1.5\times 10^{-5}\ [\tilde{\nu}_{1L}]^2$	$B_d^0 \to \mu\bar{\mu}$	Corr.(<) [60]
122 123	$1.2\ \times 10^{-5}\ [\tilde{\nu}_{1L}]^2$	$B_s^0 \to \mu\bar{\mu}$	$1.7\times 10^{-5}\ [\tilde{\nu}_{1L}]^2$	$B_d^0 \to K^0\mu\bar{\mu}$	Upd. [68]
122 131	$6.2\ \times 10^{-6}\ [\tilde{\nu}_{1L}]^2$	$B_d^0 \to \mu\bar{\mu}$	$1.5\times 10^{-5}\ [\tilde{\nu}_{1L}]^2$	$B_d^0 \to \mu\bar{\mu}$	Corr.(<) [60]
122 132	$1.2\ \times 10^{-5}\ [\tilde{\nu}_{1L}]^2$	$B_s^0 \to \mu\bar{\mu}$	$1.8\times 10^{-5}\ [\tilde{\nu}_{1L}]^2$	$B_d^0 \to K^0\mu\bar{\mu}$	Upd. [68]
123 111	$6.7\ \times 10^{-5}\ [\tilde{\nu}_{1L}]^2$	$\tau \to \mu\eta$	$1.7\times 10^{-3}\ [\tilde{\nu}_{1L}]^2$	$\tau \to \mu\eta$	Upd. [64]
	$1.0\ \times 10^{-3}\ [\tilde{\nu}_{1L}]^2$	$\tau \to \mu\pi^0$			
123 112	$1.0\ \times 10^{-3}\ [\tilde{\nu}_{1L}]^2$	$\tau \to \mu K_S$	none	n/a	New
123 113	$2.2\ \times 10^{-4}\ [\tilde{\nu}_{1L}]^2$	$B_d^0 \to \mu\bar{\tau}$	$6.2\times 10^{-4}\ [\tilde{\nu}_{1L}]^2$	$B_d^0 \to \mu\bar{\tau}$	Corr.(<) [60]
123 121	$1.0\ \times 10^{-3}\ [\tilde{\nu}_{1L}]^2$	$\tau \to \mu K_S$	$7.6\times 10^{-2}\ [\tilde{\nu}_{1L}]^2$	$\tau \to \mu K^0$	Upd. [64]
123 122	$3.7\ \times 10^{-4}\ [\tilde{\nu}_{1L}]^2$	$\tau \to \mu\eta$	$1.7\times 10^{-2}\ [\tilde{\nu}_{1L}]^2$	$\tau \to \mu\eta$	Upd. [64]
123 131	$2.2\ \times 10^{-4}\ [\tilde{\nu}_{1L}]^2$	$B_d^0 \to \tau\bar{\mu}$	$6.2\times 10^{-4}\ [\tilde{\nu}_{1L}]^2$	$B_d^0 \to \mu\bar{\tau}$	Corr.(<) [60]
131 111	$8.5\ \times 10^{-5}\ [\tilde{\nu}_{1L}]^2$	$\tau \to e\eta$	$1.6\times 10^{-3}\ [\tilde{\nu}_{1L}]^2$	$\tau \to e\eta$	Upd. [64]
	$7.1\ \times 10^{-4}\ [\tilde{\nu}_{1L}]^2$	$\tau \to e\pi^0$			
131 112	$9.7\ \times 10^{-4}\ [\tilde{\nu}_{1L}]^2$	$\tau \to eK_S$	$8.5\times 10^{-2}\ [\tilde{\nu}_{1L}]^2$	$\tau \to eK^0$	Upd. [64]
131 113	$3.7\ \times 10^{-4}\ [\tilde{\nu}_{1L}]^2$	$B_d^0 \to \tau\bar{e}$	$4.9\times 10^{-4}\ [\tilde{\nu}_{1L}]^2$	$B_d^0 \to \tau\bar{e}$	Corr.(<) [60]
131 121	$9.7\ \times 10^{-4}\ [\tilde{\nu}_{1L}]^2$	$\tau \to eK_S$	none	n/a	New
131 122	$4.6\ \times 10^{-4}\ [\tilde{\nu}_{1L}]^2$	$\tau \to e\eta$	$1.6\times 10^{-2}\ [\tilde{\nu}_{1L}]^2$	$\tau \to e\eta$	Upd. [64]
131 131	$3.7\ \times 10^{-4}\ [\tilde{\nu}_{1L}]^2$	$B_d^0 \to e\bar{\tau}$	$4.9\times 10^{-4}\ [\tilde{\nu}_{1L}]^2$	$B_d^0 \to e\bar{\tau}$	Corr.(<) [60]

Table 3.5: Bounds on $(\lambda_{\mathbf{ijk}}\lambda'_{\mathbf{lmn}})$.

$(\lambda_{ijk}\ \lambda'_{lmn})$	From reference [1]		Previously published		
$ijk\ lmn$	Bound	Decay	Bound	Decay	Key
132 111	$6.7\ \times10^{-5}\ [\tilde{\nu}_{1L}]^2$	$\tau\to\mu\eta$	$1.7\times10^{-3}\ [\tilde{\nu}_{1L}]^2$	$\tau\to\mu\eta$	Upd. [64]
	$1.0\ \times10^{-3}\ [\tilde{\nu}_{1L}]^2$	$\tau\to\mu\pi^0$			
132 112	$1.0\ \times10^{-3}\ [\tilde{\nu}_{1L}]^2$	$\tau\to\mu K_S$	$7.6\times10^{-2}\ [\tilde{\nu}_{1L}]^2$	$\tau\to\mu K^0$	Upd. [64]
132 113	$2.2\ \times10^{-4}\ [\tilde{\nu}_{1L}]^2$	$B^0_d\to\tau\bar{\mu}$	$6.2\times10^{-4}\ [\tilde{\nu}_{1L}]^2$	$B^0_d\to\mu\bar{\tau}$	Corr.(<) [60]
132 121	$1.0\ \times10^{-3}\ [\tilde{\nu}_{1L}]^2$	$\tau\to\mu K_S$	none	n/a	New
132 122	$3.7\ \times10^{-4}\ [\tilde{\nu}_{1L}]^2$	$\tau\to\mu\eta$	$1.7\times10^{-2}\ [\tilde{\nu}_{1L}]^2$	$\tau\to\mu\eta$	Upd. [64]
132 131	$2.2\ \times10^{-4}\ [\tilde{\nu}_{1L}]^2$	$B^0_d\to\mu\bar{\tau}$	$6.2\times10^{-4}\ [\tilde{\nu}_{1L}]^2$	$B^0_d\to\mu\bar{\tau}$	Corr.(<) [60]
211 213	$4.1\ \times10^{-5}\ [\tilde{\nu}_{2L}]^2$	$B^0_d\to e\bar{e}$	$1.7\times10^{-5}\ [\tilde{\nu}_{2L}]^2$	$B^0_d\to e\bar{e}$	Corr.(>) [60]
211 223	$2.3\ \times10^{-4}\ [\tilde{\nu}_{2L}]^2$	$B^0_s\to e\bar{e}$	$1.4\times10^{-4}\ [\tilde{\nu}_{2L}]^2$	$B^0_d\to K^0 e\bar{e}$	Unimp. [68]
211 231	$4.1\ \times10^{-5}\ [\tilde{\nu}_{2L}]^2$	$B^0_d\to e\bar{e}$	$1.7\times10^{-5}\ [\tilde{\nu}_{2L}]^2$	$B^0_d\to e\bar{e}$	Corr.(>) [60]
211 232	$2.3\ \times10^{-4}\ [\tilde{\nu}_{2L}]^2$	$B^0_s\to e\bar{e}$	$2.3\times10^{-5}\ [\tilde{\nu}_{2L}]^2$	$B^0_d\to K^0 e\bar{e}$	Unimp. [68]
212 211	$1.2\ \times10^{-2}\ [\tilde{\nu}_{2L}]^2$	$\pi^0\to e\bar{\mu}$	$2.1\times10^{-8}\ [\tilde{\nu}_{2L}]^2$	$\mu\to e$ in ^{48}Ti	Unimp. [67]
	$0.38\ [\tilde{\nu}_{2L}]^2$	$\eta\to\mu\bar{e}+e\bar{\mu}$			
	$0.41\ [\tilde{\nu}_{2L}]^2$	$\pi^0\to\mu\bar{e}$			
	$16\ [\tilde{\nu}_{2L}]^2$	$\eta'\to\mu\bar{e}/e\bar{\mu}$			
212 212	$6.7\ \times10^{-9}\ [\tilde{\nu}_{2L}]^2$	$K^0_L\to\mu\bar{e}/e\bar{\mu}$	$6\ \times10^{-9}\ [\tilde{\nu}_{2L}]^2$	$K^0_L\to\mu\bar{e}/e\bar{\mu}$	$^{\dagger(-)}$ Agr. [63]
212 213	$1.3\ \times10^{-5}\ [\tilde{\nu}_{2L}]^2$	$B^0_d\to e\bar{\mu}$	$2.3\times10^{-5}\ [\tilde{\nu}_{2L}]^2$	$B^0_d\to e\bar{\mu}$	Corr.(>) [60]
212 221	$6.7\ \times10^{-9}\ [\tilde{\nu}_{2L}]^2$	$K^0_L\to\mu\bar{e}/e\bar{\mu}$	$6\ \times10^{-9}\ [\tilde{\nu}_{2L}]^2$	$K^0_L\to\mu\bar{e}/e\bar{\mu}$	$^{\dagger(-)}$ Agr. [63]
212 222	$2.1\ [\tilde{\nu}_{2L}]^2$	$\eta\to\mu\bar{e}+e\bar{\mu}$	none	n/a	New
	$3.6\ \times10^{+4}\ [\tilde{\nu}_{2L}]^2$	$\eta'\to\mu\bar{e}/e\bar{\mu}$			
212 223	$7.6\ \times10^{-5}\ [\tilde{\nu}_{2L}]^2$	$B^0_s\to e\bar{\mu}$	$4.7\times10^{-5}\ [\tilde{\nu}_{2L}]^2$	$B^0_s\to e\bar{\mu}$	Corr.(>) [60]
212 231	$1.3\ \times10^{-5}\ [\tilde{\nu}_{2L}]^2$	$B^0_d\to\mu\bar{e}$	$2.3\times10^{-5}\ [\tilde{\nu}_{2L}]^2$	$B^0_d\to\mu\bar{e}$	Corr.(<) [60]
212 232	$7.6\ \times10^{-5}\ [\tilde{\nu}_{2L}]^2$	$B^0_s\to\mu\bar{e}$	$4.7\times10^{-5}\ [\tilde{\nu}_{2L}]^2$	$B^0_s\to e\bar{\mu}$	Corr.(>) [60]
213 211	$8.5\ \times10^{-5}\ [\tilde{\nu}_{2L}]^2$	$\tau\to e\eta$	$1.6\times10^{-3}\ [\tilde{\nu}_{2L}]^2$	$\tau\to e\eta$	Upd. [64]
	$7.1\ \times10^{-4}\ [\tilde{\nu}_{2L}]^2$	$\tau\to e\pi^0$			
213 212	$9.7\ \times10^{-4}\ [\tilde{\nu}_{2L}]^2$	$\tau\to eK_S$	none	n/a	New
213 213	$3.7\ \times10^{-4}\ [\tilde{\nu}_{2L}]^2$	$B^0_d\to e\bar{\tau}$	$4.9\times10^{-4}\ [\tilde{\nu}_{2L}]^2$	$B^0_d\to e\bar{\tau}$	Corr.(<) [60]
213 221	$9.7\ \times10^{-4}\ [\tilde{\nu}_{2L}]^2$	$\tau\to eK_S$	$8.5\times10^{-2}\ [\tilde{\nu}_{2L}]^2$	$\tau\to eK^0$	Upd. [64]
213 222	$4.6\ \times10^{-4}\ [\tilde{\nu}_{2L}]^2$	$\tau\to e\eta$	$1.6\times10^{-2}\ [\tilde{\nu}_{2L}]^2$	$\tau\to e\eta$	Upd. [64]
213 231	$3.7\ \times10^{-4}\ [\tilde{\nu}_{2L}]^2$	$B^0_d\to\tau\bar{e}$	$4.9\times10^{-4}\ [\tilde{\nu}_{2L}]^2$	$B^0_d\to\tau\bar{e}$	Corr.(<) [60]

Table 3.6: Bounds on $(\lambda_{\mathbf{ijk}}\lambda'_{\mathbf{lmn}})$ continued.

$(\lambda_{ijk}\ \lambda'_{lmn})$	From reference [1]		Previously published		
$ijk\ lmn$	Bound	Decay	Bound	Decay	Key
231 211	$8.5\ \times10^{-5}\ [\tilde{\nu}_{2L}]^2$	$\tau\to e\eta$	$1.6\times10^{-3}\ [\tilde{\nu}_{2L}]^2$	$\tau\to e\eta$	Upd. [64]
	$7.1\ \times10^{-4}\ [\tilde{\nu}_{2L}]^2$	$\tau\to e\pi^0$			
231 212	$9.7\ \times10^{-4}\ [\tilde{\nu}_{2L}]^2$	$\tau\to eK_S$	$8.5\times10^{-2}\ [\tilde{\nu}_{2L}]^2$	$\tau\to eK^0$	Upd. [64]
231 213	$3.7\ \times10^{-4}\ [\tilde{\nu}_{2L}]^2$	$B_d^0\to\tau\bar{e}$	$4.9\times10^{-4}\ [\tilde{\nu}_{2L}]^2$	$B_d^0\to\tau\bar{e}$	Corr.(<) [60]
231 221	$9.7\ \times10^{-4}\ [\tilde{\nu}_{2L}]^2$	$\tau\to eK_S$	none	n/a	New
231 222	$4.6\ \times10^{-4}\ [\tilde{\nu}_{2L}]^2$	$\tau\to e\eta$	$1.6\times10^{-2}\ [\tilde{\nu}_{2L}]^2$	$\tau\to e\eta$	Upd. [64]
231 231	$3.7\ \times10^{-4}\ [\tilde{\nu}_{2L}]^2$	$B_d^0\to e\bar{\tau}$	$4.9\times10^{-4}\ [\tilde{\nu}_{2L}]^2$	$B_d^0\to e\bar{\tau}$	Corr.(<) [60]
232 211	$6.7\ \times10^{-5}\ [\tilde{\nu}_{2L}]^2$	$\tau\to\mu\eta$	$1.7\times10^{-3}\ [\tilde{\nu}_{2L}]^2$	$\tau\to\mu\eta$	Upd. [64]
	$1.0\ \times10^{-3}\ [\tilde{\nu}_{2L}]^2$	$\tau\to\mu\pi^0$			
232 212	$1.0\ \times10^{-3}\ [\tilde{\nu}_{2L}]^2$	$\tau\to\mu K_S$	$7.6\times10^{-2}\ [\tilde{\nu}_{2L}]^2$	$\tau\to\mu K^0$	Upd. [64]
232 213	$2.2\ \times10^{-4}\ [\tilde{\nu}_{2L}]^2$	$B_d^0\to\tau\bar{\mu}$	$6.2\times10^{-4}\ [\tilde{\nu}_{2L}]^2$	$B_d^0\to\mu\bar{\tau}$	Corr.(<) [60]
232 221	$1.0\ \times10^{-3}\ [\tilde{\nu}_{2L}]^2$	$\tau\to\mu K_S$	none	n/a	New
232 222	$3.7\ \times10^{-4}\ [\tilde{\nu}_{2L}]^2$	$\tau\to\mu\eta$	$1.7\times10^{-2}\ [\tilde{\nu}_{2L}]^2$	$\tau\to\mu\eta$	Upd. [64]
232 231	$2.2\ \times10^{-4}\ [\tilde{\nu}_{2L}]^2$	$B_d^0\to\mu\bar{\tau}$	$6.2\times10^{-4}\ [\tilde{\nu}_{2L}]^2$	$B_d^0\to\mu\bar{\tau}$	Corr.(<) [60]
311 313	$4.1\ \times10^{-5}\ [\tilde{\nu}_{3L}]^2$	$B_d^0\to e\bar{e}$	$1.7\times10^{-5}\ [\tilde{\nu}_{3L}]^3$	$B_d^0\to e\bar{e}$	Corr.(>) [60]
311 323	$2.3\ \times10^{-4}\ [\tilde{\nu}_{3L}]^2$	$B_s^0\to e\bar{e}$	$2.3\times10^{-5}\ [\tilde{\nu}_{3L}]^2$	$B_d^0\to K^0e\bar{e}$	Unimp. [68]
311 331	$4.1\ \times10^{-5}\ [\tilde{\nu}_{3L}]^2$	$B_d^0\to e\bar{e}$	$1.7\times10^{-5}\ [\tilde{\nu}_{3L}]^2$	$B_d^0\to e\bar{e}$	Corr.(>) [60]
311 332	$2.3\ \times10^{-4}\ [\tilde{\nu}_{3L}]^2$	$B_s^0\to e\bar{e}$	$2.3\times10^{-5}\ [\tilde{\nu}_{3L}]^2$	$B_d^0\to K^0e\bar{e}$	Unimp. [68]
312 311	$1.2\ \times10^{-2}\ [\tilde{\nu}_{3L}]^2$	$\pi^0\to e\bar{\mu}$	$2.1\times10^{-8}\ [\tilde{\nu}_{3L}]^2$	$\mu\to e$ in ^{48}Ti	Unimp. [67]
	$0.38\ [\tilde{\nu}_{3L}]^2$	$\eta\to\mu\bar{e}+e\bar{\mu}$			
	$0.41\ [\tilde{\nu}_{3L}]^2$	$\pi^0\to\mu\bar{e}$			
	$16\ [\tilde{\nu}_{3L}]^2$	$\eta'\to\mu\bar{e}/e\bar{\mu}$			
312 312	$6.7\ \times10^{-9}\ [\tilde{\nu}_{3L}]^2$	$K_L^0\to\mu\bar{e}/e\bar{\mu}$	$6\ \times10^{-9}\ [\tilde{\nu}_{3L}]^3$	$K_L^0\to\mu\bar{e}/e\bar{\mu}$	$^{\dagger(-)}$ Agr. [63]
312 313	$1.3\ \times10^{-5}\ [\tilde{\nu}_{3L}]^2$	$B_d^0\to e\bar{\mu}$	$2.3\times10^{-5}\ [\tilde{\nu}_{3L}]^2$	$B_d^0\to e\bar{\mu}$	Corr.(<) [60]
312 321	$6.7\ \times10^{-9}\ [\tilde{\nu}_{3L}]^2$	$K_L^0\to\mu\bar{e}/e\bar{\mu}$	$6\ \times10^{-9}\ [\tilde{\nu}_{3L}]^3$	$K_L^0\to\mu\bar{e}/e\bar{\mu}$	$^{\dagger(-)}$ Agr. [63]
312 322	$2.1\ [\tilde{\nu}_{3L}]^2$	$\eta\to\mu\bar{e}+e\bar{\mu}$	none	n/a	New
	$3.6\ \times10^{+4}\ [\tilde{\nu}_{3L}]^2$	$\eta'\to\mu\bar{e}/e\bar{\mu}$			
312 323	$7.6\ \times10^{-5}\ [\tilde{\nu}_{3L}]^2$	$B_s^0\to e\bar{\mu}$	$4.7\times10^{-5}\ [\tilde{\nu}_{3L}]^2$	$B_s^0\to e\bar{\mu}$	Corr.(>) [60]
312 331	$1.3\ \times10^{-5}\ [\tilde{\nu}_{3L}]^2$	$B_d^0\to\mu\bar{e}$	$2.3\times10^{-5}\ [\tilde{\nu}_{3L}]^2$	$B_d^0\to\mu\bar{e}$	Corr.(<) [60]
312 332	$7.6\ \times10^{-5}\ [\tilde{\nu}_{3L}]^2$	$B_s^0\to\mu\bar{e}$	$4.7\times10^{-5}\ [\tilde{\nu}_{3L}]^2$	$B_s^0\to\mu\bar{e}$	Corr.(>) [60]

Table 3.7: Bounds on $(\lambda_{\mathbf{ijk}}\lambda'_{\mathbf{lmn}})$ continued.

$(\lambda_{ijk}\ \lambda'_{lmn})$	From reference [1]		Previously published		
$ijk\ lmn$	Bound	Decay	Bound	Decay	Key
313 311	$8.5\ \times10^{-5}\ [\tilde{\nu}_{3L}]^2$	$\tau\to e\eta$	$1.6\times10^{-3}\ [\tilde{\nu}_{3L}]^2$	$\tau\to e\eta$	Upd. [64]
	$7.1\ \times10^{-4}\ [\tilde{\nu}_{3L}]^2$	$\tau\to e\pi^0$			
313 312	$9.7\ \times10^{-4}\ [\tilde{\nu}_{3L}]^2$	$\tau\to eK_S$	none	n/a	New
313 313	$3.7\ \times10^{-4}\ [\tilde{\nu}_{3L}]^2$	$B^0_d\to e\bar{\tau}$	$4.9\times10^{-4}\ [\tilde{\nu}_{3L}]^2$	$B^0_d\to e\bar{\tau}$	Corr.(<) [60]
313 321	$9.7\ \times10^{-4}\ [\tilde{\nu}_{3L}]^2$	$\tau\to eK_S$	$8.5\times10^{-2}\ [\tilde{\nu}_{3L}]^2$	$\tau\to eK^0$	Upd. [64]
313 322	$4.6\ \times10^{-4}\ [\tilde{\nu}_{3L}]^2$	$\tau\to e\eta$	$1.6\times10^{-2}\ [\tilde{\nu}_{3L}]^2$	$\tau\to e\eta$	Upd. [64]
313 331	$3.7\ \times10^{-4}\ [\tilde{\nu}_{3L}]^2$	$B^0_d\to\tau\bar{e}$	$4.9\times10^{-4}\ [\tilde{\nu}_{3L}]^2$	$B^0_d\to\tau\bar{e}$	Corr.(<) [60]
321 311	$1.2\ \times10^{-2}\ [\tilde{\nu}_{3L}]^2$	$\pi^0\to e\bar{\mu}$	$2.1\times10^{-8}\ [\tilde{\nu}_{3L}]^2$	$\mu\to e$ in ^{48}Ti	Unimp. [67]
	$0.38\ [\tilde{\nu}_{3L}]^2$	$\eta\to\mu\bar{e}+e\bar{\mu}$			
	$0.41\ [\tilde{\nu}_{3L}]^2$	$\pi^0\to\mu\bar{e}$			
	$16\ [\tilde{\nu}_{3L}]^2$	$\eta'\to\mu\bar{e}/e\bar{\mu}$			
321 312	$6.7\ \times10^{-9}\ [\tilde{\nu}_{3L}]^2$	$K^0_L\to\mu\bar{e}/e\bar{\mu}$	$6\ \times10^{-9}\ [\tilde{\nu}_{3L}]^3$	$K^0_L\to\mu\bar{e}/e\bar{\mu}$	$^{\dagger(-)}$ Agr. [63]
321 313	$1.3\ \times10^{-5}\ [\tilde{\nu}_{3L}]^2$	$B^0_d\to\mu\bar{e}$	$2.3\times10^{-5}\ [\tilde{\nu}_{3L}]^2$	$B^0_d\to\mu\bar{e}$	Corr.(<) [60]
321 321	$6.7\ \times10^{-9}\ [\tilde{\nu}_{3L}]^2$	$K^0_L\to\mu\bar{e}/e\bar{\mu}$	$6\ \times10^{-9}\ [\tilde{\nu}_{3L}]^3$	$K^0_L\to\mu\bar{e}/e\bar{\mu}$	$^{\dagger(-)}$ Agr. [63]
321 322	$2.1\ [\tilde{\nu}_{3L}]^2$	$\eta\to\mu\bar{e}+e\bar{\mu}$	none	n/a	New
	$3.6\ \times10^{+4}\ [\tilde{\nu}_{3L}]^2$	$\eta'\to\mu\bar{e}/e\bar{\mu}$			
321 323	$7.6\ \times10^{-5}\ [\tilde{\nu}_{3L}]^2$	$B^0_s\to\mu\bar{e}$	$4.7\times10^{-5}\ [\tilde{\nu}_{3L}]^2$	$B^0_s\to\mu\bar{e}$	Corr.(>) [60]
321 331	$1.3\ \times10^{-5}\ [\tilde{\nu}_{3L}]^2$	$B^0_d\to e\bar{\mu}$	$2.3\times10^{-5}\ [\tilde{\nu}_{3L}]^2$	$B^0_d\to e\bar{\mu}$	Corr.(<) [60]
321 332	$7.6\ \times10^{-5}\ [\tilde{\nu}_{3L}]^2$	$B^0_s\to e\bar{\mu}$	$4.7\times10^{-5}\ [\tilde{\nu}_{3L}]^2$	$B^0_s\to e\bar{\mu}$	Corr.(>) [60]
322 313	$6.2\ \times10^{-6}\ [\tilde{\nu}_{3L}]^2$	$B^0_d\to\mu\bar{\mu}$	$1.5\times10^{-5}\ [\tilde{\nu}_{3L}]^2$	$B^0_d\to\mu\bar{\mu}$	Corr.(<) [60]
322 323	$1.2\ \times10^{-5}\ [\tilde{\nu}_{3L}]^2$	$B^0_s\to\mu\bar{\mu}$	$1.7\times10^{-5}\ [\tilde{\nu}_{3L}]^2$	$B^0_d\to K^0\mu\bar{\mu}$	Upd. [68]
322 331	$6.2\ \times10^{-6}\ [\tilde{\nu}_{3L}]^2$	$B^0_d\to\mu\bar{\mu}$	$1.5\times10^{-5}\ [\tilde{\nu}_{3L}]^2$	$B^0_d\to\mu\bar{\mu}$	Corr.(<) [60]
322 332	$1.2\ \times10^{-5}\ [\tilde{\nu}_{3L}]^2$	$B^0_s\to\mu\bar{\mu}$	$1.8\times10^{-5}\ [\tilde{\nu}_{3L}]^3$	$B^0_d\to K^0\mu\bar{\mu}$	Upd. [68]
323 311	$6.7\ \times10^{-5}\ [\tilde{\nu}_{3L}]^2$	$\tau\to\mu\eta$	$1.7\times10^{-3}\ [\tilde{\nu}_{3L}]^2$	$\tau\to\mu\eta$	Upd. [64]
	$1.0\ \times10^{-3}\ [\tilde{\nu}_{3L}]^2$	$\tau\to\mu\pi^0$			
323 312	$1.0\ \times10^{-3}\ [\tilde{\nu}_{3L}]^2$	$\tau\to\mu K_S$	none	n/a	New
323 313	$2.2\ \times10^{-4}\ [\tilde{\nu}_{3L}]^2$	$B^0_d\to\mu\bar{\tau}$	$6.2\times10^{-4}\ [\tilde{\nu}_{3L}]^2$	$B^0_d\to\mu\bar{\tau}$	Corr.(<) [60]
323 321	$1.0\ \times10^{-3}\ [\tilde{\nu}_{3L}]^2$	$\tau\to\mu K_S$	$7.6\times10^{-2}\ [\tilde{\nu}_{3L}]^2$	$\tau\to\mu K^0$	Upd. [64]
323 322	$3.7\ \times10^{-4}\ [\tilde{\nu}_{3L}]^2$	$\tau\to\mu\eta$	$1.7\times10^{-2}\ [\tilde{\nu}_{3L}]^2$	$\tau\to\mu\eta$	Upd. [64]
323 331	$2.2\ \times10^{-4}\ [\tilde{\nu}_{3L}]^2$	$B^0_d\to\tau\bar{\mu}$	$6.2\times10^{-4}\ [\tilde{\nu}_{3L}]^2$	$B^0_d\to\mu\bar{\tau}$	Corr.(<) [60]

Table 3.8: Bounds on $(\lambda_{\mathbf{ijk}}\lambda'_{\mathbf{lmn}})$ continued.

$(\lambda'_{ijk}\ \lambda'_{lmn})$	From reference [1]		Previously published		
$ijk\ lmn$	Bound	Decay	Bound	Decay	Key
111 113	$2.6\ \times10^{-2}\ [\tilde{u}_{1L}]^2$	$B^0_d \to e\bar{e}$	$0.03\ [\tilde{u}_{1L}]$ $\times 0.18\ [\tilde{u}_{1L}]$	APV in Cs A^b_{FB}	Unimp. [26], [26]
111 211	$0.36\ [\tilde{d}_{1R}]^2$	$\pi^0 \to e\bar{\mu}$	$4.5\ \times10^{-8}\ [\tilde{d}_{1R}]^2$	$\mu \to e$ in ^{48}Ti	Unimp. [67]
	$11\ [\tilde{d}_{1R}]^2$	$\pi^0 \to \mu\bar{e}$			
	$1.5\ \times10^{+2}\ [\tilde{d}_{1R}]^2$	$\eta \to \mu\bar{e} + e\bar{\mu}$			
	$1.9\ \times10^{+4}\ [\tilde{d}_{1R}]^2$	$\eta' \to \mu\bar{e}/e\bar{\mu}$			
111 211	$0.36\ [\tilde{u}_{1L}]^2$	$\pi^0 \to e\bar{\mu}$	$4.3\ \times10^{-8}\ [\tilde{u}_{1L}]^2$	$\mu \to e$ in ^{48}Ti	Unimp. [67]
	$11\ [\tilde{u}_{1L}]^2$	$\pi^0 \to \mu\bar{e}$			
	$1.5\ \times10^{+2}\ [\tilde{u}_{1L}]^2$	$\eta \to \mu\bar{e} + e\bar{\mu}$			
	$1.9\ \times10^{+4}\ [\tilde{u}_{1L}]^2$	$\eta' \to \mu\bar{e}$			
111 212	$2.7\ \times10^{-7}\ [\tilde{u}_{1L}]^2$	$K^0_L \to \mu\bar{e}/e\bar{\mu}$	$3\ \times10^{-7}\ [\tilde{u}_{1L}]^2$	$K^0_L \to \mu\bar{e}/e\bar{\mu}$	$^{\dagger(-)}$ Agr. [63]
111 213	$1.6\ \times10^{-3}\ [\tilde{u}_{1L}]^2$	$B^0_d \to e\bar{\mu}$	$4.7\ \times10^{-3}\ [\tilde{u}_{1L}]^2$	$B^0_d \to e\bar{\mu}$	Upd. [60]
111 221	$2.8\ \times10^{-2}\ [\tilde{d}_{1R}]^2$	$D^0 \to e\bar{\mu}$	$0.02\ [\tilde{d}_{1R}]$ $\times 0.21\ [\tilde{d}_{1R}]$	APV in Cs $\frac{\tau\to\pi^-\nu}{\pi^-\to\mu\bar{\nu}}$	Unimp. [26], [69]
111 311	$1.2\ \times10^{-3}\ [\tilde{d}_{1R}]^2$	$\tau \to e\pi^0$	$0.02\ [\tilde{d}_{1R}]$ $\times 0.12\ [\tilde{d}_{1R}]$	APV in Cs $\frac{\tau\to\pi^-\nu}{\pi^-\to\mu\bar{\nu}}$	Upd. [26], [26]
	$2.0\ \times10^{-3}\ [\tilde{d}_{1R}]^2$	$\tau \to e\eta$			
	$2.4\ \times10^{-3}\ [\tilde{d}_{1R}]^2$	$\tau \to e\rho^0$			
111 311	$1.2\ \times10^{-3}\ [\tilde{u}_{1L}]^2$	$\tau \to e\pi^0$	$2.4\ \times10^{-3}\ [\tilde{u}_{1L}]^2$	$\tau \to e\rho^0$	Upd. [64] $^{\dagger(-)}$
	$2.0\ \times10^{-3}\ [\tilde{u}_{1L}]^2$	$\tau \to e\eta$			
	$2.4\ \times10^{-3}\ [\tilde{u}_{1L}]^2$	$\tau \to e\rho^0$			
111 312	$2.3\ \times10^{-3}\ [\tilde{u}_{1L}]^2$	$\tau \to eK_S$	none	n/a	New
	$3.6\ \times10^{-3}\ [\tilde{u}_{1L}]^2$	$\tau \to e\bar{K}^{*0}$			
111 313	$2.7\ \times10^{-3}\ [\tilde{u}_{1L}]^2$	$B^0_d \to e\bar{\tau}$	$5.9\ \times10^{-3}\ [\tilde{u}_{1L}]^2$	$B^0_d \to e\bar{\tau}$	Upd. [60]
112 113	$9.3\ [\tilde{u}_{1L}]^2$	$B^0_s \to e\bar{e}$	$0.18\ [\tilde{u}_{1L}]$ $\times 0.28\ [\tilde{u}_{1L}]$	A^b_{FB} A^s_{FB}	Unimp. [26], [26]
112 211	$2.7\ \times10^{-7}\ [\tilde{u}_{1L}]^2$	$K^0_L \to \mu\bar{e}/e\bar{\mu}$	$3\ \times10^{-7}\ [\tilde{u}_{1L}]^2$	$K^0_L \to \mu\bar{e}/e\bar{\mu}$	$^{\dagger(-)}$ Agr. [63]
112 212	$0.36\ [\tilde{d}_{2R}]^2$	$\pi^0 \to e\bar{\mu}$	$4.5\ \times10^{-8}\ [\tilde{d}_{2R}]^2$	$\mu \to e$ in ^{48}Ti	Unimp. [67]
	$1.1\ [\tilde{d}_{2R}]^2$	$\pi^0 \to \mu\bar{e}$			
	$1.6\ \times10^{+2}\ [\tilde{d}_{2R}]^2$	$\eta \to \mu\bar{e} + e\bar{\mu}$			
	$1.9\ \times10^{+4}\ [\tilde{d}_{2R}]^2$	$\eta' \to \mu\bar{e}/e\bar{\mu}$			

Table 3.9: Bounds on $(\lambda'_{\mathbf{ijk}}\lambda'_{\mathbf{lmn}})$.

$(\lambda'_{ijk}\ \lambda'_{lmn})$	From reference [1]		Previously published		
$ijk\ lmn$	Bound	Decay	Bound	Decay	Key
112 212	76 $[\tilde{u}_{1L}]^2$	$\eta\to\mu\bar{e}+e\bar{\mu}$	none	n/a	New
	1.1 $\times10^{+5}$ $[\tilde{u}_{1L}]^2$	$\eta'\to\mu\bar{e}$			
112 213	9.4 $\times10^{-3}$ $[\tilde{u}_{1L}]^2$	$B^0_s\to e\bar{\mu}$	9.6 $\times10^{-3}$ $[\tilde{u}_{1L}]^2$	$B^0_s\to e\bar{\mu}$	Upd. [60]
112 222	2.8 $\times10^{-2}$ $[\tilde{d}_{2R}]^2$	$D^0\to e\bar{\mu}$	0.02 $[\tilde{d}_{2R}]$ $\times0.21$ $[\tilde{d}_{2R}]$	APV in Cs $\frac{\tau\to\pi^-\nu}{\pi^-\to\mu\bar{\nu}}$	Unimp. [26], [69]
112 311	2.3 $\times10^{-3}$ $[\tilde{u}_{1L}]^2$	$\tau\to eK_S$	2.7 $\times10^{-3}$ $[\tilde{u}_{1L}]^2$	$\tau\to eK^{0*}$	Upd. [64]
	2.9 $\times10^{-3}$ $[\tilde{u}_{1L}]^2$	$\tau\to eK^{*0}$			
112 312	1.2 $\times10^{-3}$ $[\tilde{d}_{2R}]^2$	$\tau\to e\pi^0$	0.02 $[\tilde{d}_{2R}]$ $\times0.12$ $[\tilde{d}_{2R}]$	APV in Cs $\frac{\tau\to\pi^-\nu}{\pi^-\to\mu\bar{\nu}}$	Upd. [26], [26]
	2.0 $\times10^{-3}$ $[\tilde{d}_{2R}]^2$	$\tau\to e\eta$			
	2.4 $\times10^{-3}$ $[\tilde{d}_{2R}]^2$	$\tau\to e\rho^0$			
112 312	1.2 $\times10^{-3}$ $[\tilde{u}_{1L}]^2$	$\tau\to e\eta$	none	n/a	$^{\dagger(-)}$ New
	3.4 $\times10^{-3}$ $[\tilde{u}_{1L}]^2$	$\tau\to e\phi$			
113 211	1.6 $\times10^{-3}$ $[\tilde{u}_{1L}]^2$	$B^0_d\to\mu\bar{e}$	4.7 $\times10^{-3}$ $[\tilde{u}_{1L}]^2$	$B^0_d\to\mu\bar{e}$	Upd. [60]
113 212	9.4 $\times10^{-3}$ $[\tilde{u}_{1L}]^2$	$B^0_s\to\mu\bar{e}$	9.6 $\times10^{-3}$ $[\tilde{u}_{1L}]^2$	$B^0_s\to\mu\bar{e}$	Upd. [60]
113 213	0.36 $[\tilde{d}_{3R}]^2$	$\pi^0\to e\bar{\mu}$	4.5 $\times10^{-8}$ $[\tilde{d}_{3R}]^2$	$\mu\to e$ in ^{48}Ti	Unimp. [67]
	11 $[\tilde{d}_{3R}]^2$	$\pi^0\to\mu\bar{e}$			
	1.5 $\times10^{+2}$ $[\tilde{d}_{3R}]^2$	$\eta\to\mu\bar{e}+e\bar{\mu}$			
	1.9 $\times10^{+4}$ $[\tilde{d}_{3R}]^2$	$\eta'\to\mu\bar{e}/e\bar{\mu}$			
113 223	2.8 $\times10^{-2}$ $[\tilde{d}_{3R}]^2$	$D^0\to e\bar{\mu}$	0.02 $[\tilde{d}_{3R}]$ $\times0.21$ $[\tilde{d}_{3R}]$	APV in Cs $\frac{\tau\to\pi^-\nu}{\pi^-\to\mu\bar{\nu}}$	Unimp. [26], [69]
113 311	2.7 $\times10^{-3}$ $[\tilde{u}_{1L}]^2$	$B^0_d\to\tau\bar{e}$	5.9 $\times10^{-3}$ $[\tilde{u}_{1L}]^2$	$B^0_d\to\tau\bar{e}$	Upd. [60]
113 313	1.2 $\times10^{-3}$ $[\tilde{d}_{3R}]^2$	$\tau\to e\pi^0$	0.02 $[\tilde{d}_{3R}]$ $\times0.12$ $[\tilde{d}_{3R}]$	APV in Cs $\frac{\tau\to\pi^-\nu}{\pi^-\to\mu\bar{\nu}}$	Upd. [26], [26]
	2.0 $\times10^{-3}$ $[\tilde{d}_{3R}]^2$	$\tau\to e\eta$			
	2.4 $\times10^{-3}$ $[\tilde{d}_{3R}]^2$	$\tau\to e\rho^0$			
121 123	2.6 $\times10^{-2}$ $[\tilde{u}_{2L}]^2$	$B^0_d\to e\bar{e}$	0.03 $[\tilde{u}_{2L}]$ $\times0.18$ $[\tilde{u}_{2L}]$	APV in Cs A^b_{FB}	Unimp. [26], [26]
121 211	9.0 $\times10^{-3}$ $[\tilde{d}_{1R}]^2$	$D^0\to\mu\bar{e}$	0.21 $[\tilde{d}_{1R}]$ $\times5.9$ $\times10^{-2}$ $[\tilde{d}_{1R}]$	A^c_{FB} $\frac{\pi^-\to e\bar{\nu}}{\pi^-\to\mu\bar{\nu}}$	Upd. [26], [65]
121 221	1.6 $[\tilde{d}_{1R}]^2$	$J/\psi\to\mu\bar{e}/e\bar{\mu}$	0.21 $[\tilde{d}_{1R}]$ $\times0.21$ $[\tilde{d}_{1R}]$	A^c_{FB} $\frac{D^0\to\nu\bar{\mu}K^-}{D^0\to\nu\bar{e}K^-}$	Unimp. [26], [69]

Table 3.10: Bounds on $(\lambda'_{\mathbf{ijk}}\lambda'_{\mathbf{lmn}})$ continued.

$(\lambda'_{ijk}\ \lambda'_{lmn})$	From reference [1]		Previously published		
$ijk\ lmn$	Bound	Decay	Bound	Decay	Key
121 221	$0.36 \quad [\tilde{u}_{2L}]^2$	$\pi^0 \to e\bar{\mu}$	$4.3 \times 10^{-8}\ [\tilde{u}_{2L}]^2$	$\mu \to e$ in ^{48}Ti	Unimp. [67]
	$11 \quad [\tilde{u}_{2L}]^2$	$\pi^0 \to \mu\bar{e}$			
	$1.5 \times 10^{+2}\ [\tilde{u}_{2L}]^2$	$\eta \to \mu\bar{e} + e\bar{\mu}$			
	$1.9 \times 10^{+4}\ [\tilde{u}_{2L}]^2$	$\eta' \to \mu\bar{e}$			
121 222	$2.7 \times 10^{-7}\ [\tilde{u}_{2L}]^2$	$K_L^0 \to \mu\bar{e}/e\bar{\mu}$	$3 \times 10^{-7}\ [\tilde{u}_{2L}]^2$	$K_L^0 \to \mu\bar{e}/e\bar{\mu}$	$^{\dagger(-)}$ Agr. [63]
121 223	$1.6 \times 10^{-3}\ [\tilde{u}_{2L}]^2$	$B_d^0 \to e\bar{\mu}$	$4.7 \times 10^{-3}\ [\tilde{u}_{2L}]^2$	$B_d^0 \to e\bar{\mu}$	Upd. [60]
121 321	$5.9 \quad [\tilde{d}_{1R}]^2$	$J/\psi \to \tau\bar{e}/e\bar{\tau}$	$0.21 \quad [\tilde{d}_{1R}]$ $\times 0.52 \quad [\tilde{d}_{1R}]$	A_{FB}^c $\frac{D_s^- \to \tau\bar{\nu}}{D_s^- \to \mu\bar{\nu}}$	Unimp. [26], [70]
121 321	$1.2 \times 10^{-3}\ [\tilde{u}_{2L}]^2$	$\tau \to e\pi^0$	$2.4 \times 10^{-3}\ [\tilde{u}_{2L}]^2$	$\tau \to e\rho^0$	Upd. [64] $^{\dagger(-)}$
	$2.0 \times 10^{-3}\ [\tilde{u}_{2L}]^2$	$\tau \to e\eta$			
	$2.4 \times 10^{-3}\ [\tilde{u}_{2L}]^2$	$\tau \to e\rho^0$			
121 322	$2.3 \times 10^{-3}\ [\tilde{u}_{2L}]^2$	$\tau \to eK_S$	none	n/a	New
	$3.6 \times 10^{-3}\ [\tilde{u}_{2L}]^2$	$\tau \to e\bar{K}^{*0}$			
121 323	$2.7 \times 10^{-3}\ [\tilde{u}_{2L}]^2$	$B_d^0 \to e\bar{\tau}$	$5.9 \times 10^{-3}\ [\tilde{u}_{2L}]^2$	$B_d^0 \to e\bar{\tau}$	Upd. [60]
122 123	$4.1 \quad [\tilde{u}_{2L}]^2$	$B_s^0 \to e\bar{e}$	$0.18 \quad [\tilde{u}_{2L}]$ $\times 0.28 \quad [\tilde{u}_{2L}]$	A_{FB}^b A_{FB}^s	Unimp. [26], [26]
122 212	$9.0 \times 10^{-3}\ [\tilde{d}_{2R}]^2$	$D^0 \to \mu\bar{e}$	$0.21 \quad [\tilde{d}_{2R}]$ $\times 5.9 \times 10^{-2}\ [\tilde{d}_{2R}]$	A_{FB}^c $\frac{\pi^- \to e\bar{\nu}}{\pi^- \to \mu\bar{\nu}}$	Upd. [26], [65]
122 221	$2.7 \times 10^{-7}\ [\tilde{u}_{2L}]^2$	$K_L^0 \to \mu\bar{e}/e\bar{\mu}$	$3 \times 10^{-7}\ [\tilde{u}_{2L}]^2$	$K_L^0 \to \mu\bar{e}/e\bar{\mu}$	$^{\dagger(-)}$ Agr. [63]
122 222	$1.6 \quad [\tilde{d}_{2R}]^2$	$J/\psi \to \mu\bar{e}/e\bar{\mu}$	$0.21 \quad [\tilde{d}_{2R}]$ $\times 0.21 \quad [\tilde{d}_{2R}]$	A_{FB}^c $\frac{D^0 \to \nu\bar{\mu}K^-}{D^0 \to \nu\bar{e}K^-}$	Unimp. [26], [69]
122 222	$76 \quad [\tilde{u}_{2L}]^2$	$\eta \to \mu\bar{e} + e\bar{\mu}$	none	n/a	New
	$1.1 \times 10^{+5}\ [\tilde{u}_{2L}]^2$	$\eta' \to \mu\bar{e}$			
122 223	$9.4 \times 10^{-3}\ [\tilde{u}_{2L}]^2$	$B_s^0 \to e\bar{\mu}$	$9.6 \times 10^{-3}\ [\tilde{u}_{2L}]^2$	$B_s^0 \to e\bar{\mu}$	Upd. [60]
122 321	$2.3 \times 10^{-3}\ [\tilde{u}_{2L}]^2$	$\tau \to eK_S$	$2.7 \times 10^{-3}\ [\tilde{u}_{2L}]^2$	$\tau \to eK^{0*}$	Upd. [64]
	$2.9 \times 10^{-3}\ [\tilde{u}_{2L}]^2$	$\tau \to eK^{*0}$			
122 322	$5.9 \quad [\tilde{d}_{2R}]^2$	$J/\psi \to \tau\bar{e}/e\bar{\tau}$	$0.21 \quad [\tilde{d}_{2R}]$ $\times 0.52 \quad [\tilde{d}_{2R}]$	A_{FB}^c $\frac{D_s^- \to \tau\bar{\nu}}{D_s^- \to \mu\bar{\nu}}$	Unimp. [26], [70]
122 322	$1.2 \times 10^{-3}\ [\tilde{u}_{2L}]^2$	$\tau \to e\eta$	none	n/a	$^{\dagger(-)}$ New
	$3.4 \times 10^{-3}\ [\tilde{u}_{2L}]^2$	$\tau \to e\phi$			

Table 3.11: Bounds on $(\lambda'_{\mathbf{ijk}}\lambda'_{\mathbf{lmn}})$ continued.

$(\lambda'_{ijk}\ \lambda'_{lmn})$	From reference [1]		Previously published		
$ijk\ lmn$	Bound	Decay	Bound	Decay	Key
123 213	$9.0\ \times 10^{-3}\ [\tilde{d}_{3R}]^2$	$D^0 \to \mu\bar{e}$	$0.21\ [\tilde{d}_{3R}]$ $\times 5.9\ \times 10^{-2}\ [\tilde{d}_{3R}]$	A^c_{FB} $\frac{\pi^- \to e\bar{\nu}}{\pi^- \to \mu\bar{\nu}}$	Upd. [26], [65]
123 221	$1.6\ \times 10^{-3}\ [\tilde{u}_{2L}]^2$	$B^0_d \to \mu\bar{e}$	$4.7\ \times 10^{-3}\ [\tilde{u}_{2L}]^2$	$B^0_d \to \mu\bar{e}$	Upd. [60]
123 222	$9.4\ \times 10^{-3}\ [\tilde{u}_{2L}]^2$	$B^0_s \to \mu\bar{e}$	$9.6\ \times 10^{-3}\ [\tilde{u}_{2L}]^2$	$B^0_s \to \mu\bar{e}$	Upd. [60]
123 223	$1.6\ [\tilde{d}_{3R}]^2$	$J/\psi \to \mu\bar{e}/e\bar{\mu}$	$0.21\ [\tilde{d}_{3R}]$ $\times 0.21\ [\tilde{d}_{3R}]$	A^c_{FB} $\frac{D^0 \to \nu\bar{\mu}K^-}{D^0 \to \nu\bar{e}K^-}$	Unimp. [26], [69]
123 321	$2.7\ \times 10^{-3}\ [\tilde{u}_{2L}]^2$	$B^0_d \to \tau\bar{e}$	$5.9\ \times 10^{-3}\ [\tilde{u}_{2L}]^2$	$B^0_d \to \tau\bar{e}$	Upd. [60]
123 323	$5.9\ [\tilde{d}_{3R}]^2$	$J/\psi \to \tau\bar{e}/e\bar{\tau}$	$0.21\ [\tilde{d}_{3R}]$ $\times 0.52\ [\tilde{d}_{3R}]$	A^c_{FB} $\frac{D_s^- \to \tau\bar{\nu}}{D_s^- \to \mu\bar{\nu}}$	Unimp. [26], [70]
131 133	$2.6\ \times 10^{-2}\ [\tilde{u}_{3L}]^2$	$B^0_d \to e\bar{e}$	$0.03\ [\tilde{u}_{3L}]$ $\times 0.18\ [\tilde{u}_{3L}]$	APV in Cs A^b_{FB}	Unimp. [26], [26]
131 231	$0.36\ [\tilde{u}_{3L}]^2$	$\pi^0 \to e\bar{\mu}$	$4.3\ \times 10^{-8}\ [\tilde{u}_{3L}]^2$	$\mu \to e$ in ^{48}Ti	Unimp. [67]
	$11\ [\tilde{u}_{3L}]^2$	$\pi^0 \to \mu\bar{e}$			
	$1.5\ \times 10^{+2}\ [\tilde{u}_{3L}]^2$	$\eta \to \mu\bar{e} + e\bar{\mu}$			
	$1.9\ \times 10^{+4}\ [\tilde{u}_{3L}]^2$	$\eta' \to \mu\bar{e}$			
131 232	$2.7\ \times 10^{-7}\ [\tilde{u}_{3L}]^2$	$K^0_L \to \mu\bar{e}/e\bar{\mu}$	$3\ \times 10^{-7}\ [\tilde{u}_{3L}]^2$	$K^0_L \to \mu\bar{e}/e\bar{\mu}$	$^{\dagger(-)}$ Agr. [63]
131 233	$1.6\ \times 10^{-3}\ [\tilde{u}_{3L}]^2$	$B^0_d \to e\bar{\mu}$	$4.7\ \times 10^{-3}\ [\tilde{u}_{3L}]^2$	$B^0_d \to e\bar{\mu}$	Upd. [60]
131 331	$1.2\ \times 10^{-3}\ [\tilde{u}_{3L}]^2$	$\tau \to e\pi^0$	$2.4\ \times 10^{-3}\ [\tilde{u}_{3L}]^2$	$\tau \to e\rho^0$	Upd. [64] $^{\dagger(-)}$
	$2.0\ \times 10^{-3}\ [\tilde{u}_{3L}]^2$	$\tau \to e\eta$			
	$2.4\ \times 10^{-3}\ [\tilde{u}_{3L}]^2$	$\tau \to e\rho^0$			
131 332	$2.3\ \times 10^{-3}\ [\tilde{u}_{3L}]^2$	$\tau \to eK_S$	none	n/a	New
	$3.6\ \times 10^{-3}\ [\tilde{u}_{3L}]^2$	$\tau \to e\bar{K}^{*0}$			
131 333	$2.7\ \times 10^{-3}\ [\tilde{u}_{3L}]^2$	$B^0_d \to e\bar{\tau}$	$5.9\ \times 10^{-3}\ [\tilde{u}_{3L}]^2$	$B^0_d \to e\bar{\tau}$	Upd. [60]
132 133	$4.1\ [\tilde{u}_{3L}]^2$	$B^0_s \to e\bar{e}$	$0.18\ [\tilde{u}_{3L}]$ $\times 0.28\ [\tilde{u}_{3L}]$	A^b_{FB} A^s_{FB}	Unimp. [26], [26]
132 231	$2.7\ \times 10^{-7}\ [\tilde{u}_{3L}]^2$	$K^0_L \to \mu\bar{e}/e\bar{\mu}$	$3\ \times 10^{-7}\ [\tilde{u}_{3L}]^2$	$K^0_L \to \mu\bar{e}/e\bar{\mu}$	$^{\dagger(-)}$ Agr. [63]
132 232	$76\ [\tilde{u}_{3L}]^2$	$\eta \to \mu\bar{e} + e\bar{\mu}$	none	n/a	New
	$1.1\ \times 10^{+5}\ [\tilde{u}_{3L}]^2$	$\eta' \to \mu\bar{e}$			
132 233	$9.4\ \times 10^{-3}\ [\tilde{u}_{3L}]^2$	$B^0_s \to e\bar{\mu}$	$9.6\ \times 10^{-3}\ [\tilde{u}_{3L}]^2$	$B^0_s \to e\bar{\mu}$	Upd. [60]

Table 3.12: Bounds on $(\lambda'_{\mathbf{ijk}}\lambda'_{\mathbf{lmn}})$ continued.

$(\lambda'_{ijk}\ \lambda'_{lmn})$	From reference [1]		Previously published		
$ijk\ lmn$	Bound	Decay	Bound	Decay	Key
132 331	$2.3\times10^{-3}\ [\tilde{u}_{3L}]^2$	$\tau\to eK_S$	$2.7\times10^{-3}\ [\tilde{u}_{3L}]^2$	$\tau\to eK^{0*}$	Upd. [64]
	$2.9\times10^{-3}\ [\tilde{u}_{3L}]^2$	$\tau\to eK^{*0}$			
132 332	$1.2\times10^{-3}\ [\tilde{u}_{3L}]^2$	$\tau\to e\eta$	none	n/a	$^{\dagger(-)}$ New
	$3.4\times10^{-3}\ [\tilde{u}_{3L}]^2$	$\tau\to e\phi$			
133 231	$1.6\times10^{-3}\ [\tilde{u}_{3L}]^2$	$B^0_d\to\mu\bar{e}$	$4.7\times10^{-3}\ [\tilde{u}_{3L}]^2$	$B^0_d\to\mu\bar{e}$	Upd. [60]
133 232	$9.4\times10^{-3}\ [\tilde{u}_{3L}]^2$	$B^0_s\to\mu\bar{e}$	$9.6\times10^{-3}\ [\tilde{u}_{3L}]^2$	$B^0_s\to\mu\bar{e}$	Upd. [60]
133 331	$2.7\times10^{-3}\ [\tilde{u}_{3L}]^2$	$B^0_d\to\tau\bar{e}$	$5.9\times10^{-3}\ [\tilde{u}_{3L}]^2$	$B^0_d\to\tau\bar{e}$	Upd. [60]
211 213	$5.4\times10^{-4}\ [\tilde{u}_{1L}]^2$	$B^0_d\to\mu\bar{\mu}$	$2.1\times10^{-3}\ [\tilde{u}_{1L}]^2$	$B^0_d\to\mu\bar{\mu}$	Upd. [60]
211 311	$1.6\times10^{-3}\ [\tilde{d}_{1R}]^2$	$\tau\to\mu\eta$	$4.4\times10^{-3}\ [\tilde{d}_{1R}]^2$	$\tau\to\mu\rho^0$	Upd. [64]
	$1.8\times10^{-3}\ [\tilde{d}_{1R}]^2$	$\tau\to\mu\pi^0$			
	$4.3\times10^{-3}\ [\tilde{d}_{1R}]^2$	$\tau\to\mu\rho^0$			
211 311	$1.6\times10^{-3}\ [\tilde{u}_{1L}]^2$	$\tau\to\mu\eta$	$4.4\times10^{-3}\ [\tilde{u}_{1L}]^2$	$\tau\to\mu\rho^0$	$^{\dagger(-)}$ Upd. [64]
	$1.8\times10^{-3}\ [\tilde{u}_{1L}]^2$	$\tau\to\mu\pi^0$			
	$4.3\times10^{-3}\ [\tilde{u}_{1L}]^2$	$\tau\to\mu\rho^0$			
211 312	$2.4\times10^{-3}\ [\tilde{u}_{1L}]^2$	$\tau\to\mu K_S$	none	n/a	New
	$3.6\times10^{-3}\ [\tilde{u}_{1L}]^2$	$\tau\to\mu\bar{K}^{*0}$			
211 313	$1.6\times10^{-3}\ [\tilde{u}_{1L}]^2$	$B^0_d\to\mu\bar{\tau}$	$7.3\times10^{-3}\ [\tilde{u}_{1L}]^2$	$B^0_d\to\mu\bar{\tau}$	Upd. [60]
212 213	$1.0\times10^{-3}\ [\tilde{u}_{1L}]^2$	$B^0_s\to\mu\bar{\mu}$	$4.6\times10^{-5}\ [\tilde{u}_{1L}]^2$	$B^0_d\to K^0\mu\bar{\mu}$	Unimp. [68]
212 311	$2.4\times10^{-3}\ [\tilde{u}_{1L}]^2$	$\tau\to\mu K_S$	$3.4\times10^{-3}\ [\tilde{u}_{1L}]^2$	$\tau\to\mu K^{0*}$	Upd. [64]
	$3.6\times10^{-3}\ [\tilde{u}_{1L}]^2$	$\tau\to\mu K^{*0}$			
212 312	$1.6\times10^{-3}\ [\tilde{d}_{2R}]^2$	$\tau\to\mu\eta$	$4.4\times10^{-3}\ [\tilde{d}_{2R}]^2$	$\tau\to\mu\rho^0$	Upd. [64]
	$1.8\times10^{-3}\ [\tilde{d}_{2R}]^2$	$\tau\to\mu\pi^0$			
	$4.3\times10^{-3}\ [\tilde{d}_{2R}]^2$	$\tau\to\mu\rho^0$			
212 312	$9.2\times10^{-4}\ [\tilde{u}_{1L}]^2$	$\tau\to\mu\eta$	none	n/a	$^{\dagger(-)}$ New
	$3.4\times10^{-3}\ [\tilde{u}_{1L}]^2$	$\tau\to\mu\phi$			
213 311	$1.6\times10^{-3}\ [\tilde{u}_{1L}]^2$	$B^0_d\to\tau\bar{\mu}$	$7.3\times10^{-3}\ [\tilde{u}_{1L}]^2$	$B^0_d\to\tau\bar{\mu}$	Upd. [60]
213 313	$1.6\times10^{-3}\ [\tilde{d}_{3R}]^2$	$\tau\to\mu\eta$	$4.4\times10^{-3}\ [\tilde{d}_{3R}]^2$	$\tau\to\mu\rho^0$	Upd. [64]
	$1.8\times10^{-3}\ [\tilde{d}_{3R}]^2$	$\tau\to\mu\pi^0$			
	$4.3\times10^{-3}\ [\tilde{d}_{3R}]^2$	$\tau\to\mu\rho^0$			
221 223	$5.4\times10^{-4}\ [\tilde{u}_{2L}]^2$	$B^0_d\to\mu\bar{\mu}$	$2.1\times10^{-3}\ [\tilde{u}_{2L}]^2$	$B^0_d\to\mu\bar{\mu}$	Upd. [60]

Table 3.13: Bounds on $(\lambda'_{\mathbf{ijk}}\lambda'_{\mathbf{lmn}})$ continued.

$(\lambda'_{ijk}\ \lambda'_{lmn})$	From reference [1]		Previously published		
$ijk\ lmn$	Bound	Decay	Bound	Decay	Key
221 321	2.9 $[\tilde{d}_{1R}]^2$	$J/\psi \to \tau\bar{\mu}/\mu\bar{\tau}$	0.21 $[\tilde{d}_{1R}]$ $\times 0.52$ $[\tilde{d}_{1R}]$	$\frac{D^0\to\nu\bar{\mu}K^-}{D^0\to\nu\bar{e}K^-}$ $\frac{D_s^-\to\tau\bar{\nu}}{D_s^-\to\mu\bar{\nu}}$	Unimp. [69], [70]
221 321	1.6×10^{-3} $[\tilde{u}_{2L}]^2$	$\tau\to\mu\eta$	4.4×10^{-3} $[\tilde{u}_{2L}]^2$	$\tau\to\mu\rho^0$	$^{\dagger(-)}$ Upd. [64]
	1.8×10^{-3} $[\tilde{u}_{2L}]^2$	$\tau\to\mu\pi^0$			
	4.3×10^{-3} $[\tilde{u}_{2L}]^2$	$\tau\to\mu\rho^0$			
221 322	2.4×10^{-3} $[\tilde{u}_{2L}]^2$	$\tau\to\mu K_S$	none	n/a	New
	3.6×10^{-3} $[\tilde{u}_{2L}]^2$	$\tau\to\mu\bar{K}^{*0}$			
221 323	1.6×10^{-3} $[\tilde{u}_{2L}]^2$	$B_d^0\to\mu\bar{\tau}$	7.3×10^{-3} $[\tilde{u}_{2L}]^2$	$B_d^0\to\mu\bar{\tau}$	Upd. [60]
222 223	1.0×10^{-3} $[\tilde{u}_{2L}]^2$	$B_s^0\to\mu\bar{\mu}$	4.6×10^{-5} $[\tilde{u}_{2L}]^2$	$B_d^0\to K^0\mu\bar{\mu}$	Unimp. [68]
222 321	2.4×10^{-3} $[\tilde{u}_{2L}]^2$	$\tau\to\mu K_S$	3.4×10^{-3} $[\tilde{u}_{2L}]^2$	$\tau\to\mu K^{0*}$	Upd. [64]
	3.6×10^{-3} $[\tilde{u}_{2L}]^2$	$\tau\to\mu K^{*0}$			
222 322	2.9 $[\tilde{d}_{2R}]^2$	$J/\psi \to \tau\bar{\mu}/\mu\bar{\tau}$	0.21 $[\tilde{d}_{2R}]$ $\times 0.52$ $[\tilde{d}_{2R}]$	$\frac{D^0\to\nu\bar{\mu}K^-}{D^0\to\nu\bar{e}K^-}$ $\frac{D_s^-\to\tau\bar{\nu}}{D_s^-\to\mu\bar{\nu}}$	Unimp. [69], [70]
222 322	9.2×10^{-4} $[\tilde{u}_{2L}]^2$	$\tau\to\mu\eta$	none	n/a	$^{\dagger(-)}$ New
	3.4×10^{-3} $[\tilde{u}_{2L}]^2$	$\tau\to\mu\phi$			
223 321	1.6×10^{-3} $[\tilde{u}_{2L}]^2$	$B_d^0\to\tau\bar{\mu}$	7.3×10^{-3} $[\tilde{u}_{2L}]^2$	$B_d^0\to\tau\bar{\mu}$	Upd. [60]
223 323	2.9 $[\tilde{d}_{3R}]^2$	$J/\psi \to \tau\bar{\mu}/\mu\bar{\tau}$	0.21 $[\tilde{d}_{3R}]$ $\times 0.52$ $[\tilde{d}_{3R}]$	$\frac{D^0\to\nu\bar{\mu}K^-}{D^0\to\nu\bar{e}K^-}$ $\frac{D_s^-\to\tau\bar{\nu}}{D_s^-\to\mu\bar{\nu}}$	Unimp. [69], [70]
231 233	5.4×10^{-4} $[\tilde{u}_{3L}]^2$	$B_d^0\to\mu\bar{\mu}$	2.1×10^{-3} $[\tilde{u}_{3L}]^2$	$B_d^0\to\mu\bar{\mu}$	Upd. [60]
231 331	1.6×10^{-3} $[\tilde{u}_{3L}]^2$	$\tau\to\mu\eta$	4.4×10^{-3} $[\tilde{u}_{3L}]^2$	$\tau\to\mu\rho^0$	$^{\dagger(-)}$ Upd. [64]
	1.8×10^{-3} $[\tilde{u}_{3L}]^2$	$\tau\to\mu\pi^0$			
	4.3×10^{-3} $[\tilde{u}_{3L}]^2$	$\tau\to\mu\rho^0$			
231 332	2.4×10^{-3} $[\tilde{u}_{3L}]^2$	$\tau\to\mu K_S$	none	n/a	New
	3.6×10^{-3} $[\tilde{u}_{3L}]^2$	$\tau\to\mu\bar{K}^{*0}$			
231 333	1.6×10^{-3} $[\tilde{u}_{3L}]^2$	$B_d^0\to\mu\bar{\tau}$	7.3×10^{-3} $[\tilde{u}_{3L}]^2$	$B_d^0\to\mu\bar{\tau}$	Upd. [60]
232 233	1.0×10^{-3} $[\tilde{u}_{3L}]^2$	$B_s^0\to\mu\bar{\mu}$	4.6×10^{-5} $[\tilde{u}_{3L}]^2$	$B_d^0\to K^0\mu\bar{\mu}$	Unimp. [68]
232 331	2.4×10^{-3} $[\tilde{u}_{3L}]^2$	$\tau\to\mu K_S$	3.4×10^{-3} $[\tilde{u}_{3L}]^2$	$\tau\to\mu K^{0*}$	Upd. [64]
	3.6×10^{-3} $[\tilde{u}_{3L}]^2$	$\tau\to\mu K^{*0}$			
232 332	9.2×10^{-4} $[\tilde{u}_{3L}]^2$	$\tau\to\mu\eta$	none	n/a	$^{\dagger(-)}$ New
	3.4×10^{-3} $[\tilde{u}_{3L}]^2$	$\tau\to\mu\phi$			
233 331	1.6×10^{-3} $[\tilde{u}_{3L}]^2$	$B_d^0\to\tau\bar{\mu}$	7.3×10^{-3} $[\tilde{u}_{3L}]^2$	$B_d^0\to\tau\bar{\mu}$	Upd. [60]

Table 3.14: Bounds on $(\lambda'_{\mathbf{ijk}}\lambda'_{\mathbf{lmn}})$ continued.

Chapter 4

Bounds On R–Parity Violating Terms from OPAL

The OPAL collaboration searched for lepton flavor violation in electron–positron collisions at LEP2 energies [71], and provided 95% confidence limits on the cross–sections for $e^+e^- \to e^\mp\mu^\pm / e^\mp\tau^\pm / \mu^\mp\tau^\pm$. This allows one to set bounds on $\lambda_{ijk}\lambda_{lmn}$–type combinations, though with a dependence on the mediating sneutrino mass that is not linear. These may be compared to the relevant bounds from τ lepton and muon decay data, and may possibly complement them through the different mass dependence.

4.1 Analytic Expressions

The Feynman diagrams and matrix elements for the appropriate processes are very similar to those from the purely leptonic decay of heavy leptons in section 3.2.2. The only difference, bar which values the flavor indices take, is to replace an outgoing charged lepton with an incoming charged anti–lepton, as shown in figure 4.1. For the matrix element, this entails that the spinor $\bar{u}(p_{e_b})$ for an outgoing lepton of flavor b is replaced by $\bar{v}(p_{e_b})$ for an incoming anti–lepton of flavor b, and that the propagator $i/(p^2_{\tilde{\nu}_{gL}} - m^2_{\tilde{\nu}_{gL}})$ can *not* be approximated as $-i/m^2_{\tilde{\nu}_{gL}}$. Instead, $p^2_{\tilde{\nu}_{gL}}$ is replaced by one of either of the Mandelstam variables s or t. The choice of s or t is related to the choice of which of the flavor indices a, b, c and d are chosen to represent which of the leptons. The following choice is made: e_a is the incoming lepton, $\bar{e}_b$ is the incoming anti–lepton, e_c is the outgoing lepton and $\bar{e}_d$ is the outgoing anti–lepton. Hence $a = b = 1$. The Mandelstam variable t is defined to be $(p_{e_a} - p_{e_c})^2$, and $s = (p_{e_a} + p_{\bar{e}_b})^2$. The momentum–squared of the sneutrino appearing in the propagator is then s for the terms involving lepton e_a and anti–lepton $\bar{e}_b$ at a vertex, *i.e.* those terms involving λ_{gab} or λ^*_{gba}, or t for the terms involving lepton e_a and lepton e_c at a vertex, *i.e.* those terms involving λ_{gac} or λ^*_{gca}. Also, the fact that the sneutrino can decay must be taken into account by the relativistic Breit–Wigner form of the propagator, which dampens the s–channel resonance. The fact that the sneutrino can decay into on–shell particles implies that its self–energy corrections to its mass gain an imaginary part, hence the propagator can be written in the form $i/(p^2_{\tilde{\nu}_{gL}} - m^2_{\tilde{\nu}_{gL}} + im_{\tilde{\nu}_{gL}}\Gamma_{\tilde{\nu}_{gL}})$, where $\Gamma_{\tilde{\nu}_{gL}}$ is the decay width of the sneutrino, in the approximation that the imaginary part of the self–energy is small. The s–channel propagator is then taken to be $i/(p^2_{\tilde{\nu}_{gL}} - m^2_{\tilde{\nu}_{gL}} + ir_\Gamma m^2_{\tilde{\nu}_{gL}})$, parametrizing the decay width of the sneutrino as r_Γ times its mass. Since the decay width of the sneutrino in the RPVMSSM involves many unknowns, in the analysis r_Γ is set to be 5% and 10%. For comparison, the Z boson decay width is roughly 3% of m_Z and the $W^\pm$ boson decay width is roughly 3% of m_W.

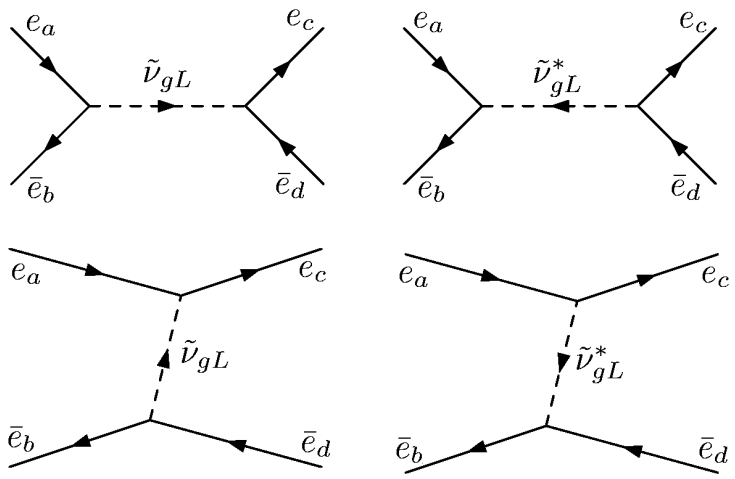

Figure 4.1: The Feynman diagrams for the process of a charged lepton of flavor a interacting with a charged anti–lepton of flavor b to form a charged lepton of flavor c and a charged anti–lepton of flavor d.

4.1.1 Matrix Element

The matrix element for this process is given by

$$\begin{aligned} i\mathcal{M}_{e_a\bar{e}_b\to e_c\bar{e}_d} &= \langle e_c(p_{e_c}),\bar{e}_d(p_{\bar{e}_d})|[\bar{e}_k(-i)\lambda_{jik}P_L e_i\tilde{\nu}_{jL}][\bar{e}_l(-i)\lambda^*_{mln}P_R e_n\tilde{\nu}^*_{mL}]|e_a(p_{e_a}),\bar{e}_b(p_{\bar{e}_b})\rangle \\ &= \frac{i}{(s-m^2_{\tilde{\nu}_{gL}}+ir_\Gamma m^2_{\tilde{\nu}_{gL}})}([\bar{v}(p_{\bar{e}_b})\lambda^*_{gba}P_R u(p_{e_a})][\bar{u}(p_{e_c})\lambda_{gdc}P_L v(p_{\bar{e}_d})] \\ &\quad +[\bar{v}(p_{e_b})\lambda_{gab}P_L u(p_{e_a})][\bar{u}(p_{e_c})\lambda^*_{gcd}P_R v(p_{\bar{e}_d})]) \\ &\quad -\frac{i}{(t-m^2_{\tilde{\nu}_{gL}})}([\bar{v}(p_{\bar{e}_b})\lambda_{gdb}P_L v(p_{\bar{e}_d})][\bar{u}(p_{e_c})\lambda^*_{gca}P_R u(p_{e_a})] \\ &\quad +[\bar{u}(p_{e_c})\lambda_{gac}P_L u(p_{e_a})][\bar{v}(p_{\bar{e}_b})\lambda^*_{gbd}P_R v(p_{\bar{e}_d})]) \end{aligned} \tag{4.1}$$

4.1.2 Differential Cross–Section

Squaring the matrix element, summing over final spins and averaging over initial spins, gives the following differential cross–section:

$$\begin{aligned} \left(\frac{\mathrm{d}\sigma}{\mathrm{d}\Omega}\right)_{e_a\bar{e}_b\to e_c\bar{e}_d} &= \frac{1}{256\pi^2 s}\left(\frac{s^2}{((s-m^2_{\tilde{\nu}_{gL}})^2+r^2_\Gamma m^4_{\tilde{\nu}_{gL}})}(|\lambda_{gdc}|^2|\lambda_{gba}|^2+|\lambda_{gcd}|^2|\lambda_{gab}|^2)\right. \\ &\quad \left. +\frac{t^2}{(t-m^2_{\tilde{\nu}_{gL}})^2}(|\lambda_{gdb}|^2|\lambda_{gca}|^2+|\lambda_{gbd}|^2|\lambda_{gac}|^2)\right) \end{aligned} \tag{4.2}$$

approximating all the (anti–)leptons as massless compared to the center–of–momentum energy $\sqrt{s}$. In making this massless lepton approximation, the cross–terms between the s– and t–channel matrix elements drop out, since they are proportional to the lepton masses.

Setting $a=b=1$ and then summing over the two final states $e_c\bar{e}_d$ plus $e_d\bar{e}_c$ for comparison with the data (given in reference [71] for combined searches, where, for example, no distinction

between $e^-\tau^+$ and $e^+\tau^-$ was made), this reduces to the following three cases:

$$\left(\frac{\mathrm{d}\sigma}{\mathrm{d}\Omega}\right)_{e\bar{e}\to e\mu} = \frac{1}{128\pi^2 s}\left(\frac{s^2}{((s-m^2_{\tilde{\nu}_{gL}})^2+r^2_\Gamma m^4_{\tilde{\nu}_{gL}})}+\frac{t^2}{(t-m^2_{\tilde{\nu}_{gL}})^2}\right) \times(|\lambda_{g21}|^2|\lambda_{g11}|^2+|\lambda_{g12}|^2|\lambda_{g11}|^2) \tag{4.3}$$

$$\left(\frac{\mathrm{d}\sigma}{\mathrm{d}\Omega}\right)_{e\bar{e}\to e\tau} = \frac{1}{128\pi^2 s}\left(\frac{s^2}{((s-m^2_{\tilde{\nu}_{gL}})^2+r^2_\Gamma m^4_{\tilde{\nu}_{gL}})}+\frac{t^2}{(t-m^2_{\tilde{\nu}_{gL}})^2}\right) \times(|\lambda_{g21}|^2|\lambda_{g11}|^2+|\lambda_{g12}|^2|\lambda_{g11}|^2) \tag{4.4}$$

$$\left(\frac{\mathrm{d}\sigma}{\mathrm{d}\Omega}\right)_{e\bar{e}\to \mu\tau} = \frac{1}{128\pi^2 s}\left(\frac{s^2}{((s-m^2_{\tilde{\nu}_{gL}})^2+r^2_\Gamma m^4_{\tilde{\nu}_{gL}})}(|\lambda_{g23}|^2|\lambda_{g11}|^2+|\lambda_{g32}|^2|\lambda_{g11}|^2) + \frac{t^2}{(t-m^2_{\tilde{\nu}_{gL}})^2}(|\lambda_{g21}|^2|\lambda_{g31}|^2+|\lambda_{g12}|^2|\lambda_{g13}|^2)\right) \tag{4.5}$$

4.2 Numerical Results

The bounds on the appropriate $\lambda_{ijk}\lambda_{lmn}$–combinations as a function of the sneutrino mass $m_{\tilde{\nu}_{gL}}$ are calculated by comparing the integrals over the solid angles of the differential cross–sections presented in equations (4.4), (4.5) and (4.5) to the 95% confidence upper limits on the relevant cross–sections given in reference [71]. These bounds are shown in figures 4.2, 4.3 and 4.4, respectively, along with the bounds on the same coupling combinations, using the double coupling dominance convention, from table 3.4 as a function of $m_{\tilde{\nu}_{gL}}$. In figures 4.2 and 4.3, both the s– and the t–channels contribute to the bound on each coupling combination, and in figure 4.4 the s–channel cross–section is dependent on $(|\lambda_{g23}|^2|\lambda_{g11}|^2+|\lambda_{g32}|^2|\lambda_{g11}|^2)$ while the t–channel cross–section is dependent on $(|\lambda_{g21}|^2|\lambda_{g31}|^2+|\lambda_{g12}|^2|\lambda_{g13}|^2)$, so there are two different dependences on the sneutrino mass. In calculating the bounds, an average value of $\sqrt{s}=204.5$ GeV was used though the data were taken in the range $\sqrt{s}=200$ GeV to 209 GeV, hence there is potentially a 2% error associated with this.

4.3 Discussion

As can be seen in figures 4.2, 4.3 and 4.4, unless the sneutrino mass is very close to the center–of–momentum energy of $\sqrt{s}\approx 200$ GeV, the bounds from the non–observation of LFV in τ lepton and muon decays are much stronger than those from the non–observation of LFV at the OPAL experiment. Even considering the mass of the sneutrino to be in the region of such a resonance, where the bounds are very dependent on the decay width of the sneutrino, the bounds are only better if, in the case of $e^+e^-\to e^\mp\tau^\pm/\mu^\mp\tau^\pm$, the decay width is 10% of the mass (*i.e.* 20 GeV) or lower. In the case of $e^+e^-\to e^\mp\mu^\pm$, if the decay width is used as a variable, the value for which the collider bound is better than the decay bound is less than 36 MeV, which is far below the energy resolution of the experiment (for example, the electromagnetic calorimeter resolution was about 3.5% for electrons with momenta above 70 GeV [71]). This result suggests that the signal for $e^+e^-\to e^\mp\mu^\pm$ at a high–energy linear collider predicted by Sun *et al.* [72] is 10^{+4} to 10^{+6} times too large, as the values of the couplings taken are those for the bounds on *individual* couplings, which are far weaker than those on the products.

Though the collider bounds are not as tight as the decay bounds away from the potential resonance, one may deduce that data collected at energies below $\sqrt{s}\approx 200$ GeV might enhance

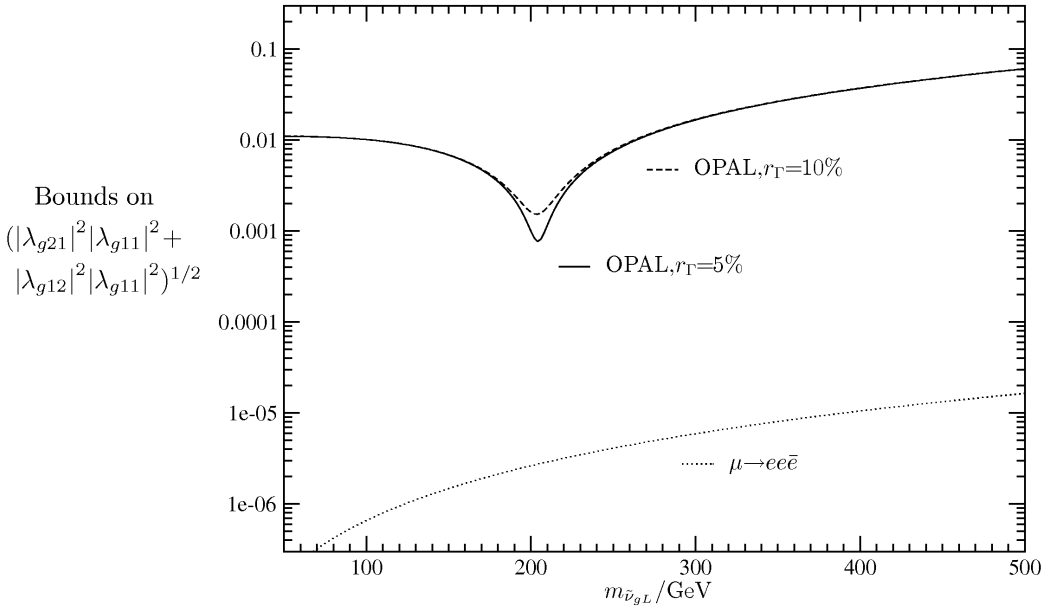

Figure 4.2: The bounds on $(|\lambda_{g21}|^2|\lambda_{g11}|^2 + |\lambda_{g12}|^2|\lambda_{g11}|^2)^{1/2}$ as a function of $m_{\tilde{\nu}_{gL}}$ from the search for $e\bar{e}\to\mu\bar{e}/e\bar{\mu}$ by OPAL in the range 200 GeV $\leq\sqrt{s}\leq$209 GeV.

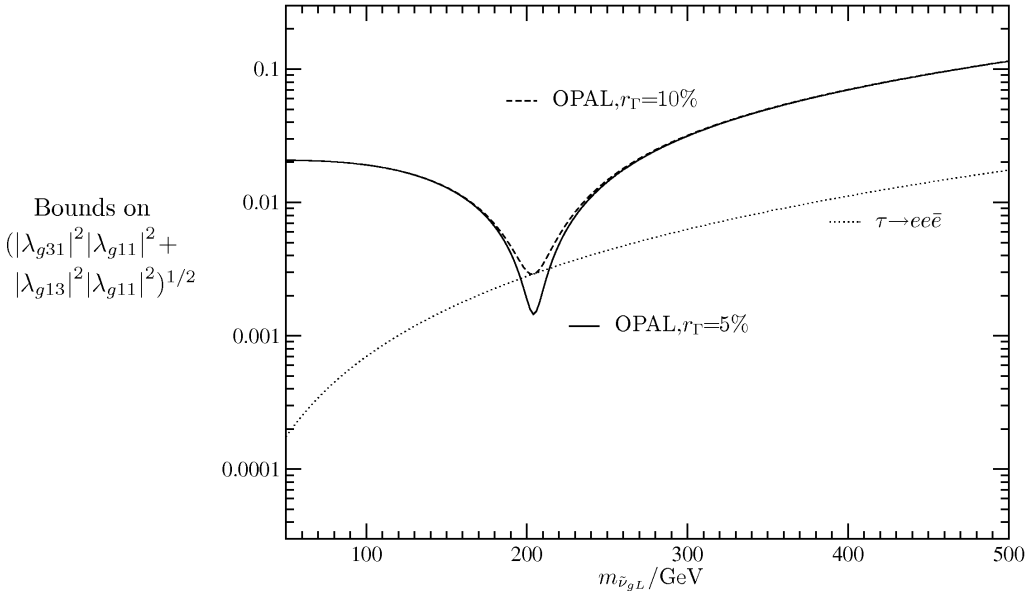

Figure 4.3: The bounds on $(|\lambda_{g31}|^2|\lambda_{g11}|^2 + |\lambda_{g13}|^2|\lambda_{g11}|^2)^{1/2}$ as a function of $m_{\tilde{\nu}_{gL}}$ from the search for $e\bar{e}\to\tau\bar{e}/e\bar{\tau}$ by OPAL in the range 200 GeV $\leq\sqrt{s}\leq$209 GeV.

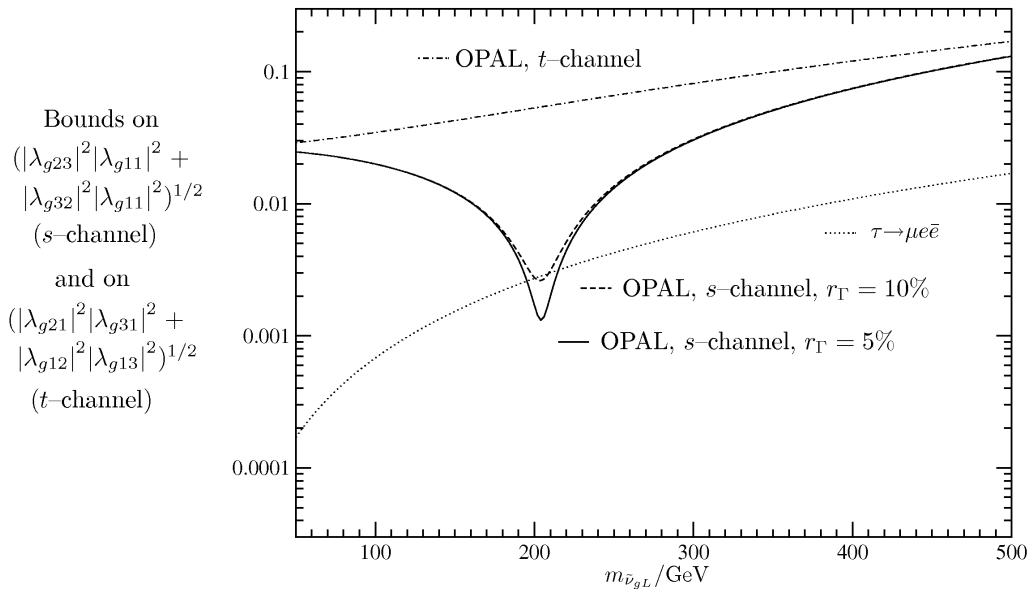

Figure 4.4: The bounds on $(|\lambda_{g23}|^2|\lambda_{g11}|^2 + |\lambda_{g32}|^2|\lambda_{g11}|^2)^{1/2}$ (s–channel) and $(|\lambda_{g21}|^2|\lambda_{g31}|^2 + |\lambda_{g12}|^2|\lambda_{g13}|^2)^{1/2}$ (t–channel) as a function of $m_{\tilde{\nu}_{gL}}$ from the search for $e\bar{e} \to \tau\bar{\mu}/\mu\bar{\tau}$ by OPAL in the range 200 GeV $\leq\sqrt{s}\leq$209 GeV.

the bounds, since there would be a series of potential resonances. However, there has been no experimental analysis by the OPAL collaboration below $\sqrt{s} = 189$ GeV, and there is less integrated luminosity between $\sqrt{s} = 189$ GeV and $\sqrt{s} = 200$ GeV to the extent that the bounds are a factor of 3 less tight. Hence such bounds would be almost entirely covered by the bounds obtained in this chapter.

Chapter 5

Signals of R–Parity–Violating Supersymmetry at Present Lepton Colliders Through Single b Quark Production

This chapter is based on the work published in reference [2], updated with results from chapter 3. Since reference [1] had not been published at the time of writing reference [2], reference [2] uses the previously published bounds, from the examinations of bounds from B meson decays by Saha and Kundu [60] and by Xu, Wang and Yang [68] which utilized decay data from the Particle Data Group in 2000, and from BaBar, Belle, CDF and the Particle Data Group as well (but from 2006), respectively, and from analysis by Barbier *et al.* [26] of data from the search for atomic parity violation in caesium [73]. The results were also calculated using the results of chapter 3, but were not included in reference [2]. Both sets of results, using references [26], [68] and [73], and using chapter 3 respectively, are presented here. This chapter investigates the potential signal of single B meson production at electron–positron colliders with energies in the range 6 to 20 GeV, with special attention given to the case of a center–of–mass energy of 10.58 GeV, at which BaBar and Belle currently run. The lower limit is chosen as slightly above the threshold for creating a BK meson pair, and the upper limit is arbitrarily chosen, as for energies very much greater than m_B accurately identifying single B meson production is unfeasible.

5.1 Signal

The Standard Model predicts quark flavor violation through CKM mixing, but the cross–sections for $e\bar{e}\rightarrow b\bar{s}$ or $b\bar{d}$ are extremely small. Detection of flavor violation in significant excess to the Standard Model prediction would be an exciting signal of new physics.

As described in section 2.4.3, quark flavor violation can be mediated at tree–level by sfermions. A non–zero λ and λ' combination allows single b quark production along with a light down–type anti–quark through the Feynman diagrams shown in figure 5.1.

5.1.1 Single b Quark Production With A High–Energy Photon

As is discussed in section 5.2, the production of a single B meson — light meson pair is not necessarily a clean signal. Hence the cases of an additional final–state photon for the single

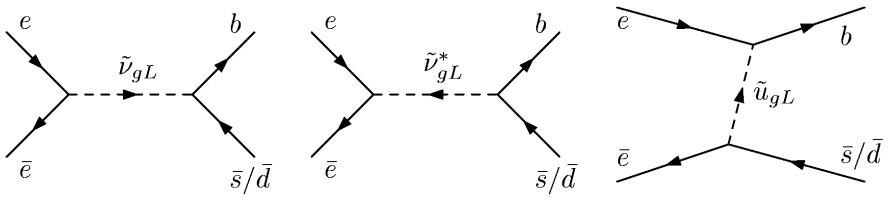

Figure 5.1: Sneutrino– and squark–mediated single b quark production diagrams.

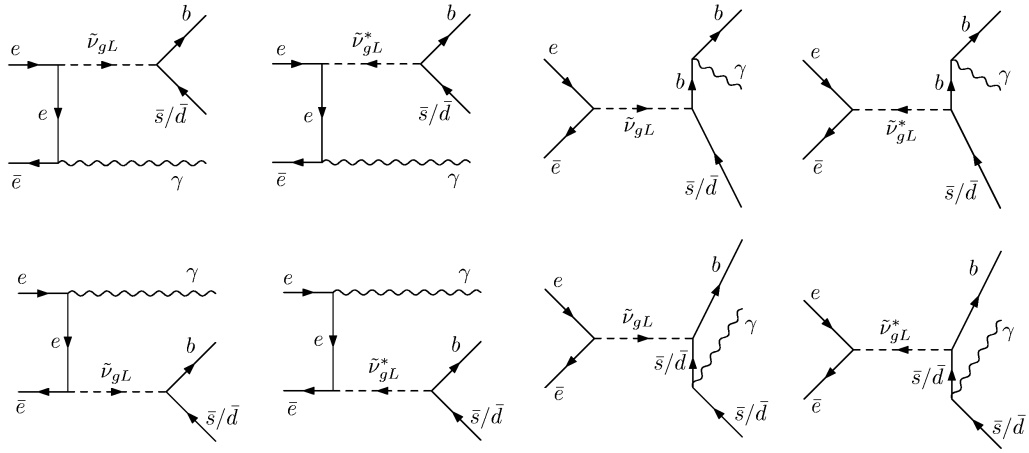

Figure 5.2: Sneutrino–mediated diagrams for single b quark production with a final state photon.

b quark signals are also considered, which may prove to be a cleaner signal as the energy of the B meson does not have to be measured — for a sufficiently energetic photon, $\bar{B}B$ pair production is kinematically excluded, in analogy to using radiative return to measure hadronic cross–sections for lower energies than those at which an experiment runs [74]. The Feynman diagrams are shown in figures 5.2 and 5.3. Diagrams where the photon is emitted by the virtual squark have matrix elements suppressed by another power of order $s/m^2_{\tilde{u}_{gL}}$, hence they are neglected.

5.1.2 Analytic Expressions

Once more, the sfermion propagators are approximated as $-i/m^2_{\tilde{f}}$, and the convention that only either the squark–mediated process or the sneutrino–mediated process dominates is also adopted.

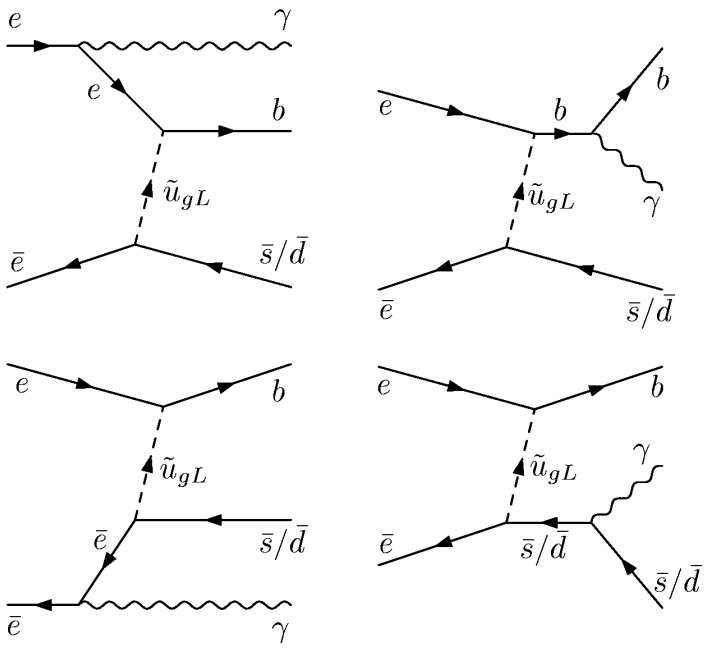

Figure 5.3: Squark–mediated diagrams for single b quark production with a final state photon.

Matrix Elements

The matrix elements for the processes shown in figure 5.1 are given by:

$$\begin{aligned} i\mathcal{M}^{bs}_{\tilde{\nu}} &= \langle b,\bar{s}/\bar{d}|T\left([\bar{e}_k(-i)(\lambda_{jik}P_L\tilde{\nu}_{jL}+\lambda^*_{jki}\tilde{\nu}^*_{jL}P_R)e_i]\right. \\ &\quad \left.\times\,[\bar{d}_n(-i)(\lambda'_{tmn}P_L\tilde{\nu}_{tL}+\lambda'^*_{tnm}P_R\tilde{\nu}^*_{tL})d_m]\right)|e,\bar{e}\rangle \\ &= \bar{v}(p_{\bar{e}})(-i\lambda^*_{g11}P_R)u(p_e)\left(\frac{-i}{m^2_{\tilde{\nu}_{gL}}}\right)\bar{u}(p_b)(-i\lambda'_{g23}P_L)v(p_{\bar{s}}) \\ &\quad +\bar{v}(p_{\bar{e}})(-i\lambda_{g11}P_L)u(p_e)\left(\frac{-i}{m^2_{\tilde{\nu}_{gL}}}\right)\bar{u}(p_b)(-i\lambda'^*_{g32}P_R)v(p_{\bar{s}}) \end{aligned} \tag{5.1}$$

for the s–channel sneutrino graph, or

$$\begin{aligned} i\mathcal{M}^{bs}_{\tilde{u}} &= \langle b,\bar{s}/\bar{d}|T\big([i\lambda'_{ijn}\bar{d}_{Rn}e_{Li}\tilde{u}_{jL}][i\lambda'^*_{ktm}\bar{e}_{kL}d_{mR}\tilde{u}^*_{tL}]\big)|e,\bar{e}\rangle \\ &= \bar{v}(p_{\bar{e}})(i\lambda'^*_{1g2}P_R)u(p_e)\left(\frac{-i}{m^2_{\tilde{u}_{gL}}}\right)\bar{u}(p_b)(i\lambda'_{1g3}P_L)v(p_{\bar{s}}) \end{aligned} \tag{5.2}$$

for the t–channel up–type–squark graph. The matrix elements for down anti–quarks in the final state instead of strange anti–quarks are the same but with $p_{\bar{d}}$ instead of $p_{\bar{s}}$ and either λ'_{g13} instead of λ'_{g23} or λ'_{1g1} instead of λ'_{1g2}.

The matrix elements for the processes with a final–state photon, shown in figures 5.2 and 5.3,

are given by:

$$
\begin{aligned}
i\mathcal{M}^{bs\gamma}_{\tilde{\nu}} &= \left\langle b,\bar{s}/\bar{d}\right|T\left([\bar{e}_k(-i)(\lambda_{jik}P_L\tilde{\nu}_{jL}+\lambda^*_{jki}\tilde{\nu}^*_{jL}P_R)e_i]\right.\\
&\quad\times[\bar{d}_n(-i)(\lambda'_{tmn}P_L\tilde{\nu}_{tL}+\lambda'^*_{tnm}P_R\tilde{\nu}^*_{tL})d_m]\\
&\quad\left.\times([-i\bar{e}_a(-\sqrt{4\pi\alpha})\not{A}e_a]-[i\bar{d}_a\frac{1}{3}(-\sqrt{4\pi\alpha})\not{A}d_a])\right)|e,\bar{e}\rangle\\
&= \left(\bar{v}(p_{\bar{e}})\left[(-i\lambda^*_{g11}P_R)\frac{i(\not{p}_e-\not{p}_\gamma+m_e)}{(p_e-p_\gamma)^2-m_e^2}(-i(-\sqrt{4\pi\alpha})\gamma^\mu\epsilon^*_{\gamma\mu})\right.\right.\\
&\quad\left.+(-i(-\sqrt{4\pi\alpha})\gamma^\mu\epsilon^*_{\gamma\mu})\frac{i(\not{p}_\gamma-\not{p}_{\bar{e}}+m_e)}{(p_\gamma-p_{\bar{e}})^2-m_e^2}(-i\lambda^*_{g11}P_R)\right]u(p_e)\\
&\quad\times\left(\frac{-i}{m^2_{\tilde{\nu}_{gL}}}\right)\bar{u}(p_b)(-i\lambda'_{g23}P_L)v(p_{\bar{s}})\\
&\quad+\bar{v}(p_{\bar{e}})(-i\lambda^*_{g11}P_R)u(p_e)\left(\frac{-i}{m^2_{\tilde{\nu}_{gL}}}\right)\\
&\quad\times\bar{u}(p_b)\left[(-i\lambda'_{g23}P_L)\frac{i(-\not{p}_{\bar{s}}-\not{p}_\gamma+m_s)}{(-p_{\bar{s}}-p_\gamma)^2-m_s^2}\left(\frac{-i}{3}(-\sqrt{4\pi\alpha})\gamma^\mu\epsilon^*_{\gamma\mu}\right)\right.\\
&\quad\left.\left.+\left(\frac{-i}{3}(-\sqrt{4\pi\alpha})\gamma^\mu\epsilon^*_{\gamma\mu}\right)\frac{i(\not{p}_b+\not{p}_\gamma+m_b)}{(p_b+p_\gamma)^2-m_b^2}(-i\lambda'_{g23}P_L)\right]v(p_{\bar{s}})\right)\\
&\quad+\left(\bar{v}(p_{\bar{e}})\left[(-i\lambda_{g11}P_L)\frac{i(\not{p}_e-\not{p}_\gamma+m_e)}{(p_e-p_\gamma)^2-m_e^2}(-i(-\sqrt{4\pi\alpha})\gamma^\mu\epsilon^*_{\gamma\mu})\right.\right.\\
&\quad\left.+(-i(-\sqrt{4\pi\alpha})\gamma^\mu\epsilon^*_{\gamma\mu})\frac{i(\not{p}_\gamma-\not{p}_{\bar{e}}+m_e)}{(p_\gamma-p_{\bar{e}})^2-m_e^2}(-i\lambda_{g11}P_L)\right]u(p_e)\\
&\quad\times\left(\frac{-i}{m^2_{\tilde{\nu}_{gL}}}\right)\bar{u}(p_b)(-i\lambda'^*_{g32}P_R)v(p_{\bar{s}})\\
&\quad+\bar{v}(p_{\bar{e}})(-i\lambda_{g11}P_L)u(p_e)\left(\frac{-i}{m^2_{\tilde{\nu}_{gL}}}\right)\\
&\quad\times\bar{u}(p_b)\left[(-i\lambda'^*_{g32}P_R)\frac{i(-\not{p}_{\bar{s}}-\not{p}_\gamma+m_s)}{(-p_{\bar{s}}-p_\gamma)^2-m_s^2}\left(\frac{-i}{3}(-\sqrt{4\pi\alpha})\gamma^\mu\epsilon^*_{\gamma\mu}\right)\right.\\
&\quad\left.\left.+\left(\frac{-i}{3}(-\sqrt{4\pi\alpha})\gamma^\mu\epsilon^*_{\gamma\mu}\right)\frac{i(\not{p}_b+\not{p}_\gamma+m_b)}{(p_b+p_\gamma)^2-m_b^2}(-i\lambda'^*_{g32}P_R)\right]v(p_{\bar{s}})\right)
\end{aligned}
\tag{5.3}
$$

for the sneutrino–mediated graph, or

$$
\begin{aligned}
i\mathcal{M}^{bs\gamma}_{\tilde{u}} &= \langle b,\bar{s}/\bar{d}|T\left([i\lambda'_{ijn}\bar{d}_{Rn}e_{Li}\tilde{u}_{jL}][i\lambda'^{*}_{ktm}\bar{e}_{kL}d_{mR}\tilde{u}^{*}_{tL}]\right.\\
&\quad\left.\times([-i\bar{e}_a(-\sqrt{4\pi\alpha})\not{A}e_a]-[i\bar{d}_a\frac{1}{3}(-\sqrt{4\pi\alpha})\not{A}d_a])\right)|e,\bar{e}\rangle\\
&= \left(\bar{u}(p_b)\left[(i\lambda'_{1g3}P_L)\frac{i(\not{p}_e-\not{p}_\gamma+m_e)}{(p_e-p_\gamma)^2-m_e^2}(-i(-\sqrt{4\pi\alpha})\gamma^\mu\epsilon^*_{\gamma\mu})\right.\right.\\
&\quad+\left.\left(\frac{-i}{3}(-\sqrt{4\pi\alpha})\gamma^\mu\epsilon^*_{\gamma\mu}\right)\frac{i(\not{p}_b+\not{p}_\gamma+m_b)}{(p_b+p_\gamma)^2-m_b^2}(i\lambda'_{1g3}P_L)\right]u(p_e)\\
&\quad\times(\frac{-i}{m^2_{\tilde{u}_{gL}}})\bar{v}(p_{\bar{e}})(i\lambda'^{*}_{1g2}P_R)v(p_{\bar{s}})\\
&\quad+\bar{u}(p_b)(i\lambda'_{1g3}P_L)u(p_e)(\frac{-i}{m^2_{\tilde{u}_{gL}}})\\
&\quad\times\bar{v}(p_{\bar{e}})\left[(-i(-\sqrt{4\pi\alpha})\gamma^\mu\epsilon^*_{\gamma\mu})\frac{i(\not{p}_\gamma-\not{p}_{\bar{e}}+m_e)}{(p_\gamma-p_{\bar{e}})^2-m_e^2}(i\lambda'^{*}_{1g2}P_R)\right.\\
&\quad+\left.\left.(i\lambda'^{*}_{1g2}P_R)\frac{i(-\not{p}_{\bar{s}}-\not{p}_\gamma+m_s)}{(-p_{\bar{s}}-p_\gamma)^2-m_s^2}\left(\frac{-i}{3}(-\sqrt{4\pi\alpha})\gamma^\mu\epsilon^*_{\gamma\mu}\right)\right]v(p_{\bar{s}})\right)
\end{aligned}
\tag{5.4}
$$

for the up–type–squark–mediated graph.

Cross–Sections

Squaring the matrix elements, summing over final spins, averaging over initial spins, summing over the b and $\bar{b}$ final states (so any subscript with a b in the following equations in this section refers to either, and likewise a s or d subscript refers to either the quark or anti–quark, such that in total there is one quark and one anti–quark) and allowing only for one of the two R–parity violating processes to dominate leads to the differential cross–sections for the processes shown in figure 5.1:

$$
\left(\frac{d\sigma}{d\Omega}\right)^{bs}_{\tilde{\nu}}=\frac{|\mathbf{p}_b|}{|\mathbf{p}_e|}\frac{3}{128\pi^2 s}(s-2m_e^2)(s-m_b^2-m_s^2)\frac{(|\lambda_{g11}|^2|\lambda'_{g23}|^2+|\lambda_{g11}|^2|\lambda'_{g32}|^2)}{m^4_{\tilde{\nu}_{gL}}} \tag{5.5}
$$

for the sneutrino exchange process, and

$$
\left(\frac{d\sigma}{d\Omega}\right)^{bs}_{\tilde{u}}=\frac{|\mathbf{p}_b|}{|\mathbf{p}_e|}\frac{3}{128\pi^2 s}(t-m_b^2-m_e^2)(t-m_s^2-m_e^2)\frac{|\lambda'_{1g2}|^2|\lambda'_{1g3}|^2}{m^4_{\tilde{u}_{gL}}} \tag{5.6}
$$

for the squark exchange process. Here $\mathbf{p}_b$ is the three–dimensional momentum of the b quark. The case of a final–state down quark can be obtained by the appropriate changes of indices (*i.e.* replacing 2 by 1 in the coupling indices and s by d in the mass indices). The limits used on these combinations of couplings from experimental data are given in table 5.1.

For the processes shown in figures 5.2 and 5.3, summing over the b and $\bar{b}$ final states and allowing only for one of the two R–parity violating processes to dominate, the cross–sections are given by:

$$
\sigma^{bs\gamma}_{\tilde{\nu}}=\int_{-\infty}^{\infty}\frac{\mathrm{d}\boldsymbol{p_b}}{(2\pi)^3}\int_{-\infty}^{\infty}\frac{\mathrm{d}\boldsymbol{p_s}}{(2\pi)^3}\int_{-\infty}^{\infty}\frac{\mathrm{d}\boldsymbol{p_\gamma}}{(2\pi)^3}\frac{(2\pi)^4\delta^{(4)}(p_e+p_{\bar{e}}-p_b-p_s-p_\gamma)}{(2E_b)(2E_s)(2E_\gamma)}\frac{1}{2s}\left\langle\left|\mathcal{M}^{bs\gamma}_{\tilde{\nu}}\right|^2\right\rangle \tag{5.7}
$$

for the sneutrino exchange process, and

$$
\sigma^{bs\gamma}_{\tilde{u}}=\int_{-\infty}^{\infty}\frac{\mathrm{d}\boldsymbol{p_b}}{(2\pi)^3}\int_{-\infty}^{\infty}\frac{\mathrm{d}\boldsymbol{p_s}}{(2\pi)^3}\int_{-\infty}^{\infty}\frac{\mathrm{d}\boldsymbol{p_\gamma}}{(2\pi)^3}\frac{(2\pi)^4\delta^{(4)}(p_e+p_{\bar{e}}-p_b-p_s-p_\gamma)}{(2E_b)(2E_s)(2E_\gamma)}\frac{1}{2s}\left\langle\left|\mathcal{M}^{bs\gamma}_{\tilde{u}}\right|^2\right\rangle \tag{5.8}
$$

for the squark exchange process. Angle brackets denote averaging over initial spins and summing over final spins. Again, in equations (5.7), (5.8), (5.9) and (5.10), the case of a final–state down quark can be obtained by the appropriate changes of indices (*i.e.* replacing 2 by 1 in the coupling indices and s by d in the mass and momenta indices).

The squared matrix elements are given by:

$$
\begin{aligned}
\left\langle \left| \mathcal{M}_{\tilde{\nu}}^{bs\gamma} \right|^2 \right\rangle \;=\; & \frac{8\pi\alpha}{3} \frac{(|\lambda_{g11}|^2 |\lambda'_{g23}|^2 + |\lambda_{g11}|^2 |\lambda'_{g32}|^2)}{m^4_{\tilde{\nu}_{gL}}} \left(\frac{1}{(p_e{\cdot}p_\gamma)(p_b{\cdot}p_\gamma)} [6(p_e{\cdot}p_{\bar{e}})(p_e{\cdot}p_b)(p_b{\cdot}p_s) \right. \\
& +3(p_e{\cdot}p_{\bar{e}})(p_e{\cdot}p_b)(p_s{\cdot}p_\gamma) \\
& -3(p_e{\cdot}p_{\bar{e}})(p_e{\cdot}p_s)(p_b{\cdot}p_\gamma) + 3(p_e{\cdot}p_{\bar{e}})(p_e{\cdot}p_\gamma)(p_b{\cdot}p_s) - 3(p_e{\cdot}p_{\bar{e}})(p_b{\cdot}p_s)(p_b{\cdot}p_\gamma) \\
& -3(p_e{\cdot}p_b)(p_{\bar{e}}{\cdot}p_\gamma)(p_b{\cdot}p_s) + 3(p_e{\cdot}p_\gamma)(p_{\bar{e}}{\cdot}p_b)(p_b{\cdot}p_s)] \\
& + \frac{1}{(p_e{\cdot}p_\gamma)(p_s{\cdot}p_\gamma)} [3(p_e{\cdot}p_{\bar{e}})(p_e{\cdot}p_b)(p_s{\cdot}p_\gamma) - 6(p_e{\cdot}p_{\bar{e}})(p_e{\cdot}p_s)(p_b{\cdot}p_s) \\
& -3(p_e{\cdot}p_{\bar{e}})(p_e{\cdot}p_s)(p_b{\cdot}p_\gamma) - 3(p_e{\cdot}p_{\bar{e}})(p_e{\cdot}p_\gamma)(p_b{\cdot}p_s) + 3(p_e{\cdot}p_{\bar{e}})(p_b{\cdot}p_s)(p_s{\cdot}p_\gamma) \\
& +3(p_e{\cdot}p_s)(p_{\bar{e}}{\cdot}p_\gamma)(p_b{\cdot}p_s) - 3(p_e{\cdot}p_\gamma)(p_{\bar{e}}{\cdot}p_s)(p_b{\cdot}p_s)] \\
& + \frac{1}{(p_e{\cdot}p_\gamma)(p_{\bar{e}}{\cdot}p_\gamma)} [18(p_e{\cdot}p_{\bar{e}})^2(p_b{\cdot}p_s) - 18(p_e{\cdot}p_{\bar{e}})(p_e{\cdot}p_\gamma)(p_b{\cdot}p_s) \\
& -18(p_e{\cdot}p_{\bar{e}})(p_{\bar{e}}{\cdot}p_\gamma)(p_b{\cdot}p_s) + 18(p_e{\cdot}p_\gamma)(p_{\bar{e}}{\cdot}p_\gamma)(p_b{\cdot}p_s) \\
& +9(p_e{\cdot}p_\gamma)(p_b{\cdot}p_s)m_e^2 + 9(p_{\bar{e}}{\cdot}p_\gamma)(p_b{\cdot}p_s)m_e^2] \\
& + \frac{1}{(p_{\bar{e}}{\cdot}p_\gamma)(p_b{\cdot}p_\gamma)} [3(p_e{\cdot}p_{\bar{e}})(p_{\bar{e}}{\cdot}p_s)(p_b{\cdot}p_\gamma) - 6(p_e{\cdot}p_{\bar{e}})(p_{\bar{e}}{\cdot}p_b)(p_b{\cdot}p_s) \\
& -3(p_e{\cdot}p_{\bar{e}})(p_{\bar{e}}{\cdot}p_b)(p_s{\cdot}p_\gamma) - 3(p_e{\cdot}p_{\bar{e}})(p_{\bar{e}}{\cdot}p_\gamma)(p_b{\cdot}p_s) + 3(p_e{\cdot}p_{\bar{e}})(p_b{\cdot}p_s)(p_b{\cdot}p_\gamma) \\
& -3(p_e{\cdot}p_b)(p_{\bar{e}}{\cdot}p_\gamma)(p_b{\cdot}p_s) + 3(p_e{\cdot}p_\gamma)(p_{\bar{e}}{\cdot}p_b)(p_b{\cdot}p_s)] \\
& + \frac{1}{(p_{\bar{e}}{\cdot}p_\gamma)(p_s{\cdot}p_\gamma)} [6(p_e{\cdot}p_{\bar{e}})(p_{\bar{e}}{\cdot}p_s)(p_b{\cdot}p_s) - 3(p_e{\cdot}p_{\bar{e}})(p_{\bar{e}}{\cdot}p_b)(p_s{\cdot}p_\gamma) \\
& +3(p_e{\cdot}p_{\bar{e}})(p_{\bar{e}}{\cdot}p_s)(p_b{\cdot}p_\gamma) + 3(p_e{\cdot}p_{\bar{e}})(p_{\bar{e}}{\cdot}p_\gamma)(p_b{\cdot}p_s) - 3(p_e{\cdot}p_{\bar{e}})(p_b{\cdot}p_s)(p_s{\cdot}p_\gamma) \\
& +3(p_e{\cdot}p_s)(p_{\bar{e}}{\cdot}p_\gamma)(p_b{\cdot}p_s) - 3(p_e{\cdot}p_\gamma)(p_{\bar{e}}{\cdot}p_s)(p_b{\cdot}p_s)] \\
& + \frac{1}{(p_b{\cdot}p_\gamma)(p_s{\cdot}p_\gamma)} [2(p_e{\cdot}p_{\bar{e}})(p_b{\cdot}p_s)(p_b{\cdot}p_\gamma) + 2(p_e{\cdot}p_{\bar{e}})(p_b{\cdot}p_s)(p_s{\cdot}p_\gamma) \\
& +2(p_e{\cdot}p_{\bar{e}})(p_b{\cdot}p_s)^2 + 2(p_e{\cdot}p_{\bar{e}})(p_b{\cdot}p_\gamma)(p_s{\cdot}p_\gamma) \\
& -(p_e{\cdot}p_{\bar{e}})(p_b{\cdot}p_\gamma)m_s^2 - (p_e{\cdot}p_{\bar{e}})(p_s{\cdot}p_\gamma)m_b^2] \\
& + \frac{1}{(p_e{\cdot}p_\gamma)^2} [9(p_e{\cdot}p_\gamma)(p_{\bar{e}}{\cdot}p_\gamma)(p_b{\cdot}p_s) - 9(p_e{\cdot}p_{\bar{e}})(p_b{\cdot}p_s)m_e^2 + 9(p_{\bar{e}}{\cdot}p_\gamma)(p_b{\cdot}p_s)m_e^2] \\
& + \frac{1}{(p_{\bar{e}}{\cdot}p_\gamma)^2} [9(p_e{\cdot}p_\gamma)(p_{\bar{e}}{\cdot}p_\gamma)(p_b{\cdot}p_s) - 9(p_e{\cdot}p_{\bar{e}})(p_b{\cdot}p_s)m_e^2 + 9(p_e{\cdot}p_\gamma)(p_b{\cdot}p_s)m_e^2] \\
& + \frac{1}{(p_s{\cdot}p_\gamma)^2} [(p_e{\cdot}p_{\bar{e}})(p_b{\cdot}p_\gamma)(p_s{\cdot}p_\gamma) - (p_e{\cdot}p_{\bar{e}})(p_b{\cdot}p_s)m_s^2 - (p_e{\cdot}p_{\bar{e}})(p_b{\cdot}p_\gamma)m_s^2] \\
& \left. + \frac{1}{(p_b{\cdot}p_\gamma)^2} [(p_e{\cdot}p_{\bar{e}})(p_b{\cdot}p_\gamma)(p_s{\cdot}p_\gamma) - (p_e{\cdot}p_{\bar{e}})(p_b{\cdot}p_s)m_b^2 - (p_e{\cdot}p_{\bar{e}})(p_s{\cdot}p_\gamma)m_b^2] \right)
\end{aligned}
\tag{5.9}
$$

and

$$
\begin{aligned}
\left\langle \left| \mathcal{M}_{\tilde{u}}^{bs\gamma} \right|^2 \right\rangle \;=\; & \frac{8\pi\alpha}{3} \frac{|\lambda'_{1g2}|^2 |\lambda'_{1g3}|^2}{m^4_{\tilde{u}_{gL}}} \left(\frac{1}{(p_e{\cdot}p_\gamma)(p_b{\cdot}p_\gamma)} [6(p_e{\cdot}p_b)(p_{\bar{e}}{\cdot}p_s)(p_b{\cdot}p_\gamma) \right. \\
& -6(p_e{\cdot}p_b)(p_e{\cdot}p_\gamma)(p_{\bar{e}}{\cdot}p_s) \\
& -6(p_e{\cdot}p_b)^2(p_{\bar{e}}{\cdot}p_s) + 6(p_e{\cdot}p_\gamma)(p_{\bar{e}}{\cdot}p_s)(p_b{\cdot}p_\gamma) \\
& -3(p_e{\cdot}p_\gamma)(p_{\bar{e}}{\cdot}p_s)m_b^2 + 3(p_{\bar{e}}{\cdot}p_s)(p_b{\cdot}p_\gamma)m_e^2] \\
& + \frac{1}{(p_e{\cdot}p_\gamma)(p_s{\cdot}p_\gamma)} [6(p_e{\cdot}p_b)(p_e{\cdot}p_s)(p_{\bar{e}}{\cdot}p_s) - 3(p_e{\cdot}p_{\bar{e}})(p_e{\cdot}p_b)(p_s{\cdot}p_\gamma) \\
& +3(p_e{\cdot}p_b)(p_e{\cdot}p_s)(p_{\bar{e}}{\cdot}p_\gamma) + 3(p_e{\cdot}p_b)(p_e{\cdot}p_\gamma)(p_{\bar{e}}{\cdot}p_s) - 3(p_e{\cdot}p_b)(p_{\bar{e}}{\cdot}p_s)(p_s{\cdot}p_\gamma) \\
& -3(p_e{\cdot}p_s)(p_{\bar{e}}{\cdot}p_s)(p_b{\cdot}p_\gamma) + 3(p_e{\cdot}p_\gamma)(p_{\bar{e}}{\cdot}p_s)(p_b{\cdot}p_s)] \\
& + \frac{1}{(p_e{\cdot}p_\gamma)(p_{\bar{e}}{\cdot}p_\gamma)} [9(p_e{\cdot}p_{\bar{e}})(p_e{\cdot}p_b)(p_s{\cdot}p_\gamma) - 18(p_e{\cdot}p_{\bar{e}})(p_e{\cdot}p_b)(p_{\bar{e}}{\cdot}p_s) \\
& +9(p_e{\cdot}p_{\bar{e}})(p_{\bar{e}}{\cdot}p_s)(p_b{\cdot}p_\gamma) - 9(p_e{\cdot}p_b)(p_e{\cdot}p_s)(p_{\bar{e}}{\cdot}p_\gamma) + 9(p_e{\cdot}p_b)(p_e{\cdot}p_\gamma)(p_{\bar{e}}{\cdot}p_s) \\
& +9(p_e{\cdot}p_b)(p_{\bar{e}}{\cdot}p_s)(p_{\bar{e}}{\cdot}p_\gamma) - 9(p_e{\cdot}p_\gamma)(p_{\bar{e}}{\cdot}p_b)(p_{\bar{e}}{\cdot}p_s)] \\
& + \frac{1}{(p_{\bar{e}}{\cdot}p_\gamma)(p_b{\cdot}p_\gamma)} [6(p_e{\cdot}p_b)(p_{\bar{e}}{\cdot}p_b)(p_{\bar{e}}{\cdot}p_s) - 3(p_e{\cdot}p_{\bar{e}})(p_{\bar{e}}{\cdot}p_s)(p_b{\cdot}p_\gamma) \\
& -3(p_e{\cdot}p_b)(p_{\bar{e}}{\cdot}p_b)(p_s{\cdot}p_\gamma) + 3(p_e{\cdot}p_b)(p_{\bar{e}}{\cdot}p_s)(p_{\bar{e}}{\cdot}p_\gamma) - 3(p_e{\cdot}p_b)(p_{\bar{e}}{\cdot}p_s)(p_b{\cdot}p_\gamma) \\
& +3(p_e{\cdot}p_b)(p_{\bar{e}}{\cdot}p_\gamma)(p_b{\cdot}p_s) + 3(p_e{\cdot}p_\gamma)(p_{\bar{e}}{\cdot}p_b)(p_{\bar{e}}{\cdot}p_s)] \\
& + \frac{1}{(p_{\bar{e}}{\cdot}p_\gamma)(p_s{\cdot}p_\gamma)} [6(p_e{\cdot}p_b)(p_{\bar{e}}{\cdot}p_s)(p_s{\cdot}p_\gamma) - 6(p_e{\cdot}p_b)(p_{\bar{e}}{\cdot}p_s)(p_{\bar{e}}{\cdot}p_\gamma) \\
& -6(p_e{\cdot}p_b)(p_{\bar{e}}{\cdot}p_s)^2 + 6(p_e{\cdot}p_b)(p_{\bar{e}}{\cdot}p_\gamma)(p_s{\cdot}p_\gamma) \\
& -3(p_e{\cdot}p_b)(p_{\bar{e}}{\cdot}p_\gamma)m_s^2 + 3(p_e{\cdot}p_b)(p_s{\cdot}p_\gamma)m_e^2] \\
& + \frac{1}{(p_b{\cdot}p_\gamma)(p_s{\cdot}p_\gamma)} [(p_e{\cdot}p_b)(p_{\bar{e}}{\cdot}p_b)(p_s{\cdot}p_\gamma) - 2(p_e{\cdot}p_b)(p_{\bar{e}}{\cdot}p_s)(p_b{\cdot}p_s) \\
& -(p_e{\cdot}p_b)(p_{\bar{e}}{\cdot}p_s)(p_b{\cdot}p_\gamma) - (p_e{\cdot}p_b)(p_{\bar{e}}{\cdot}p_s)(p_s{\cdot}p_\gamma) - (p_e{\cdot}p_b)(p_{\bar{e}}{\cdot}p_\gamma)(p_b{\cdot}p_s) \\
& +(p_e{\cdot}p_s)(p_{\bar{e}}{\cdot}p_s)(p_b{\cdot}p_\gamma) - (p_e{\cdot}p_\gamma)(p_{\bar{e}}{\cdot}p_s)(p_b{\cdot}p_s)] \\
& + \frac{1}{(p_e{\cdot}p_\gamma)^2} [9(p_e{\cdot}p_b)(p_{\bar{e}}{\cdot}p_s)m_e^2 - 9(p_e{\cdot}p_\gamma)(p_{\bar{e}}{\cdot}p_s)(p_b{\cdot}p_\gamma) - 9(p_{\bar{e}}{\cdot}p_s)(p_b{\cdot}p_\gamma)m_e^2] \\
& + \frac{1}{(p_{\bar{e}}{\cdot}p_\gamma)^2} [9(p_e{\cdot}p_b)(p_{\bar{e}}{\cdot}p_s)m_e^2 - 9(p_e{\cdot}p_b)(p_{\bar{e}}{\cdot}p_\gamma)(p_s{\cdot}p_\gamma) - 9(p_e{\cdot}p_b)(p_s{\cdot}p_\gamma)m_e^2] \\
& + \frac{1}{(p_s{\cdot}p_\gamma)^2} [(p_e{\cdot}p_b)(p_{\bar{e}}{\cdot}p_s)m_s^2 - (p_e{\cdot}p_b)(p_{\bar{e}}{\cdot}p_\gamma)(p_s{\cdot}p_\gamma) + (p_e{\cdot}p_b)(p_{\bar{e}}{\cdot}p_\gamma)m_s^2] \\
& \left. + \frac{1}{(p_b{\cdot}p_\gamma)^2} [(p_e{\cdot}p_b)(p_{\bar{e}}{\cdot}p_s)m_b^2 - (p_e{\cdot}p_\gamma)(p_{\bar{e}}{\cdot}p_s)(p_b{\cdot}p_\gamma) + (p_e{\cdot}p_\gamma)(p_{\bar{e}}{\cdot}p_s)m_b^2] \right)
\end{aligned}
\tag{5.10}
$$

where the γ–matrix algebra was performed with FORM [75], as were the sums over Lorentz indices. These expressions were integrated using Monte–Carlo methods, utilizing the changes of variables detailed in appendix E. The matrix element was checked to satisfy the Ward identity that replacing the photon polarization vector in the matrix element with the photon momentum gives zero.

	Published before [1] ($\equiv$ PP)		From chapter 3 ($\equiv$ TT)
Coupling	Bound in GeV^{-4}	Process	Bound in GeV^{-4}
$(\lvert\lambda_{g11}\rvert^2\lvert\lambda'_{g13}\rvert^2$ $+\lvert\lambda_{g11}\rvert^2\lvert\lambda'_{g31}\rvert^2)m_{\tilde{\nu}_{gL}}^{-4}$	2.9×10^{-18}	$B_d^0\to e\bar{e}$ [26]	6.1×10^{-19} (Corr.($<$))
$(\lvert\lambda_{g11}\rvert^2\lvert\lambda'_{g23}\rvert^2$ $+\lvert\lambda_{g11}\rvert^2\lvert\lambda'_{g32}\rvert^2)m_{\tilde{\nu}_{gL}}^{-4}$	5.9×10^{-18} GeV^{-4}	$B_s^0\to e\bar{e}$ [68]	(Unimp.)
$\lvert\lambda'_{1g1}\rvert^2\lvert\lambda'_{1g3}\rvert^2 m_{\tilde{u}_{gL}}^{-4}$	2.9×10^{-13}	APV in Cs [73], $A_{\rm FB}^b$ [26]	(Unimp.)
$\lvert\lambda'_{1g2}\rvert^2\lvert\lambda'_{1g3}\rvert^2 m_{\tilde{u}_{gL}}^{-4}$	2.2×10^{-17}	$B_d^0\to Ke\bar{e}$ [68]	(Unimp.)

Table 5.1: Used bounds on coupling combinations. The atomic parity violation bound on $\lvert\lambda'_{1g1}\rvert^2 m_{\tilde{u}_{gL}}^{-2}$ is combined with the constraint on $\lvert\lambda'_{1g3}\rvert^2 m_{\tilde{u}_{gL}}^{-2}$ from the forward–backward asymmetry of $b\bar{b}$ pair production to bound $\lvert\lambda'_{1g1}\rvert^2\lvert\lambda'_{1g3}\rvert^2 m_{\tilde{u}_{gL}}^{-4}$. The bounds from chapter 3 are only given in the cases where it makes a difference.

Channel	Using [26], [68] and [73] (PP)	Using chapter 3 (TT)
bd via $\tilde{\nu}$	3.4 $\times10^{-6}$ fb	2.8 $\times10^{-6}$ fb
bs via $\tilde{\nu}$	6.2 $\times10^{-6}$ fb	6.2 $\times10^{-6}$ fb
bd via $\tilde{u}$	0.13 fb	0.13 fb
bs via $\tilde{u}$	1.0 $\times10^{-5}$ fb	1.0 $\times10^{-5}$ fb

Table 5.2: The cross–sections for $e\bar{e}\to b\bar{s}/s\bar{b}/b\bar{d}/d\bar{b}$ at $\sqrt{s} = 10.58$ GeV.

5.1.3 Numerical Results

The cross–sections for the processes with and without the final–state photon are presented in figure 5.4 and figure 5.5, with the numerical values for $\sqrt{s} = 10.58$ GeV given in tables 5.2 and 5.3. The values used for the couplings are shown in table 5.1.

In order to exclude the possibility that it was emitted through the radiative decay of a B meson, the phase space of the photon is restricted. Since there is an upper bound $E_{\gamma\max}$ to the energy that the radiated photon can have for a B meson with a given momentum in the beam center–of–momentum frame, the photon is restricted to have 10% or more energy above this $E_{\gamma\max}$ for a B meson with half the beam energy. In this case,

$$E_{\gamma\max} = \frac{1}{2}(E_B + \sqrt{E_B^2 - m_B^2}) = \frac{1}{4}(\sqrt{s} + \sqrt{s - 4m_B^2}) \tag{5.11}$$

In doing this, the background of misidentified $\bar{B}B$ pair production is eliminated. The signal for the final–state photon case begins at 10.56 GeV as below this it is kinematically impossible to produce a $\bar{B}B$ pair, hence the advantage of the additional photon is non–existent, while still suffering from the α suppression of the signal. The restriction on the photon energy cuts out much of the phase space, and cuts out more as $\sqrt{s}$ increases, until around $\sqrt{s} = 13.8$ GeV, where the entire phase space is excluded. Unfortunately, even in the best case, close to the special value $\sqrt{s} = 10.58$ GeV, the best signal is less than 0.1 ab.

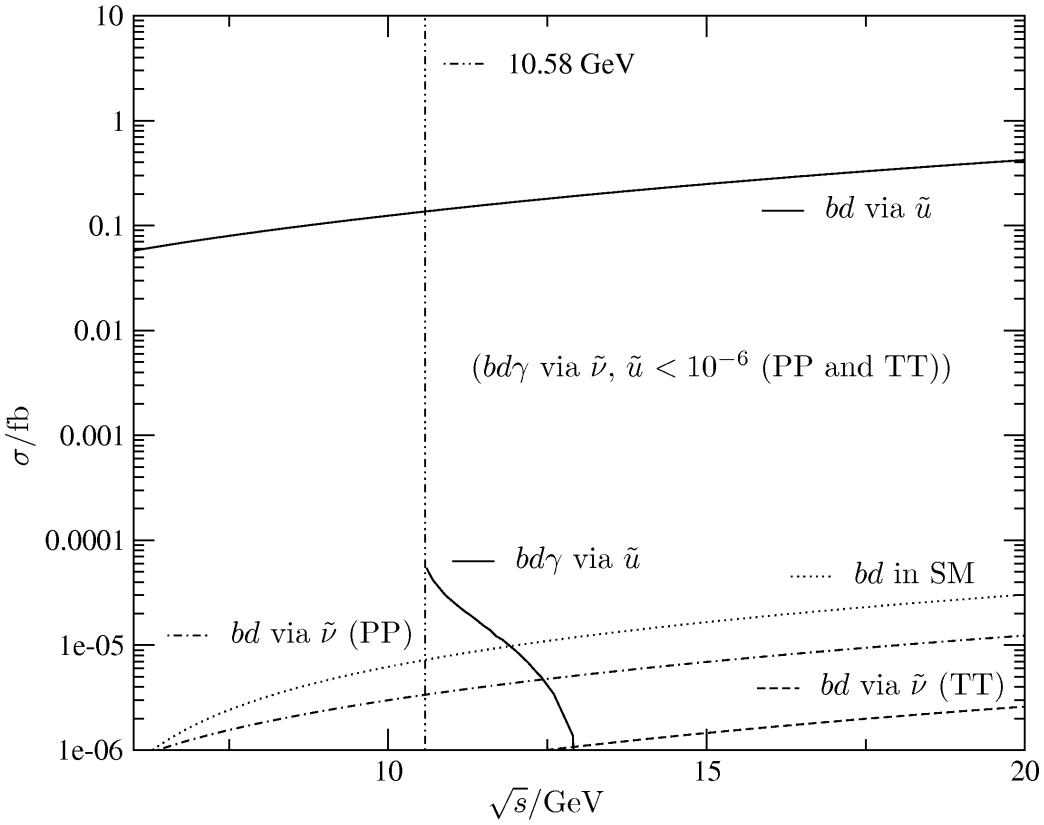

Figure 5.4: Cross–sections for $e\bar{e}\to b\bar{d}/d\bar{b}/b\bar{d}\gamma/d\bar{b}\gamma$ through R–parity violation and the SM background for $e\bar{e}\to b\bar{d}/d\bar{b}$. (PP denotes results calculated using the bounds "**p**reviously **p**ublished", *i.e.* appearing in publications before reference [1], and TT denotes results calculated using the bounds from chapter 3 in **t**his **t**hesis.)

5.1.4 Experimental Signature

The calculated signals have on–shell single quarks in the final state. The process of hadronization is not well understood, but since $\sqrt{s} \gg \Lambda_{\rm QCD}$ it is assumed that the scattering amplitude for the sum of all possible $e\bar{e}\to\bar{B}M$ is the same as for $e\bar{e}\to b\bar{q}$, where M is a light (bottomless) meson which has anti–quark constituent $\bar{q}$. In this scheme, the production of a $b\bar{d}$ pair leads to an on–shell neutral pair with an unflavored light meson ($\bar{B}_d\pi^0$, $\bar{B}_d\eta'$, $\bar{B}_d\eta'$, $\bar{B}^*_d\rho$ or $\bar{B}^*_d\omega$) 43.5% of the time and to a charged pair with an unflavored light meson ($B^-_d\pi^+$, $B^{*-}_d\rho^+$) 43.5% of the time, according to the Lund string model [76]. The remaining 13% consist of the channels where the light meson is strange ($\bar{B}_sK$ and $\bar{B}^*_sK^*$). Since the Lund string model represents the QCD force between the quarks as a string with energy density of about 0.2 GeV^2, the kinetic energy available (in the center–of–momentum frame) to the bare quarks of roughly 6 GeV is far in excess of this, leading to a naïve guess that complications from the bottom and light quarks forming an interim bound state are negligible.

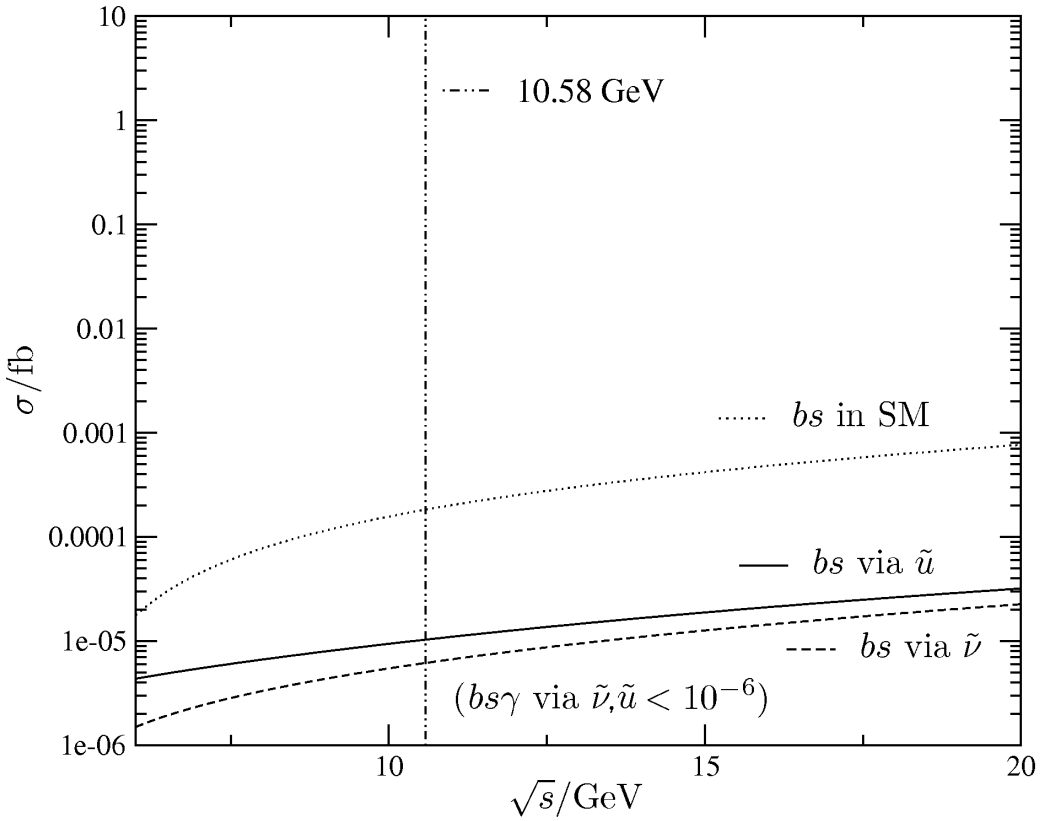

Figure 5.5: Cross–sections for $e\bar{e}\to b\bar{s}/s\bar{b}/b\bar{s}\gamma/s\bar{b}\gamma$ through R–parity violation and the SM background for $e\bar{e}\to b\bar{s}/s\bar{b}$. (PP denotes results calculated using the bounds **p**ublished **p**revious to reference [1], and TT denotes results calculated using the bounds from chapter 3 in **t**his **t**hesis.)

5.2 Backgrounds

Three sources of background to the signal are identified: direct SM $e\bar{e}\to\bar{B}M$, misidentified $\bar{B}B$ pair production, and R–parity conserving MSSM $e\bar{e}\to b\bar{s}$ or $b\bar{d}$.

5.2.1 Standard Model Background

As mentioned in section 5.1, there is a Standard Model background to the processes $e\bar{e}\to b\bar{s}, b\bar{d}$. However, its leading order contribution is at one–loop level and doubly Cabibbo suppressed. Ignoring Feynman diagrams with an electron–Higgs Yukawa coupling, there are five classes of diagrams, shown in figure 5.6 (in these diagrams the photon may be replaced by a Z boson, though this suppresses the matrix element by a further factor of s/m_Z^2).

Using FeynArts [77] and FORMCalc [78], which utilize FORM [75] and LoopTools [78], and continuing to use the assumed quark–hadron duality, the cross–sections obtained are presented in figure 5.4 and figure 5.5, with the numerical values for $\sqrt{s} = 10.58$ GeV given in table 5.4.

Considering the two–particle final states, the SM background is completely negligible compared to the squark–mediated signal for bd production. However, it is within an order of magnitude of the other three potential signals (sneutrino–mediated bd production, squark–

Channel	Using [26], [68] and [73] (PP)	Using chapter 3 (TT)
$bd\gamma$ via $\tilde{\nu}$	1.6×10^{-9} fb	3.9×10^{-10} fb
$bs\gamma$ via $\tilde{\nu}$	2.9×10^{-9} fb	2.9×10^{-9} fb
$bd\gamma$ via $\tilde{u}$	5.7×10^{-5} fb	5.7×10^{-5} fb
$bs\gamma$ via $\tilde{u}$	4.3×10^{-9} fb	4.3×10^{-9} fb

Table 5.3: The cross–sections for $e\bar{e}\to b\bar{s}\gamma/s\bar{b}\gamma/b\bar{d}\gamma/d\bar{b}\gamma$ at $\sqrt{s} = 10.58$ GeV.

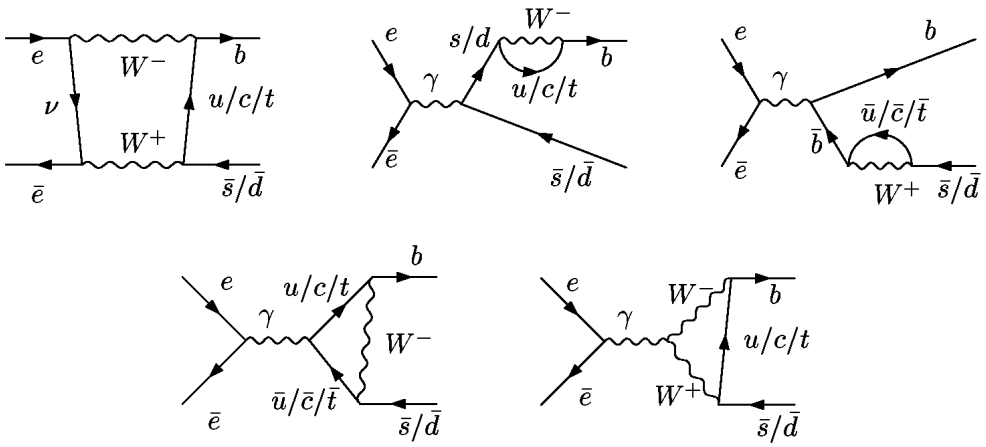

Figure 5.6: SM background single b production.

and sneutrino–mediated bs production). Unfortunately, detecting such cross–sections of 10^{-4} fb is well beyond the reach of current colliders.

There are related processes, where four quarks are created in the hard process. They can then hadronize into two mesons, either a charged pair or a neutral pair. The diagrams for the production of a charged pair are those in figure 5.7. Those for the production of a neutral pair are the same as for the charged pair, but with the down–type quarks combining to form a $\bar{B}^0$ and the up–types combining to form a light neutral meson.

Generally, it is expected that the hard matrix element for the creation of four quarks is of a similar size or less than the two–quark case. Even ignoring the suppression of the wavefunction overlap of these four quarks with the two–meson final state, one can therefore safely neglect this Standard Model background as well.

5.2.2 False Signal From $\bar{B}B$ Pair Production

Misidentification of B mesons is an extremely important concern. The RPV signal must not be confused with that of a $b\bar{b}$ pair production with one unidentified b quark. Simply looking for events that contain only a single tagged bottom quark is (quantitatively) not feasible. Hence, kinematics are used to get rid of $b\bar{b}$ events. The direct production of a B meson and a light meson of mass m_M leads to, in the beam center–of–momentum frame, the B meson taking a

bd in SM	7.3×10^{-6} fb
bs in SM	1.8×10^{-4} fb

Table 5.4: SM background cross–sections for $e\bar{e}\to b\bar{s}/s\bar{b}/b\bar{d}/d\bar{b}$ at $\sqrt{s} = 10.58$ GeV.

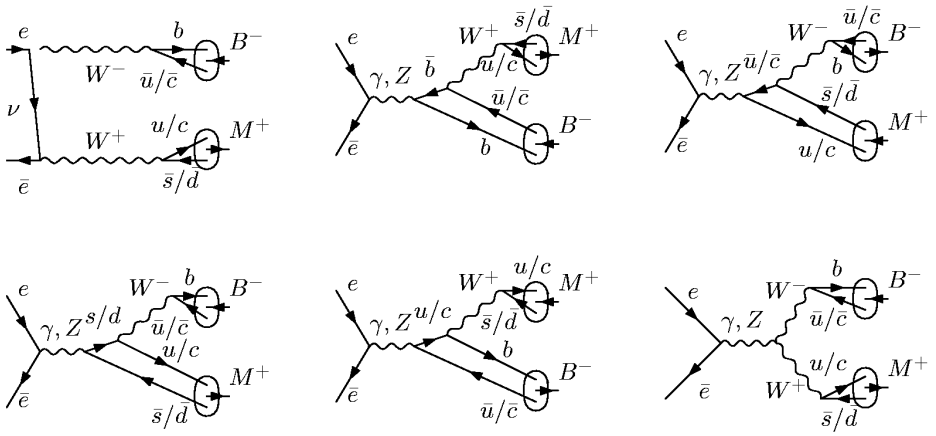

Figure 5.7: Four–quark SM single B meson production.

fraction $(s+m_B^2-m_M^2)/(2s)$ of the center–of–momentum energy $\sqrt{s}$. For the squark–mediated bd signal with $\sqrt{s} = 10.58$ GeV, the B meson will have energy between 6.56 GeV (where the light meson is an η') to 6.61 GeV (where the light meson is a π^0). This is to be compared to the case of $\bar{B}B$ production, where both have energy 5.29 GeV.

High–Energy $\bar{B}B$ Pair Production From Beam Energy Spread

The high–energy tail of the electron–positron beam can create $b\bar{b}$ pairs with enough energy that the resulting B mesons could present a false signal by both having the energy that a singly–produced B meson would have (around 6.6 GeV for $\sqrt{s} = 10.58$ GeV), and one could decay into a high–energy light meson, with the radiated photon or particle missing the detector. BaBar produces 1.1×10^6 $b\bar{b}$ pairs per fb^{-1}, and has over 350 fb^{-1} of integrated luminosity recorded [79]. This gives 385 million $b\bar{b}$ pairs. The beam energy spread is expected to be of the order of 5 MeV, estimated from the beam spread from 4.63 to 4.83 MeV on the $\Upsilon(4S)$ resonance [80]. For the false signal described, the $\bar{B}B$–pair is required to have 2.6 GeV more than the mean beam energy. This is over 400 standard deviations away, if is it assumed that the beam energy has a Gaussian distribution. The expected number of events from this channel is then insignificant (less than 10^{-250}).

Using the $\Upsilon(4S)$ resonance width of 20.7 MeV [80] as the spread, the cut is 125 standard deviations away from the mean, which still leads to an expected number of events less than 10^{-250}. These brief estimates certainly allow one to neglect beam energy spread as a background source for the RPV signal process.

This is also the source of any potential background to the case with an additional high–energy photon. For the range of energies considered, the false signal background of a $\bar{B}B$ plus

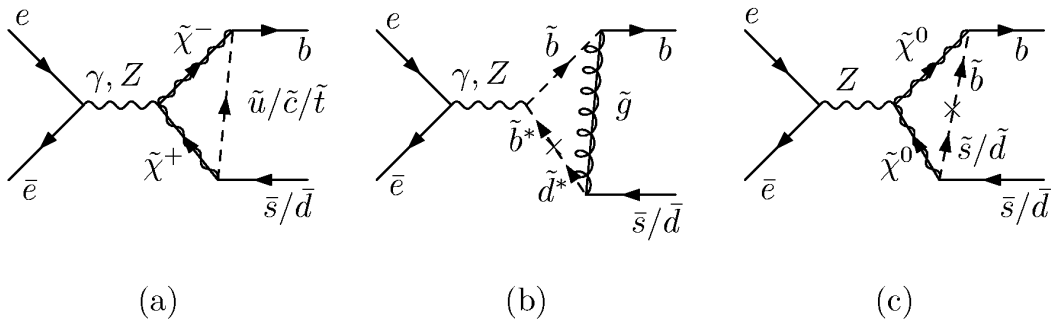

Figure 5.8: Example MSSM background diagrams: (a): flavor violation through $SU(2)_L$; (b, c): flavor violation through a mass insertion on the squark line. (b) is known as a *pengluino* diagram.

a high–energy photon requires between 1 and 2 GeV more than the mean beam energy. This is 200 to 400 standard deviations over the mean, and hence the expected number of events is less than 10^{-250}. The false signal background of a $\bar{B}B$ pair of sufficient energy that the radiative decay of one of the mesons produces a photon that passes the cut is also less than 10^{-250} events.

5.2.3 R–Parity Conserving MSSM Background

Any signal of flavor violation in significant excess of the SM prediction is an exciting signal for new physics. However, the thrust of this work is that such a signal could come from RPV couplings. Backgrounds from the R–parity conserving part of the MSSM arise from two sources: flavor violation through $SU(2)_L$ and through non–minimal squark mixing, *i.e.* general soft SUSY breaking terms [81]. (Examples of both types are shown in figure 5.8.)

The diagrams for the former case are easily obtained by replacing the Standard Model particles in SM background loop diagrams with their supersymmetric partners. The W boson mass ($m_W \gg m_B$) accounts for most of the suppression of the SM background. The charged sparticle masses are constrained to be larger than m_W. The structure of the amplitude is similar, which means that one can expect the SUSY loops without a new flavor structure to contribute below the level of the SM backgrounds. If the largest sparticle mass in the loop is increased to three times the W boson mass, these SUSY backgrounds drop below 10% of the already negligible Standard Model background rate. There are potential enhancements in the large tanβ region of the MSSM parameter space, but in the Higgs sector these destructively interfere with the SM amplitude [82], while any other enhancements are constrained by $b \to d\gamma$ to be at most close to the SM value.

The diagrams describing contributions from non–minimal flavor structure in squark sector are obtained by "supersymmetrizing" the virtual particles in the loops in the one–loop corrections to $e\bar{e} \to b\bar{b}$ (except for those diagrams without a virtual quark), and replacing the external $\bar{b}$ with a $\bar{d}$ and the internal $\tilde{b}$ with the mass eigenstate mixtures of $\tilde{b}$ and $\tilde{d}$. These contributions are not easy to calculate, as the most significant diagram, the "pengluino" (which is shown in figure 5.8), is proportional to $\alpha\alpha_s \delta m^2_{\tilde{q}}/m^2_{\tilde{g}}$, where $\delta m^2_{\tilde{q}}$ is the difference in the squared masses of the squarks (assuming that the gluino is more massive than the squarks, otherwise replace the gluino mass with the mass of the more massive squark). This, at least for b–d mixing, is not well constrained [83]. However, note that these diagrams would also contribute to $B \to \rho\gamma$, which *is* tightly constrained.

Altogether, it is expected that the R–parity conserving part of the RPV MSSM contributes to the background at a rate comparable to the Standard Model contribution at most.

5.2.4 Detection Potential

So far, there have been no searches for single B meson production. Currently BaBar has almost 400 fb^{-1} of integrated luminosity [79] and Belle has almost 650 fb^{-1} of data [84] available for analyses. Ignoring detector effects the maximum signal rate for single b production allowed by current bounds comes from t–channel squark exchange and could be as large as 100 events.

A null result, while disappointing, would still improve the bound on $|\lambda'_{1g1}|^2|\lambda'_{1g3}|^2 m_{\tilde{u}}^{-4}$. A 95% confidence limit non–observation corresponds to 95% confidence that less than three events occurred, leading to the deduction that the bound would be tightened by a factor of (expected events)/2, hence for a 0.13 fb signal with 1 ab^{-1} of luminosity, which is 130 events with perfect detection efficiency, the bound on $|\lambda'_{1g1}|^2|\lambda'_{1g3}|^2 m_{\tilde{u}}^{-4}$ would be tightened by a factor of 65.

As shown in section 5.2, the backgrounds to this process are negligible, which makes single b production a promising search channel for R–parity violation.

Chapter 6

Conclusions And Discussion

Summary In this thesis, the Standard Model of Particle Physics was outlined and the R–parity violating Minimal Supersymmetric Standard Model was described. Using all published rare decay data, bounds on combinations of many of the free parameters of the RPVMSSM were obtained. Bounds on certain combinations of these free parameters were also calculated from experimental data from high–energy electron–positron collisions, and compared to the bounds from the rare decay data. Assuming that certain couplings were equal to their upper bound from published literature and from the work in this thesis, a potential signal of the RPVMSSM at current electron–positron colliders was calculated, along with its background, and found to be viable.

Bounds From Rare Decays All flavor–violating decay modes considered yield only upper bounds on the combinations of the product of two couplings divided by the square of a sfermion mass. In general, assuming a sferion mass of 100 GeV, these bounds are still larger than the magnitude of the product of any two of almost all the Yukawa couplings in the Standard Model. The work published in reference [1] and presented in chapter 3 updates many of those bounds previously published, and in some cases bounds on combinations previously unbounded were obtained.

Bounds From Leptonic Collider Experiments It was found that the OPAL bounds on LFV in electron–positron collisions are not, except in the extreme circumstances of the sneutrino mass lying very close to the beam center–of–momentum energy along with a very narrow decay width, tighter than the same bounds from the purely leptonic decays of τ leptons and muons.

Potential Signal at Present Lepton Colliders As shown in chapter 5, high–luminosity electron–positron colliders have the potential to discover quark flavor violation in excess of SM predictions, should the RPV couplings be close to their current bounds.

Outlook

Future Lepton Colliders The large energy reach coupled with the simple initial state of electron–positron collisions makes the ILC an ideal tool for measurements of parameters at high energies. The ILC is also the ideal tool for probing single sparticle production through RPV couplings [85, 86, 87], and should pair–production of sparticles through R_p–conserving processes be viable, a very clean environment for studying sparticle decay through RPV couplings [88].

A muon–anti–muon collider would be a very interesting prospect for high–energy physics, since it combines the advantages of an electron–positron collider with the potential for much

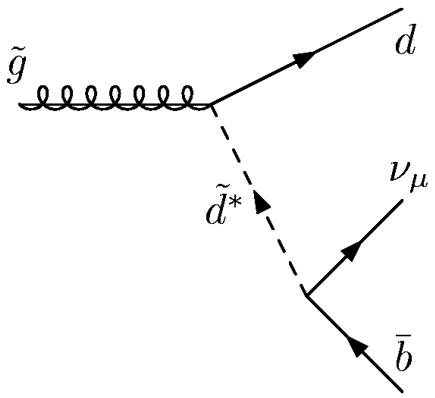

Figure 6.1: Feynman diagram of an example gluino decay chain in the RPVMSSM.

higher energies, due to the muon mass being very much greater than the electron mass. Such a collider would be able to probe different configurations of indices on RPV couplings [89], which may be of more interest because of the mystery of three generations.

Present and Future Hadron Colliders Hadron colliders offer collisions at much higher energies than electron–positron colliders, at the cost of poorly–known initial states and extremely complicated final states. Since the vast majority of the collisions are gluon–gluon, especially at the LHC, direct single sfermion production through RPV couplings would be very hard to measure, because gluons do not have any direct RPV couplings. However, the cross–sections for producing single sparticles are calculable and potentially significant [90].

LSP Decays If SUSY is realized in Nature, at an energy scale accessible to LHC, then the likely means of producing sparticles will be through $SU(3)_C$, because of the dominance of gluons in the proton parton distribution function at that scale [91, 92] and because α_s, despite asymptotic freedom [93, 94], is still large. Therefore the most copiously produced sparticles are probably going to be gluinos and squarks. These colorful sparticles must then decay, either to the MSSM LSP, since the MSSM LSP is not colorful, or, since the LSP is not stable in the RPVMSSM, through RPV couplings into stable SM particles. This decay could possibly happen through a several–stage decay chain, such as shown in figure 6.1. However, if the RPV couplings are very small, about 10^{-8} [95], a neutral, colorless LSP could escape the detector, which would render the RPVMSSM experimentally indistinguishable from the MSSM. A particularly interesting RPVMSSM scenario is if the LSP is charged or colorful (for example, in certain minimal supergravity–inspired models [96, 97]), yet still long–lived enough to impact on the walls of the detector. Such particles would provide a very different signal to typical MSSM signals [98, 99], and the cosmological bounds on charged or colorful LSPs are less stringent if they decay (lifetimes for charged LSPs are bounded at about 10^3s rather than 1s [100, 101, 102]).

Flavor Violation If the RPV couplings are over 10^{-5} or so (depending on the details of the model), then the production and decay vertices of sparticles will be within 1cm of each other [26]. In this case, the effects of R_p–violation will be felt through virtual effects. In particular, the flavor–violating aspect of the RPV couplings could come into play, especially those which are unconstrained by rare–decay data (through kinematic restrictions). However, quark–flavor violation is unlikely to be measurable at LHC, with the potential exception of

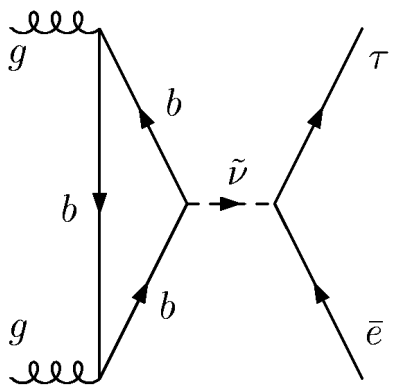

Figure 6.2: Example Feynman diagram for lepton flavor violation at the LHC in the RPVMSSM.

single top production [103] or single stop production [104] (if the process is mediated through very off–shell particles; the quark–flavor–violating decays of a neutralino through non–zero λ'' couplings can be distinguishable [105]). Lepton–flavor violation is a lot easier to detect, and has a significant potential signal [106][1], while having a negligible SM and MSSM backgrounds if no missing transverse momentum is imposed.

Viability Of The R–Parity Violating Minimal Supersymmetric Standard Model One may ask whether the bounds on the couplings rule out the RPVMSSM in any sense. In this thesis, no attempt to bound the bilinear ${\mu'}_i$ couplings was made. The work focused solely on the trilinear couplings. It was found that the majority of the bounds are still no larger than the Yukawa couplings in the Standard Model. Several couplings still remain unbounded.

One may always claim that the couplings are just below their experimental bounds. However, one of the motivations for considering the RPVMSSM is the fact that it provides mechanisms for neutrino mass. There are rough lower bounds on the trilinear couplings through their contribution to neutrino masses. There are still many combinations that contribute, and there may be many cancellations. Yet if one were to consider just the contribution to a muon–neutrino due to a τ — stau loop, one would conclude that

$$|\lambda_{233}|^2/m^2_{\tilde{\tau}_L} \approx (4\pi)^2 m_{\nu_\mu}/(\mu \tan(\beta) m^2_\tau) \tag{6.1}$$

from rearranging equation (2.14). Assuming that $\mu \approx m_{\tilde{\tau}_L} \approx 100$ GeV, $\tan\beta \approx 30$, and that $m_{\nu_\mu} \approx 0.3$ eV, this approximates to, using the notation of chapter 3,

$$|\lambda_{233}|^2 \approx 10^{-5}(m_{\tilde{\tau}_L}/100 \text{ GeV})^2 \tag{6.2}$$

which is still an order of magnitude below the bounds in table 3.4, noting of course that there is no direct comparison of couplings combined with sfermion mass.

If a top–stop loop is considered, the relevant combined couplings should be of the order of $10^{-9}(m_{\tilde{t}_L}/100 \text{ GeV})^2$. For the electron–selectron loop, the couplings need to be of the order of 1 for 100 GeV sfermion masses. This does not imply that the RPVMSSM is not viable — it is quite acceptable for the couplings to be within their bounds and the neutrino masses to be dominated by the contributions from the heavy generations.

Considering these estimates, the RPVMSSM is still a viable model.

[1]However, the signal presented in reference [106] is incorrect, since, while each individual parameter taken as input is below its current bounds, the combination of λ_{312}, ${\lambda'}_{311}$ and $m_{\tilde{\nu}}$ for example grossly violates the bounds from $\mu \to e$ conversion in ^{48}Ti [67] (by between three and five orders of magnitude, depending on the sneutrino mass).

Concluding Remarks There are many bounds on RPV couplings, but they all depend on sfermion masses. Should any one sfermion have a particularly high mass, say of the order of 10 TeV, then the bounds associated with that coupling are not very strong. If supersymmetric partners of SM particles are discovered, and their masses determined, a lot more may be said about the RPV couplings.

There are many high–precision experiments looking at the rare decays of particles (CLEO–c, BaBar, Belle, to name but a few). If their data increase by an order of magnitude, there is the exciting possibility of detection of flavor violation as predicted by the RPVMSSM, should the RPV couplings be close to the magnitude of the Yukawa couplings, other than the top–Higgs coupling, in the SM.

The prospect of the discovery of supersymmetry at the LHC brings with it the potential for many interesting signals of R_p–violation, which would lead to a better understanding of Nature.

Appendix A

Conventions

This is a reference for the conventions that are used in the thesis, with notes on how to convert these conventions into others.

A.1 Units

In this thesis, the speed of light in a vacuum, c, is defined to be 1. Planck's constant, $\hbar$, is also defined to be 1. Hence all quantities may be given in units of energy or some power (including inverse powers), or are dimensionless (*i.e.* have units of energy to the zeroth power). In particular, displacements in both time and space have units of inverse energy, while spatial momenta have units of energy. Mass has units of energy.

In particular, Giga–electron–Volts (GeV) are used as units of energy. These may be converted to femtometres (fm) using table A.1.

A.2 Spacetime

Coordinates are denoted by the contravariant vector x^μ, where here μ is a Lorentz index, and runs from 0 to 3. The time component is x^0, and the three spatial components are x^1, x^2 and x^3. The covariant vector x_μ is defined as $\eta_{\mu\nu}x^\nu$.

Unless otherwise stated, "momentum" means the four–component energy–momentum vector, where the zeroth component is the energy and the three spatial components are the three–dimensional momentum, *e.g.* for a momentum p, p^0 is the energy and p^i is the component of momentum in the direction of the spatial basis vector i where i runs from 1 to 3. The spatial momentum as a three–component vector is denoted by $\boldsymbol{p}$. A subscript denotes which particle has the momentum, *e.g.* a particle X has momentum p_X. The energy of a particle X is often denoted E_X.

$\int_{-\infty}^{\infty}\mathrm{d}\boldsymbol{p}$ denotes the integral over three variables $\int_{-\infty}^{\infty}\mathrm{d}p^1\int_{-\infty}^{\infty}\mathrm{d}p^2\int_{-\infty}^{\infty}\mathrm{d}p^3$.

A.2.1 Metric

The form of the flat–space Minkowski metric used is $(+,-,-,-)$, *i.e.*:

$$\eta_{\mu\nu} = \begin{pmatrix} +1 & 0 & 0 & 0 \\ 0 & -1 & 0 & 0 \\ 0 & 0 & -1 & 0 \\ 0 & 0 & 0 & -1 \end{pmatrix}_{\mu\nu} \tag{A.1}$$

1 GeV c^{-2}	=	1.783×10^{-27} kg	=	1.074 atomic mass units
1 GeV^{-1} $\hbar c$	=	1.973×10^{-16} m	=	0.1973fm
1 GeV^{-2} $\hbar^2c^2$	=	3.894×10^{-32} m^2	=	3.894 $\times10^{11}$ fb

Table A.1: Conversions between units.

as is common in quantum field theory textbooks [107, 108, 109, 110, 111]. This leads to a Klein–Gordon equation of the form

$$(\partial_\mu\partial^\mu + m^2)\phi = 0 \tag{A.2}$$

for a field ϕ, and a Dirac equation of the form

$$(i\partial\!\!\!/ - m)\psi = 0 \tag{A.3}$$

for a spinor field ψ, where Feynman "slashed" notation has been used. The "slash" indicates the dot product of a vector with the γ matrices of the Clifford algebra (see appendix B), *e.g.*:

$$p\!\!\!/ = \gamma^\mu\eta_{\mu\nu}p^\nu \tag{A.4}$$

so

$$\partial\!\!\!/ = \gamma^\mu\eta_{\mu\nu}\partial^\nu = \gamma^\mu\eta_{\mu\nu}\frac{\partial}{\partial x_\nu} = \gamma^\mu\frac{\partial}{\partial x^\mu} = \gamma_\mu\eta^{\mu\nu}\partial_\nu \tag{A.5}$$

A.2.2 Spinors

The normalization of spinors used is consistent with references [108] and [107], in which the spinors are normalized such that for a four–component spinor $u(p)$ with momentum p,

$$\bar{u}^\alpha(p)u^\beta(p) = 2m\delta^{\alpha\beta} \tag{A.6}$$

where α and β are spin indices. (This is in part dependent on using the $(+,-,-,-)$ metric.)

When summed over spins, this leads to

$$\sum_{\text{spins}} u^\alpha(p)\bar{u}^\beta(p) = (p\!\!\!/ + m)^{\alpha\beta} \tag{A.7}$$

and

$$\sum_{\text{spins}} v^\alpha(p)\bar{v}^\beta(p) = (p\!\!\!/ - m)^{\alpha\beta} \tag{A.8}$$

for anti–particle spinors $v(p)$. The particle density is then $1/(2E)$ for both fermions and bosons.

A.2.3 Polarization Vectors

The polarization vectors $\epsilon^{(i)\mu}$ used are normalized to -1, so that

$$\sum_i \epsilon^{(i)\mu*}\epsilon^{(i)\nu} = -\eta^{\mu\nu} \tag{A.9}$$

for massless particles or

$$\sum_i \epsilon^{(i)\mu*}\epsilon^{(i)\nu} = -\eta^{\mu\nu} + \frac{(p^\mu p^\nu)}{p^2} \tag{A.10}$$

for massive particles, where p is the momentum of the particle, μ and ν are Lorentz indices, and i labels the different polarization vectors.

A.3 Supersymmetry

The conventions followed are those laid out in reference [112], rather than in reference [113], which uses the $(-,+,+,+)$ metric and different normalizations.

The fermionic coordinates are denoted by θ, which are two–component (Weyl) spinors with complex Grassman (*i.e.* anticommuting) components, while the bosonic commuting coordinates continue to be denoted by real scalars x^μ.

A.3.1 Indices

Whether the index denoting a fermionic component is raised or lowered is important: $\theta^1 \neq \theta_1$. Instead, the rank two antisymmetric tensor $\epsilon_{\alpha\beta}$ lowers raised fermionic indices and $\epsilon^{\alpha\beta}$ raises them.

The convention adopted is that

$$\epsilon_{\alpha\beta} = \begin{pmatrix} 0 & +1 \\ -1 & 0 \end{pmatrix}_{\alpha\beta} \tag{A.11}$$

and that $\epsilon^{\alpha\beta} = -\epsilon_{\alpha\beta}$, in line with the convention that $\epsilon_{12} = +1$ (in section A.4).

By default, spinors have undotted indices and their complex conjugates have dotted indices, *e.g.* χ_α and its complex conjugate $\bar{\chi}_{\dot{\alpha}}$. Complex conjugation for a Weyl spinor is denoted by a bar over the letter, and does not mean the same as the operation denoted by a bar on a Dirac spinor, as discussed in section B.1.

Also, if indices are omitted, the convention is that pairs of adjacent spinors without indices are dot–products defined by

$$\psi\chi \equiv \psi^\alpha \chi_\alpha = -\chi_\alpha \psi^\alpha = -\epsilon_{\alpha\beta}\chi^\beta \psi^\alpha = \epsilon_{\beta\alpha}\chi^\beta \psi^\alpha = \chi^\beta \psi_\beta \equiv \chi\psi \tag{A.12}$$

Similarly

$$\bar{\psi}\bar{\chi} \equiv \bar{\psi}_{\dot{\alpha}}\bar{\chi}^{\dot{\alpha}} = -\bar{\chi}^{\dot{\alpha}}\bar{\psi}_{\dot{\alpha}} = -\epsilon^{\dot{\alpha}\dot{\beta}}\bar{\chi}_{\dot{\beta}}\bar{\psi}_{\dot{\alpha}} = \epsilon^{\dot{\beta}\dot{\alpha}}\bar{\chi}_{\dot{\beta}}\bar{\psi}_{\dot{\alpha}} = \bar{\chi}_{\dot{\beta}}\bar{\psi}^{\dot{\beta}} \equiv \bar{\chi}\bar{\psi} \tag{A.13}$$

and that the σ^μ have a lower undotted index then a lower dotted index, so

$$\psi\sigma^\mu\bar{\chi} \equiv \psi^\alpha \sigma^\mu_{\alpha\dot{\beta}}\bar{\chi}^{\dot{\beta}} \tag{A.14}$$

Similarly the $\bar{\sigma}^\mu$ have an upper dotted index then an upper undotted index, so

$$\bar{\chi}\bar{\sigma}^\mu\psi \equiv \bar{\chi}_{\dot{\alpha}}\bar{\sigma}^{\mu\dot{\alpha}\beta}\psi_\beta \tag{A.15}$$

This leads to

$$\psi\sigma^\mu\bar{\chi} \equiv \psi^\alpha \sigma^\mu_{\alpha\dot{\beta}}\bar{\chi}^{\dot{\beta}} = -\bar{\chi}^{\dot{\beta}}\sigma^\mu_{\alpha\dot{\beta}}\psi^\alpha = -\epsilon^{\dot{\beta}\dot{\gamma}}\bar{\chi}_{\dot{\gamma}}\sigma^\mu_{\alpha\dot{\beta}}\epsilon^{\alpha\delta}\psi_\delta = \bar{\chi}_{\dot{\gamma}}\epsilon^{\dot{\gamma}\dot{\beta}}\sigma^{\mu T}_{\dot{\beta}\alpha}\epsilon^{\alpha\delta}\psi_\delta = -\bar{\chi}\bar{\sigma}^\mu\psi \tag{A.16}$$

because

$$\epsilon^{\dot{\gamma}\dot{\beta}}\sigma^{\mu T}_{\dot{\beta}\alpha}\epsilon^{\alpha\delta} = \bar{\sigma}^{\mu\dot{\gamma}\delta} \tag{A.17}$$

A.3.2 Superfields

When the SM field is denoted by a lowercase letter (*e.g.* u for an up quark) it is common for the superfield to be denoted by the uppercase version (*e.g.* U for the superfield which has the up quark as its fermionic component). However, this can cause confusion in some cases (*e.g.* uppercase t and uppercase τ are identical in most fonts), and the electroweak bosons are denoted in the SM by uppercase letters already. Also, while the Higgs field is often denoted by ϕ in the SM, the notation of $H_{u/d}$ does not follow the rule, and there is the potentially

confusing notation that H_u and H_d denote the superfields (though in some older literature they are denoted H_1 and H_2 or even S and T), while $H^{\pm}$ denote the charged bosons remaining after the Goldstone bosons are absorbed into the massive vector bosons and H denotes the heavier neutral boson. As mentioned in section 2.1, in this thesis an accent is used to denote the superfields, *e.g.* $\breve{\nu}_e$ denotes the superfield which contains the SM electron–neutrino, while ν_e is reserved exclusively to represent the electron–neutrino fermion field.

Matter superfields are all "left–chiral", *i.e.*:

$$\bar{D}_{\dot{\alpha}}\breve{\psi}(x,\theta,\bar{\theta}) = 0 \tag{A.18}$$

for a chiral superfield $\breve{\psi}(x,\theta,\bar{\theta})$ (adopting the convention that its defining field is its fermion, ψ, hence $\tilde{\psi}$ is the bosonic component), where the fermionic derivative $\bar{D}_{\dot{\alpha}}$ is defined as

$$\bar{D}_{\dot{\alpha}} = -\frac{\partial}{\partial\bar{\theta}^{\dot{\alpha}}} + i\theta^{\beta}\sigma^{\mu}_{\beta\dot{\alpha}}\partial_{\mu} \tag{A.19}$$

Changing variables to $y^{\mu} = x^{\mu} - i\theta\sigma^{\mu}\bar{\theta}$ leads to

$$\bar{D}_{\dot{\alpha}}\Big|_{y,\theta} = -\frac{\partial}{\partial\bar{\theta}^{\dot{\alpha}}} \tag{A.20}$$

Hence

$$\breve{\psi}(y,\theta) = \tilde{\psi}(y) + \sqrt{2}\theta\psi(y) + \theta\theta F_{\psi}(y) \tag{A.21}$$

is the most general solution for a chiral superfield. Changing spacetime variables back to x^{μ}, one obtains

$$\begin{aligned}\breve{\psi}(x,\theta,\bar{\theta}) &= \tilde{\psi}(x) - i\theta\sigma^{\mu}\bar{\theta}\partial_{\mu}\tilde{\psi}(x) - \frac{1}{2}\theta\sigma^{\mu}\bar{\theta}\theta\sigma^{\nu}\bar{\theta}\partial_{\mu}\partial_{\nu}\tilde{\psi}(x) + \sqrt{2}\theta\psi(x) - i\sqrt{2}\theta\sigma^{\mu}\bar{\theta}\theta\partial_{\mu}\psi(x) \\ &\quad +\theta\theta F_{\psi}(x) \\ &= \tilde{\psi}(x) + \sqrt{2}\theta\psi(x) + \theta\theta F_{\psi}(x) - i\partial_{\mu}\tilde{\psi}(x) + \frac{i}{\sqrt{2}}\theta\theta\partial_{\mu}\psi(x)\sigma^{\mu}\bar{\theta} - \frac{1}{4}\bar{\theta}\bar{\theta}\theta\theta\partial^{\mu}\partial_{\mu}\tilde{\psi}(x)\end{aligned} \tag{A.22}$$

This means that the right–handed $SU(2)_L$ singlet electron field is represented by the charge conjugate of the left–handed $SU(2)_L$ singlet positron field. The superfields associated with the $SU(2)_L$ singlets have a superscript c, *e.g.* the left–handed $SU(2)_L$ singlet positron field is denoted e^c_R, and the Dirac spinor for the electron is given by

$$e = \begin{pmatrix} e_L \\ (\bar{e}^c_R)^T \end{pmatrix} \tag{A.23}$$

In ordinary SM terms, $(\bar{e}^c_R)^T$ would be denoted e_R. The subscript R in e^c_R denotes that its antiparticle, which is the field which is combined into a Dirac spinor with the left–handed chirality of the familiar SM field, is right–handed.

A.3.3 Number Of Supersymmetries

In this thesis, only one pair (the generator and its complex conjugate) of fermionic generators for the supersymmetry are considered. This is referred to as $N = 1$ supersymmetry. For a number of pairs of generators $N > 1$, there would be many more spin states — each fermionic generator acting on a spin–0 boson would create a spin–1/2 fermion, but so would acting on it with one fermionic generator, then a different fermionic generator, then the conjugate of a third different fermionic generator. A problem with attempting to build models of Nature with $N > 1$ supersymmetries is that there would have to be left– and right–handed chiralities transforming in the same way for each gauge group, which is in opposition to the experimental fact of $SU(2)_L$ acting only on left–handed chiralities.

A.4 Antisymmetric Tensors And γ Matrices

A.4.1 Antisymmetric Tensors

For the completely antisymmetric tensor of rank n, $\epsilon_{\alpha_1\alpha_2\alpha_3\ldots\alpha_n}$, the property that it is antisymmetric under the interchange of any two of its indices is enough to define it completely, up to an overall sign. The convention adopted in this thesis is such that

$$\epsilon_{123\ldots n} = +1 \tag{A.24}$$

and indices are raised and lowered in the manner appropriate to the index (*e.g.* for Lorentz indices, they are raised and lowered using the space–time metric, while for spinor indices, they are raised and lowered by the rank two antisymmetric tensor).

A.4.2 γ Matrices

The γ matrices are those that satisfy the Clifford algebra, *i.e.*:

$$\{\gamma_\mu, \gamma_\nu\} = 2\eta_{\mu\nu} I_{4\times 4} \tag{A.25}$$

where $I_{4\times 4}$ is the four–by–four identity matrix.

In this thesis, nothing in the main body depends on an explicit representation of the γ matrices, but in the appendices it is most useful to adopt an explicit representation when discussing spinors and supersymmetry. Hence the following representation, the *Weyl* representation, of the γ matrices is used, for $\mu = 0, 1, 2, 3$:

$$\gamma^\mu = \begin{pmatrix} 0_{2\times 2} & \sigma^\mu \\ \bar{\sigma}^\mu & 0_{2\times 2} \end{pmatrix} \tag{A.26}$$

where the four–by–four component γ matrix is written in terms of blocks of two–by–two component matrices. The entries of $0_{2\times 2}$ in the top–left and bottom–right are two–by–two matrices with 0 for all components. The σ matrices are defined as follows:

$$\sigma^0 = \begin{pmatrix} 1 & 0 \\ 0 & 1 \end{pmatrix} = I_{2\times 2} \tag{A.27}$$

$$\sigma^1 = \begin{pmatrix} 0 & 1 \\ 1 & 0 \end{pmatrix} \tag{A.28}$$

$$\sigma^2 = \begin{pmatrix} 0 & -i \\ i & 0 \end{pmatrix} \tag{A.29}$$

$$\sigma^3 = \begin{pmatrix} 1 & 0 \\ 0 & -1 \end{pmatrix} \tag{A.30}$$

Hence σ^0 is the two–by–two identity matrix, $I_{2\times 2}$, and σ^i for $i = 1, 2, 3$ are the Pauli matrices. The $\bar{\sigma}$ matrices are defined as follows:

$$\bar{\sigma}^0 = \sigma^0 \tag{A.31}$$

$$\bar{\sigma}^i = -\sigma^i \ \text{(for } i = 1, 2, 3) \tag{A.32}$$

The matrix γ^5 is defined as follows:

$$\gamma^5 = i\gamma^0\gamma^1\gamma^2\gamma^3 = \frac{i}{24}\epsilon_{\mu\nu\rho\sigma}\gamma^\mu\gamma^\nu\gamma^\rho\gamma^\sigma = \frac{i}{24}\epsilon^{\mu\nu\rho\sigma}\gamma_\mu\gamma_\nu\gamma_\rho\gamma_\sigma \tag{A.33}$$

and so, in the explicit representation used,

$$\gamma^5 = \begin{pmatrix} -I_{2\times 2} & 0 \\ 0 & I_{2\times 2} \end{pmatrix} \tag{A.34}$$

A particularly useful identity is that

$$(\gamma^5)^2 = I_{4\times 4} \tag{A.35}$$

The chiral projection operators P_L and P_R are defined by:

$$P_L = \frac{1}{2}(I_{4\times 4} - \gamma^5) \tag{A.36}$$

$$P_R = \frac{1}{2}(I_{4\times 4} + \gamma^5) \tag{A.37}$$

Hence in the explicit representation used,

$$P_L = \begin{pmatrix} I_{2\times 2} & 0_{2\times 2} \\ 0_{2\times 2} & 0_{2\times 2} \end{pmatrix} \tag{A.38}$$

$$P_R = \begin{pmatrix} 0_{2\times 2} & 0_{2\times 2} \\ 0_{2\times 2} & I_{2\times 2} \end{pmatrix} \tag{A.39}$$

A particular identity from this is that for example a left–handed electron–neutrino ν_L and a left–handed strange quark s_L,

$$\nu_{eL} s_L = \nu_L^\alpha s_{L\alpha} = \nu_{eL\beta}\epsilon^{\alpha\beta} s_{L\alpha} = -\nu_{eL\beta}\epsilon^{\beta\alpha} s_{L\alpha} = -i\nu_{eL\beta}\bar{\sigma}^{2\alpha\beta} s_{L\alpha} = \nu_e(-i)\gamma^0\gamma^2 P_L s \tag{A.40}$$

A.5 Feynman Diagrams

All Feynman diagrams are drawn with initial–state particles on the left and final–state particles on the right, rather than initial–state particles on the bottom and final–state particles on the top.

A.6 Time–Ordering

The time–ordered product of the field creation/annihilation operators $\psi_1(x^\mu)$ and $\psi_2(x'^\mu)$ is denoted by $T(\psi_1\psi_2)$. This means that

$$T(\psi_1\psi_2) = \theta(x^0 - x'^0)\psi_1(x^\mu)\psi_2(x'^\mu) + \theta(x'^0 - x^0)\psi_2(x'^\mu)\psi_1(x^\mu) = \begin{cases} \psi_1(x^\mu)\psi_2(x'^\mu) \text{ if } x^0 > x'^0 \\ \psi_2(x'^\mu)\psi_1(x^\mu) \text{ if } x^0 < x'^0 \end{cases} \tag{A.41}$$

where $\theta(x^0 - x'^0)$ is the Heaviside step function.

Appendix B

Spinors And Fermionic Fields

For a more complete treatment of the properties of spinors and fermionic fields, see for example the first chapter of reference [112] or the third chapter of reference [108], upon which most of the material in this appendix is based.

Fermionic fields are represented by creation and annihilation operators which are anticommuting objects, and these are arranged in two– or four–component spinors, and then the whole object is often referred to as a spinor. In this appendix, the term is used to just refer to the objects with a half–integer spin Lorentz transformation, while a spinor with complex anticommuting operator elements is referred to as a fermionic field. However, both aspects (Lorentz transformations and the anticommuting nature) of fermionic fields are discussed here, as are the various types of spinor (Weyl, Dirac and Majorana).

All the following assumes four space–time dimensions. In different numbers of dimensions, spinors have different numbers of components, and it is just a coincidence that in four space–time dimensions spinors have four components. Also, it is not possible to decompose Dirac spinors into Weyl spinors in an odd number of space–time dimensions.

B.1 Dirac Spinors

One can show that the object

$$\frac{1}{2}\Sigma^{\mu\nu} = \frac{i}{4}[\gamma^\mu, \gamma^\nu] \tag{B.1}$$

satisfies the Lie algebra for the Lorentz transformations (simply by plugging it into the commutation relations and repeatedly using equation (A.25)). Using the Weyl representation of the γ matrices, the boost generators are

$$\frac{1}{2}\Sigma^{0i} = \frac{-i}{2}\begin{pmatrix} \sigma^i & 0_{2\times 2} \\ 0_{2\times 2} & -\sigma^i \end{pmatrix} \tag{B.2}$$

where i runs from 1 to 3. The rotation generators are

$$\frac{1}{2}\Sigma^{ij} = \frac{-i}{2}\epsilon^{ij}{}_k \begin{pmatrix} \sigma^k & 0_{2\times 2} \\ 0_{2\times 2} & \sigma^k \end{pmatrix} \tag{B.3}$$

where i, j and k run from 1 to 3.

A *Dirac spinor* is defined to be a four–component object that transforms according to these generators.

The bar operation on a Dirac spinor ψ is defined thus:

$$\bar{\psi} = \psi^\dagger \gamma^0 \tag{B.4}$$

and does not mean the same as it does for a Weyl spinor, where a bar over the letter denotes complex conjugation. However, it leads conveniently to the following for a Dirac spinor ψ, where ψ_L and ψ_R are Weyl spinors defined by equations (B.12) and (B.13):

$$\psi = \begin{pmatrix} \psi_L \\ \psi_R \end{pmatrix} \tag{B.5}$$

$$\bar{\psi} = (\bar{\psi}_R, \bar{\psi}_L) \tag{B.6}$$

$$\overline{(P_L\psi)} = (P_L\psi)^\dagger\gamma^0 = \psi^\dagger P_L\gamma^0 = \psi^\dagger\gamma^0 P_R = \bar{\psi}P_R = \bar{\psi}_L \tag{B.7}$$

$$\overline{(P_R\psi)} = (P_R\psi)^\dagger\gamma^0 = \psi^\dagger P_R\gamma^0 = \psi^\dagger\gamma^0 P_L = \bar{\psi}P_L = \bar{\psi}_R \tag{B.8}$$

The charge conjugate of a Dirac spinor ψ is defined to be

$$\psi^c = C\bar{\psi}^T \tag{B.9}$$

where C satisfies

$$C^{-1}\gamma^\mu C = -\gamma^{\mu T} \tag{B.10}$$

and can be chosen to be

$$C = -i\gamma^0\gamma^2 \tag{B.11}$$

B.2 Weyl Spinors

In the Weyl representation of the γ matrices, one can see that the transformation generators are block–diagonal. Using equations (A.38) and (A.39), one can define left– and right–handed *Weyl spinors*, ψ_L and ψ_R respectively, by

$$\psi_L = P_L\psi \tag{B.12}$$

$$\psi_R = P_R\psi \tag{B.13}$$

where ψ is a Dirac spinor. Both chiralities transform in the same way under spatial rotations, but have opposite transformations under boosts.

Using the identity

$$\sigma^{\mu\dagger} = -\sigma^2\bar{\sigma}^{\mu T}\sigma^2 \tag{B.14}$$

one can show that $\sigma^2\psi_L^*$ transforms as a right–handed spinor, and $\sigma^2\psi_R^*$ transforms as a left–handed spinor.

In the limit of massless fermions, the Dirac equation (equation (A.3)) reduces to

$$i\partial\!\!\!/\psi = 0 \tag{B.15}$$

which is equivalent to the decoupled equations

$$i\bar{\sigma}^\mu\partial_\mu\psi_L = 0 \tag{B.16}$$

$$i\sigma^\mu\partial_\mu\psi_R = 0 \tag{B.17}$$

B.3 Majorana Spinors

A *Majorana spinor* is defined to be a Dirac spinor that is equal to its charge conjugate. Given a Weyl spinor $\psi_{L\alpha}$ one may construct a Majorana spinor

$$\psi^M = \begin{pmatrix} \psi_{L\alpha} \\ \bar{\psi}_L^{\dot{\alpha}} \end{pmatrix} \tag{B.18}$$

B.4 Anticommutation

The Spin–Statistics Theorem [114] states that the creation and annihilation operators of integer spin quantum fields satisfy *commutation* relations, while those of half–integer spin quantum fields satisfy *anticommutation* relations. The Pauli exclusion principle is a consequence of this: two electrons in the same quantum state would have to be created by identical operators, which would then be expressible as the square of the creation operator acting on the vacuum state, but since this operator anticommutes with itself, its square is zero identically.

B.5 Fierz Identities

Some Fierz identities were used, in equations (3.1) and (3.7). Actually, really only one Fierz identity was used,

$$(\theta\psi)(\bar{\chi}\bar{\eta}) = \sum_{\mu} \frac{-1}{2} (\theta\sigma^{\mu}\bar{\eta})(\bar{\chi}\bar{\sigma}_{\mu}\psi) \tag{B.19}$$

This was used to re-write $(e_L^i u_L^m)(\bar{u}_L^n \bar{e}_L^k)$ and $(\bar{d}_R^n e_L^i)(\bar{e}_L^k d_R^m)$, where the quark spinors are dotted with lepton spinors, into forms where the quarks spinors are dotted with each other.

$$\begin{aligned}
(e_L^i u_L^m)(\bar{u}_L^n \bar{e}_L^k) = (u_L^m e_L^i)(\bar{e}_L^k \bar{u}_L^n) &= \sum_{\mu} \frac{-1}{2} (u_L^m \sigma^{\mu} \bar{u}_L^n)(\bar{e}_L^k \bar{\sigma}_{\mu} e_L^i) \\
&= \sum_{\mu} \frac{1}{2} (\bar{u}_L^n \bar{\sigma}^{\mu} u_L^m)(\bar{e}_L^k \bar{\sigma}_{\mu} e_L^i) \\
&= \sum_{\mu} \frac{1}{2} (\bar{u}^n P_R \gamma^{\mu} u^m)(\bar{e}^k P_R \gamma_{\mu} e^i) \\
&= \sum_{\mu} \frac{1}{2} (\bar{u}^n \gamma^{\mu} P_L u^m)(\bar{e}^k \gamma_{\mu} P_L e^i)
\end{aligned} \tag{B.20}$$

and (writing the right-handed Weyl spinors d_R^m as $\bar{\eta}_L^m$),

$$\begin{aligned}
(\bar{d}_R^n e_L^i)(\bar{e}_L^k d_R^m) &= (\eta_L^n e_L^i)(\bar{e}_L^k \bar{\eta}_L^m) \\
&= \sum_{\mu} \frac{-1}{2} (\eta_L^n \sigma^{\mu} \bar{\eta}_L^m)(\bar{e}_L^k \bar{\sigma}_{\mu} e_L^i) \\
&= \sum_{\mu} \frac{-1}{2} (\eta^{nT} P_L \gamma^{\mu} \bar{\eta}^{mT})(\bar{e}^k P_R \gamma_{\mu} e^i) \\
&= \sum_{\mu} \frac{-1}{2} (\eta^{nT} \gamma^{\mu} P_R \bar{\eta}^{mT})(\bar{e}^k \gamma_{\mu} P_L e^i) \\
&= \sum_{\mu} \frac{-1}{2} (\bar{d}^n \gamma^{\mu} P_R d^m)(\bar{e}^k \gamma_{\mu} P_L e^i)
\end{aligned} \tag{B.21}$$

Appendix C

The SM Lagrangian Density And Feynman Rules

C.1 Lagrangian Density

As mentioned in section 1.2.1, the Lagrangian density of the SM can be separated into four pieces: the *kinetic* part, $\mathcal{L}^{\rm SM}_{\rm kin}$, the *scalar potential* part, $\mathcal{L}^{\rm SM}_{\rm pot}$, the *Yukawa* part, $\mathcal{L}^{\rm SM}_{\rm Yuk}$, and the *Yang–Mills* part, $\mathcal{L}^{\rm SM}_{\rm Y-M}$.

The notation for the fields which are fundamental representations of one or more of the gauge groups is shown in table C.1, and their spins and gauge group transformations in table C.2.

Electroweak symmetry breaking mixes the gauge vector bosons of $SU(2)_L$ and $U(1)_Y$. It is usual to denote the unmixed states as B^μ for the $U(1)_Y$ vector boson and W_1^μ, W_2^μ and W_3^μ for the $SU(2)_L$ vector bosons. After electroweak symmetry breaking, the mixed states are denoted $W^{\pm\mu} = {}^1\!/\!_{\sqrt{2}}(W_1^\mu \mp i W_2^\mu)$ (the (electrically) charged W bosons), $Z^\mu = \cos(\theta_W)W_3^\mu - \sin(\theta_W)B^\mu$ (the Z boson, which is electrically neutral) and $A^\mu = \sin(\theta_W)W_3^\mu + \cos(\theta_W)B^\mu$ (the photon, which is also electrically neutral). The weak mixing angle is denoted by θ_W, and gives the relation between the $SU(2)_L$ and $U(1)_Y$ gauge couplings, in that the ratio of the $U(1)_Y$ gauge coupling to that of $SU(2)_L$ is $\tan(\theta_W)$, and the gauge couplings are also related to the electromagnetic coupling, $(-\sqrt{4\pi\alpha})$, in that the $SU(2)_L$ gauge coupling is $\frac{(-\sqrt{4\pi\alpha})}{\sin(\theta_W)}$. (Conventionally γ is used to denote photons, hence it is used in the Feynman diagrams and in subscripts denoting quantities associated with the photon (its momentum, p_γ^μ, polarization, ϵ_γ^μ, *etc.*), but since γ^μ already denotes the matrices of the Clifford algebra, A^μ is used to denote the photon field.) The gluons are denoted by $g^\mu_{a_C}$.

C.1.1 The Kinetic Part

The kinetic part is given by

$$\mathcal{L}^{\rm SM}_{\rm kin} = i\bar{\psi}_j \not{D}\psi_j + (D^\mu\phi)^\dagger\cdot(D_\mu\phi) \tag{C.1}$$

where the ψ_j are the fermions.

The D_μ are covariant derivatives, which are different for each fermionic field depending on their gauge–transformation properties.

$$D_\mu = \partial_\mu - iq_Y\frac{(-\sqrt{4\pi\alpha})}{\cos(\theta_W)}B_\mu - iq_W\frac{(-\sqrt{4\pi\alpha})}{\sin(\theta_W)}W_{\mu a_W}t_W^{a_W} - iq_C\sqrt{4\pi\alpha_s}g_{\mu a_C}t_C^{a_C} \tag{C.2}$$

where $t_W^{a_W}$ are the generators of $SU(2)$ (and a_W runs from 1 to 3), $t_C^{a_C}$ are the generators of $SU(3)$ (and a_C runs from 1 to 8) and q_Y, q_W and q_C are such that:

Field	Symbol
Higgs doublet	$\phi = \begin{pmatrix} \phi^+ \\ \phi^0 \end{pmatrix}$
Right–handed electron	$e_{1R} = e_R$
Right–handed muon	$e_{2R} = \mu_R$
Right–handed τ lepton	$e_{3R} = \tau_R$
Left–handed electron doublet	$L_{1L} = \begin{pmatrix} \nu_{eL} \\ e_L \end{pmatrix}$
Left–handed muon doublet	$L_{2L} = \begin{pmatrix} \nu_{\mu L} \\ \mu_L \end{pmatrix}$
Left–handed τ lepton doublet	$L_{3L} = \begin{pmatrix} \nu_{\tau L} \\ \tau_L \end{pmatrix}$
Right–handed up quarks	$u_{1R} = u_R^{\text{red}}, u_R^{\text{green}}, u_R^{\text{blue}}$
Right–handed charm quarks	$u_{2R} = c_R^{\text{red}}, c_R^{\text{green}}, c_R^{\text{blue}}$
Right–handed top quarks	$u_{3R} = t_R^{\text{red}}, t_R^{\text{green}}, t_R^{\text{blue}}$
Right–handed down quarks	$d_{1R} = d_R^{\text{red}}, d_R^{\text{green}}, d_R^{\text{blue}}$
Right–handed strange quarks	$d_{2R} = s_R^{\text{red}}, s_R^{\text{green}}, s_R^{\text{blue}}$
Right–handed bottom quarks	$d_{3R} = b_R^{\text{red}}, b_R^{\text{green}}, b_R^{\text{blue}}$
Left–handed up–down quark doublets	$Q_{1L} = \begin{pmatrix} u_{1L} \\ d_{1L} \end{pmatrix} = \begin{pmatrix} u_L \\ d_L \end{pmatrix}^{\text{red}}, \begin{pmatrix} u_L \\ d_L \end{pmatrix}^{\text{green}}, \begin{pmatrix} u_L \\ d_L \end{pmatrix}^{\text{blue}}$
Left–handed charm–strange quark doublets	$Q_{2L} = \begin{pmatrix} u_{2L} \\ d_{2L} \end{pmatrix} = \begin{pmatrix} c_L \\ s_L \end{pmatrix}^{\text{red}}, \begin{pmatrix} c_L \\ s_L \end{pmatrix}^{\text{green}}, \begin{pmatrix} c_L \\ s_L \end{pmatrix}^{\text{blue}}$
Left–handed top–bottom quark doublets	$Q_{3L} = \begin{pmatrix} u_{3L} \\ d_{3L} \end{pmatrix} = \begin{pmatrix} t_L \\ b_L \end{pmatrix}^{\text{red}}, \begin{pmatrix} t_L \\ b_L \end{pmatrix}^{\text{green}}, \begin{pmatrix} t_L \\ b_L \end{pmatrix}^{\text{blue}}$

Table C.1: Notation for fields except gauge vector bosons.

q_Y is the hypercharge of the field upon which D_μ is acting, as given in table C.1;
q_W is 1 for an $SU(2)_L$ doublet and 0 for an $SU(2)_L$ singlet; and
q_C is 1 for an $SU(3)_C$ triplet and 0 for an $SU(3)_C$ singlet.

So, for example, sum of the left– and right–handed electron terms is

$$\begin{aligned}
\mathcal{L}_{\rm kin}^{{\rm SM}\ e} &= i\bar{e}_{1R}\left(i\partial\!\!\!/ - i(-1)\frac{(-\sqrt{4\pi\alpha})}{\cos(\theta_W)}B\!\!\!/\right)e_{1R} \\
&\quad + i\bar{L}_{1L}\left(\partial\!\!\!/ - i\left(\frac{-1}{2}\right)\frac{(-\sqrt{4\pi\alpha})}{\cos(\theta_W)}B\!\!\!/ - i\frac{(-\sqrt{4\pi\alpha})}{\sin(\theta_W)}W\!\!\!/_{a_W}t_W^{a_W}\right)L_{1L} \\
&= \bar{e}_R\left(i\partial\!\!\!/ - \frac{(-\sqrt{4\pi\alpha})}{\cos(\theta_W)}B\!\!\!/\right)e_R \\
&\quad + (\bar{\nu}_{eL}\bar{e}_L)\left(i\partial_\mu - \frac{1}{2}\frac{(-\sqrt{4\pi\alpha})}{\cos(\theta_W)}B\!\!\!/\right. \\
&\quad \left. + \frac{(-\sqrt{4\pi\alpha})}{\sin(\theta_W)}\frac{1}{2}\begin{pmatrix} W\!\!\!/_3 & (W\!\!\!/_1 - iW\!\!\!/_2) \\ (W\!\!\!/_1 + iW\!\!\!/_2) & -W\!\!\!/_3 \end{pmatrix}\right)\begin{pmatrix}\nu_{eL}\\ e_L\end{pmatrix} \\
&= \bar{e}\left(i\partial\!\!\!/ - (-\sqrt{4\pi\alpha})\left(A\!\!\!/ - \frac{\sin(\theta_W)}{\cos(\theta_W)}Z\!\!\!/\right)\right)P_R e \\
&\quad + (\bar{\nu}_{eL}\bar{e}_L)\left(i\partial\!\!\!/ - \frac{(-\sqrt{4\pi\alpha})}{2}\left(A\!\!\!/ - \frac{\sin(\theta_W)}{\cos(\theta_W)}Z\!\!\!/\right)\right. \\
&\quad \left. + \frac{(-\sqrt{4\pi\alpha})}{2}\begin{pmatrix} (A\!\!\!/ + \frac{\cos(\theta_W)}{\sin(\theta_W)}Z\!\!\!/) & \frac{\sqrt{2}}{\sin(\theta_W)}W\!\!\!/^+ \\ \frac{\sqrt{2}}{\sin(\theta_W)}W\!\!\!/^- & -(A\!\!\!/ + \frac{\cos(\theta_W)}{\sin(\theta_W)}Z\!\!\!/) \end{pmatrix}\right)\begin{pmatrix}\nu_{eL}\\ e_L\end{pmatrix} \\
&= \bar{e}\left(i\partial\!\!\!/ + q_e(-\sqrt{4\pi\alpha})A\!\!\!/\right. \\
&\quad - (-\sqrt{4\pi\alpha})Z\!\!\!/\left(\left(\frac{1}{2\sin(\theta_W)\cos(\theta_W)} + q_e\frac{\sin(\theta_W)}{\cos(\theta_W)}\right)P_L + q_e\frac{\sin(\theta_W)}{\cos(\theta_W)}P_R\right)\Big)e \\
&\quad + \bar{e}_L\frac{(-\sqrt{4\pi\alpha})}{\sin(\theta_W)\sqrt{2}}W\!\!\!/^-\nu_{eL} + \bar{\nu}_{eL}\frac{(-\sqrt{4\pi\alpha})}{\sin(\theta_W)\sqrt{2}}W\!\!\!/^+ e_L \\
&\quad + \bar{\nu}_e\left(i\partial\!\!\!/ + \frac{(-\sqrt{4\pi\alpha})}{2}\left(\frac{\sin(\theta_W)}{\cos(\theta_W)} + \frac{\cos(\theta_W)}{\sin(\theta_W)}\right)Z\!\!\!/\right)\nu_{eL}
\end{aligned} \tag{C.3}$$

where $q_e = -1$ is the electric charge of the electron.

C.1.2 The Scalar Potential Part

The potential part of the Lagrangian density is just the potential energy density due to the Higgs boson field.

$$\mathcal{L}_{\rm pot}^{\rm SM} = \mu^2\phi^\dagger\cdot\phi - \lambda(\phi^\dagger\cdot\phi)^2 \tag{C.4}$$

noting that here μ is the mass of the Higgs boson.

C.1.3 The Yukawa Part

The Yukawa part is given by

$$\mathcal{L}_{\rm Yuk}^{\rm SM} = -Y_{jk}^l\bar{L}_{jL}\cdot\phi\, e_{kR} - Y_{jk}^d\bar{Q}_{jL}\cdot\phi\, d_{kR} - Y_{jk}^u\sum_{\rm colors}\bar{Q}_{jLa}\epsilon_{ab}\phi_b^* u_{kR} + \text{ Hermitian conjugate} \tag{C.5}$$

where a labels the components of the $SU(2)_L$ doublets. The spontaneous breaking of electroweak symmetry by the Higgs boson vacuum expectation value, v, leads to mass terms

Field	Spin	Gauge Group Representation		$U(1)_Y$ Hypercharge
		$SU(2)_L$	$SU(3)_C$	
ϕ	0	**2** (doublet)	**1** (singlet)	$\frac{+1}{2}$
e_{1R}	$\frac{1}{2}$	**1** (singlet)	**1** (singlet)	-1
e_{2R}				
e_{3R}				
L_{1L}	$\frac{1}{2}$	**2** (doublet)	**1** (singlet)	$\frac{-1}{2}$
L_{2L}				
L_{3L}				
u_{1R}	$\frac{1}{2}$	**1** (singlet)	**3** (triplet)	$\frac{+2}{3}$
u_{2R}				
u_{3R}				
d_{1R}	$\frac{1}{2}$	**1** (singlet)	**3** (triplet)	$\frac{-1}{3}$
d_{2R}				
d_{3R}				
Q_{1L}	$\frac{1}{2}$	**2** (doublet)	**3** (triplet)	$\frac{+1}{6}$
Q_{2L}				
Q_{3L}				

Table C.2: Spin and gauge group assignments for fields except gauge vector bosons.

for the charged leptons of $Y^l_{jk}v$ and for the down–type and up–type quarks of $Y^d_{jk}v$ and $Y^u_{jk}v$ respectively, and the diagonalization of these matrices leads to the CKM matrix [10, 11].

C.1.4 The Yang–Mills Part

The Yang–Mills part is given by

$$\mathcal{L}^{\rm SM}_{\rm Y-M} = \frac{-1}{4}{\rm tr}(F_{Y\mu\nu}F_Y^{\mu\nu}) - \frac{1}{4}{\rm tr}(F_{W\mu\nu}F_W^{\mu\nu}) - \frac{1}{4}{\rm tr}(F_{C\mu\nu}F_C^{\mu\nu}) \qquad \text{(C.6)}$$

where

$$F_Y^{\mu\nu} = \frac{i}{\left(\frac{(-\sqrt{4\pi\alpha})}{\cos(\theta_W)}\right)}[D_Y^\mu, D_Y^\nu] \tag{C.7}$$

$$D_Y^\mu = \partial^\mu - i\frac{(-\sqrt{4\pi\alpha})}{\cos(\theta_W)}B^\mu \tag{C.8}$$

$$F_W^{\mu\nu} = \frac{i}{\left(\frac{(-\sqrt{4\pi\alpha})}{\sin(\theta_W)}\right)}[D_W^\mu, D_W^\nu] \tag{C.9}$$

$$D_W^\mu = \partial^\mu - i\frac{(-\sqrt{4\pi\alpha})}{\sin(\theta_W)}W_{aW}^\mu t_W^{aW} \tag{C.10}$$

$$F_C^{\mu\nu} = \frac{i}{\sqrt{4\pi\alpha_s}}[D_C^\mu, D_C^\nu] \tag{C.11}$$

$$D_C^\mu = \partial^\mu - i\sqrt{4\pi\alpha_s}g_{aC}^\mu t_C^{aC} \tag{C.12}$$

C.1.5 Ghosts

The Faddeev–Popov [115] gauge–fixing of non–Abelian gauge groups introduces new fields which serve to cancel the unphysical longitudinal and time–like polarizations of the gauge bosons, and these particles are called "ghosts" because they are scalar particles that obey anticommutation relations. They only couple to the gauge bosons, and they never appear in the external states. These ghosts, labelled by c^a, where a is an adjoint representation index, have a kinetic term, and the gauge–fixing also introduces a dependence on an unphysical parameter ξ which determines the choice of gauge and does not appear in any final physical result. These additional terms are given by

$$\mathcal{L}_{\text{F–P}}^{\text{SM}} = \sum_{\text{gauge fields}} -\bar{c}^a(\partial^\mu\partial_\mu\delta_{ab} + g\partial_\mu G^{c\mu}f_{abc})c^b - \frac{1}{2\xi}\partial_\mu G^{a\mu}\partial_\nu G_a^\nu \tag{C.13}$$

where f_{abc} is defined by

$$[t_a, t_b] = if_{abc}t_c \tag{C.14}$$

for generators t_a of the gauge group, with gauge bosons G_a^μ.

C.2 Feynman Rules

The Feynman rules are given for each particle having momentum p and mass m, and, if applicable, Lorentz index μ.

C.2.1 External Lines

If quark bilinears are approximated to initial– or final–state mesons, then the mesons follow the same rules as their spin would suggest, *i.e.* pseudoscalar mesons have the same rules as scalar bosons (the difference between scalar and pseudoscalar not affecting the rules in this case) and vector mesons have the same rules as vector bosons.

Spin 0

For every external scalar boson (initial– or final–state), there is a factor of 1.

Spin 1/2

For every initial–state fermion, there is a factor of a Dirac spinor $u(p)$.
For every initial–state anti–fermion, there is a factor of a Dirac spinor $\bar{v}(p)$.
For every final–state fermion, there is a factor of a Dirac spinor $\bar{u}(p)$.
For every final–state anti–fermion, there is a factor of a Dirac spinor $v(p)$.

Spin 1

For every initial–state vector boson, there is a factor of ϵ^{μ}.
For every final–state vector boson, there is a factor of $\epsilon^{*\mu}$.

C.2.2 Internal Lines

There is a small imaginary part, $i\epsilon$, of the denominator of propagators, which serves to indicate the direction around the poles in the propagator that the contour should be taken to get the correct time–ordering of the fields.

Spin 0

For every internal boson, there is a factor of $i/(p^2 - m^2 + i\epsilon)$.

Spin 1/2

For every internal fermion, there is a factor of $i(\not{p} - m)^{-1} = i(\not{p} + m)/(p^2 - m^2 + i\epsilon)$, where the momentum is taken to flow in the sense of the particle number. Additionally, there is a Kronecker δ in fundamental color indices for quarks. (In general there is a Kronecker δ in gauge indices for any gauged internal particle, but since $SU(2)_L$ is broken (and also with a small index range), it is usual to consider each state separately.)

Spin 1

For every internal massless vector boson, there is a factor of $-i\eta_{\mu\nu}/(p^2+i\epsilon)$, using the Feynman gauge. Additionally, there is a Kronecker δ in adjoint color indices for gluons.

For massive vector bosons, there are two usual choices of gauge — the unitary gauge, where three of the Higgs boson doublet degrees of freedom are "eaten" by the $SU(2)_L$ gauge bosons, and the Feynman–'t Hooft gauge, where they are considered separately. The unitary gauge is often the most convenient for tree–level diagrams, while the Feynman–'t Hooft gauge is often more practical for loop diagrams.

In the unitary gauge, there is no propagator for the unphysical Higgs bosons, and the massive vector boson propagator is $i(-\eta_{\mu\nu} + p_\mu p_\nu/m^2)/(p^2 - m^2 + i\epsilon)$.

In the Feynman–'t Hooft gauge, the massive vector boson propagator is $-i\eta_{\mu\nu}/(p^2-m^2+i\epsilon)$, and all four of the Higgs boson degrees of freedom have the propagator $i/(p^2 - m^2 + i\epsilon)$.

Ghosts

The ghost propagator is $i/(p^2 + i\epsilon)$, with a Kronecker δ in adjoint gauge indices.

C.2.3 Vertices

The Feynman rules for vertices can be read off the Lagrangian density. Terms with three or four fields give rise to vertex rules involving those fields. A factor of a fermion field corresponds to an incoming fermion or an outgoing anti–fermion, while the barred field corresponds to an outgoing fermion or an incoming anti–fermion. A real bosonic field corresponds to either an

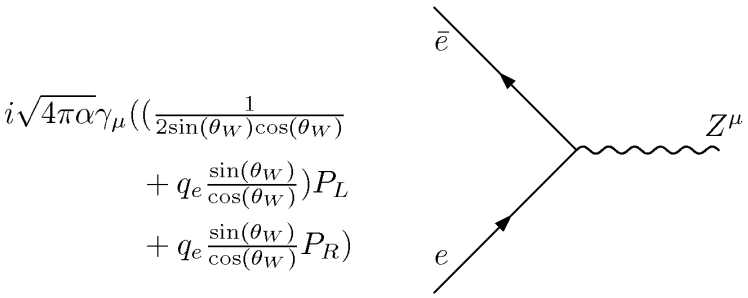

Figure C.1: Feynman vertex rule for the coupling of an electron to a Z boson.

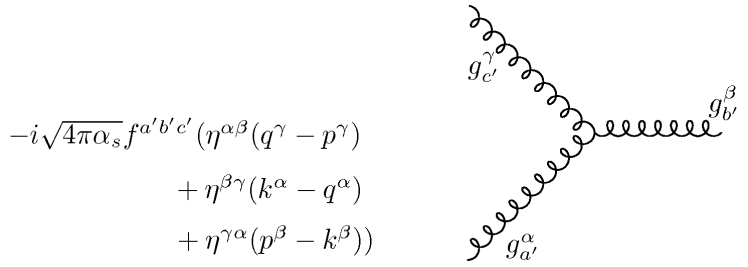

Figure C.2: Feynman vertex rule for the triple gluon vertex.

incoming or outgoing boson, while a complex bosonic field corresponds to an incoming boson or an outgoing anti–boson, and its complex conjugate to an outgoing boson or an incoming anti–boson. All the constants and γ–matrices are then the factor for the vertex in the matrix element, with an additional factor of i and potentially combinatorial factors from identical particles to avoid double–counting.

For example, the term $-(-\sqrt{4\pi\alpha})\bar{e}\not{Z}((\frac{1}{2\sin(\theta_W)\cos(\theta_W)} + q_e\frac{\sin(\theta_W)}{\cos(\theta_W)})P_L + q_e\frac{\sin(\theta_W)}{\cos(\theta_W)}P_R)e$ leads to the Feynman rule shown in figure C.1, *i.e.* the vertex brings a factor of $-i(-\sqrt{4\pi\alpha})\gamma_\mu((\frac{1}{2\sin(\theta_W)\cos(\theta_W)} + q_e\frac{\sin(\theta_W)}{\cos(\theta_W)})P_L + q_e\frac{\sin(\theta_W)}{\cos(\theta_W)}P_R)$ to the matrix element.

Terms involving derivatives have a factor of p_μ for every $i\partial_\mu$ acting on a field with momentum p. Terms involving more than one of any individual field have to have all possible contractions of the fields in the term in the Lagrangian density with the incoming and outgoing fields of the vertex. An example with both these complications is the triple gluon vertex, shown in figure C.2.

Starting with the final term from equation (C.6) and using equations (C.11) and (C.12),

$$\begin{aligned}\frac{-1}{4}\mathrm{tr}(F_{C\mu\nu}F_C^{\mu\nu}) &= \frac{-1}{4}\mathrm{tr}\big((\partial_\mu g_{a\nu}t^a_C - \partial_\nu g_{a\mu}t^a_C)(\partial^\mu g^\nu_b t^b_C - \partial^\nu g^\mu_b t^b_C)\big)\\ &\quad -\sqrt{4\pi\alpha_s}f^{abc}(\partial_\mu g_{a\nu})g^\mu_b g^\nu_c - \frac{\sqrt{4\pi\alpha_s}^2}{4}f_{eab}g^{a\mu}g^{b\nu}f^{ecd}g_{\mu c}g_{\nu d}\end{aligned} \tag{C.15}$$

For three incoming gluons to a vertex (which is the same as for any combination of the gluons incoming or outgoing, except the momenta for outgoing gluons has the opposite sign) denoted by $g^\alpha_{a'}$, $g^\beta_{b'}$ and $g^\gamma_{c'}$, with momenta p, q and k respectively, there is a factor of

$$
\begin{aligned}
i(-\sqrt{4\pi\alpha_s}f^{abc})&(p_\mu\delta_{aa'}\eta_\nu^{\ \alpha}\delta_{bb'}\eta^{\mu\beta}\delta_{cc'}\eta^{\nu\gamma} + p_\mu\delta_{aa'}\eta_\nu^{\ \alpha}\delta_{bc'}\eta^{\mu\gamma}\delta_{cb'}\eta^{\nu\beta} \\
&+q_\mu\delta_{ab'}\eta_\nu^{\ \beta}\delta_{bc'}\eta^{\mu\gamma}\delta_{ca'}\eta^{\nu\alpha} + q_\mu\delta_{ab'}\eta_\nu^{\ \beta}\delta_{ba'}\eta^{\mu\alpha}\delta_{cc'}\eta^{\nu\gamma} \\
&+k_\mu\delta_{ac'}\eta_\nu^{\ \gamma}\delta_{bb'}\eta^{\mu\beta}\delta_{ca'}\eta^{\nu\alpha} + k_\mu\delta_{ac'}\eta_\nu^{\ \gamma}\delta_{ba'}\eta^{\mu\alpha}\delta_{cb'}\eta^{\nu\beta}) \\
&= -i\sqrt{4\pi\alpha_s}f^{a'b'c'}(\eta^{\alpha\beta}(q^\gamma - p^\gamma) + \eta^{\beta\gamma}(k^\alpha - q^\alpha) + \eta^{\gamma\alpha}(p^\beta - k^\beta))
\end{aligned}
\tag{C.16}
$$

where the first term on the left–hand side comes from taking $g^\alpha_{a'}$ with the first field, $\partial_\mu g_{a\nu}$ in the second term, $-\sqrt{4\pi\alpha_s}f^{abc}(\partial_\mu g_{a\nu})g^\mu_b g^\nu_c$, on the right hand side of equation (C.15), $g^\beta_{b'}$ with the second, g^μ_b, and $g^\gamma_{c'}$ with the third, g^ν_c, and the second term comes from taking $g^\alpha_{a'}$ with the first field, $\partial_\mu g_{a\nu}$, $g^\gamma_{c'}$ with the second, g^μ_b, and $g^\beta_{b'}$ with the third, and so on. The terms on the right–hand side come from performing the sums over indices and using the antisymmetry of the structure functions.

Appendix D

Obtaining Feynman Rules From Supersymmetric Lagrangian Densities

D.1 Integrating Over Fermionic Coordinates

In supersymmetric theories, the Lagrangian density is extended from being a function of the space–time coordinates x^μ to being a function of the bosonic space–time coordinates x^μ and of fermionic coordinates θ and $\bar{\theta}$, where θ is a Weyl spinor with complex anticommuting components. Hence the action is the integral of the Lagrangian density over both the bosonic and fermionic coordinates. Performing the integration over the fermionic coordinates also happens to pick out the terms of the Lagrangian density which transform as total derivatives (with respect to the bosonic coordinates) under supersymmetry transformations.

Integration over the fermionic coordinates is defined such that

$$\int \mathrm{d}\theta^\alpha = 0 \tag{D.1}$$

$$\int \mathrm{d}\bar{\theta}_{\dot{\alpha}} = 0 \tag{D.2}$$

$$\int \mathrm{d}\theta^\alpha \theta^\beta = \delta^{\alpha\beta} \tag{D.3}$$

$$\int \mathrm{d}\bar{\theta}_{\dot{\alpha}} \bar{\theta}_{\dot{\beta}} = \delta_{\dot{\alpha}\dot{\beta}} \tag{D.4}$$

Defining

$$\mathrm{d}^2\theta = \frac{-1}{4}\mathrm{d}\theta^\alpha \mathrm{d}\theta_\alpha \tag{D.5}$$

$$\mathrm{d}^2\bar{\theta} = \frac{-1}{4}\mathrm{d}\bar{\theta}_{\dot{\alpha}} \mathrm{d}\bar{\theta}^{\dot{\alpha}} \tag{D.6}$$

then

$$\int \mathrm{d}^2\theta\theta\theta = 1 \tag{D.7}$$

$$\int \mathrm{d}^2\bar{\theta}\bar{\theta}\bar{\theta} = 1 \tag{D.8}$$

and the integral of the Lagrangian density over the fermionic coordinates is

$$\int \mathrm{d}^2\theta \mathrm{d}^2\bar{\theta}\mathcal{L} = [\mathcal{L}]_{\bar{\theta}\bar{\theta}\theta\theta} \tag{D.9}$$

where $[\mathcal{L}]_{\bar{\theta}\bar{\theta}\theta\theta}$ denotes the coefficient of $\bar{\theta}\bar{\theta}\theta\theta$ in $\mathcal{L}$. (Likewise $[W]_{\theta\theta}$ denotes the coefficient of $\theta\theta$ in W.)

D.2 Superpotentials

Since the product of left–chiral superfields is itself a left–chiral superfield, one can denote any sum of products of left–chiral superfields as a *superpotential*, and make the convention that there is a δ–function on the barred fermionic coordinates along with the superpotential in the Lagrangian density, and also that the Lagrangian density contains the Hermitian conjugate of the superpotential with a δ–function on the unbarred fermionic coordinates. In effect, one can just take the coefficients of $\theta\theta$ from the superpotential along with their Hermitian conjugates as the terms in the Lagrangian remaining after integrating over fermionic coordinates. The coefficients of $\theta\theta$ are known as F–terms.

The most generic renormalizable superpotential involving only chiral superfields is given in equation (D.10).

$$W_{\text{general}} = f_i\breve{\psi}_i + \frac{1}{2}m_{ij}\breve{\psi}_i\breve{\psi}_j + \frac{1}{3}\lambda_{ijk}\breve{\psi}_i\breve{\psi}_j\breve{\psi}_k \tag{D.10}$$

However, the tadpole term $f_i\breve{\psi}_i$ can be absorbed into a linear shift in the superfields, except in models with F–term supersymmetry breaking such as the O'Raifeartaigh model [116], where the vacuum expectation value for an auxiliary field arises as a consequence of this term. Hence consider

$$W_{\text{no tadpole}} = \frac{1}{2}m_{ij}\breve{\psi}_i\breve{\psi}_j + \frac{1}{3}\lambda_{ijk}\breve{\psi}_i\breve{\psi}_j\breve{\psi}_k \tag{D.11}$$

Using equation (A.22),

$$[W_{\text{no tadpole}}]_{\theta\theta} = m_{ij}\tilde{\psi}_i F_{\psi j} - \frac{1}{2}m_{ij}\psi_i\psi_j + \lambda_{ijk}\tilde{\psi}_i\tilde{\psi}_j F_{\psi k} - \lambda_{ijk}\psi_i\psi_j\tilde{\psi}_k \tag{D.12}$$

In more detail, the factor of $\sqrt{2}$ for the fermionic part in the definition of a chiral superfield allows one to read off the Yukawa part of a trilinear superpotential, since

$$\begin{aligned}\sqrt{2}\theta^\alpha\psi_{a\alpha}\sqrt{2}\theta^\beta\psi_{b\beta}\tilde{\psi}_c = -2\tilde{\psi}_c\theta^\alpha\theta^\beta\psi_{a\alpha}\psi_{b\beta} &= (2)\left(\frac{1}{2}\right)\tilde{\psi}_c\epsilon^{\alpha\beta}\theta^\gamma\theta_\gamma\psi_{a\alpha}\psi_{b\beta} \\ &= -\tilde{\psi}_c\epsilon^{\alpha\beta}\psi_{b\beta}\psi_{a\alpha}\theta^\gamma\theta_\gamma = -\tilde{\psi}_c\psi_b^\alpha\psi_{a\alpha}\theta^\gamma\theta_\gamma \\ &= -\psi_a^\alpha\psi_{b\alpha}\tilde{\psi}_c\theta^\gamma\theta_\gamma\end{aligned} \tag{D.13}$$

so the vertex factor for the Yukawa coupling is just $-i$ times the trilinear coefficient in the superpotential, with the appropriate left– or right–handed projection operator.

If the kinetic part of the Lagrangian density is given by a D–term of the form of equation (D.18), then the equations of motion allow one to eliminate the auxiliary fields $F_{\psi i}$ in favor of the bosonic fields $\tilde{\psi}_i$, since

$$F_{\psi i}^\dagger = -m_{ij}\tilde{\psi}_j - \lambda_{ijk}\tilde{\psi}_j\tilde{\psi}_k \tag{D.14}$$

so while the "D–term" leads to kinetic and gauge–interaction terms, this superpotential (with its Hermitian conjugate) leads to the interaction Lagrangian density

$$\begin{aligned}\mathcal{L}_W &= -(m_{ij}\tilde{\psi}_j + \lambda_{ijk}\tilde{\psi}_j\tilde{\psi}_k)^\dagger(m_{il}\tilde{\psi}_l + \lambda_{ilm}\tilde{\psi}_l\tilde{\psi}_m) \\ &\quad - \left(\left(\frac{1}{2}m_{ij}\psi_i\psi_j + \lambda_{ijk}\psi_i\psi_j\right) + \text{ Hermitian conjugate}\right) \end{aligned} \tag{D.15}$$

(incorporating the $-F^\dagger_{\psi i}F_{\psi i}$ term from the "D–term").

There is also a superpotential associated with gauge vector fields. In short, using the Wess–Zumino gauge, it is given by

$$\mathcal{L}_V = \frac{-1}{4}\mathrm{tr}\big(F^a_{\mu\nu}F^{a\mu\nu}\big) + i\tilde{V}_a\sigma^\mu D_\mu\bar{\tilde{V}}_a + \frac{1}{2}D^a_V D^a_V \tag{D.16}$$

where $F^a_{\mu\nu}$ is defined in terms of the usual field strength for the gauge group:

$$F^a_{\mu\nu}t^a = F_{\mu\nu} \tag{D.17}$$

and $\tilde{V}^a$ is the Weyl spinor associated with the gauge vector field V_a, and D_μ is the covariant derivative of the gauge group as in equation (C.12) for example, noting that the generators are in this case those for the adjoint representation. The auxiliary field for the vector field is denoted by D^a_V.

D.3 D–Terms

Consider the "D–term" of the Lagrangian density, using the Wess–Zumino gauge:

$$\begin{aligned}\mathcal{L}_D &= \left[\sum_{i,j}\breve{\psi}^\dagger_i \exp\left(2q_{ij}g_jV^j_a t^a\right)\breve{\psi}_i\right]_{\bar\theta\bar\theta\theta\theta} \\ &= \sum_{i,j}(D_\mu\tilde{\psi}_i)^\dagger(D^\mu\tilde{\psi}_i) + i\psi_i\sigma^\mu D_\mu\bar{\psi}_i + F^\dagger_{\psi i}F_{\psi i} \\ &\quad + i\sqrt{2}q_{ij}g_j(\tilde{\psi}^\dagger_i t^a\tilde{V}^j_a\psi_i - \bar{\psi}_i\bar{\tilde{V}}^j_a t^a\tilde{\psi}_i) + q_{ij}g_j\tilde{\psi}^\dagger_i t^a D^{aj}_V\tilde{\psi}_i \end{aligned} \tag{D.18}$$

where q_{ij} is a "charge" for the superfield $\breve{\psi}_i$ for the gauge group which has the vector field V_j as its adjoint representation, in the sense of $q_{Y,W,C}$ in equation (C.2) — if V_j is the vector superfield for an Abelian gauge group, q_{ij} is the charge for the superfield $\breve{\psi}_i$, while if V^j is the vector superfield for a non–Abelian gauge group, q_{ij} is 1 if $\breve{\psi}_i$ is in the fundamental representation of the gauge group, and 0 if it is a singlet under the gauge group. (As might be expected, t^a_j are the generators of the gauge group denoted by j.) The gauge group coupling is g_j.

When the auxiliary fields $F_{\psi i}$ are eliminated to obtain equation (D.15), and the D–term auxiliary fields are eliminated with their equations of motion:

$$D^{aj}_V = -\sum_{i,j}q_{ij}g_j\tilde{\psi}^\dagger_i t^a_j\tilde{\psi}_i \tag{D.19}$$

the normal SM–like Lagrangian density is recovered, along with extra "supersymmetric" terms.

Field	Symbol
"Up–mass" Higgs doublet	$\breve{H}_u = \begin{pmatrix} \breve{H}_u^+ \\ \breve{H}_u^0 \end{pmatrix}$
"Down–mass" Higgs doublet	$\breve{H}_d = \begin{pmatrix} \breve{H}_d^0 \\ \breve{H}_d^- \end{pmatrix}$
Left–handed positron	$\breve{e}^c_{1R} = \breve{e}^c_R$
Left–handed anti–muon	$\breve{e}^c_{2R} = \breve{\mu}^c_R$
Left–handed τ anti–lepton	$\breve{e}^c_{3R} = \breve{\tau}^c_R$
Left–handed electron doublet	$\breve{L}_{1L} = \begin{pmatrix} \breve{\nu}_{eL} \\ \breve{e}_L \end{pmatrix}$
Left–handed muon doublet	$\breve{L}_{2L} = \begin{pmatrix} \breve{\nu}_{\mu L} \\ \breve{\mu}_L \end{pmatrix}$
Left–handed τ lepton doublet	$\breve{L}_{3L} = \begin{pmatrix} \breve{\nu}_{\tau L} \\ \breve{\tau}_L \end{pmatrix}$
Left–handed up anti–quarks	$\breve{u}^c_{1R} = (\breve{u}^c_R)^{\text{anti–red}}, (\breve{u}^c_R)^{\text{anti–green}}, (\breve{u}^c_R)^{\text{anti–blue}}$
Left–handed charm anti–quarks	$\breve{u}^c_{2R} = (\breve{c}^c_R)^{\text{anti–red}}, (\breve{c}^c_R)^{\text{anti–green}}, (\breve{c}^c_R)^{\text{anti–blue}}$
Left–handed top anti–quarks	$\breve{u}^c_{3R} = (\breve{t}^c_R)^{\text{anti–red}}, (\breve{t}^c_R)^{\text{anti–green}}, (\breve{t}^c_R)^{\text{anti–blue}}$
Left–handed down anti–quarks	$\breve{d}^c_{1R} = (\breve{d}^c_R)^{\text{anti–red}}, (\breve{d}^c_R)^{\text{anti–green}}, (\breve{d}^c_R)^{\text{anti–blue}}$
Left–handed strange anti–quarks	$\breve{d}^c_{2R} = (\breve{s}^c_R)^{\text{anti–red}}, (\breve{s}^c_R)^{\text{anti–green}}, (\breve{s}^c_R)^{\text{anti–blue}}$
Left–handed bottom anti–quarks	$\breve{d}^c_{3R} = (\breve{b}^c_R)^{\text{anti–red}}, (\breve{b}^c_R)^{\text{anti–green}}, (\breve{b}^c_R)^{\text{anti–blue}}$
Left–handed up–down quark doublets	$\breve{Q}_{1L} = \begin{pmatrix} \breve{u}_{1L} \\ \breve{d}_{1L} \end{pmatrix} = \begin{pmatrix} \breve{u}_L \\ \breve{d}_L \end{pmatrix}^{\text{red}}, \begin{pmatrix} \breve{u}_L \\ \breve{d}_L \end{pmatrix}^{\text{green}}, \begin{pmatrix} \breve{u}_L \\ \breve{d}_L \end{pmatrix}^{\text{blue}}$
Left–handed charm–strange quark doublets	$\breve{Q}_{2L} = \begin{pmatrix} \breve{u}_{2L} \\ \breve{d}_{2L} \end{pmatrix} = \begin{pmatrix} \breve{c}_L \\ \breve{s}_L \end{pmatrix}^{\text{red}}, \begin{pmatrix} \breve{c}_L \\ \breve{s}_L \end{pmatrix}^{\text{green}}, \begin{pmatrix} \breve{c}_L \\ \breve{s}_L \end{pmatrix}^{\text{blue}}$
Left–handed top–bottom quark doublets	$\breve{Q}_{3L} = \begin{pmatrix} \breve{u}_{3L} \\ \breve{d}_{3L} \end{pmatrix} = \begin{pmatrix} \breve{t}_L \\ \breve{b}_L \end{pmatrix}^{\text{red}}, \begin{pmatrix} \breve{t}_L \\ \breve{b}_L \end{pmatrix}^{\text{green}}, \begin{pmatrix} \breve{t}_L \\ \breve{b}_L \end{pmatrix}^{\text{blue}}$

Table D.1: Notation for fields except gauge vector bosons.

D.4 MSSM/RPVMSSM Fields And Superpotential

D.4.1 MSSM Superpotential

The MSSM superpotential is given by

$$\begin{aligned} W_{R_p} \;=\; & \mu(\breve{H}_d)_a \epsilon_{ab} (\breve{H}_u)_b \\ & + Y^l_{jk} (\breve{H}_d)_a \epsilon_{ab} (\breve{L}_j)_b \breve{e}^c_{kR} + Y^d_{jk} (\breve{H}_d)_a \epsilon_{ab} (\breve{Q}_j)^p_b (\breve{d}^c_{kR})^p + Y^u_{jk} (\breve{H}_u)_a \epsilon_{ab} (\breve{Q}_j)^p_b (\breve{u}^c_{kR})^p \\ & + \text{gauge piece} \end{aligned} \tag{D.20}$$

where the gauge piece leads to the appropriate form of equation (D.16).

D.4.2 Soft SUSY–Breaking Terms

To parametrize supersymmetry–breaking, one may add certain terms to the Lagrangian density: mass terms for the gauginos and Higgsinos (which may mix these fermions if they have the same quantum numbers), mass terms for the sfermions (which may mix these bosons if they have the same quantum numbers), and A–terms, which are trilinear terms in the scalar fields. In principle these are completely unknown, but there are many benchmark scenarios that restrict them to being dependent on only a few parameters, such as the mSUGRA–type models, where

Field	R_p of bosonic component	Gauge Group Representation		$U(1)_Y$ Hypercharge
		$SU(2)_L$	$SU(3)_C$	
$\breve{H}_u$	$+1$	**2** (doublet)	**1** (singlet)	$\frac{+1}{2}$
$\breve{H}_d$	$+1$	**2** (doublet)	**1** (singlet)	$\frac{-1}{2}$
$\breve{e}^c_{1R}$	-1	**1** (singlet)	**1** (singlet)	$+1$
$\breve{e}^c_{2R}$				
$\breve{e}^c_{3R}$				
$\breve{L}_{1L}$	-1	**2** (doublet)	**1** (singlet)	$\frac{-1}{2}$
$\breve{L}_{2L}$				
$\breve{L}_{3L}$				
$\breve{u}^c_{1R}$	-1	**1** (singlet)	$\bar{\mathbf{3}}$ (anti–triplet)	$\frac{-2}{3}$
$\breve{u}^c_{2R}$				
$\breve{u}^c_{3R}$				
$\breve{d}^c_{1R}$	-1	**1** (singlet)	$\bar{\mathbf{3}}$ (anti–triplet)	$\frac{+1}{3}$
$\breve{d}^c_{2R}$				
$\breve{d}^c_{3R}$				
$\breve{Q}_{1L}$	-1	**2** (doublet)	**3** (triplet)	$\frac{+1}{6}$
$\breve{Q}_{2L}$				
$\breve{Q}_{3L}$				

Table D.2: Spin and gauge group assignments for fields except gauge vector bosons.

there is a common sfermion mass term, a common gaugino and Higgsino mass term, and a single common A–term, which typically arises through gravity–mediated supersymmetry–breaking.

D.4.3 RPVMSSM Superpotential

The RPVMSSM superpotential is equal to the MSSM superpotential plus an RPV bit, $W_{\not{R}_p}$, which is given by

$$\begin{aligned} W_{\not{R}_p} &= \mu'_i(\breve{L}_i)_\alpha \epsilon_{\alpha\beta}(\breve{H}_u)_\beta \\ &\quad + \frac{1}{2}\lambda_{ijk}(\breve{L}_i)_\alpha \epsilon_{\alpha\beta}(\breve{L}_j)_\beta \breve{e}^c_{kR} + \lambda'_{ijk}(\breve{L}_i)_\alpha \epsilon_{\alpha\beta}(\breve{Q}_j)^p_\beta (\breve{d}^c_{kR})^p \\ &\quad + \frac{1}{2}\lambda''_{ijk}\epsilon_{pqr}(\breve{u}^c_{iR})^p (\breve{d}^c_{jR})^q (\breve{d}^c_{kR})^r \end{aligned} \tag{D.21}$$

Appendix E

Obtaining Cross–Sections And Decay Widths From Matrix Elements

Calculating a cross–section or a decay width can be broken into two stages: the first stage of writing down the amplitude, and the second of turning the amplitude into a physical result. The first stage consists of drawing Feynman diagrams, writing down amplitudes using Feynman rules, and adding the amplitudes together, and the second stage of squaring the amplitude (in the sense of multiplying the amplitude by its complex conjugate) and resolving the kinematics of the process. This appendix deals with the second stage. The first stage is addressed in appendices C and D.

E.1 Spin–Averaging

In general, the amplitude is a complex number depending on the polarizations and quantum numbers, such as electric and color charge, of initial– and final–state particles, and is referred to as a *matrix element*, in the sense that the S–matrix can be written as a matrix of transition probabilities to and from states labelled by polarizations and quantum numbers. However, in most cases of interest, the initial particles are unpolarized, hence the initial polarizations must be averaged over all possible values. Also, in most cases one is not interested in the final–state polarizations, so the final polarizations must be summed over all possible values. Averaging over polarizations is equivalent to summing over polarizations and dividing by the number of polarizations for each particle, *i.e.* dividing by $(2S+1)$ for each massive particle, where S is its spin (*i.e.* 0 for a scalar boson, 1/2 for a fermion, 1 for a massive vector boson). Massless vector bosons only have two polarizations, so averaging over their polarizations only gives a factor of 1/2, rather than the 1/3 that massive vector bosons give. This summing is performed *after* squaring the matrix element. Of course, one does not have to use the methods outlined below, but explicitly inserting the expressions for each polarization and summing would still give the same answer, though with a lot more working.

In general, a matrix element will be a product of Lorentz products of polarization vectors $\epsilon_i^{\mu_i}$ (and also complex conjugates of polarization vectors) with various Lorentz objects (momenta, γ matrix Lorentz indices, other polarization vectors, *etc.*), and also of spinor products $\bar{u}\Gamma u$, $\bar{v}\Gamma u$, $\bar{u}\Gamma v$ and $\bar{v}\Gamma v$, where Γ represents any combination of γ matrices, with an arbitrary number of Lorentz indices (which of course, must be combined with themselves and the other Lorentz indices in the matrix element such that the matrix element is a Lorentz scalar). It may also

depend on other quantum numbers, but these shall be dealt with later. Hence, a matrix element $\mathcal{M}$ is of the form

$$\mathcal{M} = (\text{polarization–independent factor})\Pi\epsilon^{\mu_i}\Pi\epsilon^{\mu_j *}\Pi(\bar{u}\Gamma u)\Pi(\bar{v}\Gamma u)\Pi(\bar{u}\Gamma v)\Pi(\bar{v}\Gamma v) \tag{E.1}$$

E.1.1 Spinors

Since the spinor products are ordinary complex numbers (though with perhaps some Lorentz indices), when multiplying the matrix element with its complex conjugate, one can consider the product of each spinor product with its complex conjugate separately, taking care with Lorentz indices. Consider the spinor product $\bar{v}(q)\Gamma^{\mu\nu}u(p)$:

$$(\bar{v}(q)\Gamma^{\mu'\nu'}u(p))^* = \bar{u}(p)\gamma^0\Gamma^{\mu'\nu'\dagger}\gamma^0 v(q) \tag{E.2}$$

where the Lorentz indices receive a prime to note that the complex conjugate has its Lorentz indices combined with Lorentz indices on some other part of the complex conjugate of the matrix element. In equation (E.2) the facts that $(\gamma^0)^2 = 1_{4\times4}$ and $(\gamma^0)^\dagger = \gamma^0$ have been used.

Restoring spin indices on the spinors, the product of the spin product with its complex conjugate is

$$\begin{aligned}(\bar{v}(q)\Gamma^{\mu'\nu'}u(p))^*(\bar{v}(q)\Gamma^{\mu\nu}u(p)) &= \bar{u}^\alpha(p)(\gamma^0\Gamma^{\mu'\nu'\dagger}\gamma^0)_{\alpha\beta}v^\beta(q)\bar{v}^\gamma(q)\Gamma^{\mu\nu}_{\gamma\delta}u^\delta(p) \\ &= (\gamma^0\Gamma^{\mu'\nu'\dagger}\gamma^0)_{\alpha\beta}v^\beta(q)\bar{v}^\gamma(q)\Gamma^{\mu\nu}_{\gamma\delta}u^\delta(p)\bar{u}^\alpha(p)\end{aligned} \tag{E.3}$$

where $\bar{u}^\alpha(p)$ can be moved past all the other factors since it is just a complex number.

Using equations (A.7) and (A.8), this becomes

$$\begin{aligned}\sum_{\text{spins}}(\bar{v}(q)\Gamma^{\mu'\nu'}u(p))^*(\bar{v}(q)\Gamma^{\mu\nu}u(p)) &= (\gamma^0\Gamma^{\mu'\nu'\dagger}\gamma^0)_{\alpha\beta}(\not{q} - m_q)^{\beta\gamma}\Gamma^{\mu\nu}_{\gamma\delta}(\not{p} + m_p)^{\delta\alpha} \\ &= \text{tr}\Big(\gamma^0\Gamma^{\mu'\nu'\dagger}\gamma^0(\not{q} - m_q)\Gamma^{\mu\nu}(\not{p} + m_p)\Big)\end{aligned} \tag{E.4}$$

where m_p is the mass of the fermion with momentum p and m_q is the mass of the fermion with momentum q.

At this point one may use various *trace theorems* to evaluate this expression. These are identities for the traces of different numbers of γ matrices. These all follow from the fact that the γ matrices are traceless and the cyclic property of the trace operation. These identities can be found in appendix A of reference [108]. For example, the trace of two γ matrices is explicitly worked out.

$$\text{tr}(\gamma^\mu\gamma^\nu) = \text{tr}(-\gamma^\nu\gamma^\mu + 2\eta^{\mu\nu}I_{4\times4}) = \text{tr}(-\gamma^\mu\gamma^\nu + 2\eta^{\mu\nu}I_{4\times4}) \tag{E.5}$$

using equation (A.25) and the cyclic property of trace. Hence

$$2\text{tr}(\gamma^\mu\gamma^\nu) = 2\eta^{\mu\nu}\text{tr}(I_{4\times4}) \tag{E.6}$$

so, since

$$\text{tr}(I_{4\times4}) = 4 \tag{E.7}$$

equation (E.6) becomes

$$\text{tr}(\gamma^\mu\gamma^\nu) = 4\eta^{\mu\nu} \tag{E.8}$$

The identities for higher even numbers of γ matrices follows from repeated iteration of the above. The trace of an odd number of γ matrices is zero, which can be seen by using equation (A.35) to place a pair of γ^5s at the end of a string of γ matrices, then using the cyclic property of trace to bring one of them to the start of the string, then anticommuting it back past all the γ matrices until it is beside the other γ^5, having picked up an odd number of factors of -1 from the anticommutations, hence the trace of an odd number of γ matrices is equal to minus itself, hence is zero. For traces involving γ^5, one can use equation (A.33) to replace it with an antisymmetric tensor and a string of γ matrices.

E.1.2 Polarization Vectors

In a similar manner to the spinor product case, but much more simply, one sums over polarization vectors using equations (A.9) and (A.10) to replace terms like $\sum_{\text{polarizations}} \epsilon_i^{\mu_i} \epsilon_i^{\mu'_i *}$ in the square of the matrix element.

E.2 Color–Averaging

If any of the initial– or final–state particles have $SU(3)_C$ charge, then, since QCD confinement renders it impossible to tell the color charges of individual final–state colorful particles, the color charges must be averaged or summed over. In both the SM and the RPVMSSM, the color algebra can be factored out from the rest of the matrix element. There are color structures associated with the colorful parts of Feynman diagrams. Vertices involving an adjoint representation field (just gluons in the SM) coupling to fundamental representation fields (just quarks in the SM) have a three–by–three $SU(3)$ matrix t^a_{ij}, where the index $a = 1 \ldots 8$ is associated with the adjoint representation and the indices i and j (running from 1 to 3) are associated with the fundamental representation. Vertices involving three or four adjoint representation fields involve factors of the structure constants f^{abc}, where a, b and c are adjoint indices. Propagators have Kronecker δ matrices with indices appropriate to their representation. External fundamental representation particles have a three–component color vector, and external adjoint representation particles have an eight–component color vector. Analogously to the spinor case, the color matrices and vectors combine to form complex numbers within the matrix element, but there are useful identities that allow one to write the color factor times its complex conjugate as a trace of $SU(3)$ matrices. These are much simpler than the γ matrix case. For a three–component color vector v_i, an eight–component color vector V^a and a three–by–three color matrix t^a_{Cij}:

$$\sum_{\text{colors}} v_i v_j = \delta_{ij} \tag{E.9}$$

$$\sum_{\text{colors}} V^a V^b = \delta^{ab} \tag{E.10}$$

$$t^a_{Cij} t^b_{Cji} = \text{tr}\big(t^a t^b\big) = C(r)\delta^{ab} \tag{E.11}$$

where $C(r)$ is the Dynkin index for a representation r: in this case $C(r) = 1/2$. Since a and b run from 1 to 8, one must remember that $\delta^{aa} = 8$.

E.3 Kinematics

E.3.1 One–To–Two Body Decays

Consider a heavy particle Y decaying into two particles a and b. In the rest frame of Y, $E_Y = m_Y$ and $\boldsymbol{p}_Y = \mathbf{0}$.

The appropriate decay width differential is

$$\begin{aligned} \mathrm{d}\Gamma &= \frac{\mathrm{d}\boldsymbol{p}_a}{((2\pi)^3(2E_a))} \frac{\mathrm{d}\boldsymbol{p}_b}{((2\pi)^3(2E_b))} |\mathcal{M}|^2 \frac{((2\pi)^4 \delta^{(4)}(p_Y - p_a - p_b))}{(2m_Y)} \\ &= \frac{\mathrm{d}\boldsymbol{p}_a \mathrm{d}\boldsymbol{p}_b}{(2^5 \pi^2 m_Y E_a E_b)} |\mathcal{M}|^2 \delta^{(3)}(\mathbf{0} - \boldsymbol{p}_a - \boldsymbol{p}_b) \delta(m_Y - E_a - E_b) \end{aligned} \tag{E.12}$$

Now,

$$\begin{aligned} |\boldsymbol{p}_X|^2 &= E_X^2 - m_X^2 \\ \Rightarrow 2|\boldsymbol{p}_X| \mathrm{d}|\boldsymbol{p}_X| &= 2E_X \mathrm{d}E_X \end{aligned} \tag{E.13}$$

so

$$\mathrm{d}\boldsymbol{p}_X = \mathrm{d}\Omega_X |\boldsymbol{p}_X|^2 \mathrm{d}|\boldsymbol{p}_X| = \mathrm{d}\Omega_X \mathrm{d}E_X E_X |\boldsymbol{p}_X| \tag{E.14}$$

noting that $|\boldsymbol{p}_X|$ on the right hand side is now a function of E_X.

Now performing the integration over $\boldsymbol{p}_b$ "uses up" three of the four δ–functions:

$$\begin{aligned} \mathrm{d}\Gamma &= \frac{\mathrm{d}\Omega_a \mathrm{d}|\boldsymbol{p}_a||\boldsymbol{p}_a|^2}{(2^5\pi^2 m_Y E_a E_b(E_a))} |\mathcal{M}|^2 \delta(m_Y - E_a - E_b(E_a)) \\ &= \frac{\mathrm{d}\Omega_a \mathrm{d}E_a E_a |\boldsymbol{p}_a|}{(2^5\pi^2 m_Y E_a E_b(E_a))} |\mathcal{M}|^2 \delta(m_Y - E_a - E_b(E_a)) \end{aligned} \tag{E.15}$$

remembering that now E_b is no longer a free variable (through a change of variables from $|\boldsymbol{p}_b|$ to E_b), but is now constrained to be a function of E_a, such that

$$E_b = \sqrt{|\boldsymbol{p}_b|^2 + m_b^2} = \sqrt{|\boldsymbol{p}_a|^2 + m_b^2} = \sqrt{E_a^2 - m_a^2 + m_b^2} \tag{E.16}$$

and that $|\boldsymbol{p}_a|$ is a function of E_a as well.

Also,

$$\delta(f(x)) = \sum_{x_0 : f(x_0)=0} \left|\frac{\mathrm{d}f}{\mathrm{d}x}\right|^{-1} \delta(x - x_0) \tag{E.17}$$

so

$$\begin{aligned} \delta(m_Y - E_a - E_b(E_a)) &= \left|1 + \frac{\mathrm{d}E_b}{\mathrm{d}E_a}\right|^{-1} \delta(E_a - E_{a0}) = \left|1 + \frac{E_{a0}}{E_{b0}}\right|^{-1} \delta(E_a - E_{a0}) \\ &= \frac{E_{b0}}{(E_{a0} + E_{b0})} \delta(E_a - E_{a0}) = \frac{E_{b0}}{m_Y} \delta(E_a - E_{a0}) \end{aligned} \tag{E.18}$$

where $E_{b0} = E_b(E_{a0})$ so $E_{a0} + E_{b0} = m_Y$, and E_{a0} is the value of E_a that satisfies the constraint that $m_Y - E_a - E_b(E_a) = 0$.

Hence

$$\mathrm{d}\Gamma = \frac{\mathrm{d}\Omega_a \mathrm{d}E_a |\boldsymbol{p}_a|}{(2^5\pi^2 m_Y^2)} |\mathcal{M}|^2 \delta(E_a - E_{a0}) \tag{E.19}$$

Performing the integration over E_a, "using up" the last δ–function,

$$\Gamma = \int \mathrm{d}\Omega_a \frac{|\boldsymbol{p}_{a0}|}{(2^5\pi^2 m_Y^2)} |\mathcal{M}|^2 \tag{E.20}$$

where $|\boldsymbol{p}_{a0}|$ is $|\boldsymbol{p}_a|$ constrained such that $E_a = E_{a0}$, and all energies and momenta in $|\mathcal{M}|^2$ are now constrained by 4-momentum conservation laws:

$$\begin{aligned} E_b^2 &= |\boldsymbol{p}_b|^2 + m_b^2 = |\boldsymbol{p}_a|^2 + m_b^2 = E_a^2 - m_a^2 + m_b^2 \\ &= (m_Y - E_b)^2 - m_a^2 + m_b^2 \\ \Rightarrow E_b &= \frac{(m_Y^2 - m_a^2 + m_b^2)}{2m_Y} \end{aligned} \tag{E.21}$$

$$\Rightarrow E_a = \frac{(m_Y^2 - m_b^2 + m_a^2)}{2m_Y} \tag{E.22}$$

and

$$|\boldsymbol{p}_b| = |\boldsymbol{p}_a| = \sqrt{E_a^2 - m_a^2} = \sqrt{E_b^2 - m_b^2} \tag{E.23}$$

E.3.2 One–To–Three Body Decays

This is mainly a re–write of part of appendix B of reference [117].

Consider a heavy particle Y decaying into three particles a, b and c. In the rest frame of Y, $E_Y = m_Y$ and $\boldsymbol{p}_y = \mathbf{0}$. The following notation is used:

$$x = \frac{2E_a}{m_Y} \tag{E.24}$$

$$y = \frac{2E_b}{m_Y} \tag{E.25}$$

$$z = \frac{2E_c}{m_Y} \tag{E.26}$$

These are referred to as reduced energies, and satisfy

$$x + y + z = 2 \tag{E.27}$$

Also, the mass–squared ratios are denoted by

$$\alpha = \left(\frac{m_a}{m_Y}\right)^2 \tag{E.28}$$

$$\beta = \left(\frac{m_b}{m_Y}\right)^2 \tag{E.29}$$

$$\gamma = \left(\frac{m_c}{m_Y}\right)^2 \tag{E.30}$$

The appropriate decay width differential is

$$\begin{aligned} \mathrm{d}\Gamma &= \frac{\mathrm{d}\boldsymbol{p}_a}{(2\pi)^3}\frac{\mathrm{d}\boldsymbol{p}_b}{(2\pi)^3}\frac{\mathrm{d}\boldsymbol{p}_c}{(2\pi)^3}\frac{\delta^{(4)}(p_Y - p_a - p_b - p_c)(2\pi)^4}{(2m_Y)(2E_a)(2E_b)(2E_c)}|\mathcal{M}|^2 \\ &= \frac{\mathrm{d}\boldsymbol{p}_a\mathrm{d}\boldsymbol{p}_b\mathrm{d}\boldsymbol{p}_c|\mathcal{M}|^2\delta^{(4)}(p_Y - p_a - p_b - p_c)}{(2^9\pi^5 m_Y E_a E_b E_c)} \end{aligned} \tag{E.31}$$

Using equation (E.13), performing the integration over $\boldsymbol{p}_c$ "uses up" three of the four δ–functions:

$$\begin{aligned} \mathrm{d}\Gamma &= \frac{\mathrm{d}\Omega_a\mathrm{d}|\boldsymbol{p}_a||\boldsymbol{p}_a|^2\mathrm{d}\Omega_b|\boldsymbol{p}_b|^2\mathrm{d}|\boldsymbol{p}_b||\mathcal{M}|^2\delta(m_Y - E_a - E_b - E_c)}{(2^9\pi^5 m_Y E_a E_b E_c)} \\ &= \frac{\mathrm{d}\Omega_a\mathrm{d}E_a E_a|\boldsymbol{p}_a|\mathrm{d}\Omega_b|\boldsymbol{p}_b|\mathrm{d}E_b E_b|\mathcal{M}|^2\delta(m_Y - E_a - E_b - E_c)}{(2^9\pi^5 m_Y E_a E_b E_c)} \end{aligned} \tag{E.32}$$

Now

$$\boldsymbol{p}_c = -\boldsymbol{p}_a - \boldsymbol{p}_b \tag{E.33}$$

$$\Rightarrow E_c^2 - m_c^2 = |\boldsymbol{p}_c|^2 = (-\boldsymbol{p}_a - \boldsymbol{p}_b).(-\boldsymbol{p}_a - \boldsymbol{p}_b) = |\boldsymbol{p}_a|^2 + |\boldsymbol{p}_b|^2 + 2|\boldsymbol{p}_a||\boldsymbol{p}_b|\cos(\theta_{ab}) \tag{E.34}$$

$$\Rightarrow E_c\mathrm{d}E_c = |\boldsymbol{p}_a||\boldsymbol{p}_b|\mathrm{d}(\cos(\theta_{ab})) \tag{E.35}$$

assuming $|\boldsymbol{p}_a|$ and $|\boldsymbol{p}_b|$ are independent of E_c (changing variables from E_c to θ_{ab}, the angle between $\boldsymbol{p}_a$ and $\boldsymbol{p}_b$).

Changing variable in the decay width differential from $\mathrm{d}\Omega_b$ to $\mathrm{d}\Omega_{ab} = \mathrm{d}\phi_{ab}\mathrm{d}(\cos(\theta_{ab}))$,

$$\begin{aligned} \mathrm{d}\Gamma &= \frac{\mathrm{d}\Omega_a\mathrm{d}E_a|\boldsymbol{p}_a|\mathrm{d}(\cos(\theta_{ab}))\mathrm{d}\phi_{ab}|\boldsymbol{p}_b|\mathrm{d}E_b|\mathcal{M}|^2\delta(m_Y - E_a - E_b - E_c)}{(2^9\pi^5 m_Y E_c)} \\ &= \frac{\mathrm{d}\Omega_a\mathrm{d}E_a\mathrm{d}\phi_{ab}E_c\mathrm{d}E_c\mathrm{d}E_b|\mathcal{M}|^2\delta(m_Y - E_a - E_b - E_c)}{(2^9\pi^5 m_Y E_c)} \end{aligned} \tag{E.36}$$

Performing the integration over E_c, "using up" last δ–function,

$$\Gamma = \int \mathrm{d}\Omega_a \int \mathrm{d}\phi_{ab} \int \mathrm{d}E_a \int \mathrm{d}E_b \frac{|\mathcal{M}|^2}{(2^9\pi^5 m_Y)} \tag{E.37}$$

If $|\mathcal{M}|^2$ is independent of Ω_a and ϕ_{ab}, as it should be for a Lorentz–invariant quantity such as a spin–averaged decay in a vacuum, then, performing the angular integrations and changing variables from energies to reduced energies,

$$\Gamma = \frac{m_Y}{(2^8\pi^3)} \int \mathrm{d}x \int \mathrm{d}y |\mathcal{M}|^2 \tag{E.38}$$

remembering to impose energy–momentum conservation by hand.

The limits on the integrals are complicated (and can be seen in full in reference [117]), but for a decay into three massless particles, it simplifies. The most energetic particle may have up to half the total energy in the center–of–momentum frame, and the least energetic particle must have an energy of at least zero. Hence the energy of particle a can be anywhere in the range of zero to half the total energy, so the limits on the x–integral are 0 and 1. Similarly the reduced energy of particle b must be at least $(1-x)$ (making c the most energetic particle) and at most 1, so the limits on the y–integral are $(1-x)$ and 1.

At this point, $|\mathcal{M}|^2$ must be written in terms of x and y. The energies are easily translated (remembering $x+y+z=2$). Lorentz products of momenta are given by a relatively simple expression, derived as follows (in the rest frame of Y, so $\boldsymbol{p}_Y = \mathbf{0}$ and $E_Y = m_Y$):

$$\begin{aligned}
(p_a{\cdot}p_b) &= (p_Y - p_b - p_c){\cdot}(p_Y - p_a - p_c) \\
&= p_Y^2 - (p_b{\cdot}p_Y) - (p_c{\cdot}p_Y) - (p_a{\cdot}p_Y) + (p_a{\cdot}p_b) + (p_c{\cdot}p_a) - (p_c{\cdot}p_Y) + (p_b{\cdot}p_c) + p_c^2 \\
&= m_Y^2 - E_b m_Y - E_c m_Y - E_a m_Y + (p_a{\cdot}p_b) + (p_b{\cdot}p_c) + (p_c{\cdot}p_a) - E_c m_Y + m_c^2 \\
&= (p_a{\cdot}p_b) + (p_b{\cdot}p_c) + (p_c{\cdot}p_a) - E_c m_Y + m_c^2
\end{aligned} \tag{E.39}$$

since $E_a + E_b + E_c = m_Y$. Similarly

$$(p_b{\cdot}p_c) = (p_a{\cdot}p_b) + (p_b{\cdot}p_c) + (p_c{\cdot}p_a) - E_a m_Y + m_a^2 \tag{E.40}$$

$$(p_c{\cdot}p_a) = (p_a{\cdot}p_b) + (p_b{\cdot}p_c) + (p_c{\cdot}p_a) - E_b m_Y + m_b^2 \tag{E.41}$$

$$\tag{E.42}$$

so

$$\begin{aligned}
(p_a{\cdot}p_b) + (p_b{\cdot}p_c) + (p_c{\cdot}p_a) &= 3((p_a{\cdot}p_b) + (p_b{\cdot}p_c) + (p_c{\cdot}p_a)) \\
&\quad -(E_a + E_b + E_c)m_Y + m_a^2 + m_b^2 + m_c^2 \\
\Rightarrow (p_a{\cdot}p_b) + (p_b{\cdot}p_c) + (p_c{\cdot}p_a) &= \frac{(m_Y^2(1-\alpha-\beta-\gamma))}{2} \\
\Rightarrow (p_a{\cdot}p_b) &= \frac{(m_Y^2(1-\alpha-\beta-\gamma+z+2\gamma))}{2} \\
&= \frac{(m_Y^2(x+y-1-\alpha-\beta+\gamma))}{2} \\
&= \frac{(m_Y^2(x+y-1))}{2} \text{ for massless final–state particles.}
\end{aligned} \tag{E.43}$$

E.3.3 Two–To–Two Body Processes

The differential cross–section $\mathrm{d}\sigma$ for a two–to–two body process, where the initial particles are labelled A and B and the final particles are labelled a and b, is given by

$$\begin{aligned}\mathrm{d}\sigma &= (\text{incident flux factor})\times(\text{amplitude squared})\times(\text{final state phase space differential}) \\ &\quad \times(\text{momentum conservation } \delta\text{–functions}) \\ &= \frac{1}{2E_A 2E_B|v_A - v_B|}\times|\mathcal{M}|^2\times\left(\frac{\mathrm{d}\boldsymbol{p}_a}{(2\pi)^3 2E_a}\frac{\mathrm{d}\boldsymbol{p}_b}{(2\pi)^3 2E_b}\right)\times((2\pi)^4\delta^{(4)}((p_A+p_B)-(p_a+p_b)))\end{aligned} \tag{E.44}$$

Using the same manipulations as in section E.3.1, such as in equations (E.14) and (E.18) with m_Y replaced by $(E_A + E_B)$, one can obtain

$$\begin{aligned}\int\frac{\mathrm{d}\boldsymbol{p}_a\mathrm{d}\boldsymbol{p}_b(2\pi)^4\delta^{(4)}((p_A+p_B)-(p_a+p_b))}{(2\pi)^3 2E_a(2\pi)^3 2E_b} &= \int\frac{(2\pi)\delta((E_A+E_B)-(E_a+E_b))}{(2\pi)^3 2E_a 2E_b}\mathrm{d}\Omega_a\mathrm{d}E_a E_a|\boldsymbol{p}_a| \\ &= \int\frac{(2\pi)\delta(E_a-E_{a0})}{(2\pi)^3 2E_a 2E_b}\mathrm{d}\Omega_a\mathrm{d}E_a E_a|\boldsymbol{p}_a|\frac{E_{b0}}{(E_A+E_B)} \\ &= \int\frac{1}{16\pi^2}\mathrm{d}\Omega_a\frac{|\boldsymbol{p}_a|}{(E_A+E_B)}\end{aligned} \tag{E.45}$$

Hence

$$\sigma = \int\frac{1}{16\pi^2}\mathrm{d}\Omega_a\frac{|\boldsymbol{p}_a|}{(E_A+E_B)}\frac{1}{2E_A 2E_B|v_A-v_B|}|\mathcal{M}|^2 \tag{E.46}$$

For massless initial state particles, in the center–of–momentum frame, the incident flux factor $(2E_A 2E_B|v_A - v_B|)^{-1}$ is equal to $(8E_A^2)^{-1} = (2s)^{-1}$, where s is the Mandelstam variable $(p_A + p_B)^2$.

E.3.4 Two–To–Three Body Processes

The differential cross–section $\mathrm{d}\sigma$ for a two–to–three body process, where the initial particles are labelled A and B and the final particles are labelled a, b and c, is given by almost the same expression as for a two–to–two body process, with an extended final state phase space differential and conservation of momentum.

$$\begin{aligned}\mathrm{d}\sigma &= \frac{1}{2E_A 2E_B|v_A - v_B|}\times|\mathcal{M}|^2\times\left(\frac{\mathrm{d}\boldsymbol{p}_a}{(2\pi)^3 2E_a}\frac{\mathrm{d}\boldsymbol{p}_b}{(2\pi)^3 2E_b}\frac{\mathrm{d}\boldsymbol{p}_c}{(2\pi)^3 2E_c}\right) \\ &\quad \times((2\pi)^4\delta^{(4)}((p_A+p_B)-(p_a+p_b+p_c)))\end{aligned} \tag{E.47}$$

Unfortunately, there is not as easy a simplification of this expression as in the two–to–two body case. One can use many of the manipulations in section E.3.2, such as equation (E.35), changing variable in the decay width differential from $\mathrm{d}\Omega_b$ to $\mathrm{d}\Omega_{ab} = \mathrm{d}\phi_{ab}\mathrm{d}(\cos(\theta_{ab}))$, and performing the integration over $\boldsymbol{p}_c$, but if one is numerically evaluating the integrals, there is not much point in further refinement.

Appendix F

QCD Bound State Approximations

F.1 Quark Bilinear Coefficients

In chapter 3 it was assumed that meson states are separable into valence quark bilinears multiplied by form factors.

For a vector meson V, the approximation used is

$$\langle 0|\bar{q}_\alpha \gamma^\mu q_\beta|V(p_V)\rangle = iH_V^{\alpha\beta} F_V m_V \epsilon_V^\mu \tag{F.1}$$

where ϵ_V^μ is the polarization vector of V, F_V is the decay factor for the meson, m_V is the mass of the meson and $H_V^{\alpha\beta}$ is the coefficient of $\bar{q}_\alpha q_\beta$ in the quark model wavefunction of the meson.

For a pseudoscalar meson P, two approximations are used:

$$\langle 0|\bar{q}_\alpha \gamma^\mu \gamma^5 q_\beta|P(p_P)\rangle = iH_P^{\alpha\beta} F_P p_P^\mu \tag{F.2}$$

$$\langle 0|\bar{q}_\alpha \gamma^5 q_\beta|P(p_P)\rangle = \frac{iH_P^{\alpha\beta} F_P m_P^2}{\mu_P^{\alpha\beta}} \qquad \text{(no sum on } \alpha, \beta) \tag{F.3}$$

where F_P is the meson decay constant for P and $H_P^{\alpha\beta}$ is the analogue of $H_V^{\alpha\beta}$. The factor $\mu_P^{\alpha\beta}$ is described later.

This is not standard notation, so it shall be described in some detail, as it is very convenient. Firstly, it is only of relevance to the light mesons, as it is assumed that there the charmed and bottom meson wavefunctions consist entirely of one quark bilinear, *e.g.* D^0 is entirely $\bar{d}c$, so $H_{D^0}^{dc} = 1$ and all other $H_{D^0}^{\alpha\beta} = 0$. Hence for mesons which are not part of the light $SU(3)_{uds}$ octet or singlet, $H_{V/P}^{\alpha\beta} = 1$ for the relevant α and β. For the charged light mesons, this assumption is also made , *e.g.* that K^+ is entirely $\bar{s}u$, hence $H_{K^+}^{su} = 1$.

Assuming that all the momentum of the meson is carried by the valence quarks,

$$\langle 0|\sum_{\alpha,\beta} H_P^{\alpha\beta} \bar{q}_\alpha \gamma^\mu \gamma^5 q_\beta|P(p_P)\rangle = iF_P p_P^\mu \tag{F.4}$$

since the sum of the squares of $H_P^{\alpha\beta}$ for the constituent valence quark–anti–quark pairs is normalized to 1.

Now comparison with the literature is made: $H_P^{\alpha\beta}$ is related to the definition of the axial current using Gell–Mann matrices, λ^a (normalized such that $\mathrm{tr}\big(\lambda^a\lambda^b\big) = 2\delta^{ab}$; also here λ^0 is

defined as ${}^{\sqrt{2}}/_{\sqrt{3}}I_{3\times3}$). The P.D.G. [51] use the definition of the axial current A^a_μ as appearing in reference [118]:

$$A^a_\mu = \bar{q}\gamma_\mu\gamma^5\frac{1}{2}\lambda^a q \tag{F.5}$$

where the vector $q = (u, d, s)^T$, with the definition of each meson decay constant given by

$$\sqrt{2}\langle 0|A^a_\mu\big|P^b(p)\big\rangle = i\delta^{ab}f_P p_\mu \tag{F.6}$$

for a meson $P^b(p)$ defined as having valence quarks given by $\bar{q}\lambda^b q$. More generally a meson is a superposition $C^{bc}\bar{q}\lambda^c q$. From this,

$$\sqrt{2}\langle 0|A^a_\mu|P(p)\rangle = \langle 0|\sum_{\alpha,\beta}H_P^{\alpha\beta}\bar{q}_\alpha\gamma^\mu\gamma^5 q_\beta|P(p_P)\rangle \tag{F.7}$$

so the values for $H_P^{\alpha\beta}$ are just ${}^1/_{\sqrt{2}}(\lambda^a)^{\alpha\beta}$ for the pseudoscalar meson associated with the Gell–Mann matrix λ^a. This fixes the normalization; *e.g.* in this scheme the neutral pion is ${}^1/_{\sqrt{2}}(\bar{u}u - \bar{d}d)$ ($H^{uu}_{\pi^0} = {}^1/_{\sqrt{2}}$, $H^{dd}_{\pi^0} = {}^{-1}/_{\sqrt{2}}$). This also fixes which decay constant convention is used, since F_P is identified as f_P: that in which $F_\pi = 130$ MeV rather than 91 MeV. The $H_V^{\alpha\beta}$ are defined to be the same as $H_P^{\alpha\beta}$ for their pseudoscalar counterparts.

Strictly speaking, equation (F.6) should read

$$\sqrt{2}\langle 0|A^a_\mu\big|P^b(p)\big\rangle = i\delta^{ab}f_P p_\mu \exp(-ip{\cdot}x) \tag{F.8}$$

but the $\exp(-ip{\cdot}x)$ leads to a factor of 1 and enforces momentum conservation when the matrix element is squared, and so in this thesis is dropped except for the following discussion. Applying ∂^μ to both sides leads to

$$\sqrt{2}\langle 0|\partial^\mu A^a_\mu\big|P^b(p)\big\rangle = \delta^{ab}f_P p^2 \exp(-ip{\cdot}x) \tag{F.9}$$

Now

$$\begin{aligned}
\partial^\mu A^a_\mu &= \partial^\mu\left(\bar{q}\gamma_\mu\gamma^5\frac{1}{2}\lambda^a q\right) = \left(\bar{q}\overleftarrow{\partial\!\!\!/}\gamma^5\frac{1}{2}\lambda^a q + \bar{q}\partial\!\!\!/\gamma^5\frac{1}{2}\lambda^a q\right) \\
&= \left(\bar{q}\overleftarrow{\partial\!\!\!/}\gamma^5\frac{1}{2}\lambda^a q - \bar{q}\frac{1}{2}\lambda^a\gamma^5\partial\!\!\!/ q\right) = \left(\bar{q}(iM)\gamma^5\frac{1}{2}\lambda^a q - \bar{q}\frac{1}{2}\lambda^a\gamma^5(-iM)q\right) \\
&= \bar{q}\gamma^5\frac{i}{2}\{\lambda^a, M\}\,q
\end{aligned} \tag{F.10}$$

assuming that the quark fields satisfy the Dirac equation (equation (A.3)). The notation $\bar{q}\overleftarrow{\partial\!\!\!/}$ is equivalent to $(\partial_\mu q^\dagger)\gamma^0\gamma^\mu$, and M here is defined as

$$M = \begin{pmatrix} m_u & 0 & 0 \\ 0 & m_d & 0 \\ 0 & 0 & m_s \end{pmatrix} \tag{F.11}$$

Combining this result with equation (F.9) leads to

$$\langle 0|\bar{q}\gamma^5\frac{1}{2}\{\lambda^a, M\}\,q\big|P^b(p)\big\rangle = \frac{-i}{\sqrt{2}}\delta^{ab}f_P p^2 \tag{F.12}$$

(dropping the exponential function again).

Since

$$\begin{aligned}
\langle 0|\bar{q}_\alpha\gamma^5(m_{q_\alpha}+m_{q_\beta})q_\beta\big|P^b(p)\rangle &= \langle 0|\bar{q}\gamma^5\left\{(D^c_{\alpha\beta}\lambda^c),M\right\}q\big|P^b(p)\rangle \qquad \text{(F.13)}\\
\Rightarrow\langle 0|\bar{q}_\alpha\gamma^5 q_\beta\big|P^b(p)\rangle &= \frac{1}{m_{q_\alpha}+m_{q_\beta}}\langle 0|\bar{q}\gamma^5\left\{(D^c_{\alpha\beta}\lambda^c),M\right\}q\big|P^b(p)\rangle\\
&= \frac{D^c_{\alpha\beta}\sqrt{2}\delta^{cb}f_P p^2}{m_{q_\alpha}+m_{q_\beta}}\\
&= \frac{\sqrt{2}D^b_{\alpha\beta}f_P p^2}{m_{q_\alpha}+m_{q_\beta}} \qquad \text{(no sum on } \alpha,\beta) \qquad \text{(F.14)}
\end{aligned}$$

where $D^c_{\alpha\beta}$ is defined such that $\bar{q}_\alpha q_\beta = D^c_{\alpha\beta}\bar{q}\lambda^c q$.

By comparison with equation (F.3), $\mu_P^{\alpha\beta}$ is identified as

$$\mu_P^{\alpha\beta} \equiv \frac{-H_P^{\alpha\beta}(m_{q_\alpha}+m_{q_\beta})}{\sqrt{2}D^b_{\alpha\beta}} \qquad \text{(F.15)}$$

Take the neutral pion as an example:

$$\langle 0|\bar{q}\gamma^\mu\gamma^5\frac{1}{2}\lambda^3 q\big|\pi^0(p_\pi)\rangle = \frac{i}{\sqrt{2}}F_\pi p_\pi^\mu \qquad \text{(F.16)}$$

$$H^{uu}_{\pi^0} = \frac{1}{\sqrt{2}}, H^{dd}_{\pi^0} = \frac{-1}{\sqrt{2}} \qquad \text{(F.17)}$$

$$\langle 0|\bar{u}\gamma^\mu\gamma^5 u\big|\pi^0(p_\pi)\rangle = \langle 0|\bar{q}\gamma^\mu\gamma^5\frac{1}{2}(\sqrt{\frac{3}{2}}\lambda^0+\lambda^3)q\big|\pi^0(p_\pi)\rangle \qquad \text{(F.18)}$$

assuming $\langle 0|\bar{s}\gamma^\mu\gamma^5 s\big|\pi^0(p_{\pi^0})\rangle = 0$. Hence $D^0_{uu} = {}^{\sqrt{3}}\!/_{2\sqrt{2}}$ and $D^3_{uu} = {}^1\!/_2$. This leads to $\mu^{uu}_{\pi^0} = -2m_u$ and $\mu^{dd}_{\pi^0} = 2m_d$.

There are some caveats: the λ^0–λ^8 mixing is taken into account, so the used η and η' states are not exactly ${}^1\!/_{\sqrt{6}}(\bar{u}u+\bar{d}d-2\bar{s}s)$ and ${}^1\!/_{\sqrt{3}}(\bar{u}u+\bar{d}d+\bar{s}s)$, but mixtures with a mixing angle ($\theta_\eta = -11.5^\circ = 0.052$ radians, following chiral perturbation theory) given by the P.D.G. [51], likewise for ϕ and ω.

$$\langle 0|\bar{s}\gamma^5\gamma^\mu s|\eta(p_\eta)\rangle = i(\cos(\theta_\eta)H^{ss}_{\eta_8}F_{\eta_8} - \sin(\theta_\eta)H^{ss}_{\eta_0}F_{\eta_0})p_\eta^\mu \qquad \text{(F.19)}$$

The $H^{\alpha\beta}_{V/P}$ are taken to be 1 for the appropriate quark bilinears for all mesons except for π^0, K_S, K_L, η, η' and ϕ. These mesons are taken to be as in table F.1.

π^0	$\frac{1}{\sqrt{2}}(\bar{u}u - \bar{d}d)$
K_S	$\frac{1}{\sqrt{2}}(\bar{s}d + \bar{d}s)$
K_L	$\frac{1}{\sqrt{2}}(\bar{s}d - \bar{d}s)$
η	$0.515(\bar{u}u + \bar{d}d) - 0.685\bar{s}s$
η'	$0.484(\bar{u}u + \bar{d}d) + 0.729\bar{s}s$
ϕ	$\bar{s}s$

Table F.1: Non–trivial quark bilinear coefficients.

Appendix G

Input Data

The values used for the various fermion and meson masses and decay constants are shown in table G.1. All the F_P values, masses, lifetimes, decay widths and branching fractions are taken as they appeared in the P.D.G.'s listings [51] in December 2006. The masses for the quarks are the central values of the masses in the $\overline{\rm MS}$ scheme. The F_V values were calculated from $V \to e^+e^-$ and are in good agreement with [119]. F_V and F_P are defined in appendix F.

The values for decay widths and branching ratios used, taken from the P.D.G. [51] in December 2006, are given in tables G.2 and G.3.

Pseudoscalar meson	Mass (in GeV)	F_P (in GeV)	Fundamental fermion	Mass (in GeV)
π^0	0.135	0.130	e	5.11×10^{-6}
K_S	0.498	0.160	μ	0.106
K_L	0.498	0.160	τ	1.777
η	0.548	0.130	u	3.0×10^{-3}
η'	0.958	0.172	d	6.0×10^{-3}
D_0	1.86	0.25	s	0.11
B_d	5.28	0.2	c	1.25
B_s	5.37	0.2	b	4.3
Vector meson	Mass (in GeV)	F_V (in GeV)		
ρ	0.776	0.22		
K^*	0.896	0.23		
ϕ	1.020	0.23		
J/ψ	3.10	0.41		

Table G.1: Input data: masses and decay constants

Decaying particle	Decay width (GeV^{-1})	Decay channel	Branching ratio
μ	2.996×10^{-19}	$ee\bar{e}$	1.0×10^{-12}
τ	2.265×10^{-12}	$ee\bar{e}$	$2.0\ \times10^{-7}$
		$ee\bar{\mu}$	$1.1\ \times10^{-7}$
		$\mu e\bar{e}$	$1.9\ \times10^{-7}$
		$\mu e\bar{\mu}$	$2.0\ \times10^{-7}$
		$\mu\mu\bar{e}$	$1.3\ \times10^{-7}$
		$\mu\mu\bar{\mu}$	$1.9\ \times10^{-7}$
		$e\rho^0$	$2.0\ \times10^{-6}$
		$\mu\rho^0$	$6.3\ \times10^{-6}$
		$e\phi$	$6.9\ \times10^{-6}$
		$\mu\phi$	$7.0\ \times10^{-6}$
		eK^{*0}	$5.1\ \times10^{-6}$
		$e\bar{K}^{*0}$	$7.4\ \times10^{-6}$
		μK^{*0}	$7.5\ \times10^{-6}$
		$\mu\bar{K}^{*0}$	$7.5\ \times10^{-6}$
		$e\pi^0$	$1.9\ \times10^{-7}$
		$\mu\pi^0$	$4.1\ \times10^{-7}$
		$e\eta$	$2.4\ \times10^{-7}$
		$\mu\eta$	$1.5\ \times10^{-7}$
		eK_S	$9.1\ \times10^{-7}$
		μK_S	$9.5\ \times10^{-7}$

Table G.2: Input data: lepton decays

Decaying particle	Decay width (GeV^{-1})	Decay channel	Branching ratio
J/ψ	$9.3 \quad \times 10^{-5}$	$\mu\bar{e}/e\bar{\mu}$	1.1×10^{-6}
		$\tau\bar{e}/e\bar{\tau}$	8.3×10^{-6}
		$\tau\bar{\mu}/\mu\bar{\tau}$	2.0×10^{-6}
π^0	7.817×10^{-9}	$e\bar{\mu}$	3.8×10^{-10}
		$\mu\bar{e}$	3.4×10^{-9}
η	$1.29 \quad \times 10^{-6}$	$\mu\bar{e} + e\bar{\mu}$	$6 \quad \times 10^{-6}$
η'	$2.02 \quad \times 10^{-4}$	$\mu\bar{e}/e\bar{\mu}$	4.7×10^{-4}
K_L	1.263×10^{-17}	$\mu\bar{e}/e\bar{\mu}$	4.7×10^{-12}
D^0	1.602×10^{-12}	$\mu\bar{e}/e\bar{\mu}$	8.1×10^{-7}
B_d^0	4.378×10^{-13}	$\mu\bar{e}/e\bar{\mu}$	1.7×10^{-7}
		$\tau\bar{e}/e\bar{\tau}$	1.1×10^{-4}
		$\tau\bar{\mu}/\mu\bar{\tau}$	3.8×10^{-5}
		$e\bar{e}$	6.1×10^{-8}
		$\mu\bar{\mu}$	3.9×10^{-8}
B_s^0	4.378×10^{-13}	$\mu\bar{e}/e\bar{\mu}$	6.1×10^{-6}
		$e\bar{e}$	5.4×10^{-5}
		$\mu\bar{\mu}$	1.5×10^{-7}

Table G.3: Input data: meson decays

Bibliography

[1] H. K. Dreiner, M. Krämer, B. O'Leary, arXiv:hep-ph/0612278.

[2] B. O'Leary, Phys. Rev. D **75** (2007) 054027 [arXiv:hep-ph/0610413].

[3] S. L. Glashow, Nucl. Phys. **22** (1961) 579.

[4] S. Weinberg, Phys. Rev. Lett. **19** (1967) 1264.

[5] A. Salam, Svartholm: Elementary Particle Theory, Proceedings Of The Nobel Symposium Held 1968 At Lerum, Sweden, Stockholm 1968, 367–377

[6] P. W. Higgs, Phys. Lett. **12** (1964) 132.

[7] F. Englert and R. Brout, Phys. Rev. Lett. **13** (1964) 321.

[8] G. S. Guralnik, C. R. Hagen and T. W. B. Kibble, Phys. Rev. Lett. **13** (1964) 585.

[9] H. Yukawa, Proc. Phys. Math. Soc. Jap. **17** (1935) 48.

[10] N. Cabibbo, Phys. Rev. Lett. **10** (1963) 531.

[11] M. Kobayashi and T. Maskawa, Prog. Theor. Phys. **49** (1973) 652.

[12] H. Georgi and S. L. Glashow, Phys. Rev. Lett. **32** (1974) 438.

[13] H. Fritzsch and P. Minkowski, Annals Phys. **93** (1975) 193.

[14] S. Dimopoulos and H. Georgi, Nucl. Phys. B **193** (1981) 150.

[15] N. Sakai, Z. Phys. C **11** (1981) 153.

[16] T. E. Clark, T. K. Kuo and N. Nakagawa, Phys. Lett. B **115** (1982) 26.

[17] U. Amaldi, W. de Boer and H. Furstenau, Phys. Lett. B **260** (1991) 447.

[18] M. B. Green, CALT-68-1219 *IN *BATALIN, I.A. (ED.) ET AL.: QUANTUM FIELD THEORY AND QUANTUM STATISTICS, VOL. 2*, 557-577 AND CALTECH PASADENA - CALT-68-1219 (84,REC.FEB.85) 29 P. (SEE BOOK INDEX)*

[19] for an introduction to the Minimal Supersymmetric Standard Model, see *e.g.*: S. P. Martin, arXiv:hep-ph/9709356; I. J. R. Aitchison, arXiv:hep-ph/0505105.

[20] S. R. Coleman and J. Mandula, Phys. Rev. **159** (1967) 1251.

[21] J. Zinn–Justin, *Quantum Field Theory and Critical Phenomena*, Oxford University Press, 1989

[22] S. L. Adler, Phys. Rev. **177** (1969) 2426.

[23] J. S. Bell and R. Jackiw, Nuovo Cim. A **60** (1969) 47.

[24] W. de Boer and C. Sander, Phys. Lett. B **585** (2004) 276 [arXiv:hep-ph/0307049].

[25] D. Bourilkov, Int. J. Mod. Phys. A **20** (2005) 3328 [arXiv:hep-ph/0410350].

[26] R. Barbier *et al.*, Phys. Rept. **420** (2005) 1 [arXiv:hep-ph/0406039].

[27] P. Fayet, Nucl. Phys. B **90** (1975) 104.

[28] R. E. Marshak and R. N. Mohapatra, Phys. Lett. B **91** (1980) 222.

[29] J. R. Ellis, J. S. Hagelin, D. V. Nanopoulos, K. A. Olive and M. Srednicki, Nucl. Phys. B **238** (1984) 453.

[30] S. Wolfram, Phys. Lett. B **82** (1979) 65.

[31] P. F. Smith and J. R. J. Bennett, Nucl. Phys. B **149** (1979) 525.

[32] C. S. Aulakh and R. N. Mohapatra, Phys. Lett. B **119** (1982) 136.

[33] Y. Chikashige, R. N. Mohapatra and R. D. Peccei, Phys. Lett. B **98** (1981) 265.

[34] M. Gell-Mann, P. Ramond and R. Slansky, Print-80-0576 (CERN)

[35] S. F. King, Rept. Prog. Phys. **67** (2004) 107 [arXiv:hep-ph/0310204].

[36] A. Masiero and J. W. F. Valle, Phys. Lett. B **251** (1990) 273.

[37] T. Araki *et al.* [KamLAND Collaboration], Phys. Rev. Lett. **96** (2006) 101802 [arXiv:hep-ex/0512059].

[38] M. Shiozawa *et al.* [Super-Kamiokande Collaboration], Phys. Rev. Lett. **81** (1998) 3319 [arXiv:hep-ex/9806014].

[39] Y. Fukuda *et al.* [Super-Kamiokande Collaboration], Phys. Rev. Lett. **81** (1998) 1562 [arXiv:hep-ex/9807003].

[40] S. N. Ahmed *et al.* [SNO Collaboration], Phys. Rev. Lett. **92** (2004) 181301 [arXiv:nucl-ex/0309004].

[41] D. G. Michael *et al.* [MINOS Collaboration], Phys. Rev. Lett. **97** (2006) 191801 [arXiv:hep-ex/0607088].

[42] B. Pontecorvo, Sov. Phys. JETP **26** (1968) 984 [Zh. Eksp. Teor. Fiz. **53** (1967) 1717].

[43] F. Deppisch, H. Pas, A. Redelbach and R. Ruckl, Phys. Rev. D **73** (2006) 033004 [arXiv:hep-ph/0511062].

[44] S. G. Kim, N. Maekawa, A. Matsuzaki, K. Sakurai and T. Yoshikawa, arXiv:hep-ph/0612370.

[45] M. Blanke, A. J. Buras, B. Duling, A. Poschenrieder and C. Tarantino, arXiv:hep-ph/0702136.

[46] R. A. Diaz, R. Martinez and C. E. Sandoval, Eur. Phys. J. C **41** (2005) 305 [arXiv:hep-ph/0406265].

[47] A. G. Akeroyd, M. Aoki and Y. Okada, arXiv:hep-ph/0610344.

[48] C. X. Yue, L. H. Wang and W. Ma, Phys. Rev. D **74** (2006) 115018 [arXiv:hep-ph/0611054].

[49] M. Iwasaki [Belle Collaboration], arXiv:hep-ex/0406059.

[50] L. J. Hall and M. Suzuki, Nucl. Phys. B **231** (1984) 419.

[51] W. M. Yao *et al.* [Particle Data Group], J. Phys. G **33** (2006) 1.

[52] H. K. Dreiner, C. Luhn and M. Thormeier, Phys. Rev. D **73** (2006) 075007 [arXiv:hep-ph/0512163].

[53] L. E. Ibanez and G. G. Ross, Nucl. Phys. B **368** (1992) 3.

[54] H. K. Dreiner, C. Luhn, H. Murayama and M. Thormeier, arXiv:hep-ph/0610026.

[55] LEPSUSYWG, ALEPH, DELPHI, L3 and OPAL Collaborations, Preliminary results from the combination of LEP data, prepared by the LEP SUSY Working Group. LEPSUSYWG/02–01.1, 02–02.1, 02–04.1, 02–05.1, 02–06.2, 02–07.1, 02–08.1, 02–09.2, 02–10.1, 01–03.1, 01–01.1 See also http://www.cern.ch/lepsusy/.

[56] A. Dedes, S. Rimmer, J. Rosiek and M. Schmidt-Sommerfeld, Phys. Lett. B **627** (2005) 161 [arXiv:hep-ph/0506209].

[57] V. D. Barger, T. Falk, T. Han, J. Jiang, T. Li and T. Plehn, Phys. Rev. D **64** (2001) 056007 [arXiv:hep-ph/0101106].

[58] V. D. Barger, G. F. Giudice and T. Han, Phys. Rev. D **40** (1989) 2987.

[59] D. Choudhury and P. Roy, Phys. Lett. B **378** (1996) 153 [arXiv:hep-ph/9603363].

[60] J. P. Saha and A. Kundu, Phys. Rev. D **66** (2002) 054021 [arXiv:hep-ph/0205046].

[61] J. E. Kim, P. Ko and D. G. Lee, Phys. Rev. D **56** (1997) 100 [arXiv:hep-ph/9701381].

[62] J. H. Jang, J. K. Kim and J. S. Lee, Phys. Rev. D **55** (1997) 7296 [arXiv:hep-ph/9701283].

[63] H. K. Dreiner, G. Polesello and M. Thormeier, Phys. Rev. D **65** (2002) 115006 [arXiv:hep-ph/0112228].

[64] [26] updating bounds given in [61] with data published by the Particle Data Group [120] in 2002

[65] M. Herz, Diploma Thesis, arXiv:hep-ph/0301079.

[66] [26] updating bounds given in [59] with data published by the Particle Data Group in 2002 [120]

[67] [26] updating bounds given in [61] with data from
SINDRUM II Collaboration, talk given at 14th International Conference on Particles and Nuclei (PANIC), Williamsburg, Virginia, USA, 22–28 May 1996. Presented by P. Wintz. Published by World Scientific Publishing Co. Pte. Ltd. 1997, Ed. C.E. Carlson and J.J. Domingo, 458

[68] Y. G. Xu, R. M. Wang and Y. D. Yang, arXiv:hep-ph/0610338.

[69] G. Altarelli, G. F. Giudice and M. L. Mangano, Nucl. Phys. B **506** (1997) 29 [arXiv:hep-ph/9705287].
updated by [26] with data published by the Particle Data Group in 2002 [120]

[70] F. Ledroit and G. Sajot, Rapport GDR-Supersymétrie, GDR-S-008 (ISN, Grenoble, 1998) updated by [26] with data published by the Particle Data Group in 2002 [120]

[71] G. Abbiendi *et al.* [OPAL Collaboration], Phys. Lett. B **519** (2001) 23 [arXiv:hep-ex/0109011].

[72] Y. B. Sun, L. Han, W. G. Ma, F. Tabbakh, R. Y. Zhang and Y. J. Zhou, JHEP **0409** (2004) 043 [arXiv:hep-ph/0409240].

[73] [26] using data on the weak charge of Cs atoms from [121]

[74] G. Rodrigo, H. Czyz and J. H. Kuhn, eConf **C0209101** (2002) WE06 [Nucl. Phys. Proc. Suppl. **123** (2003) 167] [arXiv:hep-ph/0210287].

[75] J. Vermaseren [arXiv:math-ph/0010025].

[76] B. Andersson, G. Gustafson, G. Ingelman and T. Sjostrand, Phys. Rept. **97** (1983) 31.

[77] T. Hahn, Comput. Phys. Commun. **140** (2001) 418 [arXiv:hep-ph/0012260].

[78] T. Hahn and M. Perez-Victoria, Comput. Phys. Commun. **118** (1999) 153 [arXiv:hep-ph/9807565].

[79] http://bbr-onlwww.slac.stanford.edu:8080/babarrc/perfdata.html

[80] B. Aubert *et al.* [BABAR Collaboration], Phys. Rev. D **72** (2005) 032005 [arXiv:hep-ex/0405025].

[81] L. J. Hall, V. A. Kostelecky and S. Raby, Nucl. Phys. B **267** (1986) 415.

[82] H. E. Logan and U. Nierste, Nucl. Phys. B **586** (2000) 39 [arXiv:hep-ph/0004139].

[83] M. B. Causse and J. Orloff, Eur. Phys. J. C **23** (2002) 749 [arXiv:hep-ph/0012113].

[84] http://belle.kek.jp/bdocs/lum_day.gif

[85] V. D. Barger, G. F. Giudice and T. Han, Phys. Rev. D **40** (1989) 2987.

[86] H. K. Dreiner and S. Lola, *Prepared for Physics with e+ e- Linear Colliders (The European Working Groups 4 Feb - 1 Sep 1995: Session 3), Hamburg, Germany, 30 Aug - 1 Sep 1995*

[87] S. Lola, arXiv:hep-ph/9912217.

[88] M. Chemtob and G. Moreau, Phys. Rev. D **59** (1999) 055003 [arXiv:hep-ph/9807509].

[89] J. L. Feng, J. F. Gunion and T. Han, Phys. Rev. D **58** (1998) 071701 [arXiv:hep-ph/9711414].

[90] Y. Q. Chen, T. Han and Z. G. Si, arXiv:hep-ph/0612076.

[91] S. Chekanov *et al.* [ZEUS Collaboration], Eur. Phys. J. C **42** (2005) 1 [arXiv:hep-ph/0503274].

[92] J. Blumlein, H. Bottcher and A. Guffanti, arXiv:hep-ph/0607200.

[93] D. J. Gross and F. Wilczek, Phys. Rev. Lett. **30** (1973) 1343.

[94] H. D. Politzer, Phys. Rev. Lett. **30** (1973) 1346.

[95] H. K. Dreiner, arXiv:hep-ph/9707435.

[96] B. C. Allanach, A. Dedes and H. K. Dreiner, Phys. Rev. D **69** (2004) 115002 [Erratum-ibid. D **72** (2005) 079902] [arXiv:hep-ph/0309196].

[97] B. C. Allanach, M. A. Bernhardt, H. K. Dreiner, C. H. Kom and P. Richardson, arXiv:hep-ph/0609263.

[98] A. Nisati, S. Petrarca and G. Salvini, Mod. Phys. Lett. A **12** (1997) 2213 [arXiv:hep-ph/9707376].

[99] A. C. Kraan, J. B. Hansen and P. Nevski, arXiv:hep-ex/0511014.

[100] M. Pospelov, arXiv:hep-ph/0605215.

[101] K. Kohri and F. Takayama, arXiv:hep-ph/0605243.

[102] M. Kaplinghat and A. Rajaraman, Phys. Rev. D **74** (2006) 103004 [arXiv:astro-ph/0606209].

[103] R. J. Oakes, K. Whisnant, J. M. Yang, B. L. Young and X. Zhang, Phys. Rev. D **57** (1998) 534 [arXiv:hep-ph/9707477].

[104] E. L. Berger, B. W. Harris and Z. Sullivan, Phys. Rev. Lett. **83** (1999) 4472 [arXiv:hep-ph/9903549].

[105] B. C. Allanach, A. J. Barr, M. A. Parker, P. Richardson and B. R. Webber, JHEP **0109** (2001) 021 [arXiv:hep-ph/0106304].

[106] W. Shao-Ming, H. Liang, M. Wen-Gan, Z. Ren-You and J. Yi, Phys. Rev. D **74** (2006) 057902 [arXiv:hep-ph/0609109].

[107] D. Bailin, A. Love, *Introduction To Gauge Field Theory* Revised Edition, IOP, 1986, 1993

[108] M. Peskin, D. Schroeder, *An Introduction To Quantum Field Theory*, Westview, 1995

[109] A. Zee, *Quantum Field Theory In A Nutshell*, Princeton University Press, 2003

[110] L. Ryder, *Quantum Field Theory* Second Edition, Cambridge University Press, 1985, 1996

[111] Bjorken and Drell, *Relativistic Quamtum Fields* McGraw-Hill, 1965

[112] D. Bailin, A. Love, *Supersymmetric Gauge Field Theory And String Theory*, IOP 1994

[113] J. Wess, J. Bagger, *Supersymmetry And Supergravity*, Princeton University Press, 1983

[114] W. Pauli, Phys. Rev. **58** (1940) 716.

[115] V. N. Popov and L. D. Faddeev, FERMILAB-PUB-72-057-T *In *'t Hooft, G. (ed.): 50 years of Yang-Mills theory* 40-64*

[116] L. O'Raifeartaigh, Nucl. Phys. B **96** (1975) 331.

[117] V. D. Barger, R. J. N. Phillips, *Collider Physics Updated Edition*, Addison Wesley, 1987, 1997

[118] H. Leutwyler, Nucl. Phys. Proc. Suppl. **64** (1998) 223 [arXiv:hep-ph/9709408].

[119] M. Neubert and B. Stech, Adv. Ser. Direct. High Energy Phys. **15** (1998) 294 [arXiv:hep-ph/9705292].

[120] K. Hagiwara *et al.* [Particle Data Group], Phys. Rev. D **66** (2002) 010001.

[121] J. L. Rosner, Phys. Rev. D **65** (2002) 073026 [arXiv:hep-ph/0109239].